

AD-A183 204

AN ELECTRICAL CIRCUIT MODEL OF THE INTERFACE BETWEEN AN  
ELECTRODE AND THE... (U) AIR FORCE INST OF TECH  
WRIGHT-PATTERSON AFB OH SCHOOL OF ENGI.. J M SEDLAK

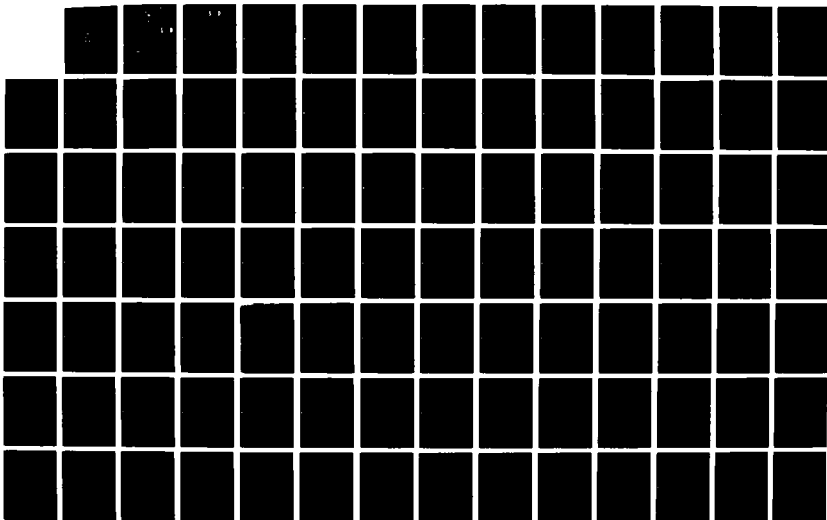
1/4

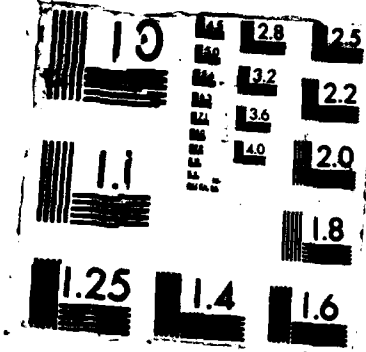
UNCLASSIFIED

31 JUL 87 AFIT/GE/EE/86D-48

F/G 9/1

NL





DTIC FILE COPY  
DTIC FILE COPY



DTIC  
ELECTE  
AUG 14 1987  
S D

AD-A183 204

Requirements for the Degree of  
Master of Science

by

**DISTRIBUTION STATEMENT A**

Approved for public release;  
Distribution Unlimited

DEPARTMENT OF THE AIR FORCE  
AIR UNIVERSITY  
**AIR FORCE INSTITUTE OF TECHNOLOGY**

Wright-Patterson Air Force Base, Ohio

87 8 11 161

AFIT/GE/EE/86D-48

DTIC  
ELECTE  
AUG 14 1987  
S ASD D

AN ELECTRICAL CIRCUIT MODEL OF THE INTERFACE BETWEEN  
AN ELECTRODE AND THE ELECTROLYTIC MEDIUM OF THE CORTEX

THESIS

Presented to the Faculty of the School of Engineering  
of the Air Force Institute of Technology

Air University

In Partial Fulfillment of the  
Requirements for the Degree of  
Master of Science

by

Jeffrey M. Sedlak, B.S.

Captain, USAF

Graduate Electrical Engineering

July 1987

Approved for public release; distribution unlimited



## Preface

Twenty years ago, Matthew Kabrisky authored a book, A Proposed Model for Visual Information Processing in the Human Brain, that proposed a method for examining the processing of visual information in the cortex of a mammalian brain. Despite the technological inability to test this precocious idea, Kabrisky had germinated a seed that remained dormant until the capability of transferring substantial electronic circuit designs onto a tiny silicon chip finally evolved. The eventual implant of a multielectrode array into a beagle in 1982 demonstrated the feasibility of direct cortical exploration, but many questions remain unanswered.

This thesis project has been undertaken to investigate the naturally occurring impedance characteristics of the conducting path between an electrode and the surface of visual processing neurons in the cortex. A saline electrolyte medium between the electrode and cortical neurons introduces a nonideal conducting path. The interpretation of data collected from direct cortical exploration must account for the nonideal conductive characteristics of this electrolytic medium.

I gratefully acknowledge the motivation and assistance provided by Maj Edward Kolesar. His wealth of experience and methodology provided much needed inspiration throughout all

phases of this undertaking. Also, I appreciate the indispensable guidance and technical expertise that were provided by Dr. Matthew Kabrisky and Capt Richard Linderman. I thank Mr. Don Smith, Mr. Bob Ewing, and the entire laboratory staff at AFIT for their assistance.

I extend a sincere heartfelt thanks to Lt Col Richard Castle and Lt Col Dennis Larsen at AFCSA/SAGF for their interest in this project and unconditional support. Without their cooperation, this thesis would not have been possible.

I especially thank my wife Cheryl for all of her support and encouragement, and I recognize the sacrifices she made on my behalf. In addition, I thank you, Cheryl, for the countless hours that you selflessly assisted me in the preparation of this thesis. Finally, I confess my indebtedness to the Creator, who gave me everything and asked only for my belief in return.

Jeffrey M. Sedlak



Accession For	
NTIS CRA&I	<input checked="" type="checkbox"/>
DTIC TAB	<input type="checkbox"/>
Unannounced	<input type="checkbox"/>
Justification	
By	
Distribution /	
Availability Codes	
Dist	Avail and/or Special
A-1	

## Contents

	<u>Page</u>
Preface .....	ii
List of Figures .....	vi
List of Tables .....	ix
Abstract .....	x
I. Introduction .....	1
Background and History .....	1
Problem Statement .....	6
Addressing the Problem .....	7
Scope .....	11
Assumptions .....	12
Summary of Current Knowledge .....	13
Approach .....	17
Materials and Equipment .....	20
Other Support .....	20
II. Theory .....	22
Metal Recording Microelectrodes .....	22
The Microelectrode/Cerebrospinal Fluid Interface .....	34
An Electrode/Electrolyte Model .....	48
Conclusion .....	55
III. Development and Implementation of a Measurement Scheme .....	57
Introduction .....	57
Choosing a Model .....	61
Nonlinear Least Squares Analysis .....	66
The Voltage Divider Measurement Technique .....	72
The Bridge Measurement Technique .....	81
Transient Response Analysis .....	84
Pulse Generation Scheme .....	94
IV. Preparation of Testable Chips .....	100
Introduction .....	100
Practice with Wafers .....	102
Passivation of Testable Chips .....	110
Summary of Processed Brain Chips .....	117

V. Results and Discussion .....	123
Test Equipment Configuration .....	124
Calibration and Baseline Procedures .....	128
Equivalent Circuit Impedance Measurements .....	132
Determination of the Maximum Scan Rate .....	145
Summary of Results .....	152
VI. Conclusions and Recommendations .....	153
Conclusions .....	153
Recommendations .....	157
Appendix A: Design of a CMOS AFIT Brain Chip .....	A-1
Appendix B: List of Equipment and Supplies .....	B-1
Appendix C: Photolithography Processing Schedule .....	C-1
Appendix D: Calculation of the Model Parameters .....	D-1
Appendix E: Nonlinear Least Squares Analysis .....	E-1
Appendix F: Calculation of the Circuit Transfer Function ..	F-1
Appendix G: Calibration and Baseline Measurements .....	G-1
Appendix H: Experimental and Calculated Frequency Response Data .....	H-1
Appendix I: Frequency Response Graphs of the Brain Chip Electrodes .....	I-1
Appendix J: Frequency Response Calculations for Scaled Inputs .....	J-1
Appendix K: The Distortion of Simulated Brain Signals .....	K-1
Bibliography .....	BIB-1
Vita .....	VIT-1

## List of Figures

Figure	Page
1-1 The Visual Pathways.....	3
2-1 Microelectrodes Used in Biopotential Recording.....	24
2-2 Effect of Amplifier Input Impedance on Bioelectrode Distortion.....	28
2-3 Distortion Characteristics of Selected Metal Electrodes.....	30
2-4 Variation of Electrode Impedance and Noise Resistance with Frequency.....	33
2-5 Experimental and Calculated Capacitance of Mercury in 0.1M and 0.01M Sodium Fluoride.....	39
2-6 Helmholtz Double Layer at Electrode Surface.....	40
2-7 Electrical Polarization of Selected Metal Electrodes.....	42
2-8 Frequency Response of a Gold Electrode.....	45
2-9 Comparison of Frequency Responses of Selected Metal Electrodes.....	46
2-10 Distortion of the EEG of a Dog Caused by Resistive Loading Effects.....	47
2-11 Reactance of Stainless-Steel Electrodes in Saline as a Function of Current Density and Frequency.....	50
2-12 Equivalent Circuit Electrical Models.....	52
2-13 The Robinson Equivalent Circuit Electrical Model...	53
3-1 Initial Model of the Electrode-Solute Interface....	62
3-2 Revised Model of the Electrode-Solute Interface....	64
3-3 Frequency-Dependent Representation of the Electrode/Electrolyte Model .....	67

3-4	Initial Voltage-Divider Measurement Scheme.....	73
3-5	Identification of a Ground Loop.....	76
3-6	Revised Voltage-Divider Measurement Scheme.....	77
3-7	Voltage Division of the Input Signal.....	79
3-8	Small Input Signal Measurement Scheme.....	80
3-9	The Bridge Measurement Scheme.....	83
3-10	Derivation of a Square Wave Pulse from the Unit Step Function.....	92
3-11	Pulse Generation Scheme with Variable Width and Timing.....	96
3-12	Connection Diagram and Truth Table of the 54121 One Shot Integrated Circuit.....	97
4-1	Wafer with 4.5 Second Exposure.....	104
4-2	Wafer with 10 Second Exposure.....	105
4-3	Partial Etch of the Polyimide.....	106
4-4	Complete Etch of the Polyimide.....	108
4-5	Wafer after the Photoresist was Removed.....	109
4-6	Wafer after Two Coats of Polyimide.....	111
4-7	Overetching of the Polyimide on a Chip.....	116
4-8	Chip after the Second Polyimide Etch.....	118
4-9	Chip after the Third Polyimide Etch.....	119
4-10	Wirebonds to the Chip.....	120
4-11	First Chip after Complete Encapsulation.....	121
5-1	Identification Codes of Array Electrodes Used in Testing.....	125
5-2	Equipment Configuration of Impedance Measurements..	127

5-3	Equipment Configuration of Array Scan Rate Tests...	129
5-4	Discrete Component Measurements of the Model.....	131
5-5	Measurements of the Model Using Actual Saline.....	133
5-6	Condition of the Electrodes after Testing.....	142
5-7	Condition of the Electrodes 24 Hours after Immersion in Saline.....	144
5-8	Determination of the Maximum Scan Rate of the Array.....	148
A-1	Brain Chip with Count-Selectable Multiplexer.....	A-4
A-2	Brain Chip with Count-Selectable Multiplexer and Multiplexed Outputs.....	A-5
A-3	Two Possible Approaches in the System Definition...	A-9
A-4	Architecture of the Fully Multiplexed Ballantine Brain Chip.....	A-11
A-5	Architecture of the CMOS AFIT Brain Chip.....	A-12
A-6	Schematic of a Quarter Section of the Decoder.....	A-15
A-7	Schematic of a Quarter Section of the Multiplexer..	A-16
A-8	The Inverter.....	A-18
A-9	The Transmission Gate.....	A-19
A-10	The Two-Input NOR Gate.....	A-20
A-11	The Three-Input NOR Gate.....	A-21
A-12	The Four-Input NAND Gate.....	A-22
A-13	Key to Symbols Used in Figures A-8 through A-12....	A-23

## List of Tables

Table		Page
2-1	Half-Cell Potentials of Selected Metals.....	35
5-1	Calculated Values of Equivalent Circuit Electrical Parameters.....	135
5-2	Corrected Values of $R_c$ .....	138
5-3	Maximum Scan Rates of the Electrodes.....	150
A-1	Comparison of nMOS and CMOS Technologies.....	A-7



### Abstract

Former research of the visual processes that occur at the cortex of mammals concentrated on the task of the design and implantation of a multielectrode array, the AFIT brain chip. Despite the importance of refining these activities, questions were generated from data collected during the first implant that need to be resolved before the next implant into a higher-level primate is attempted. The specific nature of the interface between the electrodes and the electrolytic medium at the cortex is critical to understanding and interpreting data collected during an implantation. The primary thrust of this research is to propose a qualitative model of the electrode/electrolyte interface and then to calculate the quantitative parameters of that model by immersing brain chips into a simulated electrolyte and recording empirical data. The secondary focus of this research is to investigate the limiting effect of the electrode/electrolyte interface upon the maximal scan rate of the multielectrode array. (11/12/00)

## 1. INTRODUCTION

### Background and History

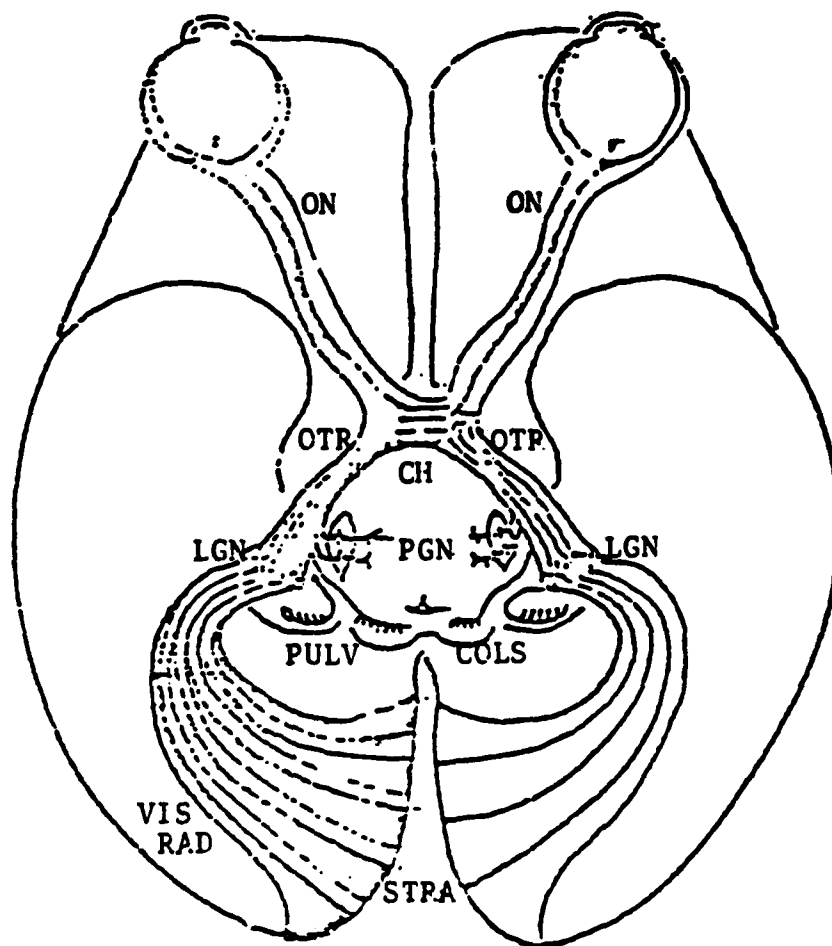
The mutual interactions between the eye and the brain, despite their transparency to the individual, are essential to the visual processes that provide eyesight to many living organisms. Because vision is such an important asset, a variety of research efforts concerning the many visual processes has been performed. Although the optical operation of the eye and certain aspects of retina functioning are well understood, the real key to vision, the brain, has baffled investigators for centuries. Some details of brain processes have been gleaned through intensive study, but the answers to most questions are still unresolved.

The importance of eyesight in our society is reflected by the classification of "handicapped" of a blind person. The devastating impact of a severe visual impairment defies any attempt to recompense the unfortunate victim. Despite federal policies enacted to ease the burden of handicapped people, the most severe form of visual impairment, blindness, disqualifies afflicted individuals from certain privileges granted to the general public. One privilege that a blind person is denied, driving an automobile, can even affect

their eligibility for certain types of employment. Any research of the visual processes that contributes to the restoration of eyesight will directly or indirectly benefit the well-being of the blind.

One project, the Air Force Institute of Technology (AFIT) brain chip, qualifies as research with the potential of restoring vision to the blind. Stated objectives of the AFIT brain chip research include, but are not limited to, fabrication and implantation of a multielectrode array (1:4), analysis of visually stimulated electrical processes in the cortex of the brain (2:1-1), and development of a surgical implantation apparatus and procedures (3:1-7). Fulfillment of these objectives would enhance the current understanding of the role of the cortex in processing visual information. The cortex ultimately receives all of the information gathered and transported by the visual pathway. As the sole source of sensory data to the cortex, the visual pathway includes the eye itself, as well as all of the nerve tissue that links the eye to the cortex. Figure 1-1 provides a representation of the visual pathway with some of its constituent components.

Ideally, biomedical engineers may someday apply the results of AFIT brain chip research to a system that bypasses the visual pathway entirely by direct stimulation of the



R: Retina	CH: Optic Chiasma
ON: Optic Nerves	STRA: Striate Area
OTR: Optic Tracts	COLS: Superior Collicuius
LCN: Lateral Geniculate Nucleus	PULV: Pulvinar of Thalamus
PGN: Pregeniculate Nucleus	VIS RAD: Visual Radiations

Figure 1-1. The Visual Pathways

visual centers of the brain. This new data channel would permit an individual with a nonfunctional visual pathway to effectively experience the neurogenic sensations of vision, provided that the visual centers of the brain still functioned. Such a mechanism might provide an alternative to the permanent loss of eyesight caused by a malfunction of a critical element in the visual pathway.

The prediction of a bypass of the visual pathway with subsequent injection of sensory data directly to the cortex is based upon the theory proposed by Brindley (4). It is well known that optical sensory data are imaged onto the visual cortex via the optic nerve, but actual perception occurs elsewhere in the brain (5). In 1979, a research project was initiated at AFIT to design an array microprobe that could be used to investigate visual processes (6:ii). The current research is concerned with the design, fabrication, passivation, optimization, and implantation of a multielectrode array.

Joseph Tatman considered the possibility of recording bioelectrical signals over the surface of the cortex in 1979 (6:vi). Tatman designed the first in a series of implantable multielectrode recording arrays, dubbed the "AFIT brain chip." This initial project in the biomedical engineering community sparked interest in successive research efforts.

In 1980, Gary Fitzgerald successfully fabricated the Tatman array; however, functional testing of the chip in a saline solution terminated within thirty seconds due to sodium ion contamination (7:108). Extending the scope of the research, George German studied the passivation problem in 1981, and recommended coating the chip with either polyimide or phosphosilicate glass (PSG) (8:59).

Using additional chips that had been fabricated by Fitzgerald, Russell Hensley and David Denton performed the first implant into a beagle dog in 1982. They developed a passivation technique that featured polyimide as the encapsulant. Initial testing of the chip in a simulated cerebrospinal fluid (CSF) saline bath enabled test chips to function for several days, and the brain chip implanted in the dog is believed to have functioned correctly for more than a week (1:70). Veterinary surgeons implanted the chip onto the visual cortex of the beagle's brain, and Hensley and Denton collected visually evoked data for seventeen days (1:81). The data clearly resembled electroencephalographic (EEG) data, but did not conclusively indicate that visual evoked response (VER) information had been collected.

In 1983, Robert Ballantine designed a new generation brain chip. He used nMOS technology and upgraded the previous 4 x 4 array of electrodes to a 16 x 16 array with

multiplexed outputs (9:I-6). Ballantine managed to fabricate the 16 x 16 array and multiplex circuitry on a chip one-fourth the size of the chip used in the beagle implant.

Ricardo Turner oriented his research in 1984 towards the next generation implant to be performed on a rhesus monkey. Turner considered the potential devastation that could be caused by the monkey's ability to grab the wires protruding from its head and fabricated a screw-in socket and connector assembly. The socket prevents movement of the brain chip inside the cranial cavity, and the 85-pin connector eliminates the undesirable interface between recording equipment and wires exiting from the skull of the monkey (3:VI-3).

#### Problem Statement

Prior to implanting an AFIT brain chip onto the visual cortex of a rhesus monkey, a quantitative electrical circuit model of the electrochemical reactions and medium between an electrode and the CSF of the brain needs to be synthesized. The inability of Hensley and Denton to ascertain the exact nature and origin of the data that they had collected (1:88-89) might have been avoided if the electrical circuit model had been available. Certainly, the development of an electrical circuit model of the electrochemical processes

that naturally occur at the interface of an electrode and the CSF will enhance future attempts to draw meaningful conclusions from collected data. An additional motivation for characterizing the parameters of the interface is the optimization of the multielectrode array scan rate. A maximal scan rate of the multielectrode array will be affected not only by the switching characteristics of pass transistors in the array, but also by the electrochemical properties of the interface itself. Knowledge of the effects of the interface upon a representative brain signal will contribute to the interpretation of collected data, as well as to the optimization of the scan rate of the array.

#### Addressing the Problem

Hensley and Denton undeniably accomplished a significant feat by implanting the AFIT brain chip into a beagle's skull. The first implant proved the feasibility of recording cortical sensory data with a multiplexed, multielectrode array, but it also generated questions that can be addressed only by performing another implant. A requirement of the next implant is that it should resolve the enigma concerning the detection of visually evoked responses beyond the level achieved by Hensley and Denton. Ideally, the EEG and VER of the rhesus monkey will be collected during the next implant,



and results of the electrical circuit model research will enable biomedical engineers to clearly distinguish evoked responses from the electrochemical processes occurring at the electrode interface. A more accurate estimate of the VER can be obtained by subtracting the distortion introduced by the interface from the signal received by an electrode. The model of the electrochemical processes should predict the perturbation of the VER that is effected by the interaction of the distributed impedance of the interface and that of the excitation. Also, the effects of electrode kinetics upon the actual brain signal will be more clearly understood.

The significant shortcoming of the research performed by Hensley and Denton was the interpretation of collected data. The data clearly resembled EEG information, but in Hensley's and Denton's own words (1:93):

Furthermore, there is evidence of VER (visual evoked response) between essentially adjacent BCE (basic computing elements), although further analysis is required to confirm this.

The lack of a detailed understanding of the dynamic propagation characteristics of a bioelectrode immersed in the CSF certainly hampered efforts by Hensley and Denton to provide a meaningful interpretation of their results (1:104).

The electrode/electrolyte interface should be modelled before the second implant into a rhesus monkey is performed

so that the nature of the collected data may be better understood. The interface kinetics and resultant effects of an array of metal electrodes upon the detection and transmission of electrical signals were not addressed by Hensley and Denton, and so their explanation of experimental results was not entirely complete. Therefore, a coherent and consistent model of the electrochemical reactions that occur at an electrode/electrolyte interface should be constructed.

Obviously, a model of the bioelectrode in a CSF environment will significantly enhance the effectiveness of future research and implant projects. The primary contribution of such a model is the isolation of the effects of the interface with the electrical signal generated at the cortex of the experimental subject. An a priori knowledge of the electrical performance impact of the interface upon the reception and transmission of brain signals will enable a more comprehensive analysis of the collected data to be made following the next implant.

E. Carstenson recognized the pervasive problem of characterizing the behavior of bioelectrodes used in a chronic implant, and devised a scheme to circumvent the electrode/electrolyte interface entirely (10). He proposed a method of encapsulating the metal recording electrodes with a ceramic insulator that had a large relative dielectric

constant (10:557). However, the frequency response and electrochemical sensitivity of the recording electrode were sacrificed in order to suppress the effects of a metal surface in contact with an electrolyte (10:558).

A requirement of the AFIT brain chip research is that the implantable multielectrode array will be used to record VER data over a large surface of the cortex (6:1). The measurement of the spatially distributed VER signals will ultimately provide information about the interconnections and interactions between the visual processing centers of the cortex (6:1). The implantation of a multielectrode array to record VER data necessitates the investigation of the chronic behavior of implanted bioelectrodes. A compromise of the frequency response and electrochemical sensitivity characteristics of an implanted bioelectrode, as in the method proposed by Carstenson, might not fulfill the requirement to record VER data in a form useful to biomedical research. Research of the optimal frequency response and electrochemical sensitivity of recording bioelectrodes will help to satisfy the objective of recording VER data that may be used by biomedical engineers to analyze elements of visual processing and pattern recognition centers in the cortex. A firm comprehension of bioelectrode dynamics will aid the interpretation of collected VER data and will contribute to

the optimization of the multielectrode array design.

### Scope

An electrical circuit model that characterizes the kinetics of the electrode/electrolyte interface will be developed, beginning with models derived for similar electrochemical processes at a solid-solute interface. Calculated resistances and capacitances will be used to identify the model's lumped parameters. Although the resistances and capacitances of the interface are, in reality, distributed parameters, the more conventional lumped-parameter approach will be invoked since the interface path lengths are much shorter than the wavelengths associated with brain signals (11:41).

A description of other activity related to the rhesus monkey implant will not appear in this thesis. Parallel thesis efforts will address the passivation of the AFIT brain chip, development of an implant procedure, adoption of a test procedure, and reduction of the measured results. This thesis will concentrate solely upon developing an electrical equivalent circuit model of the electrode/electrolyte interface and determining the maximum frequency that the multielectrode array can be scanned. In addition, the discussion of a follow-on CMOS AFIT brain chip that was

designed and fabricated in 1986 is presented in Appendix A.

### Assumptions

Throughout this research, the following assumptions are explicitly recognized:

1. In order to fit the experimental data to an electrical circuit model, an initial configuration of resistive and capacitive elements based upon prior analysis of interface kinetics will provide a starting point for the investigation. The model of an electrode/electrolyte interface proposed by David Robinson (12) will be investigated for applicability. (The Robinson model was derived from an earlier configuration proposed by E. Warburg in 1899.) (13:42).

2. The CSF of the brain will be simulated with either folded tissue paper soaked in an aqueous saline solution, or with the solution exclusively. Previous use of saline-soaked folded tissue paper by Hensley and Denton (1:14,67) and by Turner (3:IV-3) satisfactorily generated the simulated brain signals, but Turner experienced difficulty in making a good electrical contact between the electrodes and the tissue paper (3:IV-12). Turner also noted that chip failure coincided with the application of increased pressure to the chip to ensure better contact (3:IV-14). Because of the difficulties experienced by Turner, this research will proceed by first investigating the propagation of brain-like signals through a bath of saline into which a brain chip has been immersed. In this configuration, the terminals that supply the simulated brain signal are immersed in the saline solution, and the plane of the receiving electrode crosses the path of the current flow between the two terminals. If this method should fail, then the alternative method will entail the use of a saline-soaked tissue paper in the fashion described by Turner (3:IV-3).

### Summary of Current Knowledge

As an integral component of the incredibly complex brain, the cortex performs functions that are essential to the visual process. An image received by the retina is converted to electrical stimuli, transmitted through numerous channels of neurons, and mapped onto the visual area of the cortex. The processing of visual stimuli occurs in the region of the cortex (6:3), which lies on the surface of the brain at the rear of the cranium. Bundles of hundreds to thousands (14:159) of neurons that comprise functional entities, called the cortical columns, perform the processing of visual stimuli. These columns are approximately 50 to 100 microns in diameter (3:1). The specific functions of the cortical columns and their role in the visual process have not been conclusively identified (6:5), so further research of the column system may provide useful data to the biomedical and engineering communities.

Despite a preponderance of information concerning the behavior of individual neurons and interactions between small groups of neurons (6:7), researchers have not yet deciphered the complex organization and interactive processes of arrays of neurons as large as in the cortical columns. Neurocortical research has been segmented into three distinct phases (8:4-6). The recording of the intracellular data of

single cortical neurons by inserting a probe into an anesthetized animal characterized the research of Phase 1. In Phase 2, multielectrode arrays were introduced in an attempt to circumvent problems and limitations of the Phase 1 research. The chief obstacle to Phase 2 research resulted from an excessive number of wires needed to address each of the electrodes in the array. The AFIT brain chip research typifies the efforts of Phase 3. In this application, a multiplexed semiconductor array suitable for long-term implants into a higher-order mammalian subject was designed to collect data from the cortical columns.

The three neurocortical research phases described are examples of direct cortical exploration. One other method of recording brain signals, EEG, has also been used. EEG and direct cortical exploration processes constitute the current body of knowledge in the area of brain signal recording (9:I-1). EEG signal recording methods rely upon the conduction of minute currents, originating in the brain, through the skull and scalp to metallic electrodes attached to the scalp. This "action at a distance" approach to recording EEG and VER signals is somewhat analogous to the use of metal detectors at air terminal checkpoints. Although metal detectors can yield some useful information concerning the contents of luggage, the most foolproof method of

evaluating what a parcel contains is to open it and personally examine the contents. The Phase 3 method of direct cortical exploration via the implantation of a semiconductor multielectrode array replicates the personal inspection of luggage to the greatest degree technologically possible at this time.

An alternative to using a semiconductor multielectrode array for direct cortical exploration is being explored by the University of Michigan, where an instrument containing three electrodes has been proposed (15:89). For this scheme, all of the processing circuitry dedicated to the multiplexing of the electrodes is physically removed from the implantable device and connected by a harness of wires. By 1984, Michigan had not yet devised a mounting assembly or an implant procedure (15:88). An inherent weakness of the University of Michigan approach is the use of the wire harness. Each electrode requires a minimum of three wires: power, ground, and output. As the number of electrodes increases, the number of wires going through the skull is multiplied by a factor of three. Conversely, the AFIT brain chip requires only three wires regardless of the number of electrodes (16:3).

When Hensley and Denton performed the first cortical implant into a beagle dog, the form of the collected data



(1:Al-Al6) indicated that sources of distortion to the received signal were present. Further research of the propagation characteristics of the collected signal may aid in the interpretation of data collected in a future implant. Specifically, the nature of the electrode/electrolyte interface has not been ascertained, and the effects of the interface upon a received brain signal are unknown.

Information concerning the electrochemical processes that occur when an electrode is immersed in an electrolyte does exist. The earliest models of the electrode/electrolyte interface originated in the mid-1800s with Helmholtz (1853) and Quincke (1861). Helmholtz postulated that a region of localized charge forms at the electrode/electrolyte interface; this region of localized charge is called the Helmholtz double layer.

In 1899, Warburg pioneered a model of the electrode/electrolyte interface that featured frequency-dependent resistive and capacitive impedance parameters (13:47). Although various modifications of Warburg's model have been made, his original hypothesis remains valid today. In 1932, Fricke reaffirmed the validity of the basic Warburg model, but pointed out that Warburg's conception of the frequency dependent resistance and capacitance required a slight modification to an exponential

factor (13:47). Robinson published a model of the electrode/electrolyte interface in 1972 (12) that introduced an equivalent circuit configuration composed of frequency-independent electrical parameters. This model, an approximation of the more complex Warburg model, facilitates the calculation of the frequency-independent parameters that it describes. In 1982, Zimmerman described a model of an electrode/electrolyte interface (17:13-14) that was also composed of frequency-independent electrical circuit parameters. A thrust of this thesis will be to evaluate which of the equivalent circuit models best describes the behavior of the electrode/electrolyte interface.

### Approach

The starting point of this thesis is the encapsulation of AFIT brain chips with several coats of polyimide. The polyimide will adhere to the surface of the chips and protect the underlying circuitry from corrosive reactions with the disassociated ions in the saline solution. The polyimide-coated electrodes will be etched so that an electrical contact can be established with a simulated "brain."

After encapsulating and etching the chips, they will be mounted in 64-pin packages and wirebonded. Each row and

column, as well as the ground plane, will be connected to output pins of the packages. Gold wire one millimeter in diameter will be used in the wirebond procedure because of its resistance to corrosion by the saline.

Before actually immersing the chips in a saline bath, static tests will be performed on a discrete-component representation of a proposed equivalent electrical circuit model of the electrode/electrolyte interface. The equivalent circuit electrical parameters of the interface will be determined by applying a frequency-independent model to the case of a brain chip immersed in a saline electrolyte. The static tests should provide an indication of the measurement ranges of parameters of the model for actual brain chips immersed in a saline solution. In addition to the hypothetical modeling of the electrical parameters of the equivalent circuit, static tests will enable an evaluation of the test methodology and equipment configurations that will be employed during dynamic tests of the chip. Static testing of the chips will be used to provide a baseline against which the effects of the electrode/electrolyte interface may be compared, whereas dynamic testing will model the behavior of the chips in an actual CSF environment.

In order to perform dynamic testing of the chip, a simulated brain will be used to generate an electrical

signal. The immersion of chips directly into the saline will accomplish the desired simulation of an actual brain since saline is present in bodily tissues. A simulated brain signal will be generated by submersing the generator's leads in the saline with the brain chip.

After the experimental results have been obtained, a nonlinear least squares analysis will be implemented to obtain the "best-fit" for the resistive and capacitive parameters of the electrical circuit model of the electrode/electrolyte interface. Data collected for a frequency-dependent parallel impedance equivalent circuit model will be input to a nonlinear least squares computer program. The computer program will determine the "best fit" curve for the experimental data and provide the calculated values of the model's parameters as outputs (18:282-283).

Finally, the maximum scan rate of the multielectrode array will be determined from experimental data of chips immersed in a saline electrolyte. The ideal scan rate of a pulse transmitted through a lossless medium will be calculated for comparison with the actual scan rates obtained from pulse transmission in the lossy medium of the electrode/electrolyte interface. An encapsulated summary of the overall approach of this thesis consists of six milestones:

1. Encapsulate the chip with polyimide and etch to expose the electrodes.
2. Attach test leads to the chip.
3. Perform static (outside of the electrolyte) testing of the equivalent circuit electrical parameters.
4. Perform dynamic (in the electrolyte) testing of the chip.
5. Reduce the measured results consistent with the proposed electrical circuit model.
6. Determine the maximum scan frequency of the elements in the array.

#### Materials and Equipment

All of the materials and equipment necessary for this research are off-the-shelf items that will be supplied by APIT. Forty-two of the more critical items are listed in Appendix B.

#### Other Support

The nonlinear least squares computer program calculates the frequency response of a set of data by minimizing the experimental errors inherent to any measurement technique. Another software utility available to VAX 11-785 users, GRAPH, will be used to plot the frequency responses of both the experimental and calculated results. After the plot files have been generated, the laser routine will be invoked

to obtain laser-quality plots.

## 2. THEORY

The nature of the interface between an electrode and an electrolytic medium has been addressed by numerous researchers, but no single conclusive treatment of the subject has ever been published. In the specific investigation of the parameters that will govern the interface kinetics of the brain chip in contact with a saline electrolyte, a consideration of the electrodes will provide the background needed to analyze reactions that occur at the interface itself. From the analysis of the electrode/electrolyte interface, a model will be chosen that relates experimental data that is collected to the actual physical parameters of the interface.

### Metal Recording Microelectrodes

Two fundamental classes of microelectrodes that have been used to record bioelectric events exist. Biomedical engineers have employed microelectrodes of either the metal electrode or glass micropipette variety, depending upon the particular application (19:238). Both classes of electrodes were considered even though the choice of metal electrodes was derived primarily from technological considerations.

Figure 2-1 displays the distinguishing characteristics of metal electrodes and glass micropipettes. Electrodes and micropipettes use different conduction media at the tip of the probe. Conductors used in the fabrication of metal microelectrodes vary in composition and electrical characteristics depending upon the particular metal employed. In the case of glass micropipettes, an aqueous solution extending to the tip of the micropipette actually interfaces electrically with the fluid of the subject tissue. The electrode, usually composed of silver chloride, is suspended in the aqueous electrolytic solution. Biomedical personnel generally use a three-molar potassium chloride electrolytic solution in the micropipette (19:239).

Significant differences in the electrical characteristics of metal electrodes and glass micropipettes exist (19:238-239). Of the two electrode configurations, glass micropipettes prove superior for low frequency applications. Despite the superior low frequency response of glass micropipettes, there are several serious drawbacks to their widespread use. At low current levels, glass micropipettes rectify low-frequency alternating current (ac) signals. The signal-to-noise ratio of glass micropipettes is extremely poor in contrast with the extremely good signal-to-noise ratio of metal electrodes. Because of the



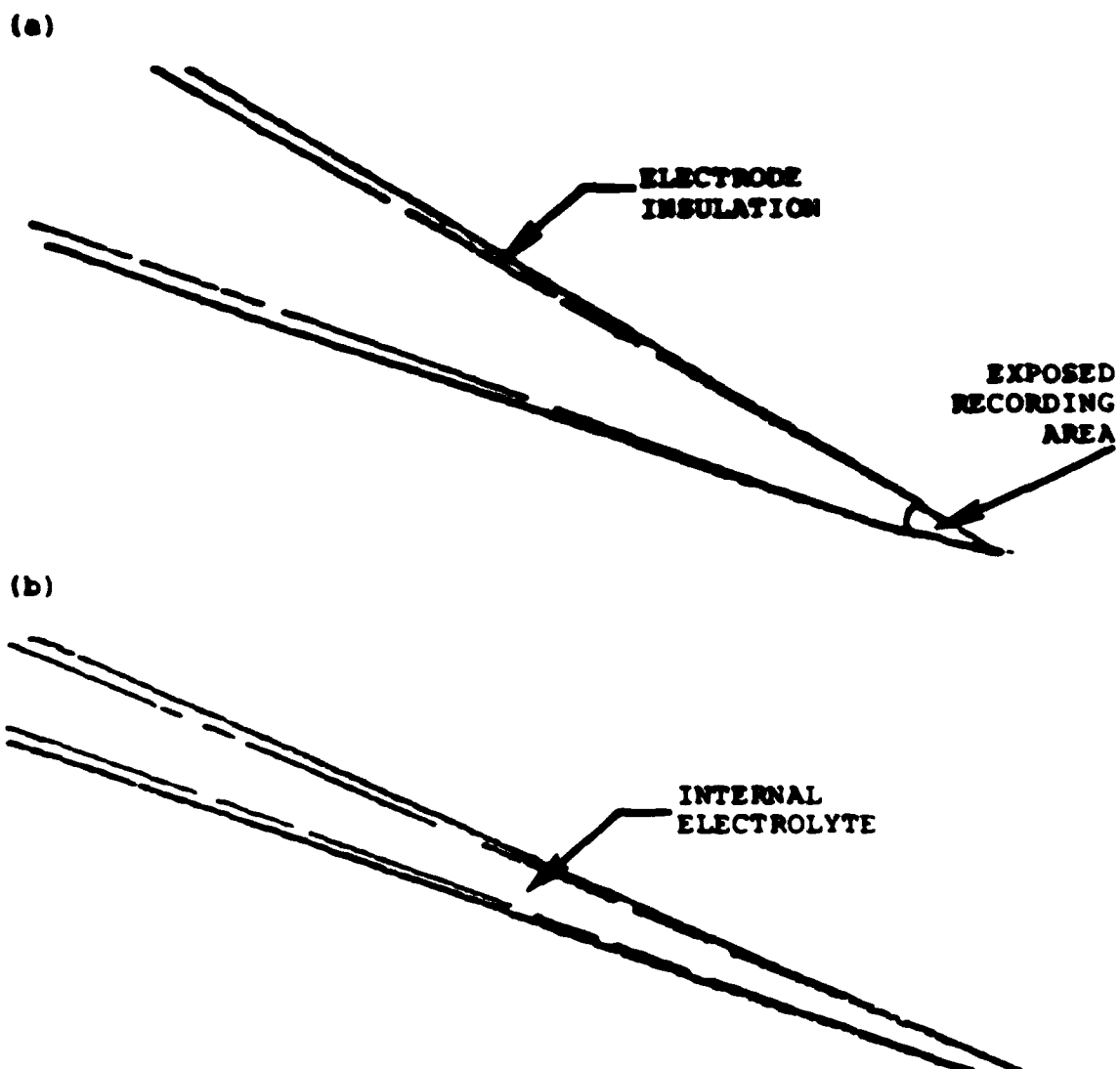


Figure 2-1. Microelectrodes Used in Biopotential Recording  
(a) metal electrode (b) glass micropipette  
(19:239)

diminutive signal levels stimulated in the cortex during VER experiments, metal electrodes exhibit a tremendous signal-to-noise advantage over their glass micropipette counterparts. The fluid tip may fail to distinguish between its inherently high signal-to-noise level and an actual VER signal. Glass micropipettes usually exhibit higher input impedances and lower drift variations than metal electrodes. Gesteland, et.al., state general application hints to decide when to use metal electrodes or glass micropipettes:

Under conditions where one is interested in propagated signals only as signals, we have found the metal probe to be most useful. When one is interested in membrane processes the fluid probe is best. (20:1856)

In the case of integrated circuit multielectrode arrays, physical properties dictate the use of metal recording electrodes rather than glass micropipettes. The single most discriminating physical property of the micropipette is the fluid-filled tip. The present level of technology of integrated circuit designs cannot accommodate the fluid-filled tip feature of glass micropipettes. Hence, the choice of metal electrodes is derived from the physical limitations of integrated circuit fabrication processes.

Another critical factor restricts the use of glass micropipettes. An analysis of VER data recorded at the

cortex of the brain requires the monitoring of cortical columns. Since cortical columns measure approximately 50 to 100 microns in diameter (3:1-1), the size of a recording microelectrode is a physical constraint that cannot be satisfied with glass micropipettes. The densely packed nature of integrated circuits coupled with the technological capability of manufacturing 50 micron electrodes contributes significantly to implantable multielectrode array research.

Wise discusses several problems plaguing conventional multielectrode arrays that integrated circuit multielectrode arrays may alleviate:

Conventional microelectrodes do not lend themselves well to the fabrication of electrode arrays since the resulting structures tend to be physically large, cause excessive disturbance when introduced into tissue, and tend to splay out when inserted, making tip locations uncertain. Thin-film technology has been explored for many years as a means for realizing structures which overcome these problems ... (15:87)

Tatman lists requirements of implantable bioelectrodes that include protection from CSF, biocompatibility with the brain tissue, long-term reliability, low input impedance, and low noise level (6:18). Integrated circuit multielectrode arrays satisfy the Tatman requirements.

The task of recording VER data may require that the recording bioelectrode have a high input impedance to

effectively isolate the input signal. Microelectrodes in the 50 to 100 square micron range could present a very high input impedance to the amplifying stage when they are placed in contact with a saline electrolyte, such as that found in the brain tissue of mammals. A good amplifier design will accommodate the high electrode impedance with a specially designed input stage. The specially designed input stage increases the amplifier impedance well above the impedance of the bioelectrode. In addition, electroplating can alter the electrode's surface topography and composition, thereby reducing the bioelectrode impedance by as many as two orders of magnitude (21:213). An example of a substance commonly electrodeposited is platinum black (21:213). Platinum black has an irregular surface topography, and the increase of surface area that can be obtained with platinum black effects a corresponding decrease of the bioelectrode impedance.

Failure to maintain an amplifier impedance much greater than the bioelectrode impedance can cause electrical loading, and result in the distortion of the input waveform. Figure 2-2 illustrates the distortion caused by descending magnitudes of amplifier input impedances. The amplifier input impedances used to generate the distorted waveforms of Figure 2-2 were electrically connected across the control signal. The relationship between bioelectrode area and

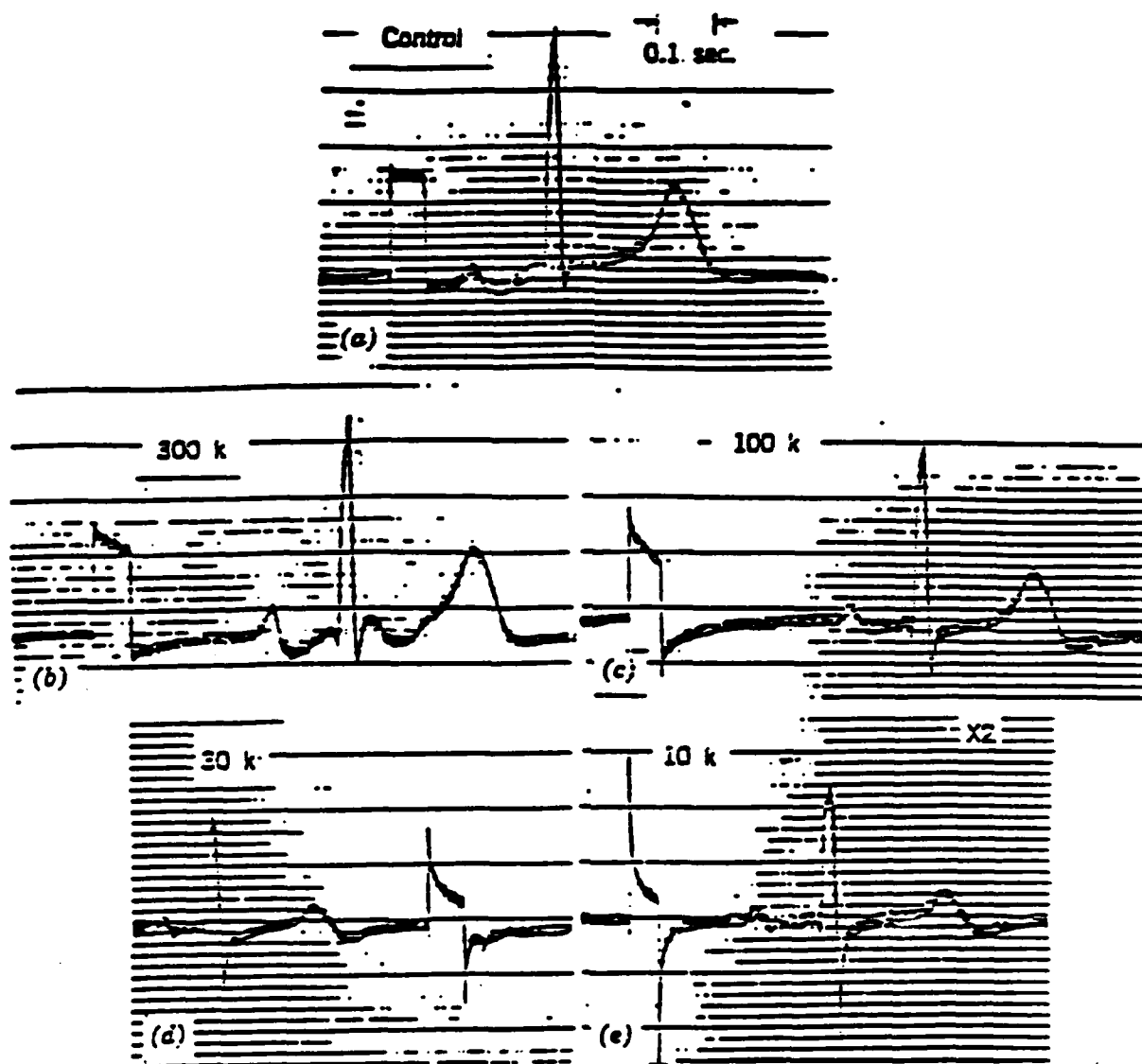


Figure 2-2. Effect of Amplifier Input Impedance on Bioelectrode Distortion (a) control signal (b) 300K ohms (c) 100K ohms (d) 30K ohms (e) 10K ohms (22:243)

amplifier input impedance differs for various metals. Figure 2-3 shows how six metal electrodes reproduced a test waveform given that all of the electrodes had a 0.1 square millimeter surface area and an amplifier input impedance of 750K ohm. Stainless steel and gold electrodes are the two most biocompatible of the six shown in Figure 2-3, but they distorted the test waveform the greatest. Stainless steel and gold bioelectrodes can faithfully reproduce the input waveform; however, the impedance match between the bioelectrode and input stage to the amplifier becomes markedly more critical in achieving low distortion in these biocompatible metals. The designer of a multielectrode array must carefully evaluate tradeoffs between distortion and biocompatibility. Various factors influence distortion, including exchange current density, electrode polarization (impedance), and amplifier loading (caused by an insufficient input impedance).

If not taken into consideration, the signal distortion that is caused by an electrode can adversely affect the successful collection of meaningful data in an experiment. Because signal amplitudes are so small for the VER of the brain (1000 microvolts or less), signal distortion could critically impact the interpretation of VER data, and thereby influence incorrect deductions. Whenever possible, a probe

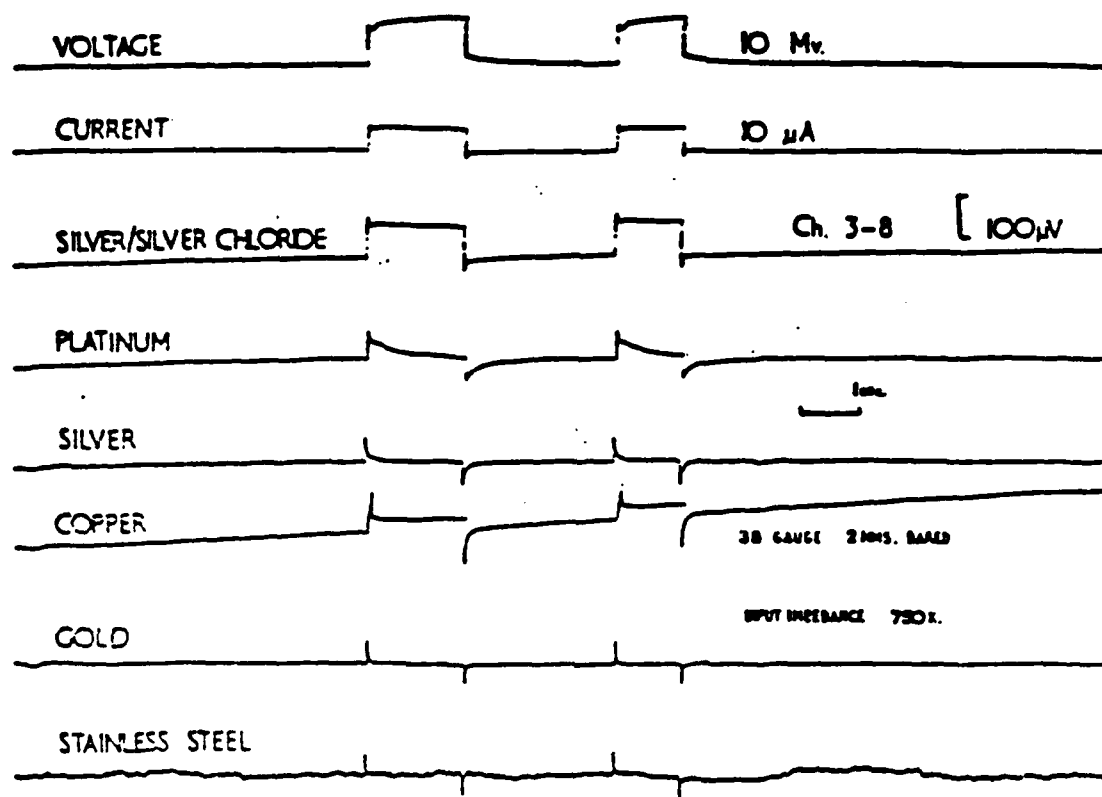


Figure 2-3. Distortion Characteristics of Selected Metal Electrodes (22:245)

designer should strive to minimize the effects of distortion inherent in the electrodes themselves.

Conventional multielectrode probe designers have reported corrective measures that they have taken to minimize undesirable coupling between the electrodes (21:213). Fortunately, an integrated circuit array of electrodes will operate with much less coupling than a conventional array of equivalent dimensions. The silicon substrate under the array and the CSF electrolyte of the brain share a common ground plane (3:E-5). Since the distance separating the substrate and brain ground planes from the electrode metal is approximately one micron, very little energy couples from one electrode to another (21:212). Researchers should ensure that the substrate ground not float on an operational chip because capacitive coupling between the electrodes and electrode pads will increase (3:IV-20). Use of narrow metal lines to connect each electrode to the multiplexer of the AFIT brain chip will further reduce capacitance between electrodes and the ground plane.

Another source of signal distortion in recording bioelectrodes is noise. Noise can couple into a recording system from various sources; the interference caused by noise can be traced to the common 60Hz power supply, cable noise, and triboelectric artifacts (potential resulting from an



unintentional movement of the recording electrode). A reduction of the high input impedance of an electrode will reduce the effects of noise on the bioelectric signal being recorded. Gesteland described the root-mean-square (RMS) noise voltage generated by a metal electrode within a specified frequency range (20:1857). The root-mean-square noise voltage,  $\langle V_{\text{RMS}} \rangle$ , can be derived from the Nyquist thermal noise theorem and is given by:

$$\langle V_{\text{RMS}} \rangle = [4kTR_n(\Delta f)]^{0.5} \quad (2-1)$$

where  $k$  is the Boltzmann's constant,  $T$  is the absolute temperature in degrees Kelvin,  $R_n$  is the equivalent noise resistance, and  $(\Delta f)$  is the operational bandwidth. The thermal noise of a metal electrode is identical to the thermal noise of the base resistance for a transistor derived by Cooke (23:1168). Therefore, the thermal noise analysis developed for transistors applies equally well to metal electrodes. Gesteland measured the noise resistance of a bright platinum microelectrode in saline solution (20:1858). The variation of measured electrode impedance (hollow circles) and noise resistance (solid circles) with changes of the frequency is shown in Figure 2-4.

Another characteristic of metal microelectrodes can create unexpected problems if not properly analyzed. When

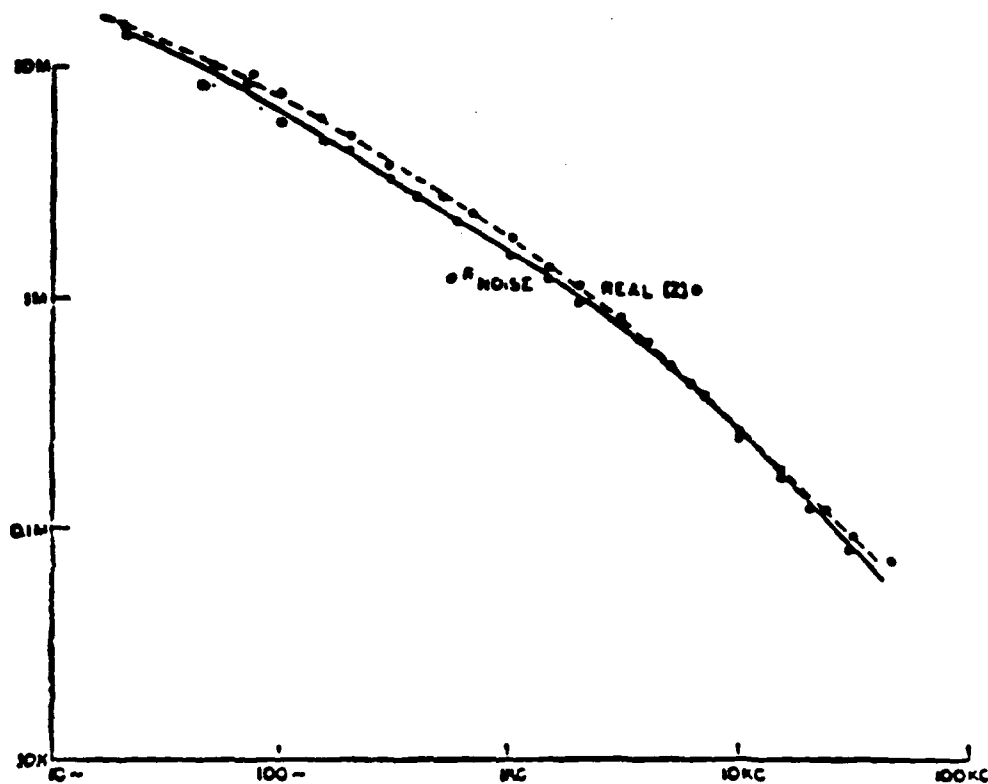


Figure 2-4. Variation of Electrode Impedance (hollow dot) and Noise Resistance (solid dot) with Frequency for Bright Platinum 851, 10 Micron Diameter Conical Tip, 5 Micron Length, in Saline (20:1858)

immersed in an electrolyte, such as the CSF of the brain, ions in the metal electrodes interact with ions in the fluid. This phenomenon, termed the half-cell potential, has been exhaustively studied and characterized by numerous researchers (22:206). Table 2-1 lists several ion-to-metal potentials. When metal electrodes conduct current, the ionization rate increases accordingly. Turner reported severe deterioration of aluminum electrodes used to record test data during simulated brain chip operational tests (3:IV-21). In the Turner experiment, aluminum electrodes that conducted current deteriorated much more rapidly than nonconducting electrodes that were exposed to the CSF. Charge transfer between an unbiased metal electrode and electrolyte eventually reaches a state of equilibrium. When equilibrium is reached, the region of electric charges at the metal electrode surface counterbalances a sheet of charges of opposite polarity in the electrolyte (13:41).

#### The Microelectrode/Cerebrospinal Fluid Interface

Analysis of the electrode/electrolyte interface reveals the alternating current impedance property that will be described physically by an electrical circuit model. Only by considering the confluence of the electrode and the electrolyte may the actual electrical circuit behavior of the

**TABLE 2-1**  
**Half-Cell Potentials of Selected Metals (22:120)**

	Potential (volts)
Aluminum <sup>+++</sup> /aluminum	-1.66
Iron <sup>++</sup> /iron	-0.44
Nickel <sup>++</sup> /nickel	-0.250
Lead <sup>++</sup> /lead	-0.126
Hydrogen <sup>-</sup> /hydrogen	0.0 (Reference)
Copper <sup>++</sup> /copper	+0.337
Copper <sup>+</sup> /copper	+0.521
Silver <sup>+</sup> /silver	+0.799
Platinum <sup>++</sup> /platinum	+1.2
Gold <sup>+</sup> /gold	+1.68
Gold <sup>+++</sup> /gold	+1.50

interface be determined. At the interface, an electrochemical reaction develops that involves the exchange of ions and electrons between the metal electrode and the saline electrolyte. An examination of the processes that naturally occur between parametric elements will be used to select an electrical circuit model that appropriately describes the reactions that occur at the interface of the electrode and electrolyte system.

When an electrode is immersed in an electrolyte, a potential develops from the difference in rates between two opposing processes:

1. ions diffuse from the metal into the electrolyte.
2. ions from the solution combine with free electrons supplied by the metal electrode (22:119).

The aqueous solution of positive sodium ( $\text{Na}^+$ ) and negative chlorine ( $\text{Cl}^-$ ) ions found in the CSF forms the basis of its electrolytic properties. Helmholtz characterized the equilibrium state as a double layer of electric charges on the surface of the electrode that counterbalance a sheet of charges of the opposite sign in the electrolyte. The charge layers can be modeled as a capacitor connected in parallel with a nonlinear resistive component. If the electrode is partially soluble in the electrolyte, then its ions

contribute to the electrolytic reaction. Otherwise, electrodes composed of an inert element contribute only electrons to the electrolytic reaction. A state of equilibrium is reached when an electric gradient equal in magnitude, but of a polarity that opposes the half-cell potential, is created by the transfer of charges between the metal and electrolyte. The electric gradient effectively negates the half-cell chemical gradient, and no further transfers of charge occur after an equilibrium state is reached.

The development of the Helmholtz double-layer model is a very significant result that was derived from the discovery of the half-cell potential. The Helmholtz double-layer qualitatively describes electrochemical processes that occur at the interface between an electrode and an electrolyte. Because a simple description of the electrochemical processes that occur at an electrode/electrolyte interface was provided by Helmholtz, a physical model can be proposed that uses electrical circuit components. The validity of such a model may then be verified through actual experimentation.

In 1913, Gouy and Chapman derived a quantitative model of the Helmholtz layer (24:2). Although overly simplistic, the model predicts electrode capacitance as a function of frequency, charge, electrode potential, and material constants

with a surprising degree of accuracy. The Gouy-Chapman model used in conjunction with a modification developed by Stern in 1924 makes predictions that closely match experimental results. In 1954, Grahame performed experiments that enabled him to measure the capacitance of mercury (Hg) in 0.1M and 0.01M solutions of sodium fluoride (NaF) by applying a variable bias. Figure 2-5 shows the Grahame experimental curves plotted against theoretical curves obtained from the Gouy-Chapman equations. Stern modified the Gouy-Chapman assumption that ions could be treated as point charges and determined that the calculated capacity of an electrode was much less if the finite size of an ion was taken into account. Also, Stern conceptualized the Helmholtz layer divided into two regions separated by a plane of closest approach. The Helmholtz double layer lies between the electrode and its plane of closest approach, and the distributed double layer extends from the plane of closest approach into the bulk of the electrolytic solution (24:36). Figure 2-6 presents a representation of the Helmholtz double layer.

Wise defines the "electrode polarization" potential ( $\eta$ ) as the change in electrode potential due to current flow in the Helmholtz double layer (25:242). The relationship between electrode current and electrode polarization

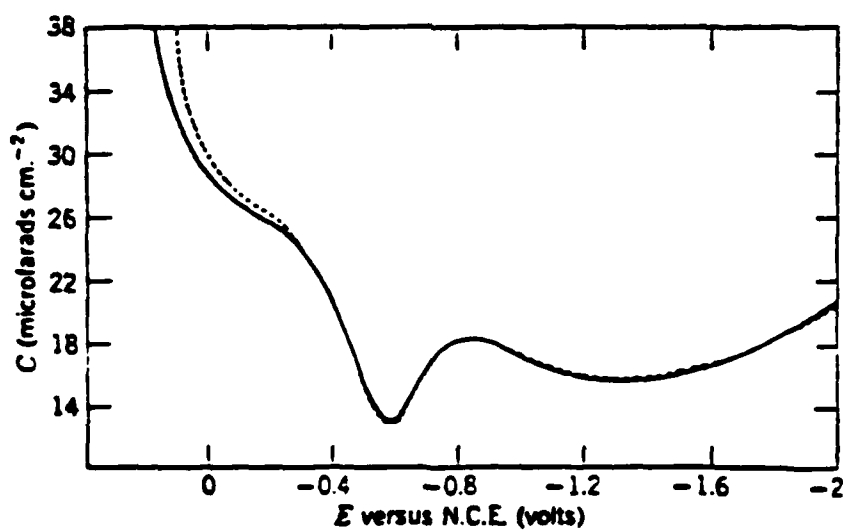
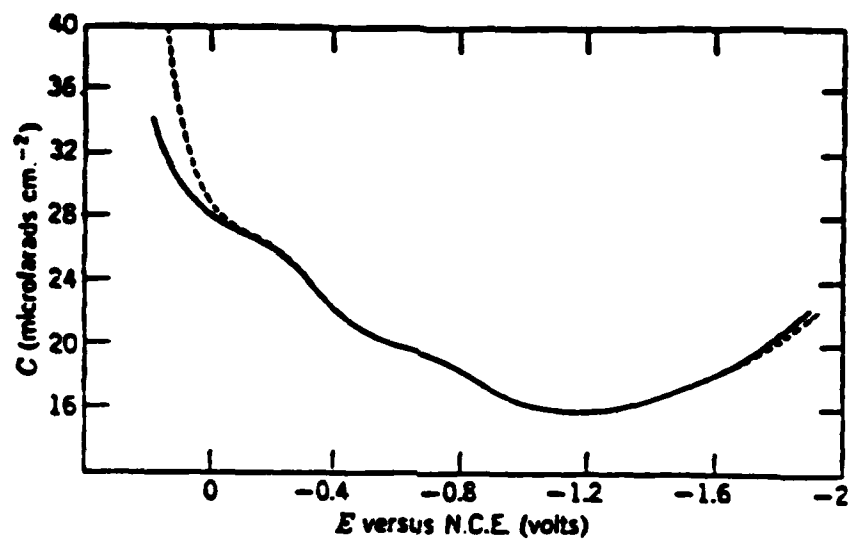


Figure 2-5. Experimental (solid) and Calculated (dashed) Capacitance of Mercury in 0.1M (top figure) and 0.01M (bottom figure) Sodium Fluoride (24:39)



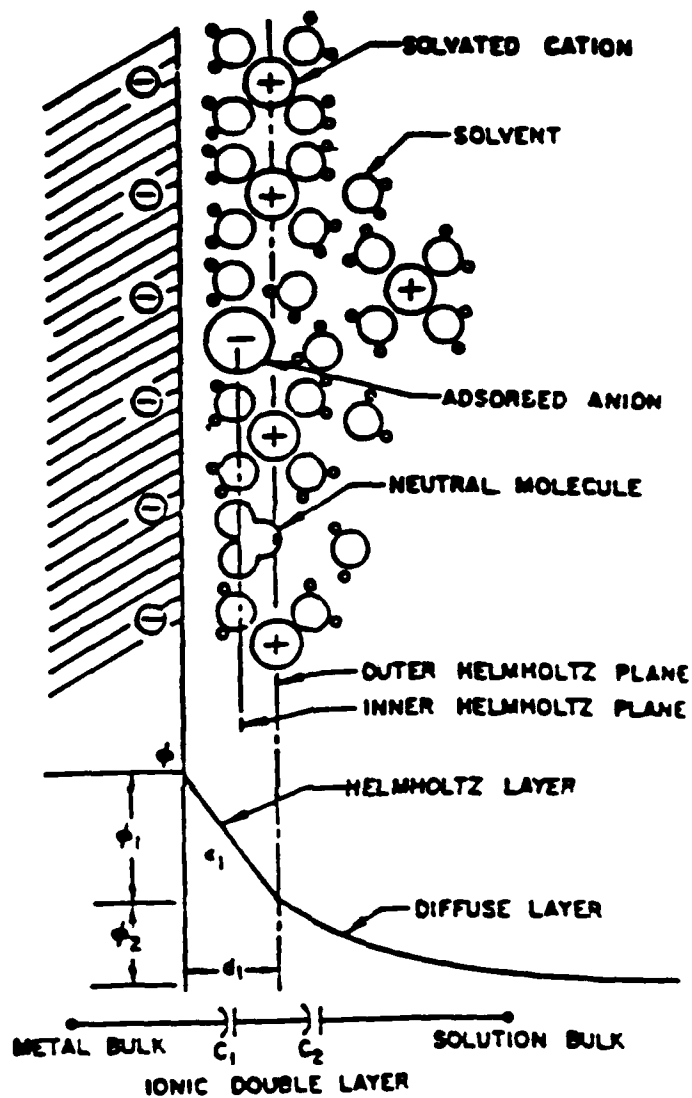


Figure 2-6. Helmholtz Double Layer at Electrode Surface (25:242)

potential is:

$$i = i_0 [\exp(\alpha qn/kT) - \exp([\alpha-1]qn/kT)] \quad (25:242) \quad (2-2)$$

where  $kT/q = 0.026$  volts at room temperature ( $T = 300$  degrees Kelvin),  $\alpha$  is a symmetry factor between zero and one, and  $i_0$  is the exchange current. For  $n < 20$  millivolts, electrode current increases linearly with respect to the polarization potential. For  $n > 50$  millivolts, however, a nonlinear expression for the polarization potential was empirically determined (25:242):

$$n = [2.3kT/(\alpha q)] (\log i - \log i_0) \quad (25:242). \quad (2-3)$$

In Figure 2-7, the dc electrode polarization potential ( $n$ ) vs. current density curves are plotted for several metals in buffered saline (6.75 gm NaCl and 2.25 gm  $\text{NaHCO}_3$  in one liter of distilled water). The low exchange current densities of the metals correspond to resistivities of  $1.4 \times 10^{-2}$  ohm- $\mu\text{m}$  for Ag to  $2.4 \times 10^{-2}$  ohm- $\mu\text{m}$  for Au (26:196). For a  $1.3 \mu\text{m}$  thick square electrode that measures 180 micrometers on each side, the total resistance ranges from  $5.6 \times 10^{-7}$  ohms for Ag to  $9.6 \times 10^{-7}$  ohms for Au. Onaral, et.al., have developed a model of the polarization phenomenon that incorporates a linear part and a nonlinear part (27:95).

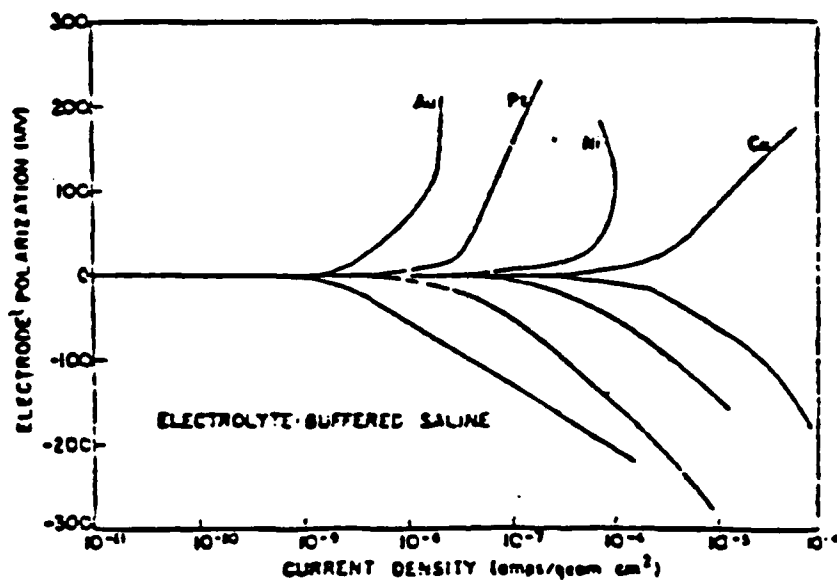
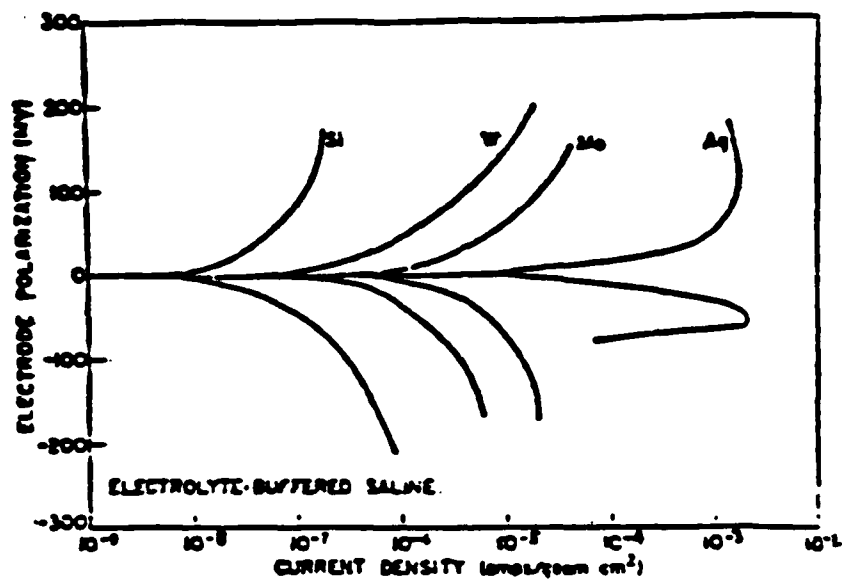


Figure 2-7. Electrical Polarization of Selected Metal Electrodes (21:214)

Although the model accurately represents polarization over a wide range of frequencies, its solution is best calculated with a computer because of the complex Discrete Fourier Transforms (DFT) employed.

Electroplating to reduce the impedance of an electrode can be traced to Kohlrausch in 1897 (13:41). Kohlrausch platinized test electrodes to reduce their impedance. The Kohlrausch technique introduced the common procedure of electrodepositing platinum black. By platinizing in a controlled process of specific duration, Kohlrausch effectively matched the 1 KHz electrode impedance with that of the electrolyte used. This technique was of great importance, particularly before amplifiers were developed.

The ac impedance of the electrode/electrolyte interface results from highly localized space charges in the Helmholtz double layer. When the thickness of the Helmholtz double layer, approximately 2 - 4 Å, is considered, the effects of irregularities at the electrode surface become significant. Microscopic surface roughness of the metal electrode can influence electrode impedance, and a chemical reaction called platinizing, or chloriding, can lower this impedance without appreciably changing the size of the electrode (25:242).

An approximate estimate of the Helmholtz double layer capacitance can be obtained from the frequency independent

expression (28:121-122)

$$C = \epsilon A/h \quad (2-4)$$

where A is the surface area of the electrode,  $\epsilon$  is the effective dielectric constant of the Helmholtz double layer, and h is the thickness of the Helmholtz double layer. The Helmholtz double layer capacitance approximates the total impedance of the electrode/electrolyte interface. Electrode impedance decreases with an increase in the frequency because of the capacitive effect of the Helmholtz double layer. Figure 2-8 shows how the impedance of metal electrodes varies with frequency. The capacitance of the Helmholtz double layer typically dominates the ac impedance of the metal/electrolyte interface (25:242-243). In Figure 2-9, differences in the impedances of the electrodes primarily reflect varying degrees of surface roughness (21:214).

Geddes outlined a method of observing the effects of the electrode/electrolyte capacitance (13:44). Using the circuit shown in Figure 2-10, Geddes created a large potential difference in the subject dog. A high input impedance amplifier produced the undistorted waveform labelled "control." By lowering variable resistance R, Geddes produced the distorted waveforms labelled "100K" and "30K". Lowering the resistance caused an increase of the current density, and

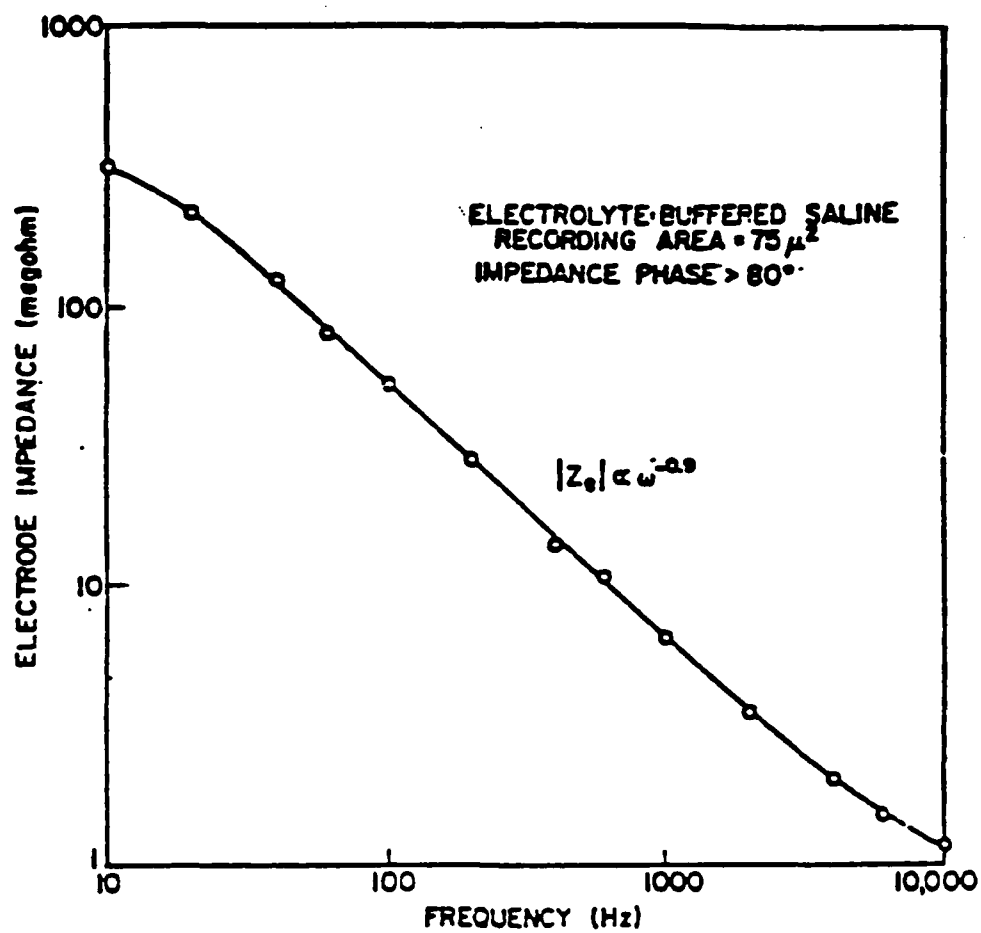


Figure 2-8. Frequency Response of a Gold Electrode  
(15:243)

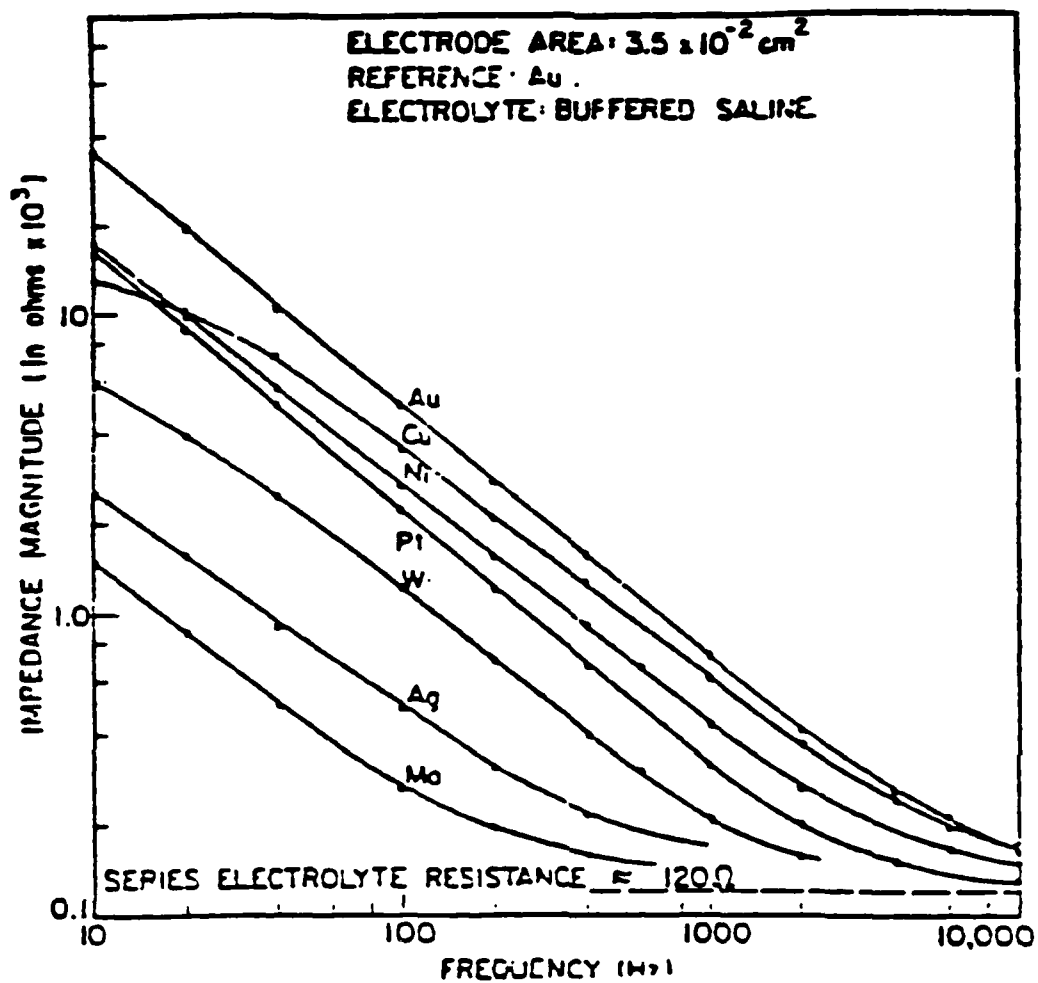


Figure 2-9. Comparison of Frequency Responses of Selected Metal Electrodes (21:214)

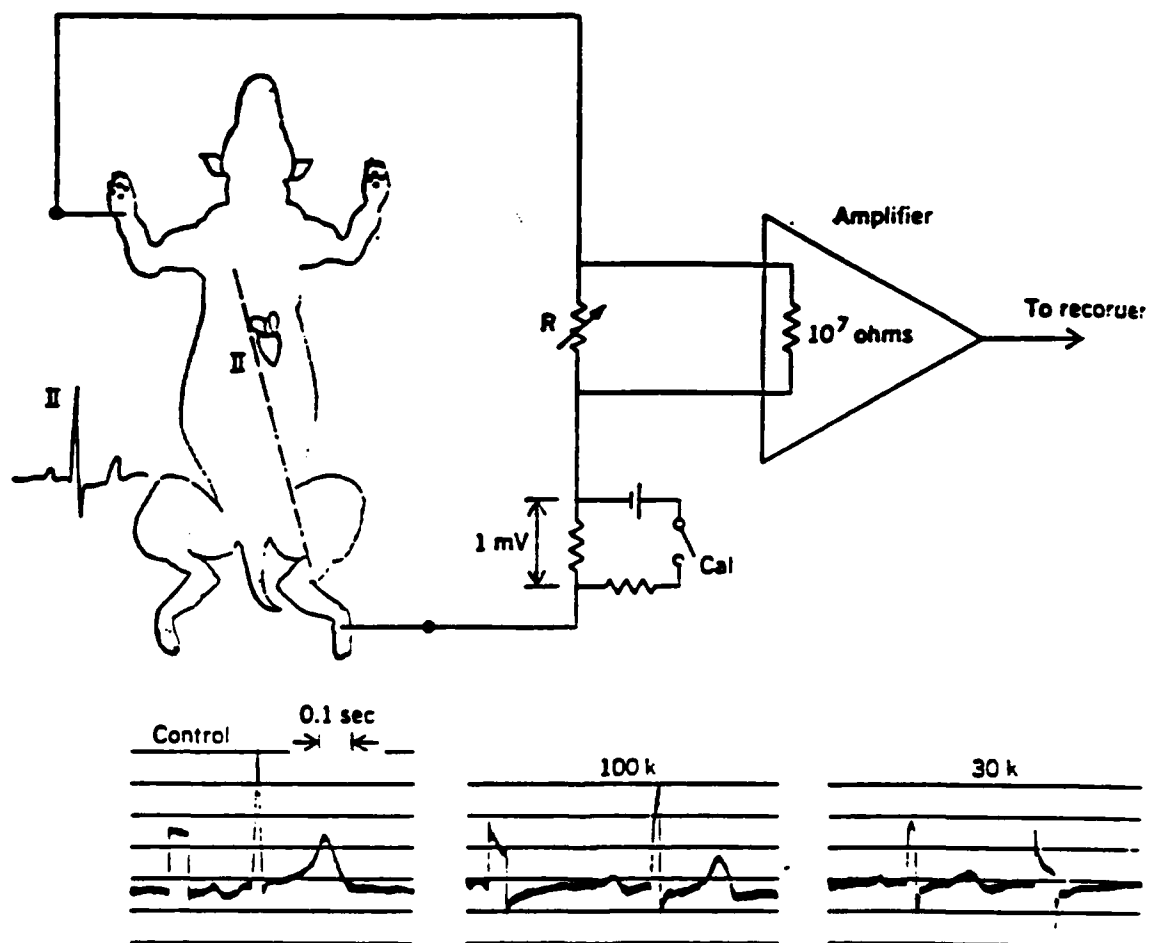


Figure 2-10. Distortion of the EEG of a Dog Caused by Resistive Loading Effects (13:44)



two forms of distortion occurred. The amplitude of the bioelectric response decreased while the capacitive decay of the square pulse appeared. This procedure demonstrates the potential distortion that can be caused by the capacitance of the Helmholtz double layer.

#### An Electrode/Electrolyte Model

The electrical behavior of the electrode/electrolyte interface can be modeled with a series circuit composed of two resistors and a capacitor (13:43). Warburg pioneered the area of modeling the electrode/electrolyte interface and published his results in 1899 (13:47). Warburg demonstrated that at a single frequency, capacitive reactance approximately equals the resistance of the Helmholtz double layer. Also, resistance and reactance vary inversely with the square root of the frequency. Algebraically, this empirical relationship can be represented as

$$x = R\omega f^{-0.5}, \quad (2-5)$$

where  $x$  is the reactance of the Helmholtz double layer,  $R$  is the resistance of the Helmholtz double layer, and  $\omega$  is a constant of proportionality. This relationship holds for a limited range of frequencies above 10Hz (13:42).

In 1932, Fricke pointed out the limitations to Warburg's

model (13:47). Although Fricke agreed that reactive and resistive components of the Helmholtz double layer impedance are approximately equal, he pointed out the subtle fact that resistance and reactance do not always vary as  $f^{-0.5}$ . In many cases, the magnitude of the exponent is actually less than 0.5. Fricke restated the Warburg equation as

$$x = R\alpha f^{-a} \quad (2-6)$$

where 'a' is less than or equal to 0.5 (13:42).

Other modifications to the theory have also been made in the electrode/electrolyte model. For instance, Varley found that the equivalent series capacitance increases as the current density increases (13:43). Varley calculated the true electrode capacitance by making measurements with decreasing current density and extrapolating the data to the zero-current threshold. He designated this quantity "initial capacity." Since the capacitance increases, the reactance decreases. Figure 2-11 shows how the reactance decreases, not only with increasing current density, but also with increasing frequency. The decrease of the reactance of Figure 2-11 results from the inherent frequency dependence of the Helmholtz double layer capacitance.

An initial representation of the electrode/electrolyte model might look like the schematic presented in Figure

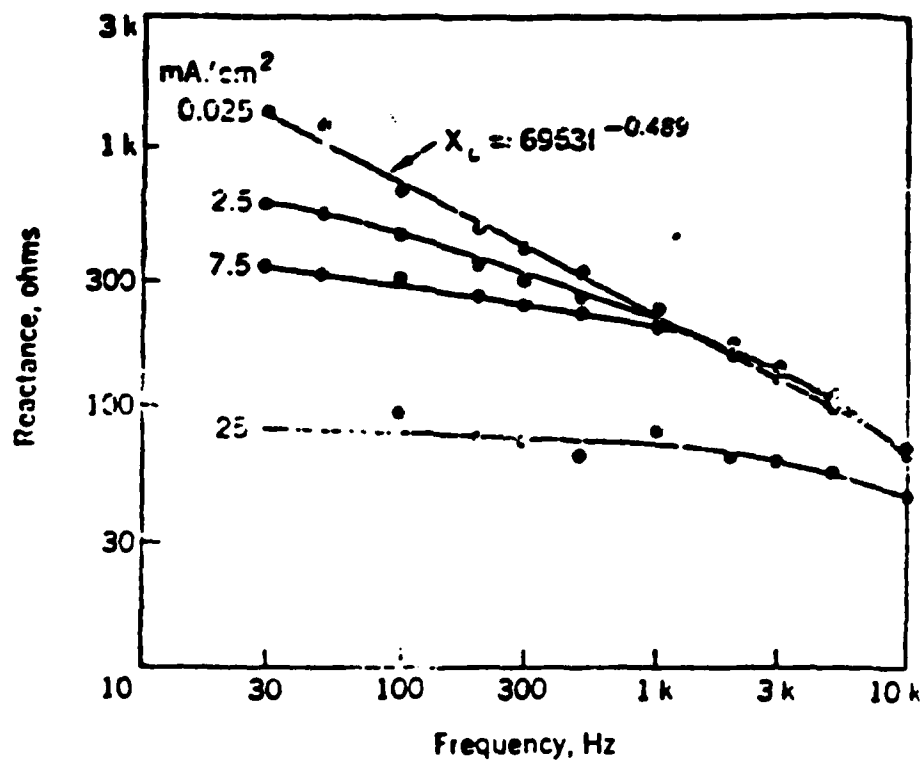


Figure 2-11. Reactance of Stainless Steel Electrodes in Saline as a Function of Current Density and Frequency (13:42)

2-12a. In the model,  $E$  is the half-cell potential of the electrode immersed in an electrolyte, and  $R(f)$  and  $C(f)$  constitute the Helmholtz double layer impedance. The situation in Figure 2-12a, whereby a direct current (dc) is blocked by the "infinite" resistance of the capacitor presents a problem. In Figure 2-12b, a finite resistance,  $R_f$ , in parallel with the resistor and capacitor facilitates the passage of current during dc operation.  $R_f$  is called the "faradaic admittance" (13:43). The  $R_f$  parameter accounts for electrolytic processes that the simpler model failed to adequately describe (13:43). Further research into the nature of  $R_f$  and its effect on the behavior of the electrode/electrolyte model would significantly enhance the current understanding of bioelectrode processes.

Robinson provides an approximation of the Warburg model that features frequency-independent parameters in place of the more complex frequency-dependent parameters developed by Warburg (12:1066). Figure 2-13 portrays the Robinson model. In Figure 2-13,  $C_s$  is the coupling capacitance of the electrode to the input of the amplifier. The  $C_s$  parameter includes the capacitance of all of the shielded connectors and wires connecting the electrode to the outside world. Robinson provides an empirical approximation that describes  $C_s$ :

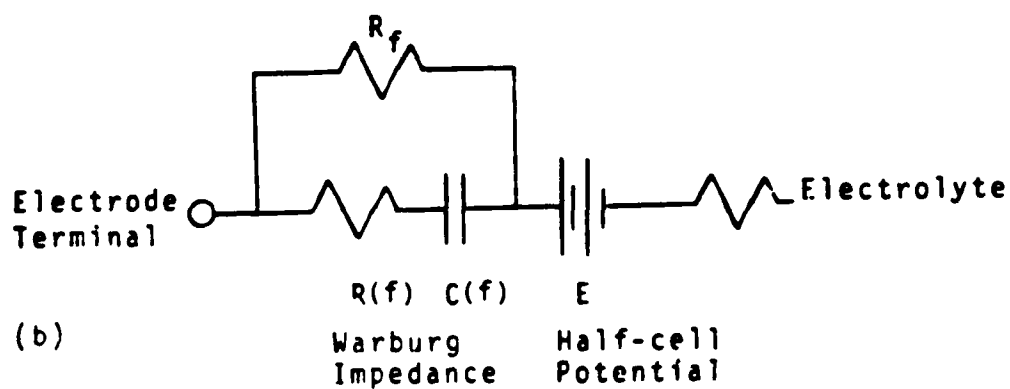
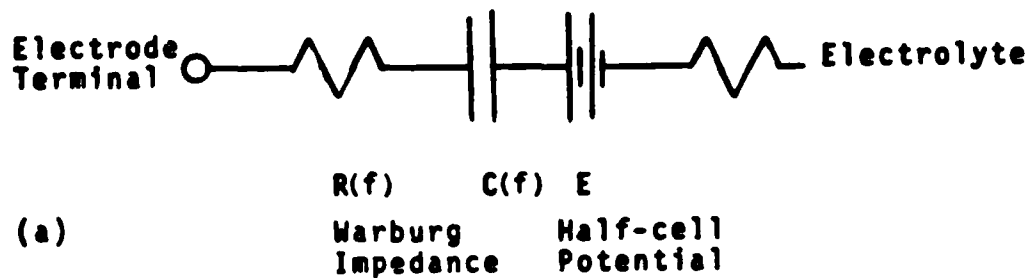


Figure 2-12. Equivalent Circuit Electrical Models  
 (a) simple Warburg model (b) modified simple Warburg model (13:243)

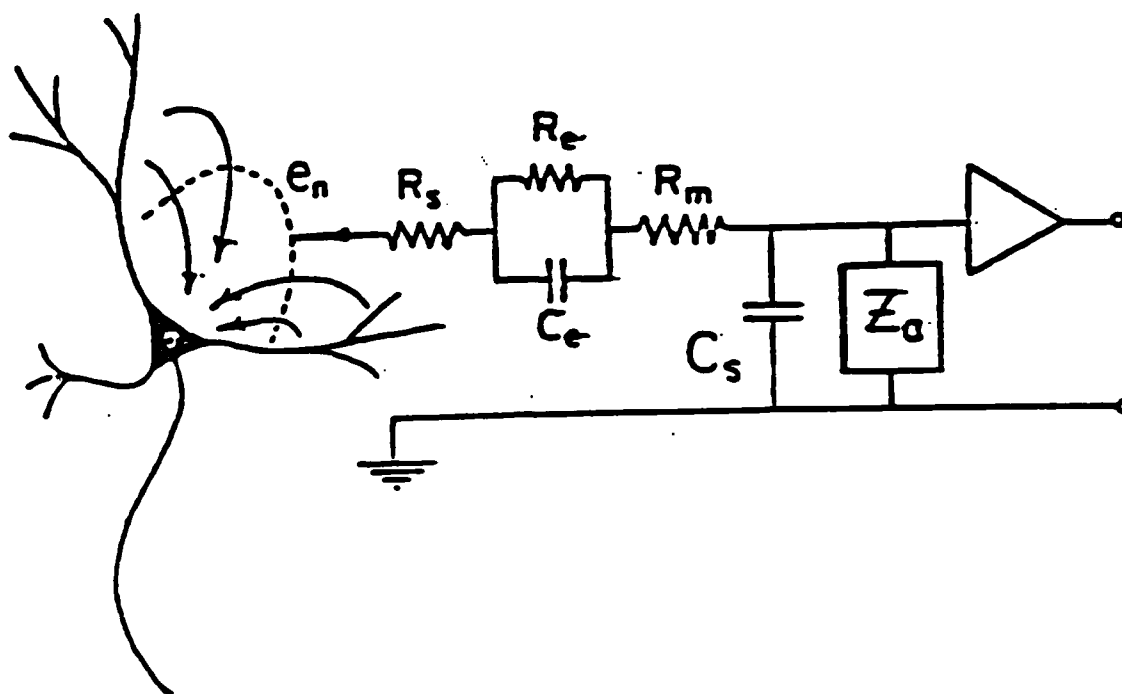


Figure 2-13. The Robinson Equivalent Circuit Electrical Model (12:1066)

$$C_s = 0.245\epsilon_r / [\log (D/d)], \quad (2-7)$$

where  $\epsilon_r$  is the relative dielectric constant,  $d$  is the electrode diameter, and  $D$  is the diameter of the electrolyte bath surrounding the immersed bioelectrode (12:1066). The  $R_m$  parameter of Figure 2-13 is the electrode resistance given by

$$R_m = 4PL/(\pi d^2), \quad (2-8)$$

where  $L$  is the length of that portion of the electrode with diameter  $d$ , and  $P$  is the resistivity of the metal. The length parameter of Equation (2-8),  $L$ , is the actual thickness of the electrode of a specified diameter ( $d$ ). In the case of a perfectly flat electrode,  $R_m = L = 0$ . Hence, reducing  $L$  effectively reduces the electrode resistance in a linear fashion. The value of resistivity  $P$  depends on the particular metal used to form the electrode. In Figure 2-13,  $C_e$  is the capacitance of the Helmholtz double layer and  $R_e$  is the purely resistive component of the Helmholtz double layer impedance. Also,  $R_s$  is the spreading resistance of the electrolyte between the Helmholtz double layer and infinity. Robinson obtained an expression for  $R_s$ :

$$R_s = P/(2\pi d), \quad (2-9)$$

where  $d$  is once again the electrode diameter (12:1070). In Figure 2-13,  $e_n$  is the recorded bioelectric potential. The

only remaining unidentified quantity in Figure 2-13,  $Z_a$ , is the input impedance of the amplifier. An amplifier input impedance several orders of magnitude greater than the electrode impedance will enhance the low-distortion recording capability of the system.

### Conclusion

The long-term objective of AFIT brain chip research is to provide a mechanism for collecting and analyzing VER data. If the data collected do not accurately reflect evoked response (minimal distortion), then the utility of the data for studying the mechanism of VER will suffer considerably. Characterization of the array bioelectrodes and the electrode/electrolyte interface precedes the ultimate goal of optimizing an implantable multielectrode array for collection of VER data. Both the characteristics of the electrode/electrolyte interface and the electrode itself affect the quality of recording a bioelectric event. The choice of a particular electrode depends upon competing criteria of different applications. If a biocompatible electrode suitable for longer term implantation is needed, then gold may satisfy the requirements better than any other choice. If the quality of the recorded data is the major concern, then silver-silver chloride might work best,



provided that a long-term implant was acceptable. For requirements between these extremes, other types of metal electrodes can be used successfully. Because of the prevalent use of aluminum contacts by integrated circuit manufacturers, only the characteristics of aluminum electrodes immersed in a saline will be investigated.

### 3. DEVELOPMENT AND IMPLEMENTATION OF A MEASUREMENT SCHEME

#### Introduction

The development of a suitable means of measuring the parameters of an electrical circuit model of the electrode/electrolyte interface is critical to the validation of the model. In this research, the model hypothesized to describe the electrode/electrolyte interface was derived from the model proposed by Robinson (12) and discussed in Chapter 2. Several simplifying assumptions were made in order to derive the equivalent electrical circuit model from the configuration proposed by Robinson. First, the shielded coaxial cable lengths were minimized and the connectors used in the test circuit are considered nonobtrusive, and the capacitance parameter of Figure 2-13,  $C_s$ , will therefore be neglected. Second, the bioelectric potential parameter of Figure 2-13,  $e_n$ , will be modelled as a square input pulse whose amplitude is one millivolt and whose period is 40 milliseconds. The capacitance and resistance parameters of this model can be supplied as inputs to the nonlinear least squares computer program for analysis and curve fitting.

The development of a technique for determining the individual components of the proposed electrode/electrolyte model proceeded through several stages of development.

Familiarization with various types of measurement apparatus characterized the first step towards the development of a measurement scheme. The application of analytical data reduction techniques to the measurement scheme followed the familiarization with the measurement apparatus. Next, a method of measuring the circuit parameters using a voltage-divider configuration was developed. The voltage-divider measurement scheme utilizes an input signal as a reference standard, so an attempt was made to collect measurements at input signal amplitudes comparable to those of the brain. The final stage of development culminated in a measurement scheme that encompassed both the measurement apparatus and a method of processing the experimental data. In this scheme, an ac impedance bridge was used to measure the experimental parameters, and data were supplied to the nonlinear least squares computer program for automated curve fitting and determination of the unknown parameters of the model.

Initial assumptions were made that impacted the techniques and analysis that evolved from the development of the measurement scheme. The actual distributed parameters of the electrode/electrolyte model were represented as discrete lumped elements in the model after the precedent set by Robinson in Figure 2-13. These lumped elements were then

treated as frequency-independent components in the corresponding analysis of the electrical circuit parameters.

The assumption of frequency independent parameters of the model is surely a simplification of the complex processes that naturally occur at an electrode-solute interface.

However, the assumption may be justified in light of the empirical data compiled by several researchers

(12:1066-1070). Intuitively, the choice of parameters in the Robinson model appears to reflect the physical arrangement of variables that interact at an electrode/electrolyte interface, and the assumption of frequency independence has indeed been integrated into the model. Aside from the judgment of whether the assumption of frequency independence should or should not have been made, the validity of representing the model as a unified entity will be investigated experimentally rather than by examining the appropriateness of Robinson's assumptions. The assumption of the frequency independence of the model's parameters has been incorporated into the nonlinear least squares computations that were used to fit experimental data to a characteristic curve.

In order to determine the maximum rate at which the electrodes of the array can be scanned, the transient response of the electrical circuit model to a square wave

input pulse was investigated. The square wave pulse was modelled to simulate the VER of the brain when a pulsed light source is used to stimulate activity (1:88). Depending upon the values of the parameters of the equivalent electrical circuit model, the introduction of transient charging and discharging effects that result from the capacitance of the Helmholtz double layer will limit the rate at which the electrodes can be scanned. The determination of the maximum rate at which the electrode array can be scanned is a prerequisite to the optimal operation of the brain chip.

An additional consideration was generated by the chemical reaction that occurs when aluminum comes into contact with sodium and chlorine ions. Unfortunately, sodium ions are very reactive and are commonly found in the cerebrospinal fluids of mammals (as well as in other bodily tissues and fluids). The reaction between sodium ions and aluminum results in a very rapid deterioration of the aluminum, and a VLSI circuit can be rendered inoperative within seconds (3:1-2). The use of polyimide as the encapsulant for the purpose of testing resulted from characteristics that satisfy criteria such as resistance to sodium penetration, compatibility with biological processes, predictability and controllability during application, resistance to liquid interactions, and the ability to be

etched and patterned (6:20). Polyimide was used as the encapsulant for the brain chips that were tested, and the process that was developed to apply it to both chips and practice wafers is provided in Appendix C.

### Choosing a Model

The equivalent electrical circuit used to model the electrode/electrolyte interface was derived from the Robinson model presented in Chapter 2. Since only the parameters relating to the interface itself are included in the equivalent electrical circuit model, an initial representation, adapted directly from Robinson's proposed configuration (12:1066), might look like the model presented in Figure 3-1. In the model of Figure 3-1,  $E_g$  is the postulated bioelectric source of brain activity,  $R_m$  is the resistance of the metallic electrode,  $C_g$  is the capacitance of the electric double layer at the interface between the electrode and the saline electrolyte,  $R_g$  is the leakage resistance of the charge carriers crossing the electric double layer, and  $R_s$  is the spreading resistance of the saline electrolyte between the electrode/electrolyte interface and the common or ground electrode.

The transformation of the equivalent electrical circuit model of Figure 3-1 into the configuration presented in

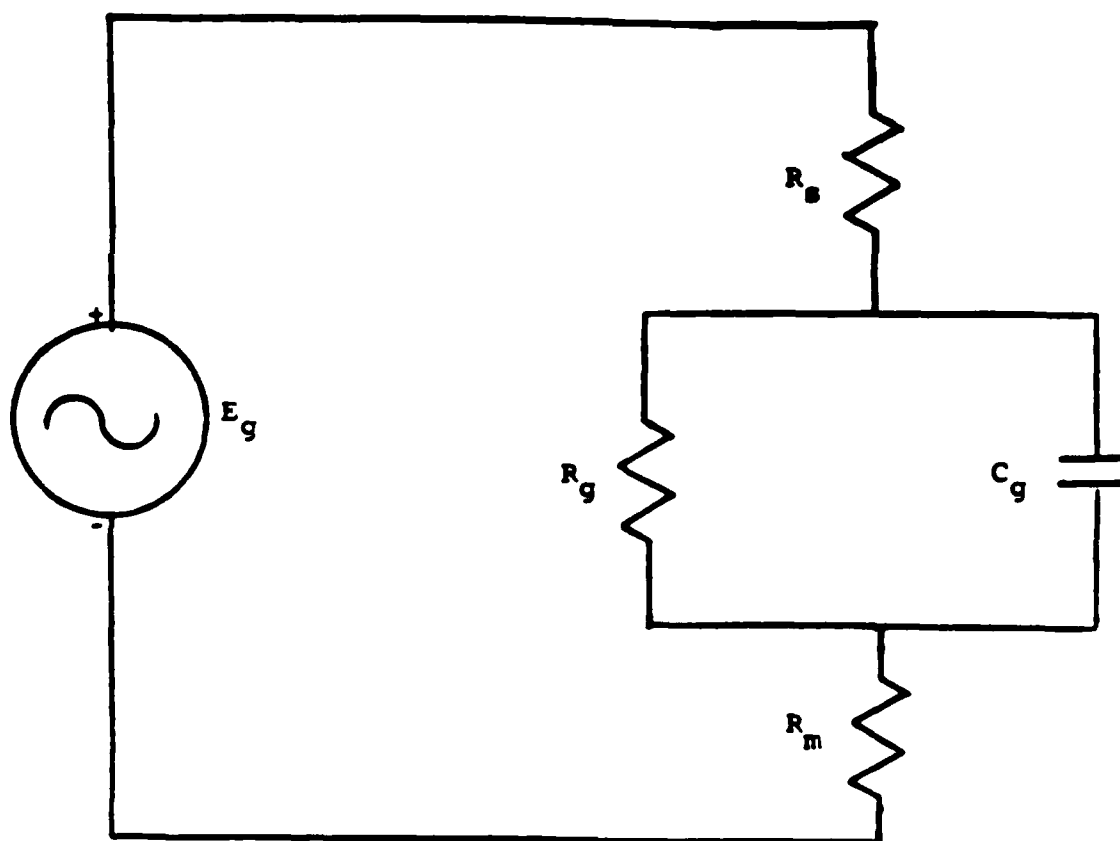


Figure 3-1. Initial Model of the Electrode-Solute Interface

Figure 3-2 can be mathematically accomplished by setting

$$R_c = R_m + R_s \quad (3-1)$$

By performing this simple transformation, a reduction of the number of inputs to the nonlinear least squares computer program was achieved, and the resultant configuration is essentially equivalent to the original circuit. The nonlinear least squares computer program will accept values of the equivalent electrical circuit model that are represented by a resistor in series with the parallel combination of a resistor and capacitor. This equivalent circuit configuration can be used to model a variety of more complicated circuits composed of lumped resistances and capacitances. Indeed, many complicated configurations of lumped resistances and capacitances can be reduced to the essentially equivalent electrical circuit model shown in Figure 3-2.

Using equations (12:1066-1070, 15:87-89) for the lumped parameters of the equivalent electrical circuit model in conjunction with the physical specifications of the brain chip, approximations of the circuit parameters were calculated. The calculated value of  $R_m$  in Figure 3-1 of  $6.42 \times 10^{-5}$  ohms was deemed insignificant in its impact upon the model, so the calculated value of  $R_s$  in Figure 3-1 of 1007



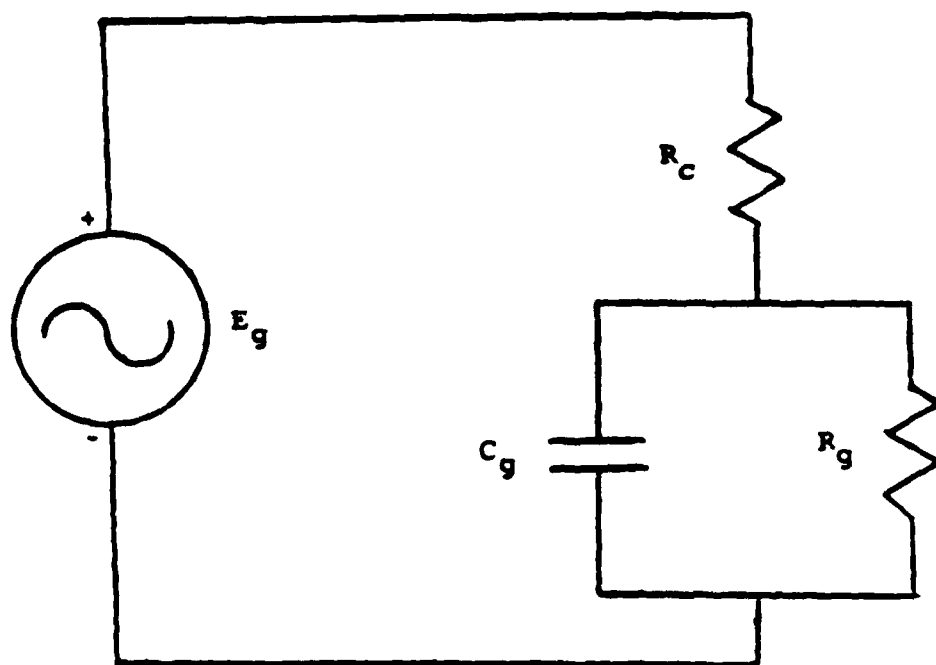


Figure 3-2. Revised Model of the Electrode-Solute Interface

ohms was used as the estimate of  $R_c$  of Figure 3-2. The calculated values of  $R_g$  and  $C_g$  of Figure 3-2 are  $4.10 \times 10^7$  ohms and  $6.48 \times 10^{-9}$  farads, respectively. The calculation of the lumped parameters of the equivalent electrical circuit model is presented in Appendix D. In the calculations of Appendix D, the resistivity of aluminum ( $10^{-5}$  ohm-cm) (12:1078), the resistivity of the saline (72.5 ohm-cm) (12:1078), the measured thickness of the aluminum in the electrode (1.3 micrometers), the length of a side of the square electrodes (180 micrometers), the relative dielectric constant (unity), and the leakage resistivity of charge carriers crossing the Helmholtz double layer ( $1.33 \times 10^4$  ohm-cm) (12:1079) were used to calculate values of the lumped parameters of the equivalent electrical circuit model.

The cerebrospinal fluid of the brain was simulated with a 0.9% saline solution. The percentage of sodium chloride by weight was obtained by mixing 0.9 grams of sodium chloride with 99.1 grams of deionized water (DIW). The simulation of the multielectrode array in contact with actual brain tissue was accomplished by flooding the bonding cavity of the 64-pin package with the 0.9% saline solution, thereby immersing the brain chip. The brain chip was encapsulated, so the saline contacted only the exposed electrodes.

## Nonlinear Least Squares Analysis

The method of nonlinear least squares can be used to calculate an unknown impedance from a collection of experimental data. The nonlinear least squares method employs the Levenburg-Marquardt algorithm to perform a computer-aided numerical analysis that minimizes the errors that naturally occur in experimental data compilation (18:282-283). Appendix E provides a discussion of the Levenburg-Marquardt algorithm used by the nonlinear least squares computer program.

In order to facilitate the analysis performed by the nonlinear least squares computer program (18:461-512), data were provided in the form of  $R_p(f)$  vs.  $f$ , where  $R_p(f)$  is the frequency-dependent effective parallel resistance of the electrode-solute interface, and  $f$  is the frequency. Figure 3-3b provides the frequency-dependent representation of the frequency-independent electrode/electrolyte model of Figure 3-3a. The impedance analyzer used to obtain the measurements, the HP4192A, was configured to provide the frequency-dependent parallel resistance parameter,  $R_p(f)$ , of Figure 3-3. The calculation routine of the nonlinear least squares computer program uses estimates of the frequency-independent model's parameters and measured values of the frequency-dependent parallel resistance,  $R_p(f)$ , to fit

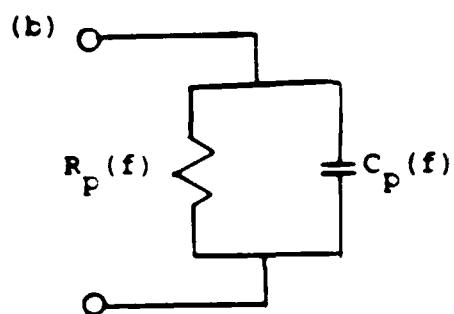
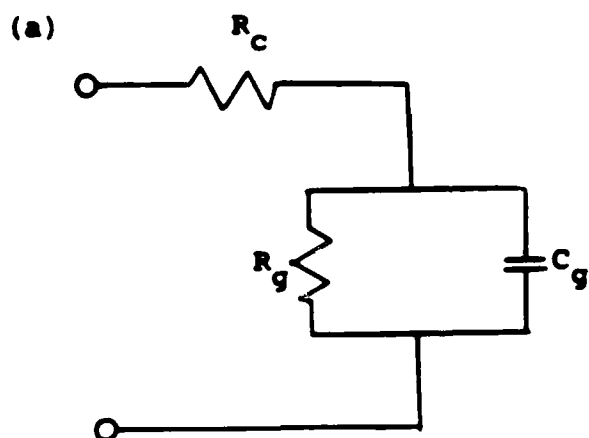


Figure 3-3. Two Configurations of the Electrode-Solute Model  
 (a) frequency-independent configuration  
 (b) frequency-dependent configuration

a curve to the data. The routine then provides values of the frequency-independent model parameters ( $R_c$ ,  $R_g$ , and  $C_g$ ). Figure 3-1 portrays the proposed (3:43, 4:250, 12:1066) equivalent electrical circuit model of the electrode-solute interface, and Figure 3-2 shows the reduced model composed of circuit elements identical to those that were supplied as estimates to the nonlinear least squares computer program.

An inspection of the model of Figure 3-2 reveals several qualitative characteristics of its frequency response behavior:

1. The dc value of the measured resistance,  $R_p(f)$ , is given by  $R_p(f) = (R_c + R_g)$ . In this case, the capacitor,  $C_g$ , acts like an open circuit.
2. The high frequency limit ( $f \rightarrow \infty$ ) of  $R_p(f)$  is given by  $R_p = R_c$ . In this case,  $C_g$  acts like a short circuit.
3. For values of the frequency  $0 < f < \infty$ ,  $R_c < R_p(f) < R_c + R_g$ . The exact value of  $R_p(f)$  is dependent upon the value of  $C_g$  as well as upon the frequency  $f$ .

In order to isolate the parameters of the equivalent electrical circuit model, an expression for  $R_p(f)$  in terms of  $R_c$ ,  $R_g$ ,  $C_g$ , and  $f$  must first be derived. The admittance,  $Y_p(f)$ , of the frequency-dependent parallel combination of  $R_p(f)$  and  $C_p(f)$  is

$$Y_p(f) = 1/Z_p(f) = R_p^{-1}(f) + j\omega C_p(f), \quad (3-2)$$

where  $\omega = 2\pi f$ ,  $j \triangleq (-1)^{0.5}$ , and  $Z_p(f)$  is the impedance of the parallel combination of  $R_p(f)$  and  $C_p(f)$ . The impedance presented by the frequency-independent parameters of the equivalent electrical circuit model,  $R_c$ ,  $R_g$ , and  $C_g$ , is given by

$$Z_q = R_c + [R_g * (j * \omega * C_g)^{-1}] / [R_g + (j * \omega * C_g)^{-1}]. \quad (3-3)$$

After simplifying,

$$Z_q = [(R_c + R_g) + j * \omega * R_c * R_g * C_g] / [1 + j * \omega * R_g * C_g]. \quad (3-4)$$

The admittance,  $Y_q$ , is found by taking the reciprocal of the expression for  $Z_q$  ( $Y_q = 1/Z_q$ ):

$$Y_q = [1 + j * \omega * R_g * C_g] / [(R_c + R_g) + j * \omega * R_c * R_g * C_g]. \quad (3-5)$$

Next,  $Y_q$  is multiplied by a factor equal to unity for mathematical convenience, and this multiplying factor is specified by forming the fractional quantity of the conjugate expression for the denominator of  $Y_q$ . Hence,

$$Y_q = \{ [1 + j * \omega * R_g * C_g] / [R_c + R_g + j * \omega * R_c * R_g * C_g] \} * \{ [R_c + R_g - j * \omega * R_c * R_g * C_g] / [R_c + R_g - j * \omega * R_c * R_g * C_g] \}. \quad (3-6)$$

This yields the expression:

$$Y_q = [(R_c + R_g) + w^2 * R_c * R_g^2 * C_g^2 + j * w * R_g^2 * C_g] / [(R_c + R_g)^2 + (w * R_c * R_g * C_g)^2]. \quad (3-7)$$

Since  $Y_p$  and  $Y_q$  are equivalent to one another ( $Y_p = Y_q$ ), and  $Y$  is a complex quantity, it follows that:

$$\text{REAL}(Y_p) = \text{REAL}(Y_q) \quad (3-8)$$

and

$$\text{IMAG}(Y_p) = \text{IMAG}(Y_q). \quad (3-9)$$

Finally, the desired relation between  $R_p(f)$  and  $R_c$ ,  $R_g$ , and  $C_g$  is found by equating the real components. This requires that:

$$1/R_p(f) = [(R_c + R_g) + R_c * (w * R_g * C_g)^2] / [(R_c + R_g)^2 + (w * R_c * R_g * C_g)^2]. \quad (3-10)$$

After simplification,

$$R_p(f) = [(R_c + R_g)^2 + (w * R_c * R_g * C_g)^2] / [(R_c + R_g) + R_c * (w * R_g * C_g)^2]. \quad (3-11)$$

The corresponding equivalency between the qualitative and quantitative results of the frequency response behavior of  $R_p(f)$  can now be shown. Using the expression for  $R_p(f)$ ,

$$\lim_{f \rightarrow \infty} R_p(f) = (R_c + R_g) \quad (3-12)$$

which agrees with qualitative characteristic (1) on page 68, and

$$\lim_{f \rightarrow \infty} R_p(f) = R_c, \quad (3-13)$$

which agrees with qualitative characteristic (2) on page 68. The qualitative characteristic (3) on page 68 agrees with the expression of  $R_p(f)$  when  $0 < f < \infty$ .

From the dc and high frequency limits of the expression for  $R_p(f)$ , the values of  $R_c$  and  $R_g$  can be experimentally determined. However, the nonlinear least squares computer program also requires that an estimate of  $C_g$  be provided (18:486). The estimate of  $C_g$  is obtained by solving the expression of  $R_p(f)$  for  $C_g$  and substituting an empirical value of  $R_p(f)$  into the resultant expression. This value of  $C_g$  is obtained at some frequency  $0 < f < \infty$ , preferably a frequency at which the effect of  $C_g$  can be observed from the variation of  $R_p(f)$ .

With estimates of  $R_c$ ,  $R_g$ , and  $C_g$  available to the nonlinear least squares computer program, the only required inputs that remain are the measured values of  $R_p(f)$ . After all of the required data have been collected, the nonlinear least squares computer program will be used to calculate a "best fit" curve of the frequency response behavior of  $R_p(f)$ .



## The Voltage-Divider Measurement Technique

The development of the voltage-divider measurement technique resulted in a method of obtaining the magnitude of the parallel resistance, but equipment limitations prevented the collection of precise phase angle information. Results obtained using the voltage divider can therefore be used to check the magnitude of the parallel resistance, but the phase angle information cannot be collected unless a vector voltmeter is used. Since a vector voltmeter that spanned a large frequency range could not be acquired, only magnitude information was obtained.

In the voltage-divider measurement scheme, a load resistance is added to the circuit of Figure 3-2, as shown in Figure 3-4. When the voltage across the load resistance,  $R_L$ , is half of the magnitude of the input voltage,  $E_g$ , then the value of the load resistance is equivalent to the magnitude of the parallel resistance  $R_p(f)$ .

The use of the voltage-divider measurement scheme requires that an input signal be applied across the model. By applying a signal comparable in magnitude to the VER of the brain, the actual measurement of lifelike electrical stimuli can be tested. Concern that the diminutive VER signal level of the brain might be hidden in the background noise stimulated this preparatory experimental effort.

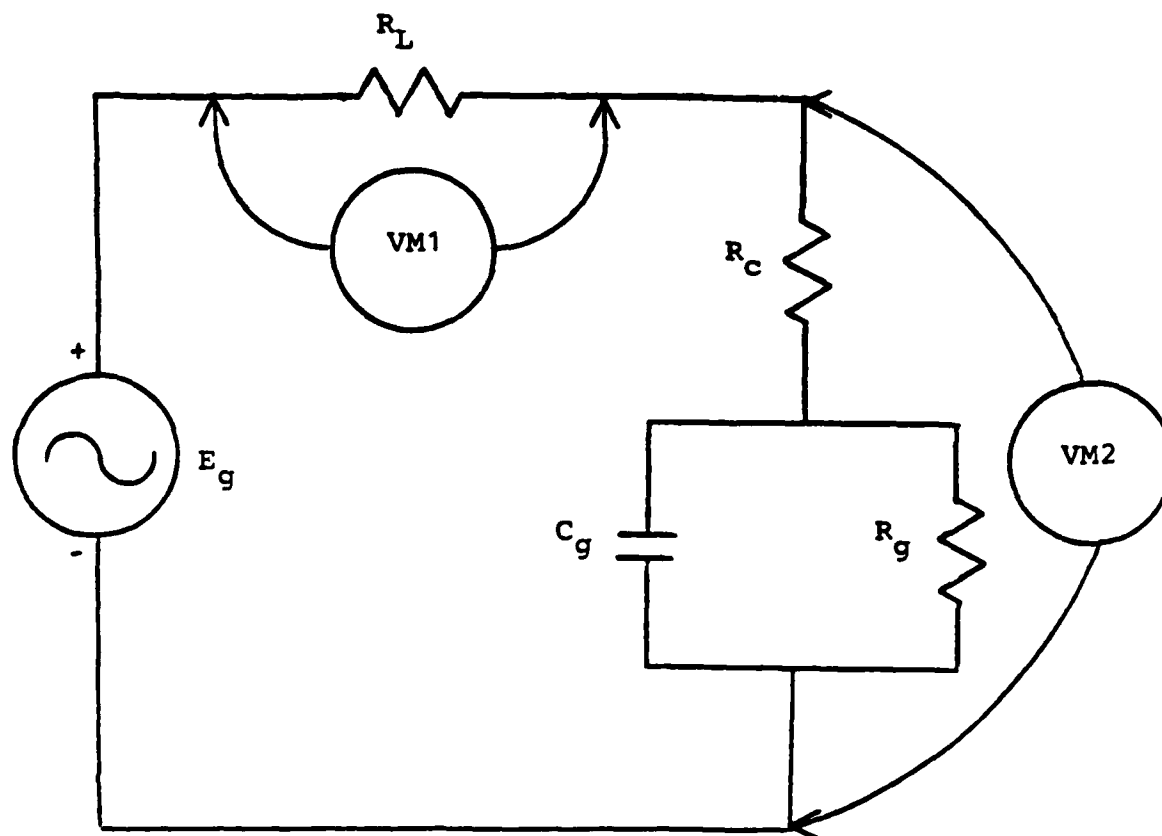


Figure 3-4. Initial Voltage-Divider Measurement Scheme

Analysis of the circuit of Figure 3-4 reveals several aspects of the operation of this circuit. First, the voltage drop across the output increases as  $R_g$  increases; this is a natural consequence of the properties of the voltage division between  $R_g$  and the output tank circuit. Second, increases in  $C_g$  cause a decrease in the observed output because of charge storage properties of the capacitor. Third, the parallel resistance decreases with corresponding increases of the frequency because of the characteristic decrease of the impedance of the capacitor.

Initial experiments were performed to measure the parallel resistance of the equivalent circuit model at very small signal amplitudes. The magnitude of the evoked responses at the cortex is less than 1000 microvolts. The measurement scheme used in these experiments is presented in Figure 3-4. At input signal levels  $E_g < 50$  millivolts, distortion of the waveform became so great that signal amplitudes became difficult to discriminate and measure in a meaningful fashion. At such small excitation levels, repeatable results could not be obtained. Obviously, data recorded in this manner are not reliable.

The problem of achieving an acceptable signal-to-noise ratio at low source amplitudes caused great concern that measurements of brain signals might be extremely difficult to

obtain. An idea that occurred was to filter out the noise. The exact origin of the noise appeared to be ambient electromagnetic 60 Hz energy as well as some indeterminate background noise. The superposition of these noise sources with the excitation signal of the generator was clearly visible on the oscilloscope trace. An examination of moderate signal levels of approximately 50 millivolts revealed a corruption of the source signal when scanned over the frequency range 0.1 Hz to 5 MHz.

Prior to investigating a filter technique, an examination of the circuit in Figure 3-4 revealed a ground loop that was introduced as a consequence of inserting VM1 and VM2 into the current path. The ground loop has been highlighted in Figure 3-5 by the dashed lines. In order to verify that this ground loop was responsible for the signal distortion, a revised scheme was conceived that eliminated the suspected ground loop of Figure 3-5. The revised scheme is shown in Figure 3-6. When the applied signal level was reduced, the output signal, though correspondingly reduced in amplitude, remained pristinely clear and undistorted. With this successful development, the next test was to attempt measurements at the microvolt signal level.

In Figure 3-6, VM1 measures the input signal from the generator and VM2 measures the voltage across the equivalent

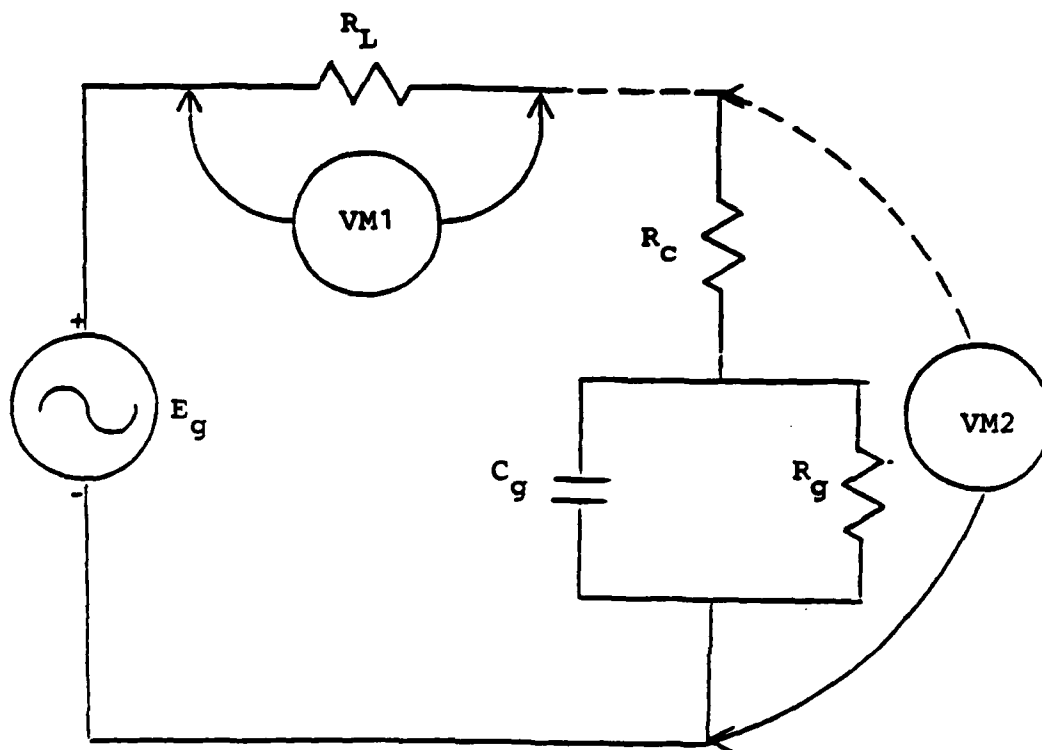


Figure 3-5. Identification of a Ground Loop (dotted lines)

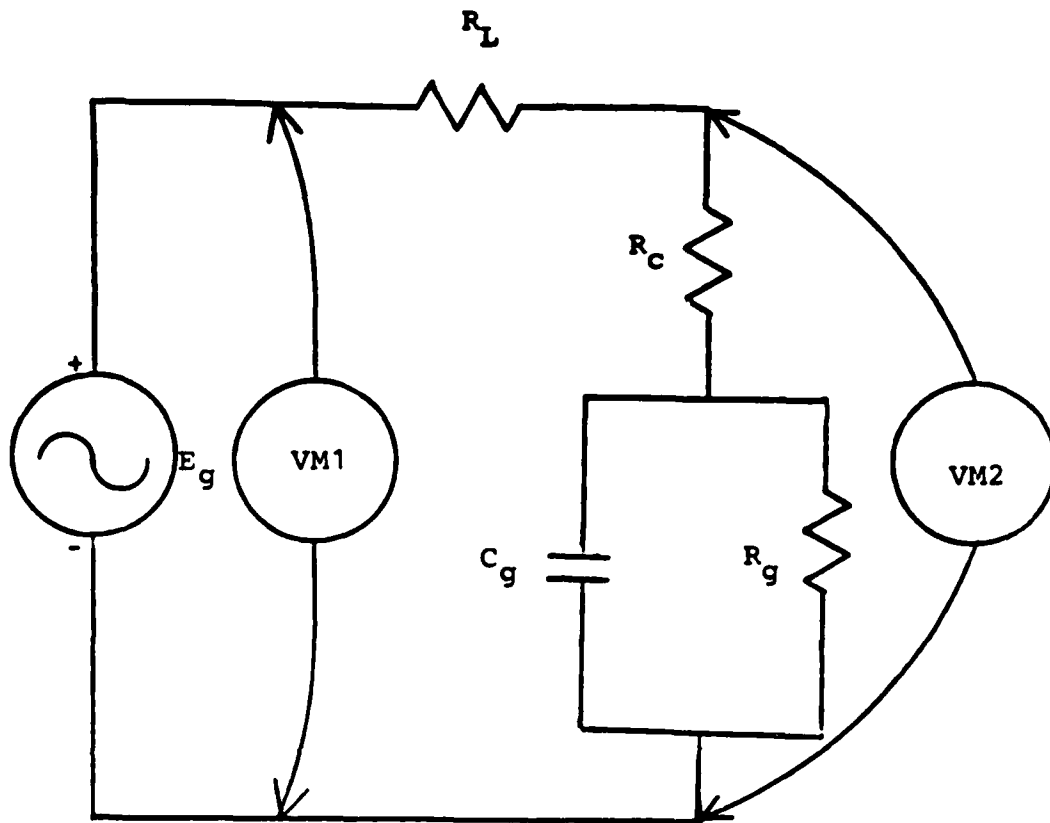


Figure 3-6. Revised Voltage-Divider Measurement Scheme

circuit composed of  $R_c$ ,  $R_g$ , and  $C_g$ . In this scheme,  $R_L$  still influences the division of the voltage, but the voltage across it is not directly measured by VM1. The value of the voltage dropped across  $R_L$  is given by the difference between VM1 and VM2. Another voltmeter could have been added to measure the voltage across  $R_L$ , but it would not contribute any new information since its measurements could be derived from VM1 and VM2.

At this point in the research, equipment limitations prevented another decrease of the excitation signal level to the microvolt range. The signal generator operates stably at the millivolt level, but microvolt levels cannot be achieved directly. This problem was partially addressed by employing an external voltage-divider. The voltage-divider was placed across the signal generator's output, as shown in Figure 3-7. By adjusting the relative magnitudes of  $R_a$  and  $R_b$ , the desired voltage division was obtained. The  $R_a:R_b$  ratio of 10,000:10 provides voltage division by a factor of 1000. Hence, the voltage developed across  $R_b$  served as the excitation to the tank circuit.

The remaining problem of equipment limitations was addressed by amplifying the output signal before it reached the oscilloscope. The instrumentation scheme of Figure 3-8 depicts how the entire configuration can be viewed as three

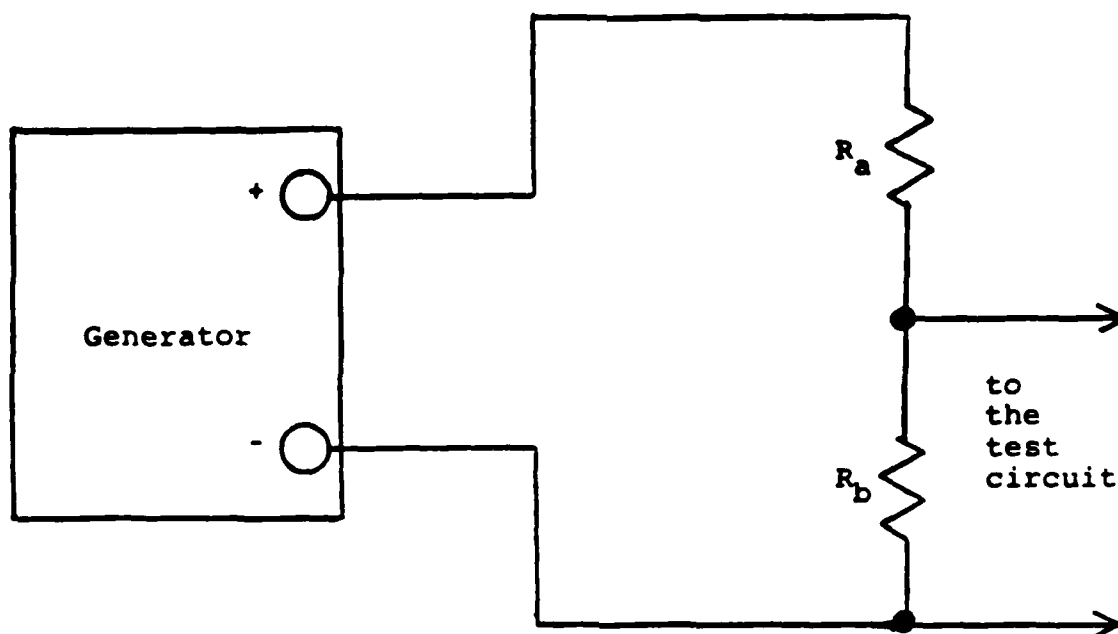


Figure 3-7. Voltage Division of the Input Signal



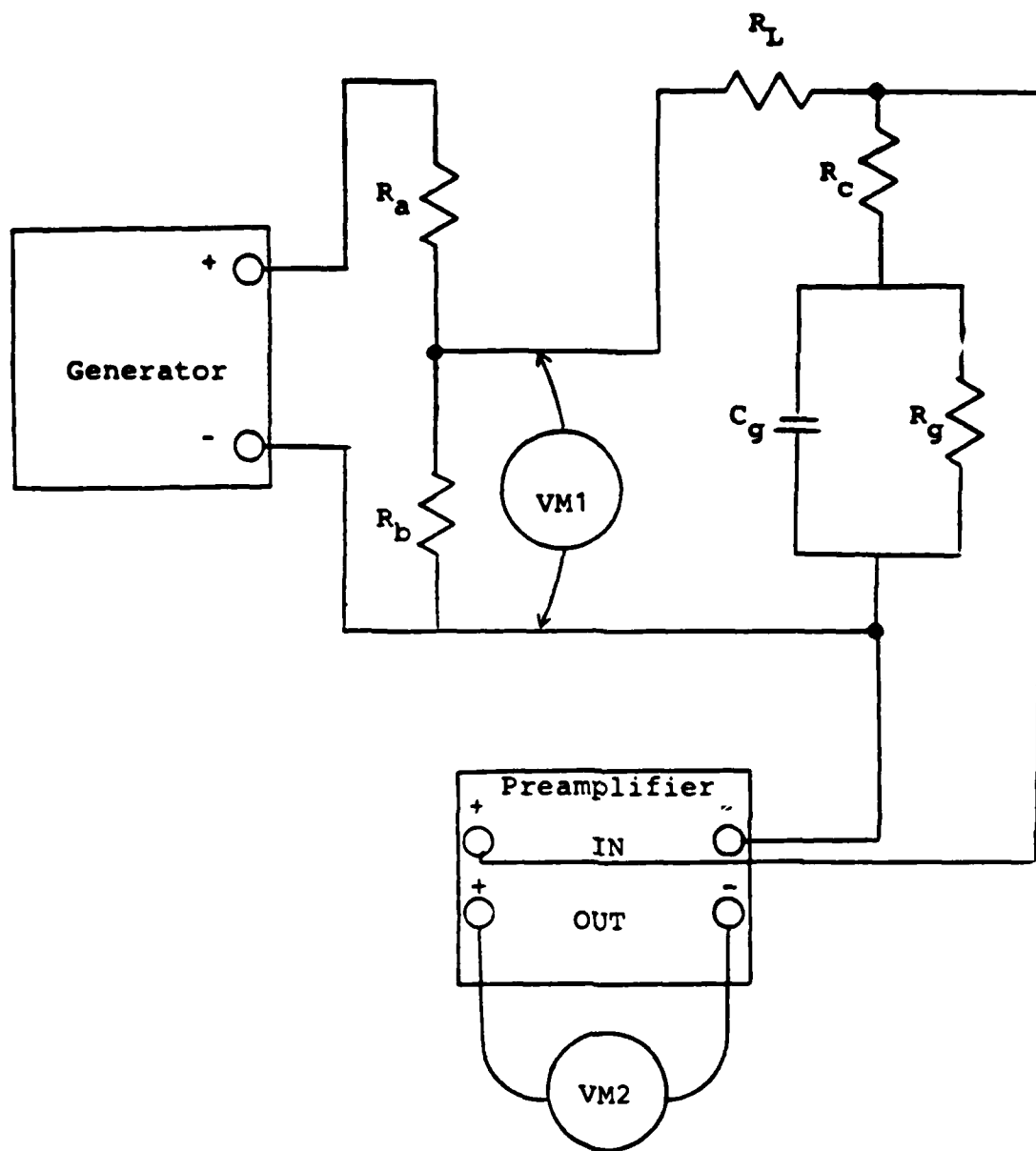


Figure 3-8. Small Input Signal Measurement Scheme

separate sections which are dependent upon the excitation signal level. Millivolts are generated, the voltage-divider ensures that microvolts are applied to the elite board, and the low-noise amplification stage (EG Parc Model 113 Preamplifier) boosts the signal to the millivolt level so that useful measurements can be discerned on the oscilloscope.

Using the circuit of Figure 3-8, additional measurements were obtained at an input signal level of 10 microvolts as measured by VML. At this signal level, noise and distortion again became more noticeable, but useful measurements could still be satisfactorily obtained.

#### The Bridge Measurement Technique

In order to address the deficiency of phase angle information that resulted from applying the voltage-divider measurement technique, an alternating current bridge method was devised. The ac bridge not only performs measurements of impedance magnitudes, but it also preserves the phase angle information of the complex impedance parameter. The HP 4192A bridge was chosen to measure the impedance parameters of the equivalent electrical circuit model.

The HP 4192A bridge performs a variety of measurement functions at the frequency, excitation signal level, and dc

bias level chosen by the operator. The frequency can be automatically or manually swept between the lower and upper limits of the operating frequency range (5 Hz to 13 MHz). The dc bias voltage is fully adjustable within the range -35 V to +35 V. The excitation signal level can be manually swept in 1 mV steps within the operating range 5 mV rms to 1.1 V rms. The HP 4192A bridge is capable of simultaneously displaying two independent, complementary impedance parameters chosen by the operator during each measurement cycle. The display of either the equivalent series or equivalent parallel impedance parameters of the device-under-test are selectable.

Using the configuration shown in Figure 3-9, a measurement of the parameters of the equivalent electrical circuit model can be obtained. In the case of the parallel component measurement arrangement, the equation for the admittance is:

$$Y = G + jB, \quad (3-14)$$

where  $G$  is the conductance and  $B$  is the susceptance of the admittance parameter. The reciprocal of the conductance yields the parallel resistance of the device-under-test, and values of the parallel resistance as a function of the frequency are provided to the nonlinear least squares

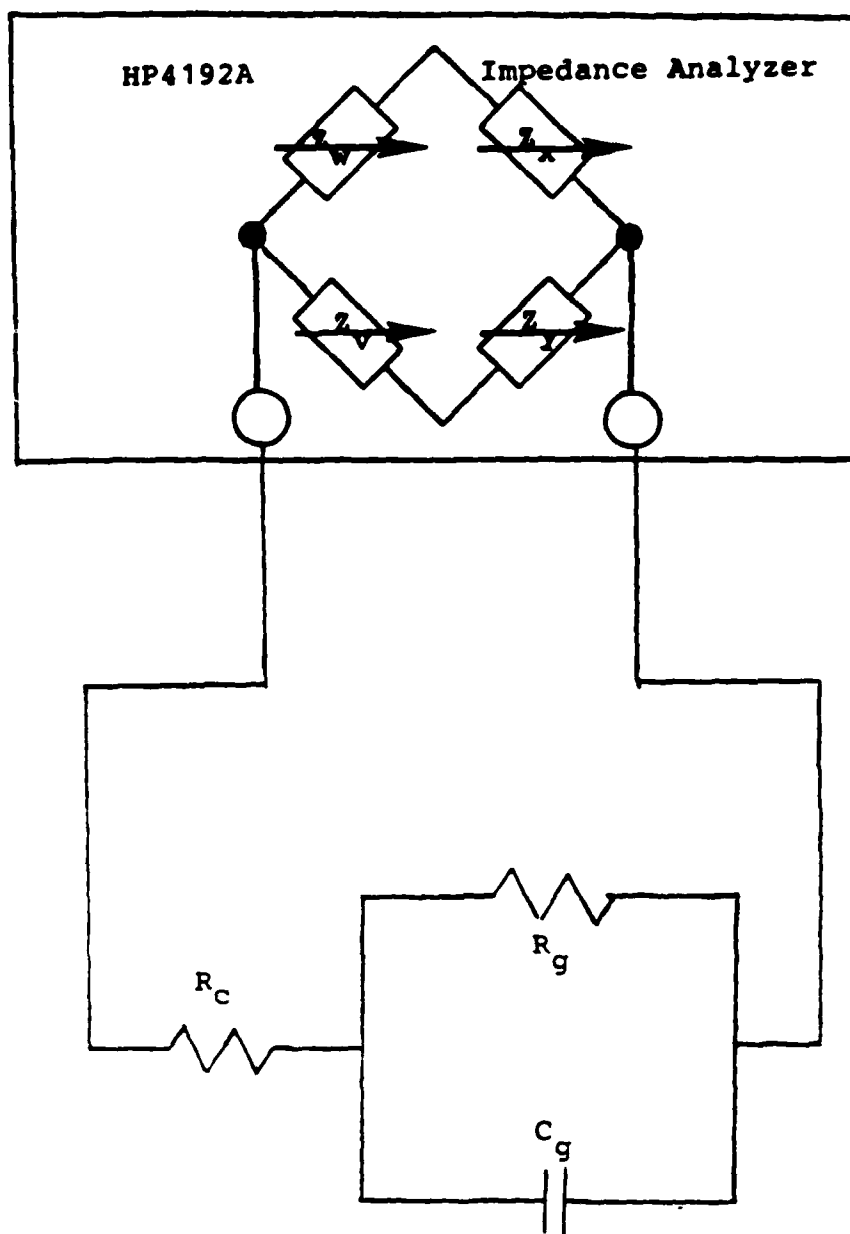


Figure 3-9. The Bridge Measurement Scheme

computer program as inputs.

Before measurements are taken with the HP 4192A bridge, a calibration procedure must be performed. The calibration procedure normally spans several frequency intervals in which measurements are to be obtained. The calibration of the bridge is achieved with a zero offset adjustment when an open circuit is applied to the measurement terminals (for the equivalent parallel circuit configuration). Zero offset adjustments are also made in each frequency interval to ensure the reliability of the data.

#### Transient Response Analysis

In the voltage-divider measurement technique, an input was applied in the form of a continuous sine wave. The sine wave sufficed to establish the feasibility of the measurement scheme, but pulsed inputs may simulate with a greater degree of accuracy the brain activity that is stimulated when a light is strobed to evoke a VER. Hence, the next battery of experiments will utilize a pulsed input. The RC effect of the tank circuit on the square pulse will be examined in order to determine the maximum scan rate of the multielectrode array.

Deviations of the output from the ideal square shape of the input pulse are anticipated because of the effect of the

Helmholtz double layer capacitance. These deviations will cause the pulse to rise and fall in an exponential fashion, thereby lengthening the effective duration of the pulse. The lengthened pulse duration will correspondingly limit the speed at which the electrode array can be scanned without losing information. A threshold value of three decibels below the maximum value of the output pulse will be used to distinguish between the pulses.

There are several variables that must be considered during this analysis. The pulse width should be known from the physiological description of how the eye transmits a pulse of information for a specific stimulation. The input and output signal waveforms are known since they can be measured. Values of  $R_c$ ,  $R_g$ , and  $C_g$  from the electrode-solute model are unknown and will be obtained by performing measurements analogous to those already described and by invoking the method of nonlinear least squares analysis to perform the necessary computations. The nonlinear least squares computer program requires that initial estimates of the model's parameters be supplied as inputs. The time constant for the exponential rise and fall of the output pulse is an unknown factor that must also be determined. The knowledge of  $R_c$ ,  $R_g$ , and  $C_g$  gives the time constant necessary to calculate the maximum operational bandwidth of the array.

AO-A103 204

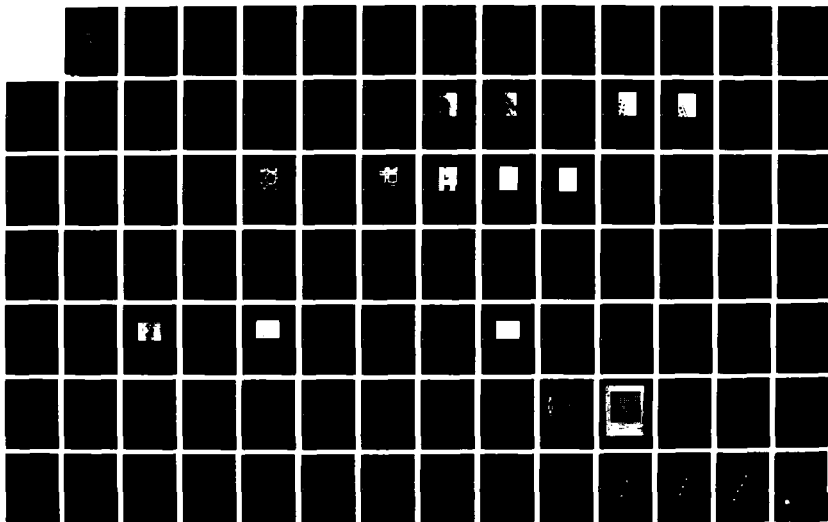
AN ELECTRICAL CIRCUIT MODEL OF THE INTERFACE BETWEEN AN 2/4  
ELECTRODE AND THE (U) AIR FORCE INST OF TECH  
WRIGHT-PATTERSON AFB OH SCHOOL OF ENGI.. J M SEDLAK

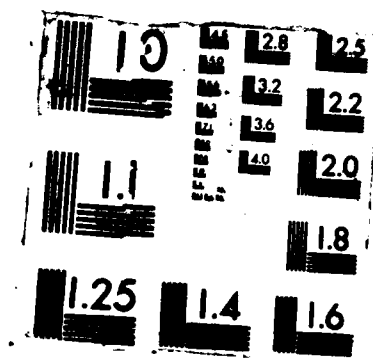
UNCLASSIFIED

31 JUL 87 AFIT/GE/EE/86D-48

F/G 9/1

NL







chip.

After the measurement and analysis methods have been mastered on an elite board, actual brain chips will be used in the experimental procedure. Additional considerations imposed by the use of brain chips include wirebonding and passivation of the chips. Once these activities have been successfully completed, actual testing of the chip in a simulated brain environment can begin. Because of the causal nature of the unknown parameters of the equivalent electrical circuit model, the values of  $R_c$ ,  $R_g$ , and  $C_g$  of the electrode-solute interface will first be determined, and then the maximum operating frequency of the chip will be specified.

When a square wave pulse is applied to the input of the equivalent circuit model of Figure 3-2, the rising and falling edges of the pulse will be altered due to the transient charging and discharging characteristics of the tank circuit. The instantaneous voltage changes of a square wave pulse, when applied to the tank circuit, are transformed into exponential growth (rising edge of the square wave pulse) and exponential decay (falling edge of the square wave pulse), which is governed by the time constant  $T = (R_c R_g C_g) / (R_c + R_g)$ . Note that a dimensional analysis of  $T$  indicates that the product of ohms and farads results in

units of seconds. For a single unit of  $T$ , the exponential function either decays to 37% of its final value or grows to 63% of its final value. A positive or negative change in the voltage results in either an exponential growth or an exponential decay, respectively.

The basic equation that governs the operation of the capacitor is:

$$i = C \cdot dv/dt. \quad (3-15)$$

From this equation, it can easily be deduced that an instantaneous change of the voltage across the capacitor would require an infinitely large current. This apparent violation of Kirchhoff's law eliminates the possibility of an instantaneous voltage change across the capacitor.

The exponential change of current that results from the effect of a capacitor upon an impressed voltage step function is given by:

$$i = I_0 \cdot \exp(\pm t/T), \quad (3-16)$$

where  $I_0$  is the value of the current at  $t = 0+$ . The initial current (29:103),  $I_0$ , is given by:

$$I_0 = V_0/R, \quad (3-17)$$

where  $V_0$  is the impressed voltage, and  $R$  is the resistance of

the circuit (29:101). Introducing a change of notation,

$$i = I_0 \cdot \exp(xt) \quad (3-18)$$

where  $x = \pm 1/T$ . The plus (+) or minus (-) sign is chosen to correspond to the growth or decay, respectively, that results from the forcing function. The units of  $x$  are 1/sec, the reciprocal of the units of the time constant  $T$ .

The time-derivative of an exponential function results in the product of a constant and the original exponential function, thereby yielding an expression differing only by the constant. Hence, the time derivative of the expression for "i" is:

$$di/dt = xI_0 \cdot \exp(xt) = xi. \quad (3-19)$$

In order to generate an expression for the impedance ( $Z$ ) looking into the equivalent circuit model, the voltage across the capacitor is defined in a fashion analogous to the current definition. Hence,

$$v = V_0 \cdot \exp(xt). \quad (3-20)$$

Taking the time-derivative of the voltage,

$$dv/dt = xV_0 \cdot \exp(xt) = xv. \quad (3-21)$$

After substituting into the expression for  $C$ , the defining

equation of the capacitor becomes:

$$i = Cxv. \quad (3-22)$$

From Ohm's law, the impedance can be described by the expression:

$$Z = 1/(Cx) = \underline{\pm} T/C. \quad (3-23)$$

Hence, an impedance can assume any positive value depending upon the circuit parameters. As a consequence of the unique property of the time-derivative of an exponential function, the impedance is a meaningless expression for other than sinusoidal forcing functions. In the case of a direct current excitation, the forcing function retains its exponential character, whereby the frequency is zero and the time constant becomes infinite. Since an impedance is defined by  $Z = v/i$ , it has the dimensions of ohms. The Kirchhoff voltage law can be applied to a circuit composed of resistive and capacitive elements that form an equivalent impedance.

At this point in the analysis, a comment concerning the dc and high frequency behavior of a capacitor needs to be made. For a dc excitation, an examination of the impedance of the capacitor results in the prediction that no current will pass through the capacitor. Thus, the capacitor acts

like an open circuit. When the capacitor voltage (in the case where no other impedances are present in the circuit) reaches a steady-state value, equivalent to the applied voltage, no further charge transfer occurs. If it did, the capacitor voltage would become greater than the applied voltage, thereby violating Kirchhoff's voltage law. At very high frequencies, an analysis of the effective impedance of a single capacitor leads to the deduction that an infinite amount of current would flow. Although this never happens in reality (an infinite source is required to generate an infinite amount of current), the capacitor does act like a short circuit.

For the circuit of Figure 3-2, the impedance  $Z(s)$  is given by:

$$Z(s) = Z(R_c) + \{Z(R_g) * Z(C_g) / [Z(R_g) + Z(C_g)]\}, \quad (3-24)$$

where  $s$  is the complex product  $j\omega$ . Making substitutions for the impedance parameters,

$$Z(s) = R_c + R_g * 1/(C_g s) / [R_g + 1/(C_g s)]. \quad (3-25)$$

After simplification,

$$Z(s) = [R_c R_g C_g s + R_c + R_g] / [R_g C_g s + 1]. \quad (3-26)$$

From the analysis of the natural response of the equivalent

circuit model for a sinusoidal excitation (previously presented), the values of  $R_C$ ,  $R_g$ , and  $C_g$  were obtained. Therefore, the impedance is a known function of the complex frequency parameter  $s$ .

In order to represent a square wave pulse, we make use of the observation that the pulse can be represented by the difference between two step functions. The unit step function is depicted in Figure 3-10a. Using the notation of a unit step function,  $u(t) = 0$  for  $t < 0$  and  $u(t) = 1$  for  $t \geq 0$ . In the step function of Figure 3-10b,  $u(t-t_0) = 0$  for  $t < t_0$  and  $u(t-t_0) = 1$  for  $t \geq t_0$ . Figure 3-10c shows the square wave pulse that results from the difference between the two unit step functions. The defining equations of a square wave pulse are  $Q(t) = 0$  for  $t < 0$  and  $t > t_0$  and  $Q(t) = 1$  for  $0 \leq t \leq t_0$ .

Despite the representation of the square wave pulse as the difference between two unit step functions, the transient analysis of the circuit of Figure 3-2 revolves around the behavior of the circuit when a single unit step input is applied. This result occurs because the transient behavior of the circuit occurs at the rising and falling edges of the square wave pulse. Except for the time when  $t = 0$ , the unit step forcing function can be treated as a dc quantity. Hence, the capacitor has an infinite impedance, and the

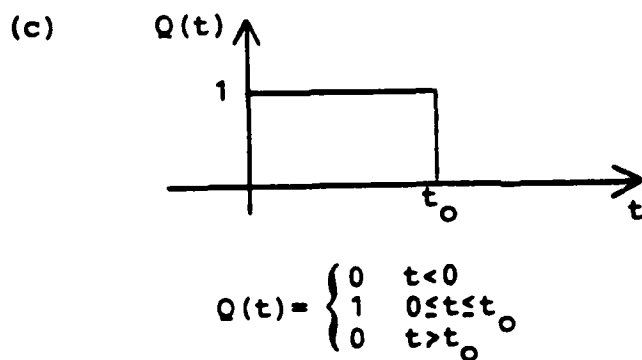
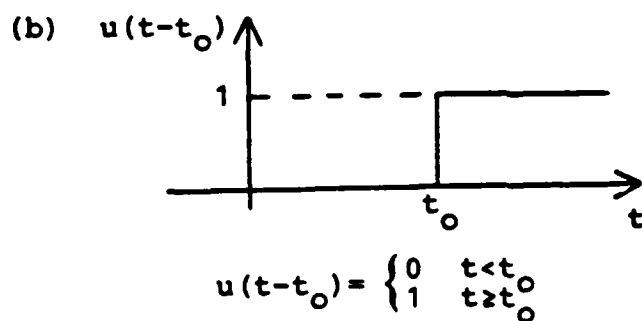
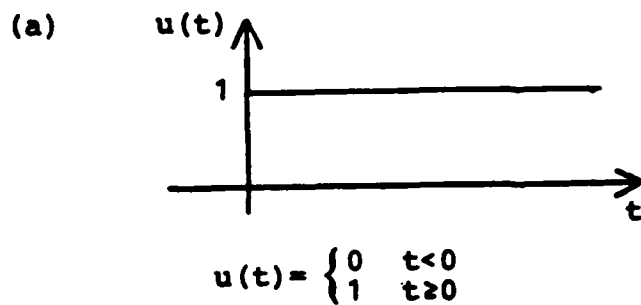


Figure 3-10. Derivation of a Square Wave Pulse from the Unit Step Function (a) unit step  
(b) shifted unit step (c) square wave pulse

forced component of the output will be determined by the division of the voltage between  $R_c$  and  $R_g$ .

The transfer function of the circuit defined by the quotient of  $V_2$  to  $V_1$ , where  $V_2$  and  $V_1$  are the output and input voltages, respectively, of the equivalent electrical circuit, is calculated in Appendix F. The result is:

$$T(s) = V_2/V_1 = 1/[R_c C_g s + (R_c + R_g)/R_g]. \quad (3-27)$$

From the transfer function, and with the use of the initial conditions [ $u(0^+) = 1$  and  $t = 0^+$ ], the total output response of the circuit is given by the sum of the forced and natural responses. After all of the calculations have been performed,

$$V_2 T = u(t) [R_g / (R_c + R_g)] \{1 - \exp[-(R_c + R_g)t / (R_c R_g C_g)]\} \quad (3-28)$$

gives the output response of the circuit to the unit step function input.

Admittedly, the square wave pulse is represented by the difference between two step inputs. If the duration of the square wave pulse,  $(t_0)$ , is greater than the settling time [ $T = R_c R_g C_g / (R_c + R_g)$ ] of the exponential response to the step input, then the output response to the square wave pulse input can be determined by examining the separate behavior of the circuit to the two step functions that represent the



square wave pulse. Since the steps are identical in magnitude but have opposing orientations (i.e. one rises and the other falls), the responses will be similar with the exception that one grows and the other decays. Hence, the calculation of the effect of the charging and discharging of the capacitive element upon the output response of the equivalent circuit model needs to be deduced only once.

#### Pulse Generation Scheme

In order to simulate a strobed light source by electrical means, a method of generating pulses of variable width, amplitude, and spacing is devised. The essential component of this method of pulse generation is a 54121 CMOS monostable multivibrator. The monostable multivibrator is also called a "one shot" since it has one stable and one unstable state that are controlled by an applied trigger. When a trigger is applied to the monostable multivibrator, the output flips from the normally "on" stable state to the unstable state. The duration of the unstable state can be controlled by using an external circuit with a suitable RC time constant.

By using two 54121 monostable multivibrators, a pulse generator can be constructed in which not only the pulse

width (or duration), but also the pulse interval, may be controlled with external circuitry. The schematic of this pulse generator is provided in Figure 3-11. The circuit diagram and truth table of the 54121 is supplied in Figure 3-12. Referring to Figure 3-11, an external clock triggers the first 54121 (on the reader's left), which then triggers the second 54121 (on the reader's right). The 54121 to the left initiates a time delay that can be used to control the interval of the pulse, and the 54121 to the right generates the actual pulse and its interval.

Kirchhoff's voltage equation  $V = V_r + V_c$  provides a means of estimating the values of  $R_{ext}$  and  $C_{ext}$  that results in the desired time constant. Hence,

$$V = I \cdot R_{ext} + 1/C_{ext} \int_0^t I \cdot dt - q(0)/C_{ext}. \quad (3-29)$$

Since the capacitor is not precharged,

$$V = I \cdot R_{ext} + 1/C_{ext} \int_0^t I \cdot dt. \quad (3-30)$$

Next, we differentiate to obtain

$$0 = R_{ext} \cdot dI/dt + I/C_{ext}. \quad (3-31)$$

The variables are then separated to yield

$$dI/I = -dt/(R_{ext} \cdot C_{ext}). \quad (3-32)$$

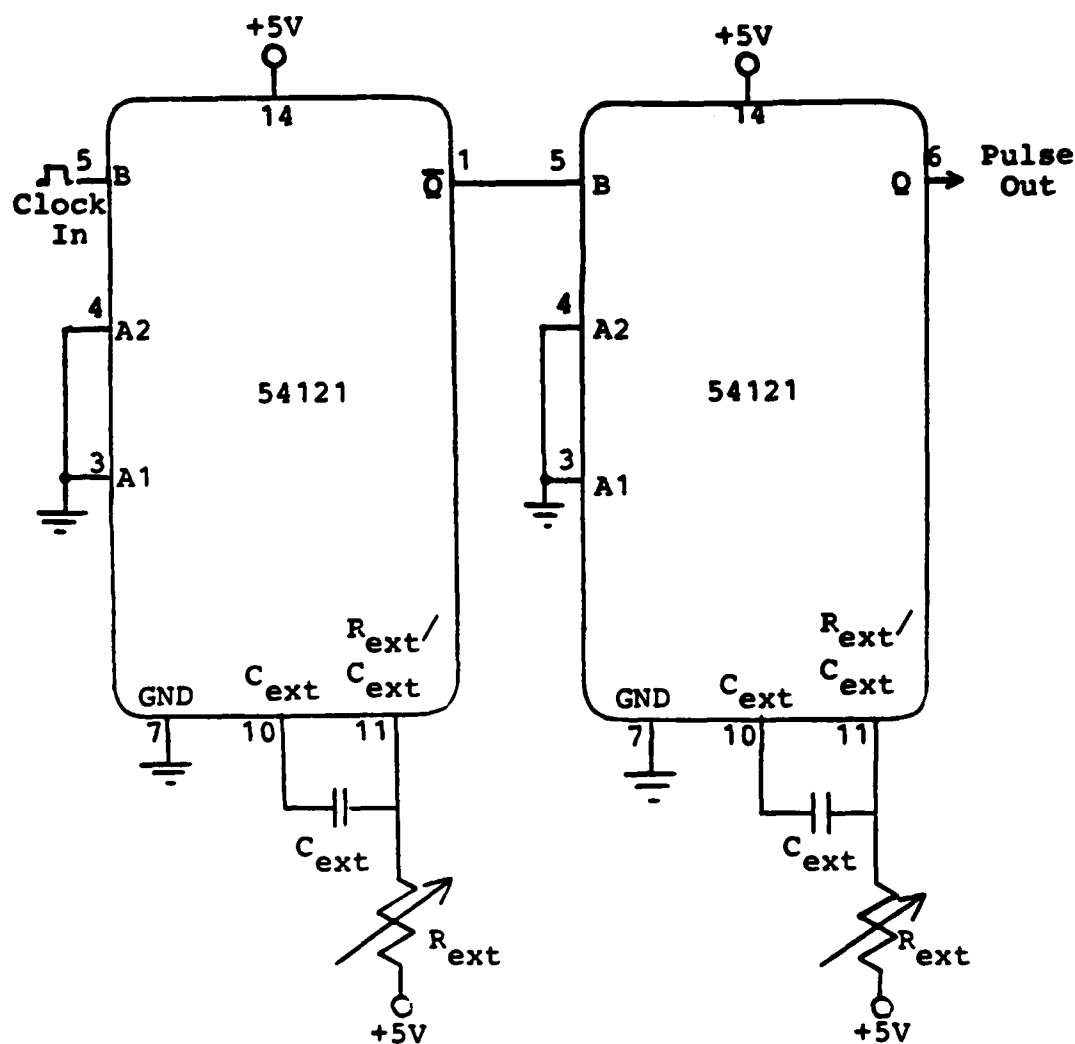
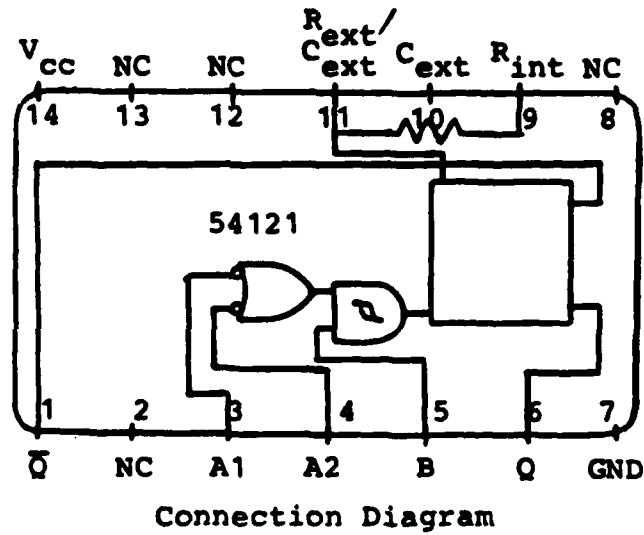


Figure 3-11. Pulse Generation Scheme with Variable Width and Timing



INPUTS			OUTPUTS	
A1	A2	B	Q	$\bar{Q}$
L	X	H	L	H
X	L	H	L	H
X	X	L	L	H
H	H	X	L	H
H	↓	H	⌋	⌋
↓	H	H	⌋	⌋
↓	↓	H	⌋	⌋
L	X	↑	⌋	⌋
X	L	↑	⌋	⌋

Truth Table

Figure 3-12. Connection Diagram and Truth Table of the 54121 One Shot

An integration of the separable first-order differential equation gives

$$\ln I = -t/(R_{\text{ext}} * C_{\text{ext}}) + K, \quad (3-33)$$

where K is a constant. Therefore,

$$\exp(\ln I) = \exp[-t/(R_{\text{ext}} * C_{\text{ext}}) + K]. \quad (3-34)$$

Simplifying,

$$I = \exp[-t/(R_{\text{ext}} * C_{\text{ext}})] * \exp(K). \quad (3-35)$$

Letting  $A = \exp(K)$ ,

$$I = A * \exp[-t/(R_{\text{ext}} * C_{\text{ext}})]. \quad (3-36)$$

Using the initial conditions for  $t=0$ ,

$$A = V/R_{\text{ext}}. \quad (3-37)$$

Therefore,

$$I = (V/R_{\text{ext}}) * \exp[-t/(R_{\text{ext}} * C_{\text{ext}})]. \quad (3-38)$$

An examination of Equation 3-36 reveals that the value of the product of  $R_{\text{ext}}$  and  $C_{\text{ext}}$  determines the time for the current to reach a particular value. A smaller  $R_{\text{ext}} * C_{\text{ext}}$  product results in a more rapid decrease of the current than a larger  $R_{\text{ext}} * C_{\text{ext}}$  product. Because  $t/(R_{\text{ext}} * C_{\text{ext}})$  is an

exponent, the  $R_{ext} * C_{ext}$  product has units of time. Hence, the time constant is given by

$$t = R_{ext} * C_{ext} \quad (3-39)$$

and has units of seconds when  $R_{ext}$  is in ohms and  $C_{ext}$  is in farads.

#### 4. PREPARATION OF TESTABLE CHIPS

##### Introduction

The requirement of a chip that will function without failure in a saline electrolyte necessitates the application of an encapsulant. A required characteristic of the encapsulant is that it not only resists the intrusion by sodium or chlorine ions, but that it also be amenable to a standard etching and patterning process. The encapsulant must prevent the electrolyte's ions from penetrating through its protective coating because the chemical reaction between the ions and the semiconductive circuit materials could devastate the device's electronic performance. The requirement to etch contact windows through the encapsulant arises from the necessity to achieve a good electrical contact with the electrodes.

Polyimide was the encapsulant that was chosen in earlier research projects (1,3), and it was likewise used in this research project. The decision to employ the polyimide was primarily generated by the chemical reaction that occurs when aluminum comes into contact with a saline. Unfortunately, sodium and chlorine ions are chemically active and are commonly found in the cerebrospinal fluids of mammals (as

well as in other bodily tissues and fluids). The reaction between chlorine and aluminum ions results in a very rapid deterioration of the aluminum; if not adequately protected, a VLSI circuit can be rendered inoperative within seconds (3:1-2). The choice of polyimide as the encapsulant of testable chips was derived from characteristics that satisfy several diverse criteria, such as resistance to ion penetration, biological compatibility, repeatability and controllability during application and processing, nonsolubility in liquids, and the ability to pattern and etch contact windows over the electrodes (6:20). Polyimide was used to encapsulate the brain chips that were tested, and the process that was developed to apply it is provided in Appendix C. A goal of applying three coats of polyimide was chosen to ensure the adequate protection of testable chips.

The decision to use a negative photolithography process for patterning the chips resulted from a lack of confidence in the controllability and repeatability characteristics of the positive photolithography process. In the positive photolithography process, the etchant that is used with polyimide, AZ351, is also the developer used with the positive photoresist. It was therefore decided that the development time for the positive photoresist would be overly critical since undercutting of the polyimide would



simultaneously occur. In the negative photolithography process that was chosen, xylene, the developer for the negative photoresist, does not interact with the polyimide coating. Polyimide is impervious to all of the substances employed in a negative photolithography process.

#### Practice with Wafers

In order to become familiar with the equipment and the procedure employed in the negative photolithography method, a set of one inch practice wafers was processed according to Schedule 1 of Appendix C. The wafers that were initially used were unpolished on both sides. After applying a coat of polyimide, these wafers were exposed for 4.5 seconds and developed in a xylene bath for 10 seconds. The pattern observed under a microscope was excessively ragged and discontinuous, so the wafers were developed for another 10 seconds; however, no noticeable improvement of the pattern's definition resulted from the added development time. Next, freshly coated wafers were exposed for 10 seconds, then developed for 20 seconds. Once again, the resultant pattern lacked definition.

The suspicion that the irregular surface of the unpolished wafers had caused the poorly defined patterns was tested by processing a batch of wafers that had a polished

surface. Using the polished surface of wafers that had a  $\langle 111 \rangle$  orientation, a vastly improved pattern was obtained after a 4.5 second exposure. The pattern that was obtained with a 4.5 second exposure is displayed in Figure 4-1. A magnification factor of 100 was used to obtain all of the figures of this section. Next, a 10 second exposure was tried, and the pattern shown in Figure 4-2 resulted. Exposure times of up to 30 seconds were also tried, but the definition of the pattern of Figure 4-2 was not significantly improved. The 10 second exposure was chosen over higher exposure times because of the characteristic "hardening" of the photoresist layer as the exposure time is increased. Since the photoresist is removed before the final cure of the polyimide, the lower exposure time simplified its removal.

Next, six wafers that had been exposed for 10 seconds and developed for 20 seconds were etched in a 60 milliliter bath of the AZ351 developer mixed in a 1:6 ratio with DIW at room temperature. An initial five-second etch time was attempted, but the polyimide was only partially removed, as shown in Figure 4-3. An additional five second etch perfunctorily stripped away all of the polyimide under the contact windows, and undercutting of the polyimide was not visible during a microscopic examination. The next wafer was etched for a full ten seconds, and the acceptable pattern

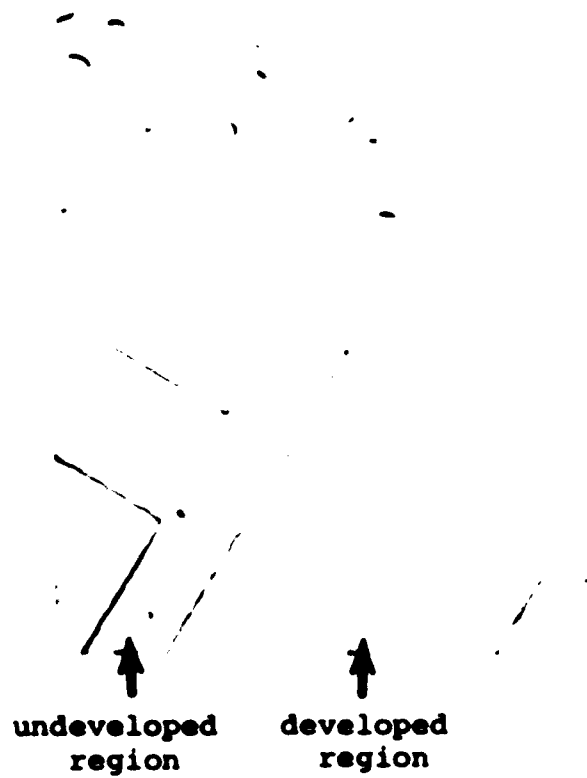


Figure 4-1. Wafer with 4.5 Second Exposure



Figure 4-2. Wafer with 10 Second Exposure

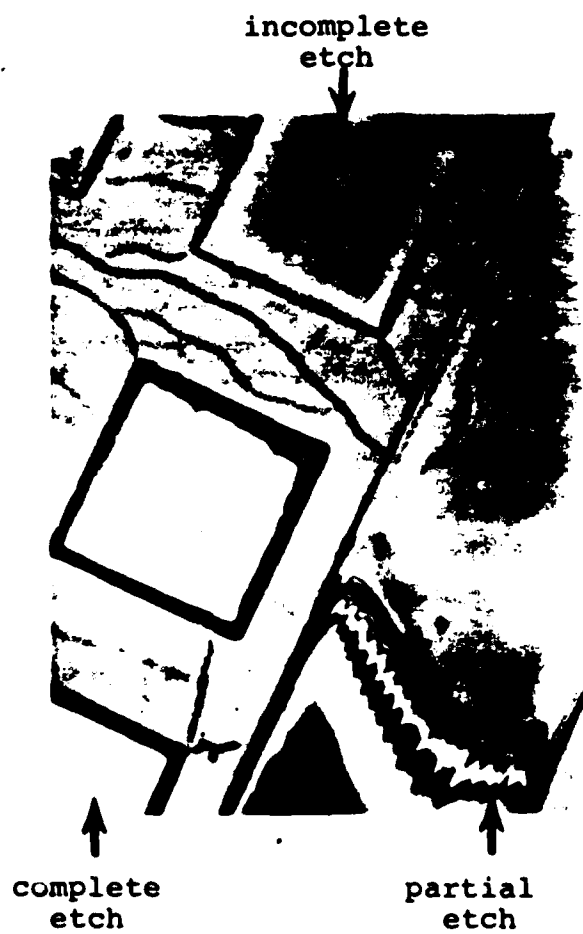


Figure 4-3. Partial Etch of the Polyimide

displayed in Figure 4-4 resulted.

The fully etched wafers were postbaked for 2 hours at 150 degrees centigrade to harden the polyimide. Unfortunately, the postbake also hardens the negative photoresist, which must be removed before another coat of polyimide is applied. The negative photoresist was removed by mechanical scrubbing with acetone, and a microscopic examination revealed that the polyimide was not defaced. The removal of the photoresist can be observed in Figure 4-5. Note the absence of cracks (shown in Figure 4-4) in the negative photoresist for the wafer depicted in Figure 4-5.

The cracking of the negative photoresist is characteristic of the exposure and development procedures that were used to pattern both the wafers and the chips. Cracks appeared each time a coat of polyimide was patterned, but they did not affect the polyimide etching since no cracks appeared in areas that were exposed. The cracks provided a convenient means of gauging the removal of the photoresist since their disappearance corresponded to the photoresist's removal.

A second coat of polyimide was applied after a two-hour cure at 180 degrees centigrade. Once again, the chip was processed according to Schedule 1 of Appendix C. The final result after the two coats of polyimide had been applied and



cracks  
in  
undeveloped  
region

Figure 4-4. Complete Etch of the Polyimide



no  
cracks  
in  
undeveloped  
region

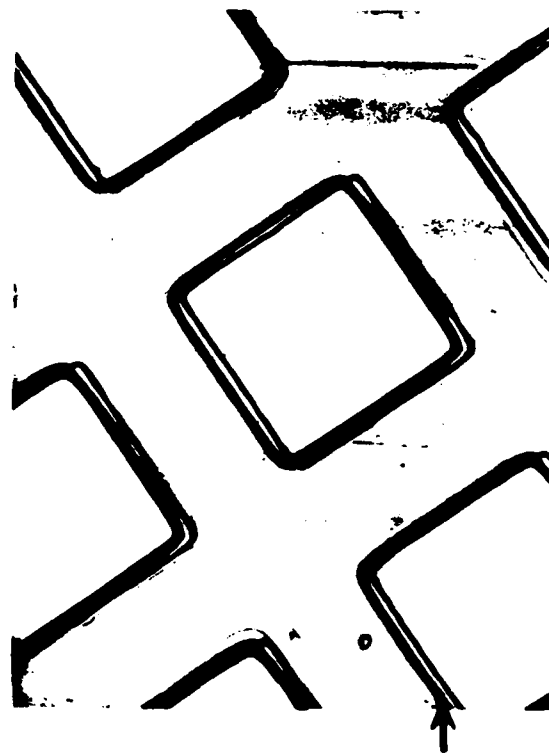
Figure 4-5. Wafer after Photoresist was Removed



processed is shown in Figure 4-6. A slight misalignment between the two patterns is visible, but it is within the tolerance necessary to effectively expose the electrodes while protecting the vulnerable areas of the integrated circuit. The size of the contact windows on the mask is actually smaller than the size of the electrodes on the chip; this feature minimized the risk of not completely protecting the vulnerable areas of the chip. The successful processing of the six wafers for a single coat of the polyimide prompted the decision to begin passivating individual chips.

#### Passivation of Testable Chips

In order to encapsulate individual chips, special techniques had to be developed because of the physical limitations of the equipment with respect to the size of the chips. Both the photoresist spinner and mask aligner are designed to accommodate one-inch or three-inch wafers, so adaptations of the processing schedule used on the wafers were necessary. Also, special precautions were required merely to handle the chips without mishap. Teflon tweezers were used to avoid unintentionally scratching the chips, and the ability to secure a chip with the tweezers while blowing nitrogen gas across their surface was hampered. A special retainer was fabricated to prevent the chips from being



misalignment

Figure 4-6. Wafer after Two Coats of Polyimide

damaged by the air flow in the baking ovens.

The smallest vacuum chuck available for the spinner was used when processing the chips, but the chips were too small to entirely cover the vacuum ports. Hence, at the instant when the vacuum was applied during a spinning operation, material that had been puddled on the chip was drawn into the vacuum line. In order to minimize the buildup of polyimide and photoresist in the vacuum line, solvents were regularly sprayed onto the chuck and into the vacuum line after each use. The polyimide, nonetheless, collected in portions of the vacuum line where the air flow was restricted.

Approximately once every two weeks it was necessary to disassemble the spinner and clean the vacuum lines. An in-line mechanical solenoid that sensed an increase in the vacuum and engaged the spinner motor proved to be the region where polyimide collected and eventually plugged the line. An adjustment of the solenoid actuator was necessary each time the spinner was disassembled for cleaning.

The use of the mask aligner with an individual chip required a modification to the procedure that had been used when processing the wafers. Placement of a chip directly upon the vacuum chuck did not interfere with the alignment of the mask, since the alignment is performed with the mask separated from the chip. The exposure of the photoresist,

however, is accomplished by first making contact between the chip and the mask. After an exposure, the chuck dropped away from the mask, but the chip invariably adhered to the mask. The task of separating the chip from the mask usually introduced scratches upon the mask and the chip, so an alternative method of alignment was devised.

The chip adhered to the mask when they made contact because of the increased pressure per unit area that is a natural consequence of using a chip in place of a wafer. This problem was alleviated by fabricating a chip holder from several silicon wafers. Strips that corresponded to the length and width of the chip were diced from several wafers, and these pieces were fitted together so that a square hole with the exact dimensions of the chip was created. This assembly was mounted on another wafer that served as a base. A vacuum hole was made in the base's center so that vacuum could be applied directly to a chip that was to be printed. Turner (3:V-4) describes the fabrication of a chip holder that was similarly constructed from silicon wafers. Initial attempts to create a vacuum hole in the center of a wafer by chemical etching, as well as by mechanical means, were either futile or too time consuming to be of any value. The  $\langle 111 \rangle$  wafers that were used fractured along their planes of crystal orientation whenever an attempt to bore a hole was made. The

anisotropic etch of a vacuum hole failed because the acid preferentially etched along the planes of crystal orientation. An isotropic etch was attempted, but after two weeks the effort was abandoned because the reaction rate was too slow.

A wafer with a vacuum hole at the center was eventually realized by a relatively simple mechanical process. Tape was applied to the unpolished side of a wafer, and pressure was applied at the center with a scribe until the wafer fractured along the planes of crystal orientation. Next, a sharp corner that intersected the center of the wafer was chipped off, and polyimide was coated over the exposed side of the wafer. The diced sections of the first wafer were mounted on the top of this wafer so that the cavity was centered over the vacuum port. After baking, the chip holder was suitable for use in the mask aligner.

After the problems peculiar to handling the chips had been resolved, actual processing of the chips began. Schedule 2 in Appendix C provides the procedure that was used. A significant change from Schedule 1 is the use of xylene rather than acetone to remove the negative photoresist after etching the polyimide. Less mechanical scrubbing was required when xylene was substituted for the acetone, and this reduced the risk of scratching the electrodes and

defacing the polyimide coating.

Another problem inherent to the processing of chips was discovered. Figure 4-7 displays the etch of a second coat of polyimide that expanded well beyond the borders of the electrodes. As a result, the pass transistors of the array were exposed by the etch. The electrodes pictured in Figure 4-7 are located near the center of the array. A few electrodes near the outer edge of the array had not been etched at all. The explanation of this phenomenon lies in the application of a viscous material such as polyimide. Around the edges of the chip, the polyimide had formed a convex meniscus that was considerably greater in depth than the more uniform layer of polyimide at the center of the chip. This phenomenon effected the underetching of electrodes farther from the center. The problem of partial etching worsened when attempts were made to etch a third coat of polyimide, indicating that the meniscus progressively thickens with the addition of polyimide coats.

In an attempt to reduce this meniscus effect, the angular velocity of the spinner was increased, but no improvement in the uniformity of a polyimide layer could be discerned. A selective etch was attempted whereby the edges of the chip were immersed in the etchant longer than the center portion of the chip. The selective etch worked



overetched

Figure 4-7. Overetching of the Polyimide on a Chip

reasonably well on the second coat of polyimide, but difficulty in etching three coats of polyimide persisted. Figure 4-8 shows the electrodes after the second etch, and Figure 4-9 shows the electrodes after an unusually successful third etch.

A difficulty with the etching process was the variable etch rate. In the first etch, the chip was uniformly immersed in the etchant for five to ten seconds. For the second and third etches, the chip was uniformly immersed in the etchant in one or two one-second intervals until the central portion of the electrodes was fully etched. After the central portion of the electrodes was etched, selective etching was conducted in order to expose electrodes closer to the edges of the chip.

After completing the processing of the chips, the chips were wirebonded. The pads were bonded with one millimeter diameter gold wire. Figure 4-10 shows the wirebonds of the first chip that was packaged. In Figure 4-11, the electrodes of the first packaged chip are shown.

#### Summary of Processed Brain Chips

A total of four chips were prepared for testing. One chip had three coats of polyimide and three chips had two coats of polyimide. Since the risk of a failure when



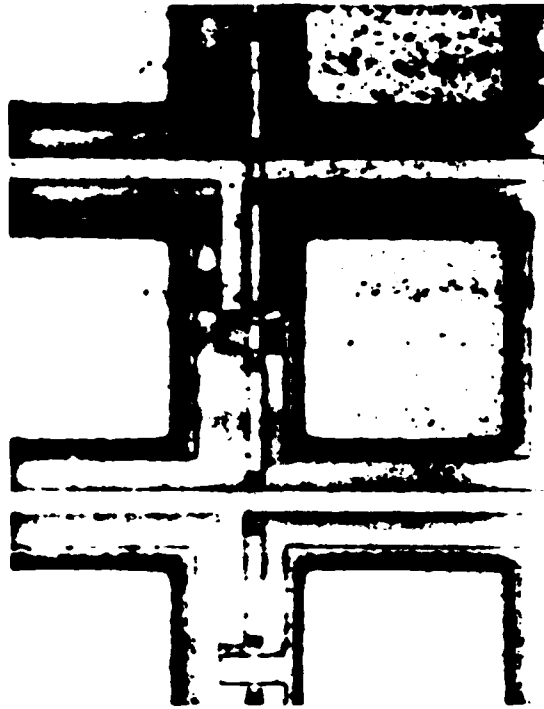


Figure 4-8. Chip after the Second Polyimide Etch



Figure 4-9. Chip after the Third Polyimide Etch



Figure 4-10. Wirebonds to the Chip

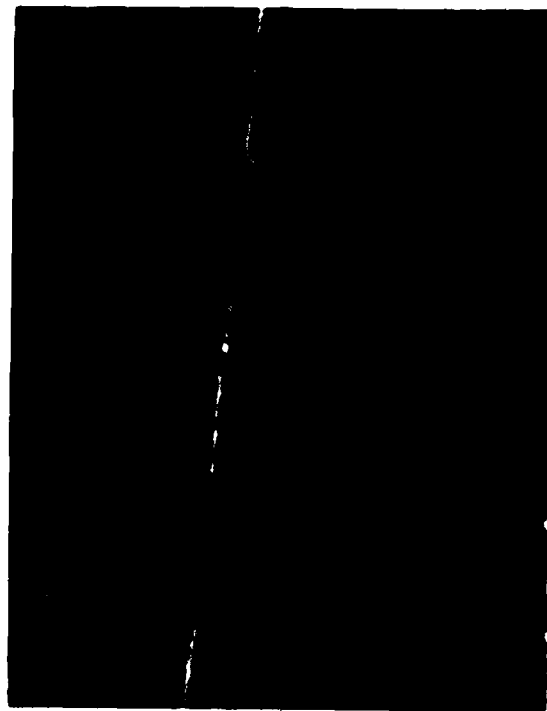


Figure 4-11. First Chip after Complete Encapsulation

applying three coats of polyimide was high in the etching process, the other three chips were given two coats of polyimide with the intention of adding additional coats if necessary. Great care was exercised during the etching of the second and third coats of polyimide. The final process of Schedule 2 was developed by trial and error, and special techniques, such as the use of a chip holder and teflon tweezers, were adopted to minimize the problems peculiar to processing discrete chips.

## 5. RESULTS AND DISCUSSION

The chips that had been processed with the polyimide encapsulant were finally ready for in vitro testing in a saline environment. Before actual chips were immersed, however, preliminary tests were accomplished to ensure that the measurement apparatus and methodology were absolutely flawless. At this stage of the research, processed chips could not be expended in the refinement of the testing procedure because of the limited quantity available--four chips. The electrodes of one of the four chips were incompletely etched, and electrical contact with these electrodes could not be achieved. Therefore, only three chips were usable in the subsequent testing.

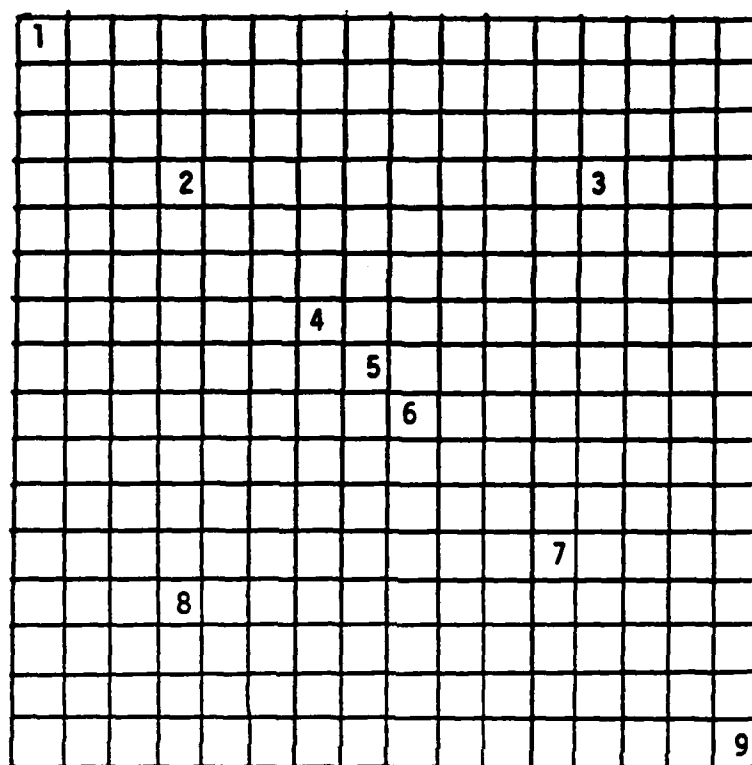
Two different types of tests were performed, and a subset of the 256 electrodes of each chip was selected for the tests. In the first test, parallel impedance measurements were obtained for frequencies in the range dc - 1.0 MHz. In the second test, a 25 Hz "brain" signal (1.0 millivolt in amplitude) was propagated through the saline, and pictures of electrode outputs were taken for 100, 1000, and 10,000 ohm load resistances. The parallel impedance measurements were obtained for all three chips, and pictures of the output signals of the electrodes were taken

for two of the chips.

Eight different electrodes were used to obtain the parallel impedance measurements of the first chip that was tested. For the latter two chips that were tested, nine different electrodes were used in both the parallel impedance and signal propagation tests. The electrodes selected for the tests are spatially oriented in varying sectors of the array, and both the propagation paths and distances from the ground plane reference electrode depend upon the actual electrode selected. Figure 5-1 portrays the 256-electrode array, and the nine electrodes used in the testing are annotated with a 3-digit code. The first digit of the code, denoted by "x", identifies which chip that the electrode originated from (x=1 for chip 1, x=2 for chip 2, and x=3 for chip 3), and the second and third digits of the code identify the row and column, respectively, of the chip being tested. Note that a hexadecimal-like number system was adopted whereby A=10, B=11, C=12, D=13, E=14, F=15, and G=16. This code will henceforth be used to distinguish the numerous sets of data that were recorded in the testing of the three chips.

#### Test Equipment Configuration

Since two different tests were performed, the equipment configurations for each of the tests varied accordingly. In



KEY

- |        |        |
|--------|--------|
| 1. X11 | 6. X99 |
| 2. X44 | 7. XCC |
| 3. X4D | 8. XD4 |
| 4. X77 | 9. XGG |
| 5. X88 |        |

Figure 5-1. Identification Codes of Array Electrodes Used in Testing



the equivalent circuit impedance measurement scheme, the HP4192A impedance analyzer was used to obtain the frequency response characteristics. Eleven different electrical parameters can be measured over the frequency range 5 Hz to 13 MHz with the HP4192A. The HP4192A measures the impedance magnitude, admittance magnitude, phase angle, resistance, reactance, conductance, susceptance, inductance, capacitance, dissipation factor, and quality factor of an unknown device or circuit component. Either series or parallel equivalent circuit measurements can be selected with the circuit mode control switch on the HP4192A. The parallel equivalent circuit measurement mode was used to collect the experimental data of the first test.

Impedance measurements of actual brain chips were facilitated by mounting the packages on an elite board and flooding the bonding cavity with saline. The appropriate row was enabled by applying +5 volts from a dc supply on the elite board. The HP4192A was then connected between the column input and the ground plane of the chip, and the equivalent circuit impedance measurements of the electrode-solute interface were recorded. Figure 5-2 shows the connection of the HP4192A to a single electrode of the array. For the second test, a more elaborate equipment configuration was required to propagate a 25 Hz pulse through

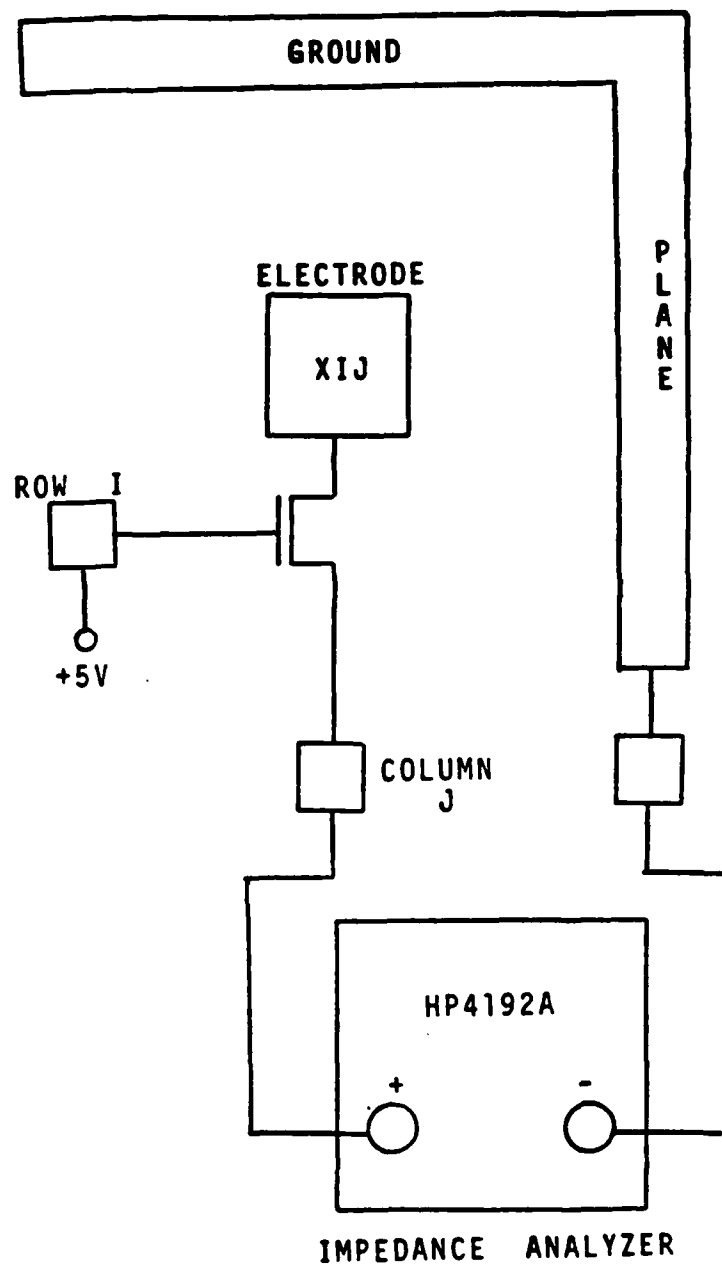


Figure 5-2. Equipment Configuration of Impedance Measurements

the saline and examine the output of an electrode. Figure 5-3 shows the equipment configuration that was used to perform the second test on a single electrode. Two signal generators, the 148 and 186 Wavetek models, were used to generate a 25 Hz pulse. The pulse interval was increased by lowering the trigger rate of the Wavetek 148 until a single 25 Hz pulse was captured on the oscilloscope trace. Channel 1 of the oscilloscope displays the output of the Wavetek 186 signal generator, and Channel 2 displays the output of an electrode. An HP198A camera and color Polaroid film were used to record the signal traces of the HP1201A oscilloscope. For all of the pictures that were taken, the horizontal sweep of the oscilloscope was 20 milliseconds per division, the vertical amplitude of the oscilloscope was 1 millivolt per division, and the shutter speed setting of the oscilloscope camera was 4.5.

#### Calibration and Baseline Procedures

To ensure the proper calibration, as well as operation, of the HP4192A impedance analyzer, tests were performed on discrete electrical circuit components. Two resistances of 1000 ohms and 40 megohms and a capacitance of 5 nanofarads were measured with the HP4192A to verify its calibration. The frequency of the measurements spanned 5 Hz to 13 MHz for

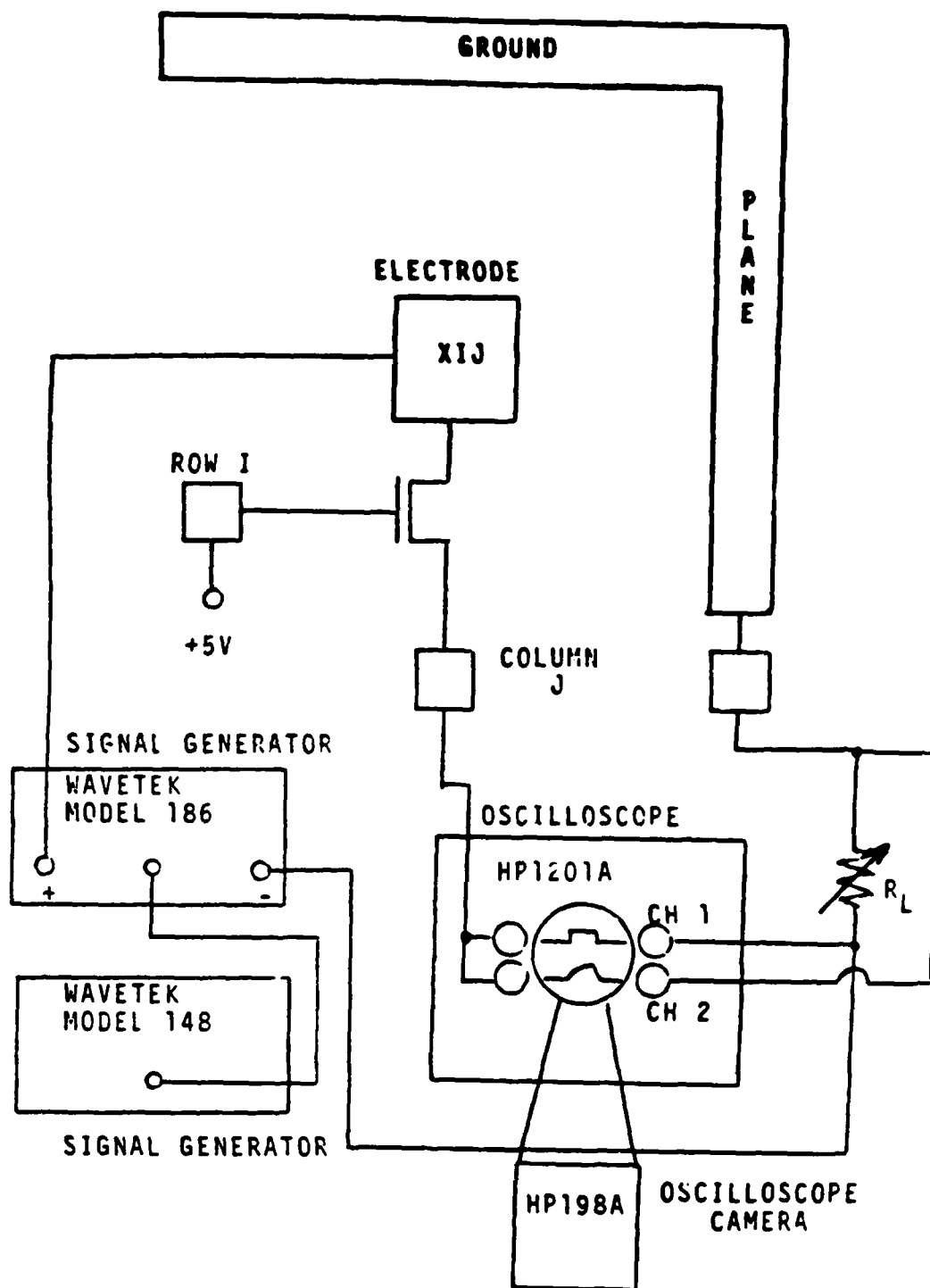


Figure 5-3. Equipment Configuration of Array Scan Rate Tests

the resistors, and 5 Hz to 9 MHz for the capacitor. At approximately 1 to 5 MHz, the measurements began to vary from expected values, thus indicating a possible degeneration of the accuracy of the measurement scheme for anticipated parameters of the equivalent electrical circuit model. In order to minimize the high frequency parasitic losses of the test probes, a zero offset adjustment was automatically performed by the HP4192A for all frequencies greater than 1 MHz. The automatic zero offset function of the HP4192A was invoked by manually performing a zero open offset calibration at 10 MHz. Therefore, the drift that was observed in the high frequency measurements of the discrete electrical circuit components was not caused by negligence in the calibration procedure of the HP4192A impedance analyzer. Values of the discrete electrical circuit components that were obtained with the HP4192A are presented in Section A of Appendix G.

After checking the calibration of the HP4192A on single discrete components, the impedance of a circuit consisting of two resistances and a capacitance configured in accordance with the equivalent electrical circuit model was obtained. Figure 5-4 shows the circuit schematic with component values indicated. The components that were used reflect the theoretical predictions of the values for the parameters in

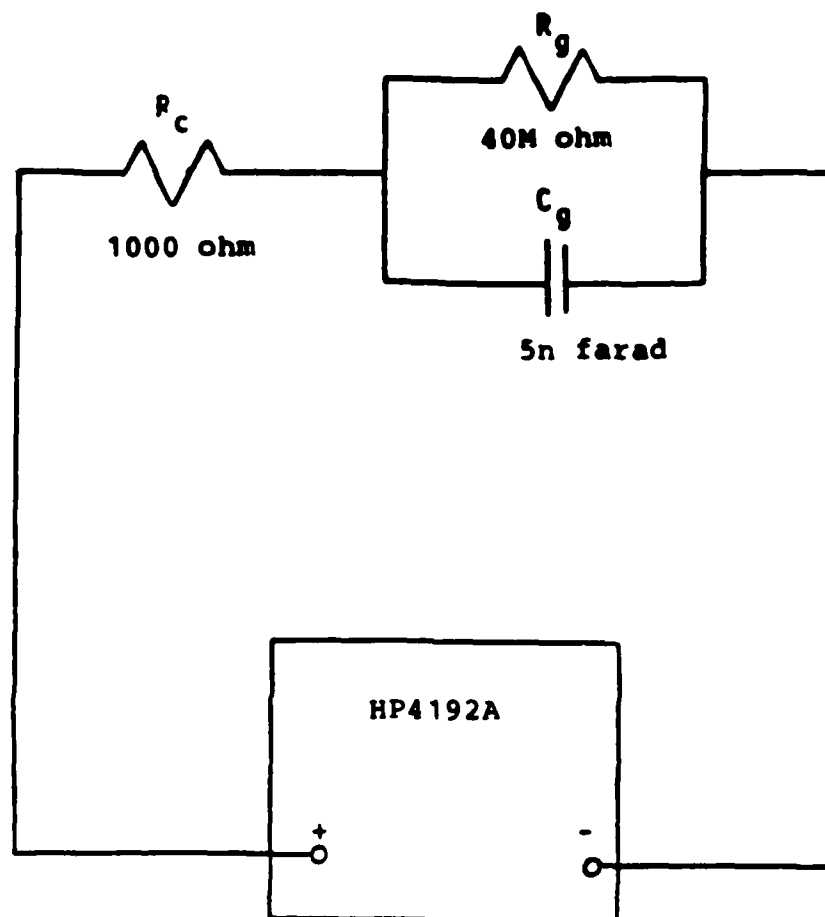


Figure 5-4. Discrete Component Measurements of the Model

the model. Section B of Appendix G supplies the impedances of the circuit of Figure 5-4 that were obtained over the frequency range 5 Hz to 13 MHz. One of the goals of modeling the electrode/electrolyte interface with discrete components was to establish a baseline against which actual measurements would later be compared.

Taking the baseline procedure one step further, the measurement scheme of Figure 5-5 was realized. Distance 'd' between the steel wire electrodes that were immersed in the saline was decreased from approximately one inch to one-half inch, and finally the separation was decreased to a few millimeters. Data collected from the configuration of Figure 5-5 for each of the three electrode separations are provided in Section C of Appendix G. An estimate of 50 ohms for the spreading resistance of the saline can be obtained from the data in Section C of Appendix G.

#### Equivalent Circuit Impedance Measurements

After performing the calibration and baseline procedures for the equivalent circuit impedance measurement scheme, measurements were recorded for actual chips immersed in the saline by using the equipment configuration of Figure 5-2. Since the HP4192A impedance analyzer operates only at frequencies greater than 5 Hz, a Keithley Model 602

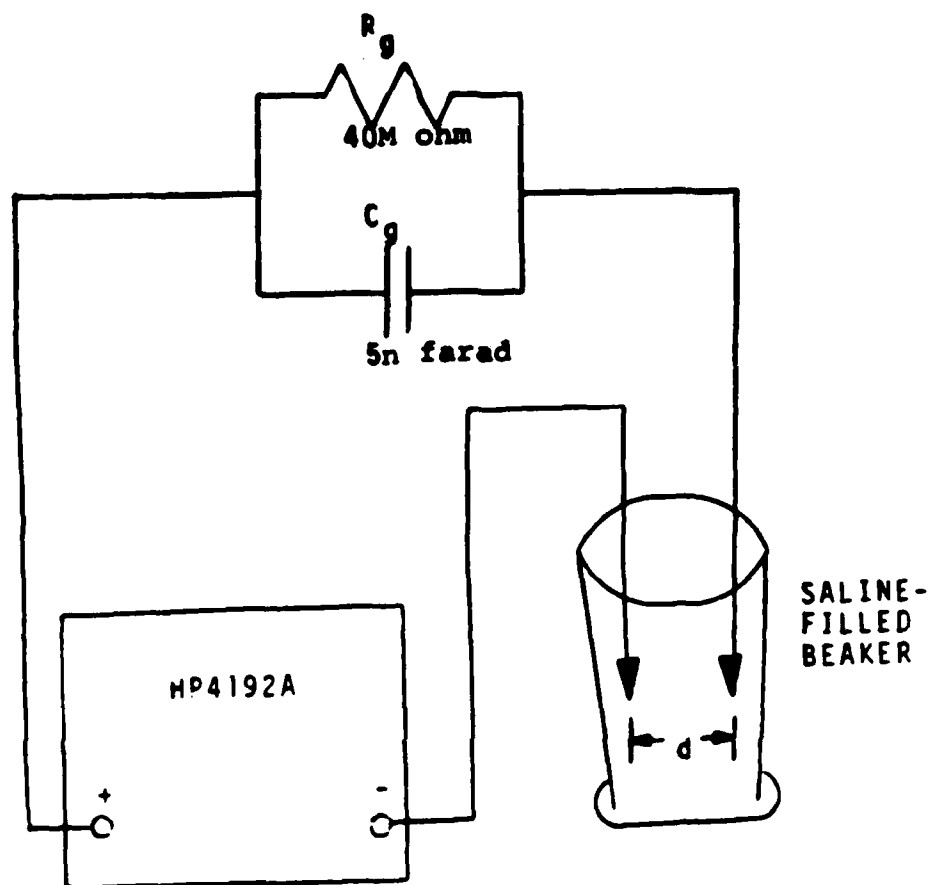


Figure 5-5. Measurements of the Model Using Actual Saline



electrometer was used to obtain the dc measurement of the parallel impedance. The Keithley Model 602 electrometer was physically substituted for the HP4192A impedance analyzer of Figure 5-2, and the dc measurements of the chips were thus realized. The data that was recorded from the three chips is provided in Appendix H in the R(f) column. The R(f) column lists only experimental data, and the R(cal) column tabulates the calculated data points obtained from the nonlinear least squares algorithm.

Prior to testing the second chip in saline, the chip was immersed in DIW and measurements were taken. For each of the nine electrodes designated in Figure 5-1, the impedance of the electrode-solute interface exceeded the measurement range of both the Keithley Model 602 and HP4192A for frequencies in the range dc - 1.0 MHz inclusive. The HP4192A displayed a message to indicate that the impedance exceeded the maximum value (1.3 megohms) of the measurement range by more than 200%. A very large impedance was expected for the entire frequency range because the resistance of DIW (approximately  $10^{16}$  ohms to  $10^{18}$  ohms) is so much greater than the resistive component of the electrode-solute interface.

The calculations of the equivalent electrical circuit parameters that appeared in Appendix H are summarized in Table 5-1. Both resistances and the capacitance of the

Table 5-1

## Calculated Values of Equivalent Electrical Circuit Parameters

Electrode	$R_c$ (kilohms)	$R_g$ (kilohms)	$C_g$ (microfarads)
188	1.49	83.7	0.67
144	1.55	89.0	0.66
1CC	1.27	73.7	0.81
111	1.61	100.2	0.63
1GG	1.57	85.2	0.65
199	1.57	100.2	0.65
177	1.61	91.5	0.64
14D	1.67	97.3	0.66
288	3.17	95.5	0.48
244	2.51	90.6	0.55
2CC	2.96	105.0	0.48
211	3.48	88.0	0.49
2GG	3.17	103.3	0.46
299	3.34	101.2	0.47
277	3.50	92.9	0.46
24D	2.70	89.0	0.55
2D4	4.01	97.9	0.38
388	3.31	91.3	0.49
344	3.77	95.3	0.42
3CC	3.72	91.0	0.44
311	2.94	104.6	0.47
3GG	4.27	83.9	0.42
399	2.76	95.8	0.53
377	3.41	91.0	0.51
34D	2.78	98.8	0.45
3D4	3.64	87.1	0.43
-----			
Mean	2.74	93.2	0.53
Standard Deviation	0.92	7.39	0.11

equivalent electrical circuit model are provided for each of the electrodes of the three chips that were tested.

In addition to the experimental data in the R(f) column of Appendix H, the data calculated by the Levenburg-Marquardt nonlinear least squares curve-fitting algorithm is provided in the R(cal) column. By invoking the Decgraph and Plot programs and the Laser software utilities on a VAX 11-785 configured with the VMS operating system, curves of the experimental and calculated data points were generated on a laser printer. The graphs of the curves for each electrode of all three chips are presented in Appendix I. Curves of both the experimental and calculated data points appear on the same graph and can be visually inspected for their "goodness of fit." All of the curves bear the characteristic "reverse S," or sigmoidal, shape that was predicted for the equivalent circuit of the electrical model.

An observation that can be made, both from the data of Appendix H as well as from the curves of Appendix I, is that the calculated data points generated by the nonlinear least squares algorithm did not settle to the high frequency value of the experimental data of approximately 100 ohms. For the first chip, the calculated data settled to approximately 1500 ohms at the high frequency limit. The suspicion that more data points were required by the nonlinear least squares

algorithm in the area of greatest change of the curve, the "knee" of the curve, prompted the collection of additional experimental data points within frequencies bounded by the knee. The additional data points were collected during testing of both the second and third chips.

As the data of Appendix H and the graphs of Appendix I show, the addition of experimental data points to the knee of the curve resulted in a greater discrepancy between the high frequency settling values of the experimental and calculated responses. The calculated data settled to approximately 3000 ohms as the frequency was increased. Since the high frequency limit of the parallel impedance approximately yields the spreading resistance of the s-line,  $R_c$ , the values of  $R_c$  that appear in Table 5-1 need to be examined further. Obviously, the value of  $R_c$  should be approximately 100 ohms since the experimental data clearly reflects this trend. Hence, the values of  $R_c$  shown in Table 5-1 need to be corrected to avoid the difficulties that had been uncovered in the method of processing the raw data. Table 5-2 presents the corrected values of  $R_c$ .

The significant deviation of the calculated data points from the experimental data points at very high frequencies can be attributed to the large spread in the magnitude of the parallel impedance for the experimental data. The range of

Table 5-2  
Corrected Values of  $R_c$

Electrode $R_c$ (ohms)	
-----	
188	127
144	118
1CC	110
111	112
1GG	77.5
199	102
177	101
14D	100
288	102
244	101
2CC	106
211	80.0
2GG	101
299	97.1
277	103
24D	111
2D4	102
388	98.0
344	111
3CC	103
311	98.0
3GG	100
399	102
377	102
34D	101
3D4	104
-----	
Mean	98.8
Standard Deviation	22.0

the parallel impedance of experimental data spans three orders of magnitude, declining from 100K ohms to 100 ohms as the frequency increases. Hence, residuals that are small in comparison to 100K ohms are large in comparison to 100 ohms. The sums of squared residuals that appear in Appendix H for each electrode should be reduced to effect a superior curvefit at the higher frequencies. Note that the standard deviations provided in Appendix H are significantly greater than the 100 ohms high frequency settling value of the experimental data. The sums of the squared residuals can be reduced by minimizing the standard deviations, and a better curvefit can be realized by decreasing the standard deviation to a value that is comparable to the high frequency parallel impedance of 100 ohms.

An attempt to reduce the residual errors was initiated by implementing a recommendation in the computer code that the initial estimates of the three input parameters ( $R_g$ ,  $C_g$ , and  $R_c$ ) should be normalized to a value between zero and one. This method was attempted on an electrode from each of the three chips. The results that derived from the scaled inputs of the three electrodes are presented in Appendix J. A comparison of the results in Appendix J to the corresponding results in Appendix H reveals that no significant changes occurred by scaling the inputs.

Although the basic shape of the curves agrees with the theoretical predictions that stem from an analysis of the equivalent electrical circuit model, the dc and very high frequency limits of the impedance differed from the values that were predicted by as many as two orders of magnitude. It is possible that, at high frequencies, the assumption of the frequency independence of the model's parameters becomes invalid. For the experimental data, the impedance at the low frequency dc limit approximates  $R_g$ , and the approximate value of 100K ohms is several orders of magnitude less than the 40M ohms value that was predicted. The impedance at the high frequency limit approximates  $R_c$ , and the approximate value of 100 ohms was one order of magnitude less than the predicted value of 1000 ohms. Although the value of the capacitance,  $C_g$ , cannot be deduced from a mere visual inspection of the frequency response curves of Appendix I ( $C_g$  impacts the breakpoints and slope of the knee of the curve), the value can nonetheless be calculated. The calculated value of  $C_g$  in the neighborhood of 0.65 microfarads is two orders of magnitude greater than the predicted value of 5 nanofarads.

Many possible explanations of the discrepancy between the theoretical and experimental values of the parameters of the equivalent electrical circuit model can be offered. First of all, the three-element (frequency-independent),

lumped-parameter model of the distributed network of complex impedance components that actually constitute an electrode/electrolyte interface is a simplification that could introduce a discrepancy between theoretical and experimental results. Second, the theoretical treatment of an electrode immersed in an electrolyte is not conclusive, as evidenced by the different models and results that have been reported. Third, the theoretical calculations relied upon certain assumptions. One such assumption is that the electrode in contact with the electrolyte was composed of pure aluminum; however, the formation of an oxide at the surface of the electrode is certainly a possibility that cannot be ignored. The processing of the chip that preceded the actual in vitro testing may certainly be responsible for deviations of the parameters that were used in the theoretical calculations. Several explanations of the discrepancy between the predicted and actual results have been offered, and other possibilities could certainly be conjectured.

A problem surfaced after tests had been performed on the first chip. As anticipated, the aluminum electrodes reacted with the saline, and a microscopic examination of the chip after it had been removed from the saline revealed that the deterioration had proceeded faster than expected. Figure 5-6





Figure 5-6. Condition of the Electrodes after Testing

shows the condition of the electrodes after performing the equivalent circuit impedance measurements on all of the electrodes that were tested. The deduction that the deterioration of the electrodes may have affected the experimental results is plausible because the surface geometry of the electrodes was certainly altered in this process. After performing a complete set of continuous measurements, the chips were carefully rinsed in DIW and mechanically agitated in an attempt to flush the reactive ions of the saline and stop the deterioration of the electrodes. The precautions that were taken, however, proved to be futile. As can be observed in Figure 5-7, the electrodes severely deteriorated in the 24-hour period following the rinse of a contaminated chip in DIW.

Despite the unexpectedly quick and massive deterioration of the exposed aluminum electrodes, the areas of the chip that were encapsulated in polyimide showed no signs of ion penetration whatsoever. No deterioration of the wirebonds occurred since they were composed of gold. The solder joints of electrode pads that were wirebonded did not deteriorate, but the exposed aluminum surrounding the joints often deteriorated severely enough to cause the wirebond to separate from the pad.

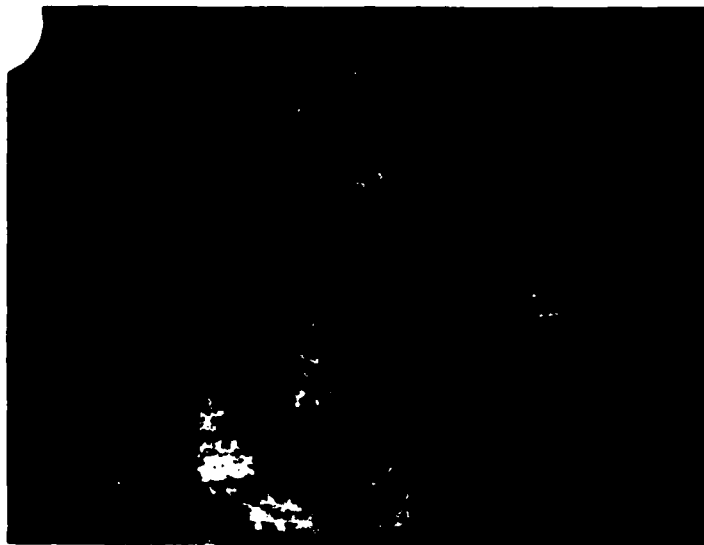


Figure 5-7. Condition of the Electrodes 24 Hours  
after Immersion in Saline

### Determination of the Maximum Scan Rate

In order to ascertain the maximum rate at which the multielectrode array can be scanned, initial assumptions had to be made concerning the nature of the brain signals that will be received. The brain signals will be received while a light strobe is employed as the external stimulus. A square pulse 1 millivolt in amplitude and 40 milliseconds in duration (25 Hz) was chosen to model an actual brain signal.

The method of determining the maximum scan rate of the array hinged upon propagating the known "brain signal" of the source into the saline and recording the signal received at an electrode. Load resistance  $R_L$  in Figure 5-3 was varied between 100, 1000, and 10,000 ohms for each electrode, and pictures were taken of the oscilloscope traces that resulted from each load resistance. Channel 1 of the oscilloscope recorded the source input pulse, and Channel 2 recorded the pulse that was received at an electrode after it had traversed the electrolytic medium and the electrode/electrolyte interface.

The second test, the determination of the maximum scan rate of the array, was conducted on only the second and third chips. Preparations to conduct the second test were not complete at the time that the first chip was immersed in a saline, and the subsequent deterioration of that chip

eliminated the possibility of performing the second test. In the tests of the second and third chips, however, two separate equipment configurations were arranged. One group of equipment was used in the first test, and another group of equipment was used in the second test. In this manner, both tests were sequentially performed on a given chip, thus minimizing the problem of chip deterioration.

The same electrodes used in the first test were also used in the second test. This arrangement facilitated the expediency of recording the results of the two tests in a timely fashion. The results are provided in Appendix K in the form of oscilloscope pictures, and the electrode codes introduced in Figure 5-1 are again used to identify the electrodes.

In a fashion analogous to that of the first test, a chip was immersed in DIW, and pictures were taken. As expected, the high resistance of the DIW resulted in the attenuation of the signal, causing the oscilloscope trace to resemble that of an open circuit. No signal whatsoever was discernible at any of the electrodes while they were immersed in DIW.

The effect of the electrode-solute interface upon the "brain signal" of the source is visible in the photos of Appendix K. The capacitive charging and discharging of the

square pulse caused a "lengthening" of that pulse, and this added delay will limit the maximum scan rate of the array. The distortion of the pulse worsened with increases of the load resistance. Obviously, the duration of a distorted pulse impacts the ability to distinguish the beginning and the end of that pulse.

The beginning of a pulse is fixed with respect to the start of the source input pulse, so only the endpoint of the pulse requires interpretation. The 3 dB point was adopted in an attempt to analytically define the cutoff of a distorted pulse. The technique employed to determine the pulse delay, which was used to calculate the maximum scan rate, involved determining the point 3 dB below the maximum value of the pulse and extrapolating to the time axis. Figure 5-8 demonstrates the technique applied to a typical electrode with  $R_L = 100K$  ohms. In Figure 5-8,  $H$  is the signal amplitude,  $H'$  is the 3 dB point,  $T$  is the period of the input pulse, and  $T'$  is the period of the received pulse. Linear measurements of these parameters were made, and the measurements were then converted to units of time to obtain the scan rate.

The maximum scan rates of the nine electrodes on both the second and third chips were determined. For each electrode, individual scan rates were calculated for each of

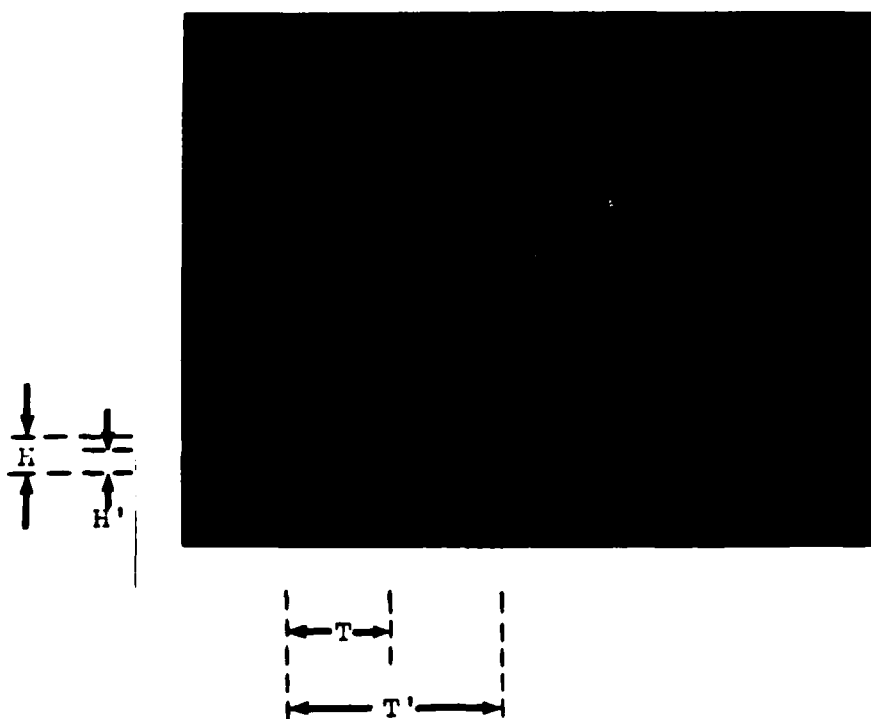


Figure 5-8. Determination of the Maximum Scan Rate of the Array

the three load resistances that were electrically connected in series with the measurement circuit. Values of the maximum scan rates of the electrodes of the second and third chips with series-connected load resistances of 100, 1000, and 10,000 ohms are presented in Table 5-3. The ideal scan rate that is obtained with an undistorted pulse is 6400 Hz. Note that for a series-connected load resistance of 100 ohms, the ideal maximum scan rate was achieved.

From the results of the second test, it is clear that a lower series-connected load resistance effectively reduces the distortion of the pulse that is received. Therefore, the scan rate of the array can be maximized by decreasing a series-connected load resistance. Alternatively, the array scan rate can be maximized by increasing the resistance of a parallel load. An amplifying stage is used to boost the actual brain signals, and the input impedance of this amplifying stage can be substituted for the load resistance of the model if the amplifier is serially connected to the measurement circuit. Hence, an amplifier should be selected so that the characteristic distortion of the input pulse is minimized. By optimizing the amplifier input impedance, the scan rate of the array can be maximized. The optimal input impedance is small if the amplifier is serially connected to the measurement circuit, or it is large if the amplifier is



Table 5-3

## Maximum Scan Rates of the Electrodes

Electrode	Scan Rate (Hz)		
	-----		
	R <sub>L</sub> (ohms)		
	100	1000	10000
-----	---	----	-----
288	6400	6180	5670
244	6400	6210	5930
2CC	6400	6210	5850
211	6400	6120	4920
2GG	6400	6340	5710
299	6400	6280	5650
277	6400	6220	5980
24D	6400	6240	5900
2D4	6400	6270	5900
388	6400	6240	5820
344	6400	6120	5770
3CC	6400	6180	5540
311	6400	6180	4790
3GG	6370	5980	4730
399	6400	6240	5840
377	6400	6210	5980
34D	6400	6190	5140
3D4	6400	6180	5800
-----			
Mean	6400	6200	5610
Standard Deviation	7.07	76.4	415

connected across the measurement circuit. From the quality of the 100 ohms series-connected load resistance pulses that appear in Appendix K, it can be deduced that further decreases of the load resistance will not significantly improve the maximum scan rate of the array. Hence, the goal of a 100 ohms (series-connected) amplifier input impedance should suffice to maximize the scan rate of the array.

The contention that the optimal array scan rate is achieved by decreasing the series-connected load resistance is supported by the observation that the low frequency limit of the model's (Figure 3-2) parallel resistance is given by:

$$\lim_{f \rightarrow 0} R_p(f) = (R_c + R_g). \quad (5-1)$$

A small series-connected load resistance effects the isolation of the bioelectric response so that the distortion of the recorded signal is minimized.

An examination of the spatial behavior of the electrodes, as presented in Appendix K, does not seem to identify a correspondence between the geographic location and the scan rates of the array electrodes. Parallels between an electrode's location and its effect upon the pulse delay do not appear to be evident. A possible explanation of this result concerns the wavelength of a 25 Hz excitation. The wavelength of a 25 Hz excitation is large in comparison with

the distances between the electrodes, and the effect of an electrode's location upon a brain wave may thus be negligible.

#### Summary of Results

The results obtained from an in vitro test of AFIT brain chips indicates a degree of validity in the model of the electrode/electrolyte interface that was chosen. Despite differences in the predicted magnitudes of the model's parameters, the basic frequency response that the model predicts was indeed descriptive of the actual response that was obtained from chips in a saline environment.

## 6. CONCLUSIONS AND RECOMMENDATIONS

### Conclusions

After reviewing several models of the interface kinetics that describe a metal electrode in contact with an electrolyte, the Robinson configuration was chosen because of a correspondence between its parameters and the physical processes that are associated with the implantation of a multielectrode array onto a cortex. A simpler, but essentially equivalent, model was derived from Robinson's configuration and applied to the task of characterizing the interface between an electrode and a saline electrolyte. Predictions concerning the measurement of electrical parameters were extracted from the model. The model's ability to characterize the interface kinetics was tested by measuring the parameters of actual brain chips immersed in a saline electrolyte. Finally, the limiting effect of the interface upon the maximum scan rate of the multielectrode array was investigated.

A total of three chips were immersed in a saline solution. Equivalent circuit impedance measurements were performed on all three of the test chips, and the maximum scan rate of the array was investigated for two of the chips.

A spatially distributed subset of electrodes of the array was used in each of the tests. Data collected in the impedance measurements were tabulated in the form of a frequency-dependent parallel impedance, and data used to determine the maximum scan rate of the array were collected in the form of oscilloscope traces of signal waveforms.

Parallel impedance measurements were used to calculate the frequency-independent parameters of the equivalent electrical circuit model. An initial attempt to measure the parallel impedance with a voltage-divider technique revealed that only the magnitude of the phasor could be collected by this method. Rather than develop a second technique to obtain the phase angle, an impedance analyzer was employed in the measurement scheme. Since the empirical data that were obtained contain measurement errors, a nonlinear least squares technique was used to generate the best-fit curve of the data. A computer program employed the Levenburg-Marquardt algorithm to generate a set of calculated data points of the fitted curves, and these data points were plotted to yield the frequency response characteristic of the electrode-solute interface.

The data (presented in Appendix H) are well-behaved at low frequencies, but, as the frequency increases, the parallel resistance parameter converges on values that are

greater than expected by one order of magnitude. The possibility that the assumption of frequency independence of the model's parameters breaks down at high frequencies cannot be ignored. The behavior of the component measurements of Appendix G at high frequencies similarly reflects the assertion that high frequency measurements may be difficult to obtain. An examination of the standard deviations that appear in Appendix H for the measurements of each electrode reveals that the deviations are significantly greater than the expected values of the high-frequency parallel impedance parameter. A better fit of the curve at high frequencies would be possible if the value of the standard deviation of the measurements was reduced.

A whole host of factors may be responsible for the variation of the theoretical model parameters from the actual results, but the tendency of the nonlinear least squares curve-fitting routine to deviate from the experimental high frequency values of the parallel impedance appears to be inherent to the algorithm employed. An investigation of either a more efficient algorithm or a more accurate calculation routine would enhance the worth of this valuable tool in future research efforts. The employment of a more accurate calculation routine, however, might be constrained by the resource limitations of the VAX 11-785 since the

existing program utilizes a sizable amount of computer resources. Within its limitations, the present program was certainly an important and useful tool for the analysis of the parallel impedance data.

The rapid deterioration of the exposed aluminum contacts should be taken into consideration before further research is performed. Since other researchers have reported superior resistance of exposed aluminum electrodes to the saline solution (1:15, 3:IV-21), other processing techniques of encapsulating a chip and etching contact windows should be investigated. An observation that can be made from this research is that multiple coats of polyimide may be redundant since the exposed aluminum deteriorates faster than ions penetrate the encapsulating layer. A reduction of the number of processing steps can provide time savings of days or even weeks. Two coats of polyimide certainly seems to be sufficient to perform tests that can be accomplished within several days.

Because of the limiting effect of the Helmholtz double layer capacitance, the maximum scan rate of the multielectrode array was influenced. A square wave pulse that simulated the VER triggered by a strobed light source was propagated into a saline bath. The electrodes of an immersed brain chip received the simulated brain signal, and

an oscilloscope trace of the signal was photographed. From these photographs, interpolated measurements were extracted and the maximum scan rate was calculated. The effect of the input impedance of an amplifying stage on the maximum scan rate was investigated by varying the series-connected load resistance of the measurement circuit. The effect of the load on the maximum scan rate of the array was significant, and an optimal series-connected load resistance of 100 ohms was found that will permit scanning the array at nearly the ideal rate without a loss of information.

#### Recommendations

The investigation of the equivalent electrical circuit model and the maximum scan rate of the array revealed several deficiencies that should be resolved in future research of the electrode-solute interface of implanted brain chips. One problem area that could be investigated is the discrepancy between the calculated and empirical values of the parameters of the model. The proposed model should either be modified or replaced, and a new model that better describes the nature of the interface kinetics could then be applied to the interpretation of results derived from the actual implantation of a brain chip. A possible area of further research is the frequency dependence of the model's parameters. Frequency



independent model parameters were assumed in this investigation. A good model of the electrode-solute interface will provide an insight into the interpretation of brain signals that are collected during an actual implant.

Another problem that surfaced was the apparent inability of the curve-fitting routine to provide a reasonable prediction of data in the high frequency spectrum of the response. Several explanations of this behavior were proposed, and methods of correcting the incongruity were attempted. The solution to this problem, however, was not found. Although analysis tools were used to supply a more accurate estimate of the saline spreading resistance, the least square curve-fitting routine should be modified so that a unified, consistent, and automated tool will be available to future investigators. A possible approach to improving the nonlinear least squares computer program is to implement a weighting system that partitions the residuals into adjacent groupings. The groupings should be partitioned so that the difference between the minimum and maximum values is less than a threshold value.

The unexpected rapid deterioration of the aluminum electrodes that were exposed to the corrosive saline did not severely hamper the experimental portion of this research, but this deterioration is unacceptable for experiments

similar to the beagle implant. A better method of processing implantable brain chips should be devised. Despite the rapid deterioration of exposed aluminum electrodes, the two coats of polyimide effectively protected the multiplex circuitry. Because of the difficulty of applying successive layers of polyimide by the traditional spinner method, three coats of polyimide were not used to protect the multiplex circuitry. In contrast with Sopko's recommendation to use five coats of polyimide (29:VI-2), two coats of polyimide successfully protected the chips used in this research. Future attempts to apply three or more coats of polyimide are not recommended since adequate protection can be obtained with two coats.

The application of a low input impedance amplifying stage in series with the measurement circuit (or high input impedance amplifying stage in parallel with the measurement circuit) to boost the received brain signals to a usable level during an implant is strongly recommended. For square wave pulses, the charging and discharging effects of the Helmholtz double layer capacitance limit the maximum scan rate of the array. The scan rate reaches its maximum value for a series-connected load resistance of approximately 100 ohms. Any reduction of the load below 100 ohms will not significantly improve the scan rate of the array.

## APPENDIX A

### Design of a CMOS AFIT Brain Chip

The design of a chip that will be implanted into a rhesus monkey must reflect the requirements that are peculiar to this special application. Two previous designs of the AFIT brain chip (1,6) exhibited a progressive pattern of development with respect to the physical, as well as functional, characteristics. The original design of the AFIT brain chip, a 4 x 4 JFET array, was conceived by 2Lt Joseph Tatman in 1979 (6). In 1983, Capt Robert Ballantine designed two versions of a new generation of AFIT brain chips (9). The new brain chips utilized nMOS technology and included a 16 x 16 array of pass transistors in addition to processing circuitry designed to limit the number of output wires by using a time multiplexing scheme. Despite making changes intended to improve various measures of performance (3:II-1), Ballantine preserved the functional characteristics of the earlier version designed by Tatman. A similar approach was adopted in creating this newly designed AFIT brain chip that succeeds Ballantine's version.

Many architectural and functional characteristics of this design correspond to characteristics of Ballantine's

approach, but various details have been altered for the sake of enhancing the capabilities of the AFIT brain chip. Numerous engineering decisions were made that impact both the design and performance of the chip. Like the vast majority of engineering designs, conflicting requirements necessitated compromises. An overall design philosophy provided a basis for making decisions that affected the layout of the chip. Elements of this overall design philosophy were reflected in the various decisions that were made before submitting the chip for fabrication. Examples of these design decisions include the commitments to minimize the complexity, reduce the number of connections between the chip and the outside world, and to fabricate electrodes as close as possible to the ideal size of 100 square microns (1:3).

#### Reasons for a New Design

Ballantine actually designed two versions of the AFIT brain chip. Functional testing of both versions by Michael McConkey (3:11-4, 11-5) revealed that the first version was fully operational, but that the second version, a modified copy of the first version, malfunctioned. The exact cause of the malfunction eluded a conclusive determination (3:F-19). Both versions feature a 16 x 16 array of electrodes controlled by a corresponding array of n-type pass

transistors. In the first version, a 16 x 1 multiplexed select line enabled and disabled a row of the pass transistors, and an output signal was obtained from the output of each of the sixteen column elements. Both the rows and columns were multiplexed in the second version, and the output signal was determined by the count states of both the row and column multiplexers. Figures A-1 and A-2 provide the physical layouts of the first and second versions, respectively.

In the first version designed by Ballantine, sixteen output leads are necessary to capture the data from each of the 256 electrodes. In the second version, only one output lead is required to effectively capture all of the electrode responses. The decrease from sixteen output leads to a single output lead significantly reduced the number of wires that had to be harnessed and routed to the chip. One desired result of the 1986 AFIT brain chip research is to minimize the number of wires that must enter the skull of the rhesus monkey. Hence, either the correction of Ballantine's second design or the development of a new version had to be accomplished.

After weighing all of the factors involved, the decision was made to redesign the circuit, but retain the basic architectural scheme that Ballantine had devised. A cursory

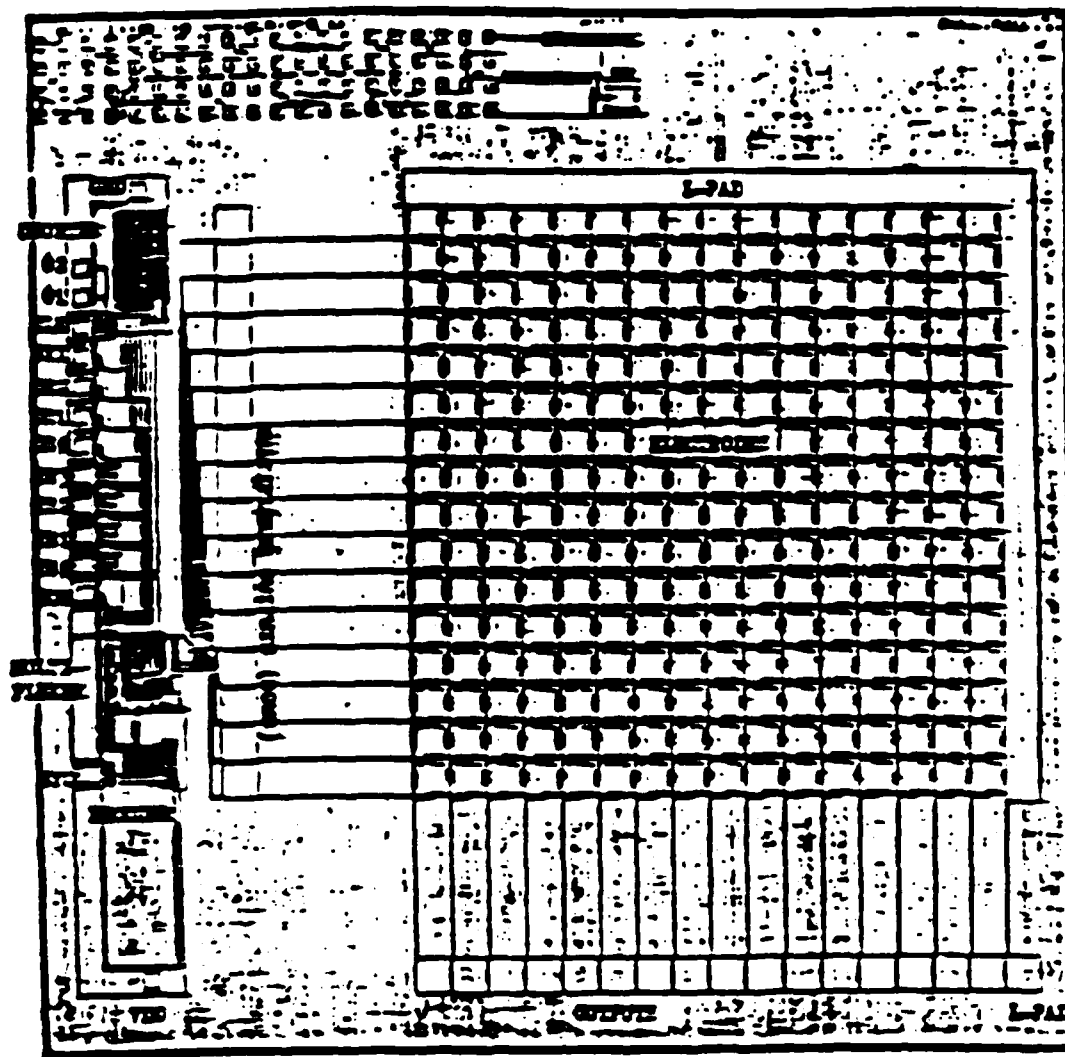


Figure A-1. Brain Chip with Count-Selectable Multiplexer  
(3:I-4)

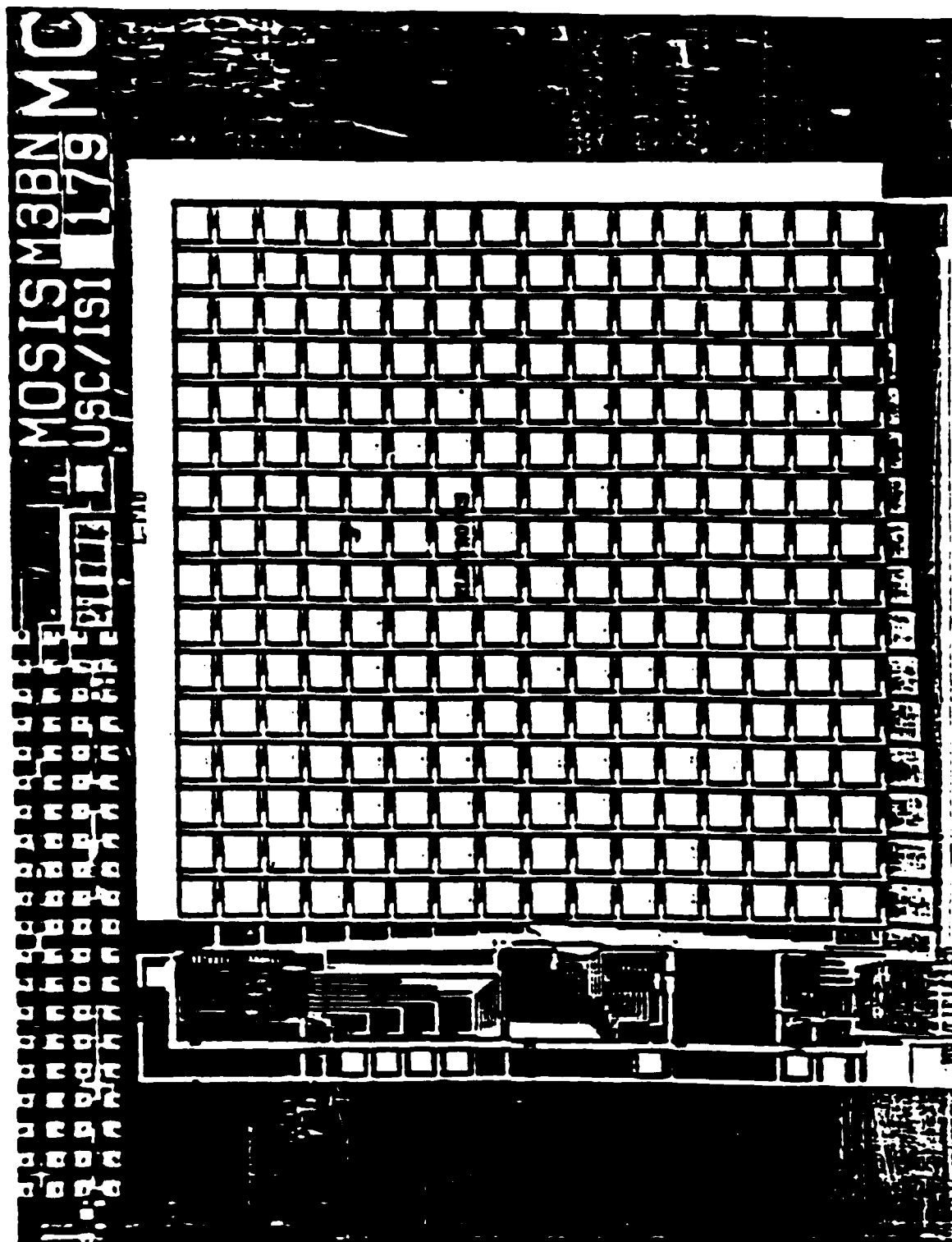


Figure A-2. Brain Chip with Count-Selectable Multiplexer and Multiplexed Outputs (3:I-6)

review of Ballantine's circuit revealed areas where both the efficiency of design, as well as the performance, might be improved. Since AFIT has demonstrated a considerable interest in 3-micron CMOS computer-aided-design (CAD) technology, as evidenced by the curriculum of EENG 695, VLSI Design, CMOS was the technology chosen for the new design. The advantages of replacing nMOS with CMOS circuitry include, but are not limited to, smaller feature size and lower power consumption (31:4). Table A-1 provides a comparison of the nMOS and CMOS technologies.

Another factor that influenced the new design of the AFIT brain chip was the optimization of the electrode surface area. Electrodes in Ballantine's chip measured 180 x 180 microns (3:II-4), encompassing approximately four times the corresponding surface area of the maximum optimal size of 100 x 100 microns of the basic computing elements, or cortical columns, of higher order mammals (3:I-1). Since the primary objective of future AFIT brain chip research is to model the electrode/electrolyte interface kinetics anticipated for the rhesus monkey implant, the decision was made to scale the electrodes down to a more physiologically appropriate dimension of 100 microns.

In all, three factors influenced the decision to design a new AFIT brain Chip. First, the desirable row and column



**TABLE A-1**  
**Comparison of nMOS and CMOS Technologies (28:28)**

CMOS	nMOS
(i) Logic Levels	
• Fully restored logic, i.e., output settles at $V_{DD}$ or $V_{SS}$ (GND).	• Output does not settle at $V_{SS}$ (GND) — hence degraded noise margin.
(ii) Transition Times	
• Rise and fall times are of the same order.	• Rise times are inherently slower than Fall times.
(iii) Transmission Gates	
• Transmission gate passes both logic levels well. The output of transmission gate can be used to drive the input of other transmission gates.	• Pass transistor transfers logic '0' well but logic '1' is degraded. Pass transistor cannot drive the gate of a second pass transistor.
(iv) Power Dissipation	
• Almost zero static power dissipation. However power is dissipated during logic transition.	• With output of a given gate = '0' power is dissipated in the circuit in addition to power dissipated during logic transitions.
(v) Precharging Characteristics	
• Both n-type and p-type devices are available for precharging a bus to $V_{DD}$ and $V_{SS}$ . Nodes can be charged fully to $V_{DD}$ or alternatively to $V_{SS}$ in a short time.	• With enhancement mode transistor the best one can do (with normal clocking) is to charge a bus to $(V_{DD} - V_t)$ . Generally use of bootstrapping or hot clocking is needed to precharge to $V_{DD}$ .
(vi) Power Supply	
• Voltage required to switch a gate is a fixed percentage of $V_{DD}$ .	• Somewhat dependent on supply voltage.
• Variable range 1.5 to 15 volts.	• Fixed.
(vii) Packing Density	
• Require $2N$ devices for $N$ inputs for complementary static gates. Less for dynamic gates.	• Require $(N + 1)$ devices for $N$ inputs
(viii) Pull-up to Pull-down Ratio	
• Load-to-driver device ratio is typically 1:1 or 2:1.	• Load-to-enhancement-driver ratio is typically 4:1 to optimize the logic '0' output level and minimize current consumption.
(ix) Layout	
• CMOS encourages regular layout styles.	• Depletion load and different driver transistor sizes inhibit layout regularity.

multiplexed design of Ballantine did not function as intended. The degree of difficulty in resolving a problem with another's design, a design more than three years old in this instance, can exceed the difficulty associated with redesigning the circuitry. Thus, a new design was accomplished as the course project for EENG 695, VLSI Design (Spring Quarter, 1986). In addition, the creation of a new design, as opposed to correcting an error in the original design, was a more positive engineering approach. Second, the predominance of available CMOS design tools and techniques and the associated advantages of CMOS processing technology favored a redesign of the AFIT brain chip. Finally, Ballantine's design did not absolutely fulfill design objectives of the rhesus monkey implant since the dimensions, 180 x 180 microns, of the electrodes were above the maximum optimal size of 100 x 100 microns.

#### Description of the Revised Design Approach

In the revised design of the AFIT brain chip, several overall approaches were considered. Two of the many possible approaches are shown in Figure A-3. In the first approach, two clock phases, one reset, one Vdd, one ground, and the single output constitute a harness of six wires that must enter the monkey's skull. Of these six leads, Vdd, ground,

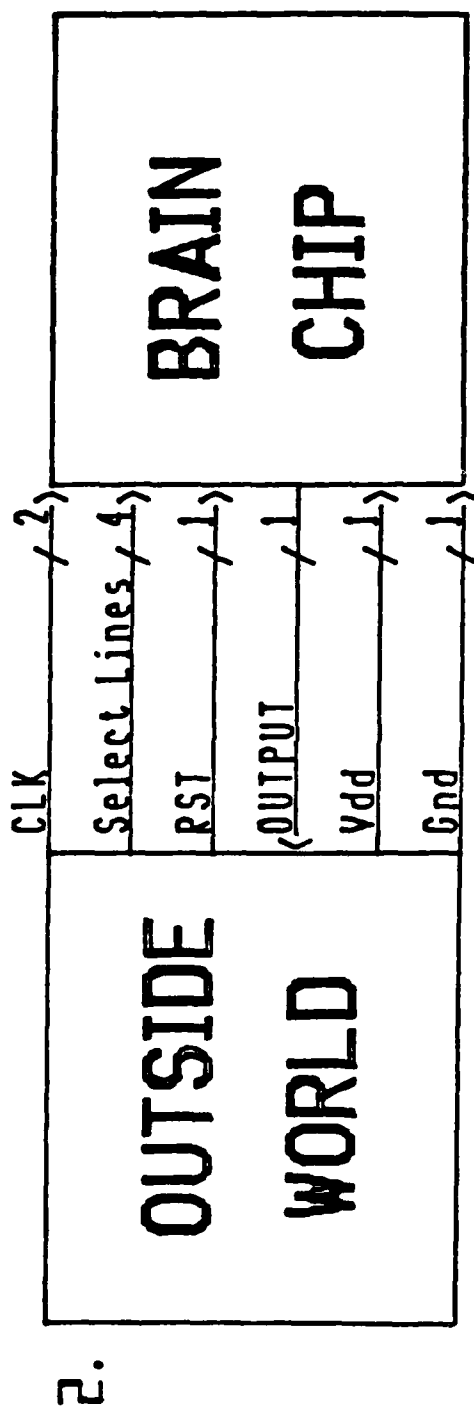
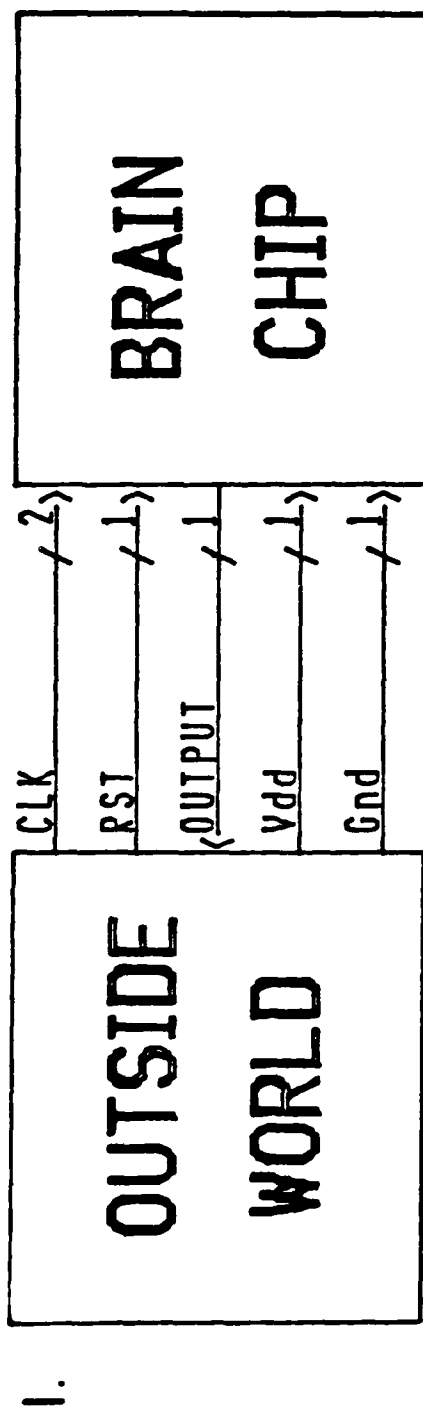


Figure A-3. Two Possible Approaches in the System Definition

and the output cannot be eliminated and must therefore enter through the monkey's skull.

In the second approach, the four control select lines needed to address each of the sixteen rows and columns of the brain chip are generated externally and transmitted through the monkey's skull via a harness of wires. Although this approach would eliminate the counter onboard the chip, and thereby reduce the complexity of the design, an undesirable penalty of an additional four wires entering the monkey's skull would be incurred. Since the number of wires entering the monkey's skull was deemed more critical than the addition of a counter to the circuitry of the brain chip, the first approach was chosen for this new design.

The system architecture of the new design resembles the architecture of Ballantine's fully multiplexed brain chip, but several features were altered for the sake of reducing the complexity and tailoring the input/output (I/O) circuitry for testing requirements of this research. The architecture of Ballantine's brain chip, shown in Figure A-4, can be compared to the architecture of the new design, shown in Figure A-5. The most obvious difference between the two designs is the number of functional units in each. Ballantine's design requires five functional units (counter, decoder, two multiplexers, and multielectrode array), whereas



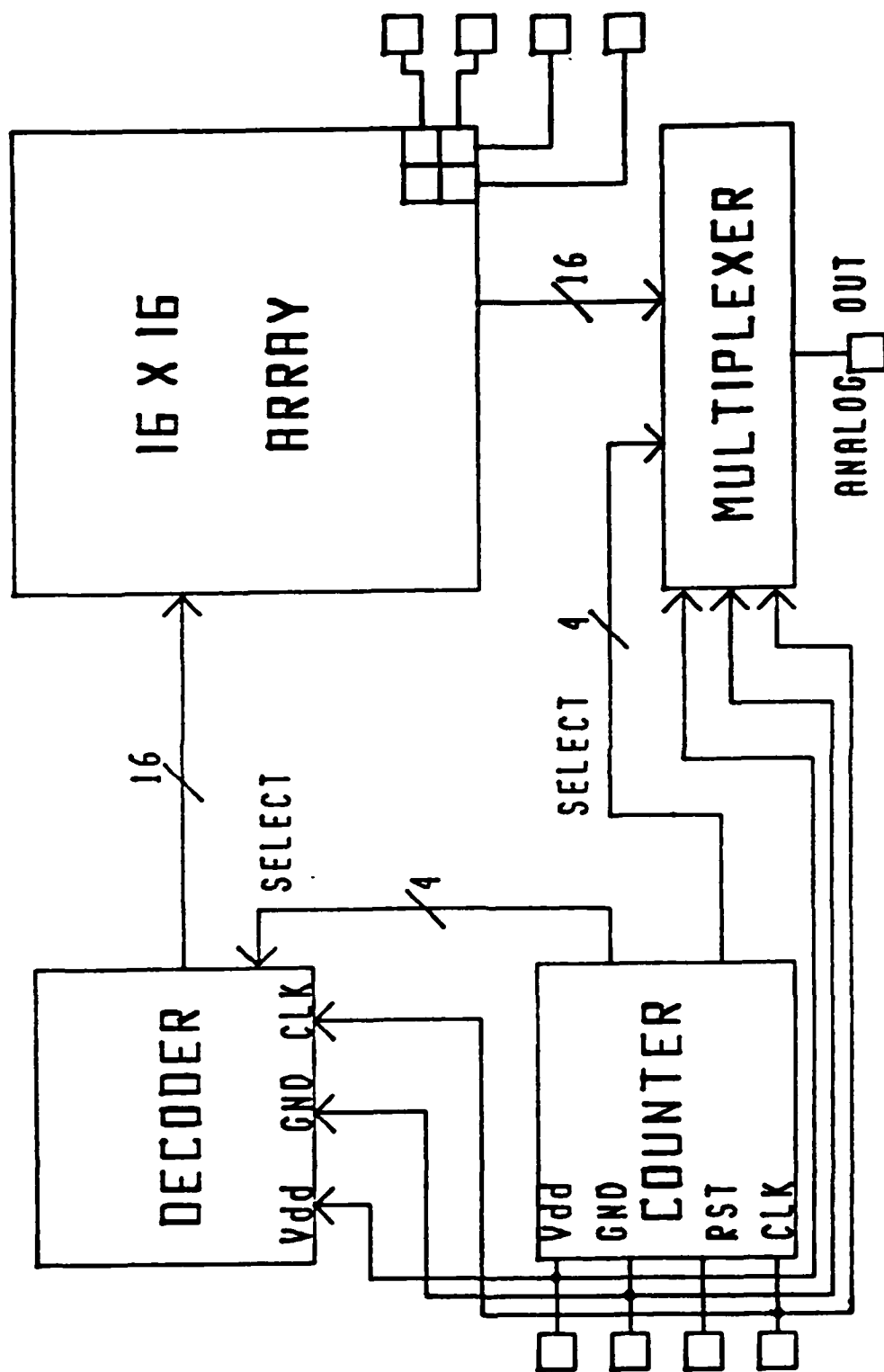


Figure A-5. Architecture of the CMOS AFIT Brain Chip

the new design requires only four functional units (counter, decoder, multiplexer, and multielectrode array). The elimination of a functional unit, and the consequential reduction in complexity, was obtained while preserving brain chip functions essential to both the next implantation and characterization of the electrode/electrolyte interface kinetics.

Other distinctions between the two designs also exist. The Ballantine design contains extra pads and circuitry necessary for manual selection of various count patterns for all of the 256 electrodes. In the new design, a 2 x 2 subset of the 16 x 16 array can be selected manually. This 2 x 2 subset array will be driven by external signals applied to the output pads. The Ballantine design utilizes an L-shaped metal strip as the reference plane for the electrodes. However, the reference plane cannot simultaneously maintain an equi-potential with respect to each of the 256 electrodes in Ballantine's design due to the varying geometrical spacings between the electrodes and the reference plane. A reference plane was unintentionally omitted in the new design; another electrode or the substrate of the chip may be used as the reference plane for testing purposes. A suggestion for future designs is to include a grid of equi-distant interconnected metal strips in the design of the

multielectrode array. In the new design, enough space is available between electrodes to include such a reference grid. This grid should be designed such that the metal strips in every row and column are equidistant from all of the electrodes in that row or column. Hence, the variable spacing between the electrodes and the reference plane would be eliminated. Unfortunately, the development of this idea occurred after the chip had been submitted for fabrication, so inclusion of this simple reference grid in the design will be left to a future circuit revision.

With the overall system description and chip architecture formulated, actual implementation of the necessary circuitry proceeded next. An unfamiliarity with VLSI design made it necessary to return to basic building blocks for the implementation of the circuitry. The basic building blocks were implemented at the gate level (AND gate, OR gate, et cetera) to produce the functional units (counter, decoder, multiplexer, et cetera) that appear in the architectural description of this chip. The actual gate-level description of the functional units was obtained from the CMOS Databook, published by National Semiconductor (32). Gate-level descriptions for quarter sections of two of the functional units, namely the decoder and the multiplexer, are shown in Figures A-6 and A-7.



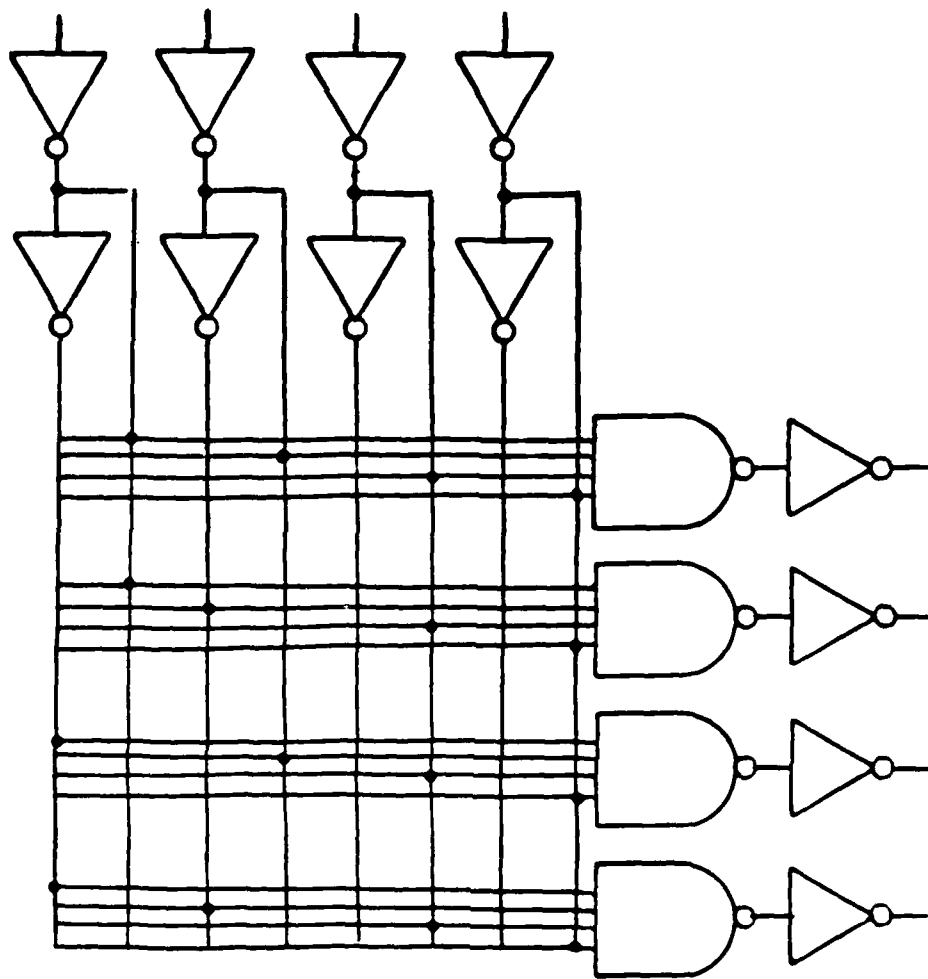


Figure A-6. Schematic of a Quarter Section of the Decoder

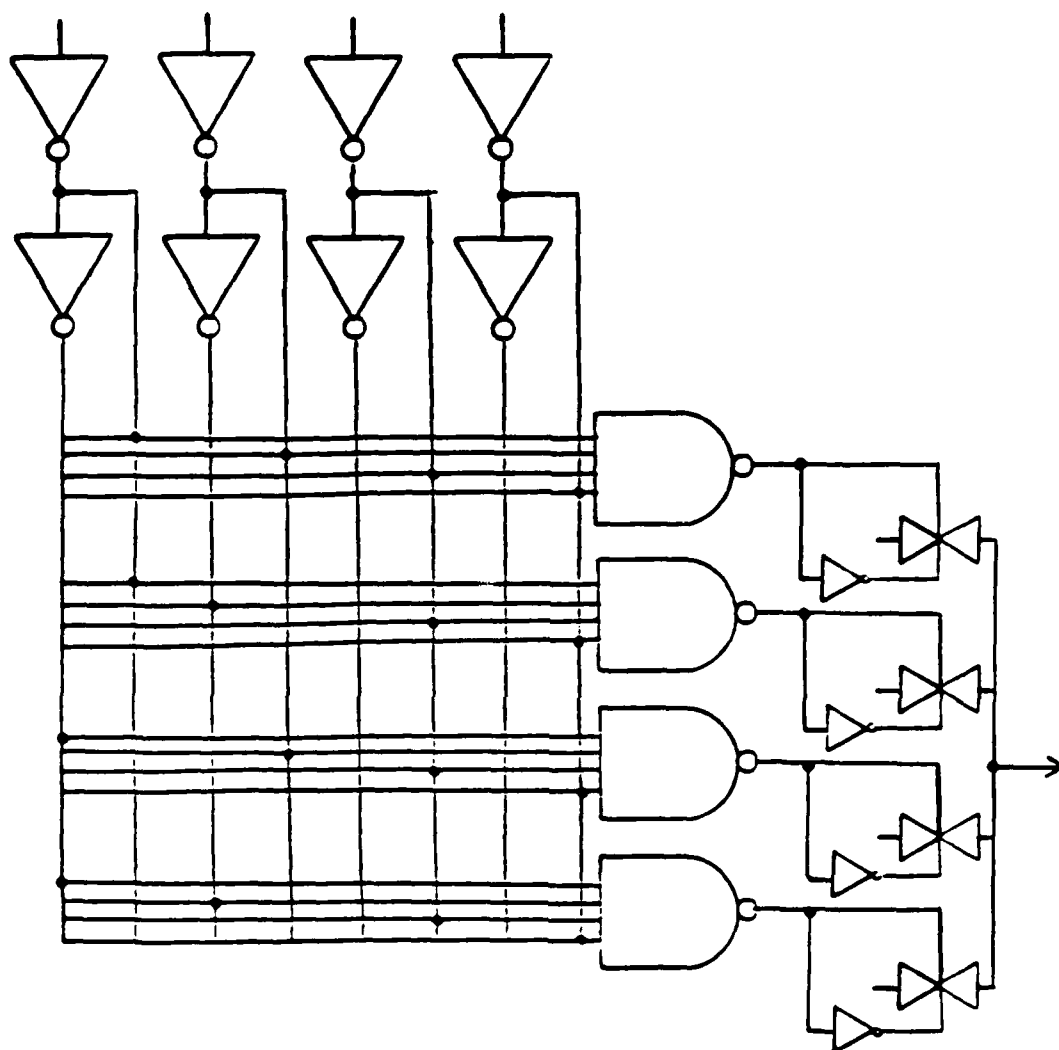


Figure A-7. Schematic of a Quarter Section of the Multiplexer

Going one step further, the gates themselves can be described with an array of transistors. Gates used in the decoder and multiplexer designs include the inverter, t-gate, 2-input NOR, 3-input NOR and 4-input NAND, which are shown in Figures A-8 through A-12, respectively. Figure A-13 provides a key of the symbols used in Figures A-8 through A-12. These gates were derived from the configurations proposed by Weste and Eshraghian (31). Simulation of the performance of these gates was accomplished using the ESIM (Electronic Circuit Simulator) and SPICE CAD tools.

The conspicuous omission of the counter from the functional units designed for the brain chip can be explained. Time constraints surrounding submission of the brain chip design for fabrication contributed to the decision to use a counter designed by another AFIT student, Capt Carl Shephard. The counter that Capt Shephard designed functions like a binary adder. The counter was chosen because it integrates smoothly into the brain chip design and requires no additional circuitry except for a dual-phase clock. Various load and preset features can be ignored and do not affect the operation of this counter. The Shephard counter conveniently interfaces with the other circuitry and complements the physical layout.

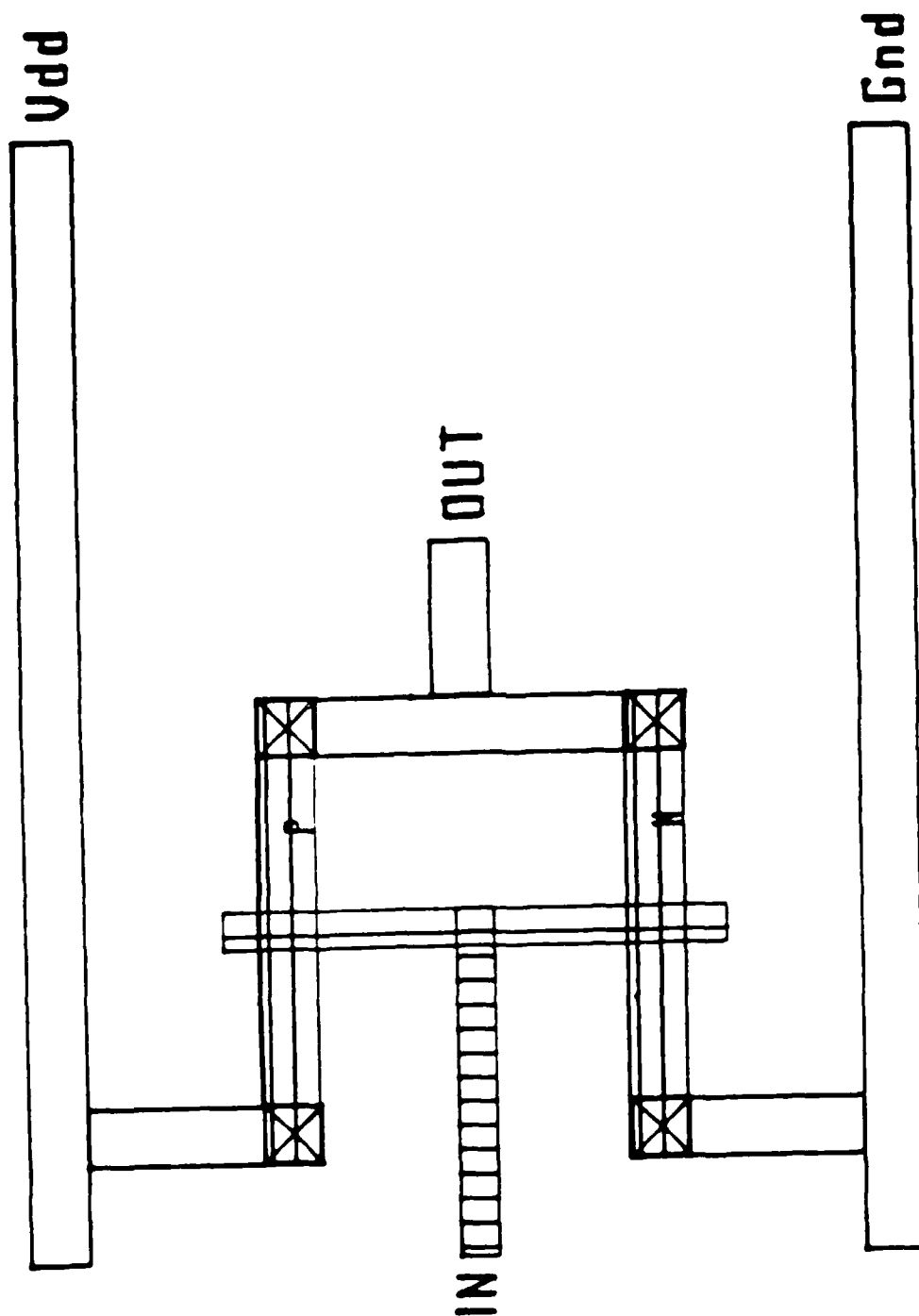


Figure A-8. The Inverter

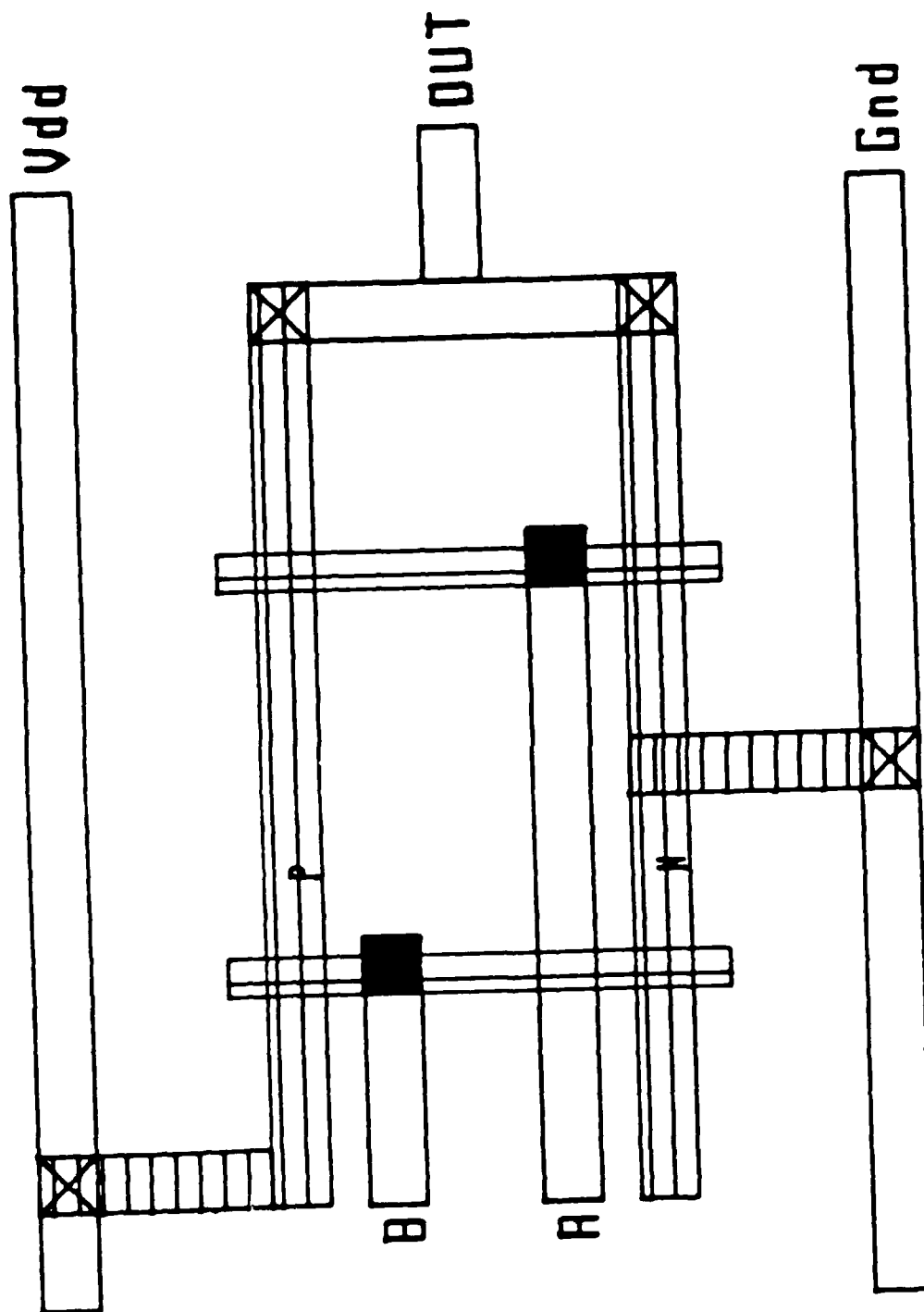


Figure A-10. The Two-Input NOR Gate

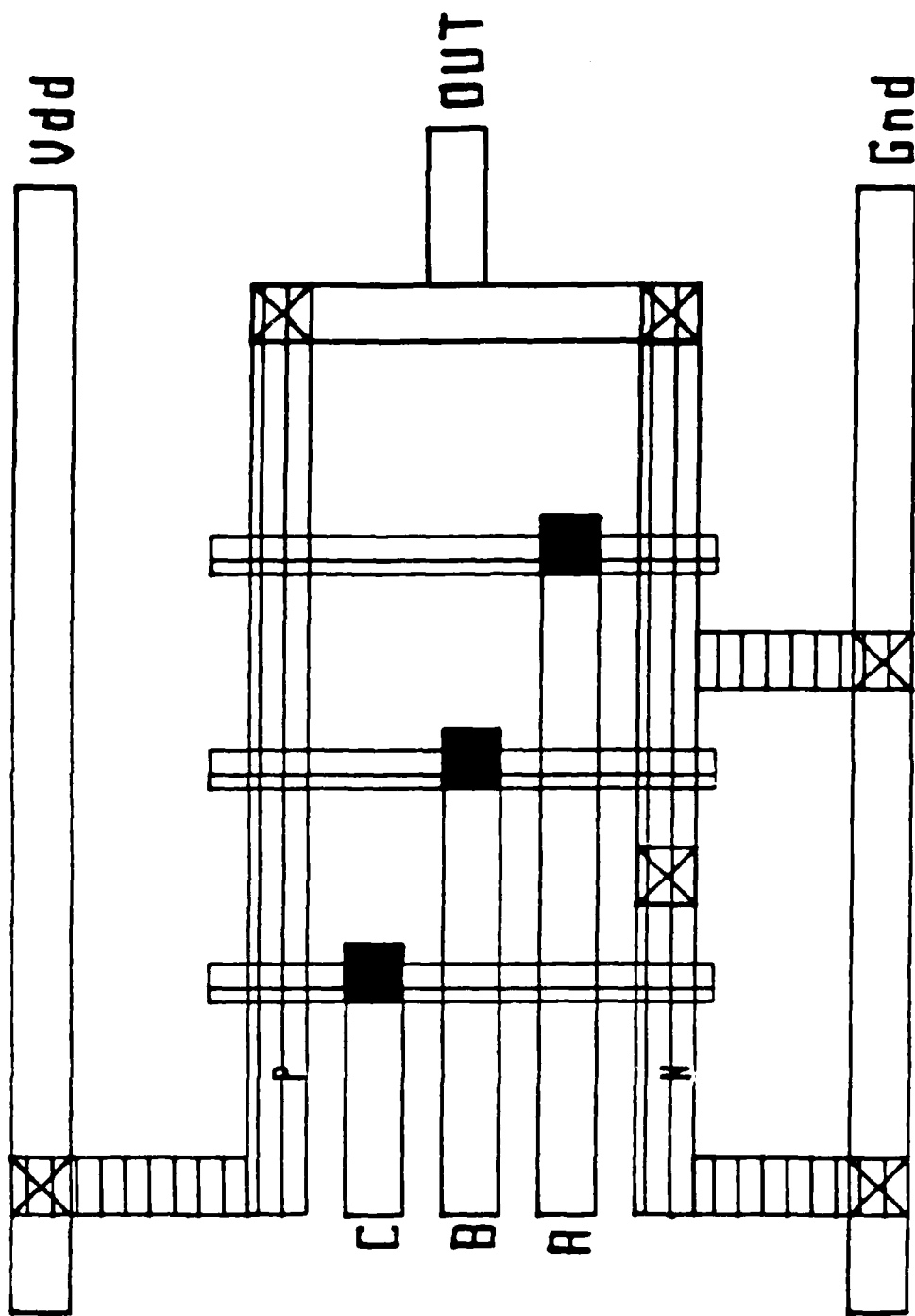


Figure A-11. The Three-Input NOR Gate

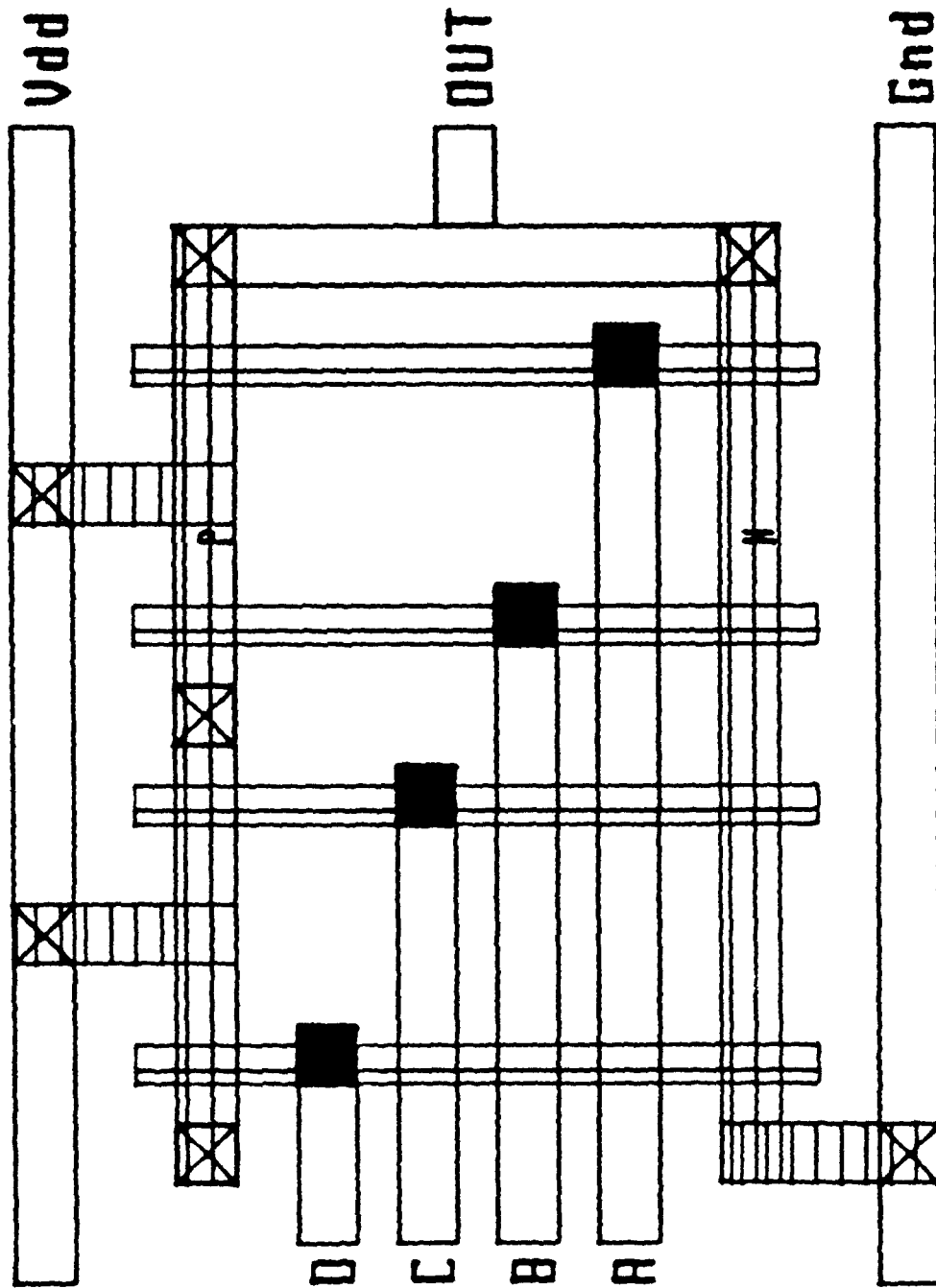
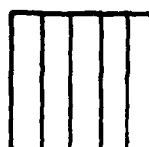


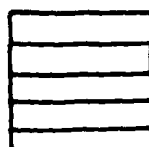
Figure A-12. The Four-Input NAND Gate



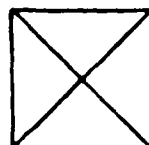
FIRST METAL



POLYSILICON



DIFFUSION



METAL-TO-DIFFUSION CONTACT



METAL-TO-POLYSILICON CONTACT

Figure A-13. Key to Symbols Used in Figures A-8 through A-12



AD-A103 204

AN ELECTRICAL CIRCUIT MODEL OF THE INTERFACE BETWEEN AN  
ELECTRODE AND THE. (U) AIR FORCE INST OF TECH  
WRIGHT-PATTERSON AFB OH SCHOOL OF ENGI.. J M SEDLAK

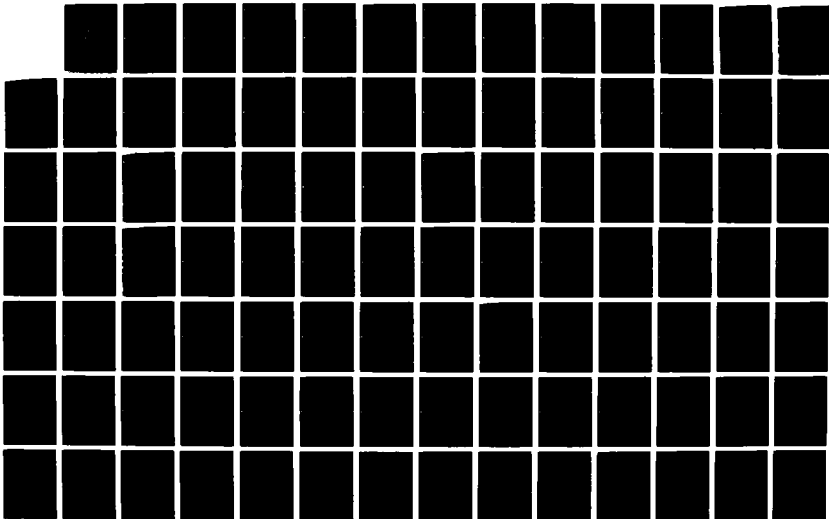
3/4

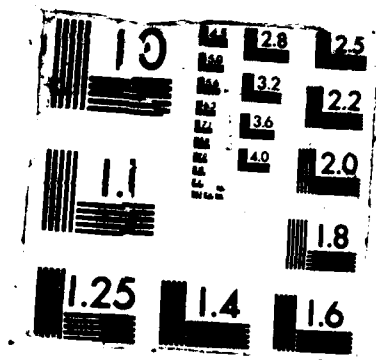
UNCLASSIFIED

31 JUL 87 AFIT/GE/EE/86D-48

F/G 9/1

NL





The basic building block approach facilitated a custom design of the brain chip. Since the design was effectively implemented at all levels of complexity, including the discrete transistor level, the opportunities for customizing appeared at each level of complexity. Hence, with the exception of the counter, it can be said that virtually every transistor in the AFIT brain chip was designed for the specific application to brain chip processing functions. A major impact of this custom design was the influence upon other characteristics of the brain chip.

#### Consequences of the Custom Design Method

The application of a custom design approach to the AFIT brain chip triggered several distinct consequences. One of the initial reasons for adopting a custom design method was to benefit from the educational aspects of building a multi-purpose chip from elemental transistors. Educational benefits encompassed the use of CAD tools as well as basic VLSI design processes. The custom design approach enabled the division of a large, complex circuit into manageable portions that could be arrayed and interconnected in a straightforward, comprehensible fashion. During this process, standard building blocks were modified when necessary to facilitate the design.

Although the complexity of the design decreased as a result of the partitioning of the brain chip into logical subdivisions, the layout, as well as the interconnection of the basic building blocks, correspondingly increased in the level of detail required in the CAD environment. Despite this seemingly anomalous circumstance, an examination of the alternative method employed in the nMOS brain chip reveals that Ballantine extensively relied upon programmable logic arrays (PLAs) to generate circuitry at the functional unit level. The multielectrode array required a special purpose design that could not be satisfied by using a PLA, but each of the remaining functional units (counter, decoder, and two multiplexers) were implemented with a PLA. Hence, four PLAs appear in the fully multiplexed nMOS AFIT brain chip of Figure A-2.

The PLA is normally available in the form of a library routine, and it may be used in a variety of general applications. Hence, PLAs can be called into the main program residing in the computer's working memory in a fashion analogous to that of a subroutine. Four subroutine calls, in addition to personalization, routing, and interconnection of the PLAs are required to generate the system architecture of the fully multiplexed nMOS brain chip. By contrast, the custom design approach adopted in the CMOS

brain chip facilitates a "pseudo-personalization" at the gate level. The increased routing and interconnection of circuit elements, to first integrate the gates into functional units, and then to integrate the functional units into the system architecture, is the penalty of a custom design approach.

#### Advantages of the New Design

The custom design approach resulted in opportunities to streamline the new AFIT brain chip; these opportunities are not generally available in the PLA approach. Because the personalization of the chip, or functional programming, was addressed at the gate, rather than at the functional unit level, a capability for increasing the compactness and efficient operation of the circuit resulted. When using a PLA, the size is fixed and efficiency gains are possible only by optimizing the descriptive algorithm of the functional unit. A custom design approach, however, presents opportunities to compact and design for efficiency at the transistor, gate, and functional unit levels of description. Hence, a more efficient and compact design can be achieved by using the custom design approach. An actual 82% reduction of the surface area of the entire AFIT brain chip resulted from this custom design procedure. The fully multiplexed nMOS design created by Ballantine encompasses  $0.5 \text{ cm}^2$  of surface

area (3:II-3), whereas the surface area of the new design measures 0.09 cm<sup>2</sup>.

Since the configuration of each building block of the new design specifically integrates into the brain chip package, the complexity of the design has been reduced. The new design contains no extraneous circuitry, such as that found in a PLA to support a general purpose application. Although the functional units used in the new design are also general purpose in nature, the circuits of each were designed for a particular application and strictly support the processing functions of the new AFIT brain chip.

A prime advantage of the new design is the degree to which it fulfills the research requirements of the next implant. One research requirement that was optimized was the reduction of inputs and outputs to six total pads. The electrodes in the multielectrode array of the previous design measured 180 x 180 microns. The new brain chip design, on the other hand, supports the predictions by Kabrisky (5:41) that cortical columns in the brains of higher order mammals are 50 to 100 microns in diameter. Therefore, the 100 x 100 microns size of the electrodes in the new design satisfies the maximum size limitation of a cortical column.

Finally, an additional advantage of the new design is that it employs CMOS technology. In addition to the inherent

advantages of CMOS technology, the application of the Berkeley CAD User's Toolbox routines to CMOS design greatly enhances the predictability and repeatability characteristics that may be necessary to fulfill future AFIT brain chip research objectives. The current availability of the CAD tools increases the likelihood of productive follow-on research.

## APPENDIX B

### List of Equipment and Supplies

1. Plastic or teflon tweezers
2. IC packages (64-pin, 40-pin)
3. Epoxy (H70E) EPOTEK
4. Ultrasonic bonder microscope
5. Polyimide (PI 2555) Dupont Pyralin (TM)
6. Polyimide adhesion promoter (VM-651) Dupont Pyralin (TM)
7. 30 gauge solid copper hookup wire with teflon insulation
8. Bottled N ultra-high purity gas
9. Practice silicon wafers
10. Mask aligner
11. Acetone
12. Methanol
13. De-ionized water (DIW)
14. Convection oven
15. Photoresist spinner apparatus
16. Negative photoresist (Waycoat Type 3, 28CP) Waycoat
17. Xylene
18. Butyl acetate
19. Positive photoresist (AZ1350J) Shipley
20. Positive photoresist developer, also used to etch polyimide (AZ351) Shipley



21. Positive photoresist adhesion promoter (HMDS) SCM, PCR Incorporated
22. Thinner (T-9035) Dupont
23. Scanning electron microscope
24. Wet sandpaper 200-300 grit
25. Elite board
26. Dual-Trace oscilloscope (HP1201A) Hewlett-Packard
27. Signal generators
28. Saline bath trough
29. 0.9% NaCl solution
30. Double-sided tape
31. Electronic sealant (Coax Seal) Universal Electronics
32. Eyedropper
33. Volt-Ohm Meter (HP3455A) Hewlett-Packard
34. Capacitance meter
35. Silicone sealant (RTV) Dow Chemical
36. X-Acto knife
37. Oscilloscope camera (HP198A) Hewlett-Packard
38. Impedance analyzer (HP4192A) Hewlett-Packard
39. AC bridge (ESI 250DA) Ericksson Scientific Instruments
40. Electrometer (VM-651) Keithley Instruments
41. Decade resistance box
42. Decade capacitance box

APPENDIX C  
Photolithography Processing Schedule

Standard Clean

The standard clean is performed before the processing of wafers or chips, and this procedure effects the elimination of organic contaminants. The standard clean was that process used by Turner (3:A-1), and the processing schedules for wafers and chips were derived from Turner's negative photolithography procedure.

1. Dip in beaker of acetone to remove organic material.
2. Blow dry with  $N_2$  gas.
3. Dip in methanol to remove more organic material.
4. Blow dry with  $N_2$  gas.
5. Flood with DIW.
6. Blow dry with  $N_2$  gas.
7. Bake for one hour at  $220^{\circ}C$  in  $N_2$  ambient convection oven to remove moisture.

### Schedule 1: Polyimide/Negative PR Process for Wafers

The photolithography process that was used on one inch practice wafers is provided in this schedule (3:A-5). Nineteen steps were required to apply a single coat of the polyimide.

1. Perform standard clean of all wafers and bake in 220°C oven.
2. Preheat second oven to 70°C.
3. Remove wafers from 220°C oven and cool.
4. Blow clean with N<sub>2</sub> to remove surface contaminants.
5. Apply polyimide adhesion promoter (VM-651):
  - puddle on wafer.
  - spin/spread at 2K rpm for 10 sec.
  - spin at 5K rpm for 30 sec.
6. Apply polyimide (PI 2555):
  - puddle on wafer.
  - spin/spread at 2K rpm for 5 sec.
  - spin at 6.5K rpm for 30 sec.
7. Prebake PI 2555 at 70°C for 20 minutes, N<sub>2</sub> ambient, to dry the polyimide without curing; place in oven immediately to minimize formation of pinholes.
8. Remove from oven and allow to cool.
9. Blow with N<sub>2</sub> gas to remove surface contaminants.
10. Apply negative photoresist (Waycoat Type 3, 28 CP):
  - puddle on wafer.
  - spin/spread at 5K rpm for 30 sec.
11. Prebake photoresist at 70°C for 20 minutes, N<sub>2</sub> ambient.
12. Blow clean with N<sub>2</sub>.
13. Align/expose for 10 sec.

14. Develop photoresist:
  - spin/spray xylene at 1K rpm for 20 seconds, keeping the surface wet while spinning.
  - spin/spray butyl acetate at 1K rpm for 20 sec.
  - spin/blow N<sub>2</sub> at 1K rpm for 30 sec.
15. Visually inspect pattern to determine if additional developing required.
16. Postbake at 120°C for 20 minutes, N<sub>2</sub> ambient, to harden photoresist.
17. Etch the polyimide:
  - AZ351 bath (one part AZ351 to 5 parts DIW) for 5 sec.
  - DIW bath for 30 sec.
  - blow dry with N<sub>2</sub>.
18. Visually inspect wafer to ensure full etch without PR lifting or pattern discontinuities; reaccomplish etch if required.
19. Cure at 180°C for 2 hours, N<sub>2</sub> ambient; cure completely before applying additional coats.

## Schedule 2: Polyimide/Negative PR Process for a Chip

The photolithography and encapsulation process for a single brain chip is provided in this schedule. Differences between this process and that of Schedule 1 resulted from the difference in the size of wafers and chips (3:A-7).

1. Perform standard clean of all wafers and bake in 220°C oven.
2. Preheat second oven to 70°C.
3. Remove chip from 220°C oven and cool.
4. Blow clean with N<sub>2</sub> to remove surface contaminants.
5. Apply polyimide adhesion promoter (VM-651):
  - puddle on chip, allowing it to spread onto chuck such that edges are coated.
  - allow promoter to flow 5 seconds to ensure good contact with edges of chip.
  - spin/spread at 2K rpm for 5 sec.
  - spin at 5K rpm for 30 sec.
6. Apply polyimide (PI 2555):
  - puddle on chip, allowing it to spread onto chuck such that edges are coated.
  - spin/spread at 2K rpm for 5 sec.
  - spin at 6.5K rpm for 30 sec.
7. Prebake PI 2555 at 70°C for 20 minutes, N<sub>2</sub> ambient, to dry the polyimide without curing; place in oven immediately to minimize formation of pinholes.
8. Remove from oven and allow to cool.
9. Blow with N<sub>2</sub> to remove surface contaminants.
10. Apply negative photoresist (Waycoat Type 3, 28 CP):
  - puddle on chip, allowing it to spread onto chuck so that edges are coated.
  - allow photoresist to flow 10 seconds to ensure good contact with edges of chip.
  - spin/spread at 5.5K rpm for 30 sec.

11. Prebake photoresist at 85°C for 20 minutes, N<sub>2</sub> ambient.
12. Blow clean with N<sub>2</sub>.
13. Align/expose for 10 sec.
14. Develop photoresist:
  - spin/spray xylene at 1K rpm for 8 seconds, keeping the surface wet while spinning.
  - spin/spray butyl acetate at 1K rpm for 10 sec.
  - spin/blow N<sub>2</sub> at 1K rpm for 30 sec.
15. Visually inspect pattern to determine if additional developing required.
16. Etch the polyimide:
  - AZ351 bath (one part AZ351 to 5 parts DIW) for 5 seconds on first coat, 1 second on additional coats.
  - DIW bath for 30 sec.
  - blow dry with N<sub>2</sub>.
17. Visually inspect chip to ensure full and uniform (on multiple coats) etch without PR lifting or pattern discontinuities; reaccomplish etch if required. Partial etch may be necessary on multiple coats, accomplish by immersing selected portions of chip in the etchant.
18. Cure at 150°C for 2 hours, N<sub>2</sub> ambient, to effect a partial cure of the polyimide.
19. Remove photoresist by gently scrubbing in xylene bath with a cotton swab; removes photoresist layer without harming polyimide layer.
20. Cure at 180°C for 2 hours, N<sub>2</sub> ambient, cure completely before applying additional coats.

## APPENDIX D

### Calculation of the Model Parameters

1.  $R_m$  = resistance of metallic electrode, circular geometry (12:1071)

$$R_m = P \frac{4L}{\pi d^2}$$

$L$  = length (thickness) =  $1.3 \mu\text{m}$  (Dektak measurement)  
 $P$  = resistivity =  $10^{-1} \Omega\text{-}\mu\text{m}$   
 $d$  = diameter

Since  $\pi d^2 = \pi \left(\frac{r}{2}\right)^2 = \frac{\pi r^2}{4} = \frac{A}{4}$ ,

then  $R_m$  for a square electrode can be derived:

$A = S^2$ , where  $A$  is the area and  $S$  ( $S = 180 \mu\text{m}$ ) is the side of a square electrode

$$R_m = P \frac{4L}{S^2/4} = 6.42 \times 10^{-5} \Omega$$

2.  $R_s$  = spreading resistance of the saline (12:1069)

For round electrode:

$$dR_s = P \frac{dr}{4\pi r^2} \quad r = \text{electrode radius}$$

$$\int_r^\infty dR_s = \frac{P}{4\pi r} = \frac{P}{2\pi d} \quad P = 72.5 \Omega\text{-cm.}$$

For square electrode:

$$dR_s = P \frac{ds}{4S^2}$$

$$\int_x dR_s = \frac{P}{4S} R_s = 1006.9 \Omega$$

3.  $R_g$  = leakage resistance of charge carriers crossing the Helmholtz double layer (12:1069)

$$PS = 1.33 \times 10^4 \Omega\text{-cm}^2$$

$$R_g = \frac{PS}{A} = 4.10 \times 10^7 \Omega$$

4.  $C_g$  = capacitance of Helmholtz double layer (12:1070)

$$C_g = \frac{\epsilon_r \epsilon_0 A}{g}$$

$\epsilon_r = 1$   
 $\epsilon_0 = 8.854 \times 10^{-14} \text{ F/cm}$   
 $g = \text{Helmholtz gap}$

$$\frac{\epsilon_r \epsilon_0}{g} = 0.2 \times 10^{-12} \text{ F}/\mu\text{m}^2$$

$$C_g = 6.48 \times 10^{-9} \text{ F}$$



## APPENDIX E

### Nonlinear Least Squares Analysis

The method of nonlinear least squares is characterized by finding constant values in the nonlinear equation that minimize the sum of the squared deviations of the observed values from those predicted by the equation. Five assumptions concerning the method of nonlinear least squares are embedded in the analysis technique (32:7-9, 33:41).

1. The correct form of the equation is known.
2. The data are representative of values predicted by the equation across the entire range of inputs and outputs.
3. The dependent variables are statistically uncorrelated.
4. Some of the coefficients of the equation are nonlinear.
5. Preliminary estimates of all of the parameters are available and do not contain an error significant enough to prevent the convergence of computed approximations.

Three types of search strategies have been implemented in nonlinear least squares computer programs (32:9):

1. The Taylor-series or Gauss-Newton method was developed by Booth and Peterson.
2. The gradient or steepest descent method was developed by Marquardt.

3. The maximum neighborhood method was developed by Marquardt and Levenburg.

The third search strategy, the Levenburg-Marquardt algorithm, displays two distinguishing features (18:473). First, a first-order Taylor series approximation is expanded about an initial, or trial, solution to reduce the residuals to a linear form. Second, the maximum neighborhood technique acts to minimize the instability and slow convergence problems that plague other techniques. A discussion of the details of the Levenburg-Marquardt algorithm was presented by Kolesar (18:472-479), and the following analysis is based upon that discourse.

To begin, consider a nonlinear function defined in terms of  $a_j$  that is expanded to a first-order approximation of a Taylor series:

$$y(x) = y_0(x) + \sum_{j=1}^n \left[ \frac{\partial y_0(x)}{\partial a_j} \cdot \delta a_j \right]. \quad (E-1)$$

This function is linear with respect to the  $a_j$  increments ( $\delta a_j$ ), and derivatives are evaluated at trial solution  $y_0(x)$ . An empirical determination of the variation of  $y(x)$  with ( $a_j$ ) is given by:

$$\frac{\partial y_0(a_j)}{\partial a_j} = \frac{y_0(a_j + \Delta a_j) - y_0(a_j - \Delta a_j)}{2\Delta a_j}. \quad (E-2)$$

With this approximation, the chi-square goodness of fit parameter,  $x^2$ , is given by:

$$x^2 = \sum_i \{ [y_i - y(x_i)]^2 \}. \quad (E-3)$$

The relative weights of the individual residuals are assumed to be unity, so Equation (E-3) can be expressed as:

$$x^2 = \sum_i \left\{ \left[ y_i - y_o(x_i) - \sum_{j=1}^n \left( \frac{y_o(x_i)}{a_j} \cdot \delta a_j \right) \right]^2 \right\}. \quad (E-4)$$

Next,  $x^2$  is minimized with respect to each  $\delta a_j$  by setting the derivatives equal to zero:

$$\frac{\partial x^2}{\partial a_k} = -2 \sum_i \left\{ \left( y_i - y_o(x_i) - \sum_{j=1}^n \left[ \frac{y_o(x_i)}{a_j} \cdot \delta a_j \right] \right) \frac{\partial y_o(x_i)}{\partial a_k} \right\} = 0. \quad (E-5)$$

Using matrix notation, let

$$\beta_k = \sum_{j=1}^n (\delta a_j a_{jk}) \quad k=1,2,3,\dots,n \quad (E-6)$$

$$\beta_k = \sum_i [y_i - y_o(x_i)] \left[ \frac{\partial y_o(x_i)}{\partial a_k} \right] = -0.5 \frac{\partial x_o^2}{\partial a_k} \quad (E-7)$$

$$a_{jk} = \sum_i \left\{ \frac{\partial y_o(x_i)}{\partial a_j} \cdot \frac{\partial y_o(x_i)}{\partial a_k} - [y_i - y_o(x_i)] \frac{\partial^2 y_o(x_i)}{\partial a_j \partial a_k} \right\} = +0.5 \frac{\partial^2 x_o^2}{\partial a_j \partial a_k}. \quad (E-8)$$

If  $x^2$  is expanded to the first-order approximation of a Taylor's series as a function of  $a_j$ , then

$$x^2 = x_o^2 + \sum_{j=1}^n \left[ \frac{\partial x_o^2}{\partial a_j} \cdot \delta a_j \right], \quad (E-9)$$

where  $x_o^2$  is the trial solution, and the nonlinear function is  $y_o(x)$ . Therefore,

$$x_o^2 = \sum_i \{ [y_i - y_o(x_i)] \}^2, \quad (E-10)$$

and the  $\delta a_j$  are increments of  $a_j$  required to reach the point where  $y(x)$  and  $x^2$  are to be determined.

The optimum values of the  $a_j$  are those which minimize  $x^2$ . Hence,

$$\frac{\partial x^2}{\partial a_k} = \frac{\partial x_0^2}{\partial a_k} + \sum_{j=1}^n \left\{ \frac{\partial^2 x_0^2}{\partial a_j \partial a_k} \cdot \delta a_j \right\} = 0 \quad k=1,2,3,\dots,n \quad (E-11)$$

Note that  $\alpha$  in Equation (E-8) is a symmetric matrix of order  $n$  with components equal to one-half of the coefficients of the  $a_j$  in Equation (E-11).

The solution of Equation (E-6) is equivalent to using a parabolic surface to approximate the  $x^2$  hypersurface. To demonstrate this equivalence,  $x^2$  can be expanded to a second order Taylor series as a function of  $a_j$ . Therefore,

$$x^2 = x_0^2 + \sum_{j=1}^n \left( \frac{\partial x_0^2}{\partial a_j} \cdot \delta a_j \right) + 0.5 \sum_{j=1}^n \sum_{k=1}^n \left( \frac{\partial^2 x_0^2}{\partial a_j \partial a_k} \cdot \delta a_j \cdot \delta a_k \right) \quad (E-12)$$

and is a function of the second-order Taylor series with respect to  $a_j$ . Equation (E-12) describes a parabolic hypersurface.

Optimal values of the increments ( $\delta a_j$ ) are found by minimizing  $x^2$ . In this fashion,

$$\frac{\partial x^2}{\partial a_k} = \frac{\partial x_0^2}{\partial a_k} + \sum_{j=1}^n \left\{ \frac{\partial^2 x_0^2}{\partial a_j \partial a_k} \cdot \delta a_j \right\} = 0 \quad k=1,2,3,\dots,n \quad (E-13)$$

which is identical to Equation (E-11). Also, by setting the derivatives of Equation (E-12) equal to zero, the same result

is obtained if the higher order terms of  $a_j$  are neglected. Hence, the solution of Equation (E-8) represents a curvature matrix. The curvature matrix is represented by

$$a_{jk} = \sum_i \left\{ \frac{\partial y_0(x_i)}{\partial a_j} \cdot \frac{\partial y_0(x_i)}{\partial a_k} \right\}. \quad (E-14)$$

Although an expansion of  $y(x)$  or  $x^2$  converges rapidly to the point of minimal  $x^2$  from neighboring points, problems arise at points outside of the parabolic region of the  $x^2$  hypersurface. In other words, a negative curvature of the  $x^2$  hypersurface forces the solution to become unstable. Another method, called the gradient search, works well when approaching the minimum from points well removed from the solution, but converges slowly inside the neighborhood of the solution. Levenburg and Marquardt combined the features of both methods such that their algorithm initially operates like a gradient search until the neighborhood of the solution is reached, then the algorithm operates like the curvature method as the search converges on a solution. Because the Taylor series needs to be valid only in the neighborhood of the minimum, a first-order expansion is sufficient.

The Levenburg-Marquardt algorithm effects the linearization of the function, and this results in the optimization of the convergence of the solution. The diagonal terms of the curvature matrix ( $a$ ) are increased by a

factor ( $\lambda$ ), and this bounds the interpolation of the algorithm between two extremes. Equations (E-6) through (E-12) can be described with the defining equations:

$$B = \lambda a a' \quad (E-15)$$

and

$$a'_{jk} = \begin{cases} a_{jk}(1+\lambda) & \text{for } j=k \\ a_{jk} & \text{for } j \neq k \end{cases} \quad (E-16)$$

For small  $\lambda$ , Equation (E-15) resembles the solution of Equations (E-6) through (E-8). For large  $\lambda$ , the diagonal terms of the curvature matrix dominate, and the matrix equation degenerates into  $n$  equations of the form:

$$B_j = \lambda \cdot \delta a_j \cdot a_{jj} \quad (E-17)$$

Equation (E-17) yields  $\delta a_j$  along the direction of the gradients ( $B_j$ ) of Equation (E-7) but with a magnitude scaled by  $a_{jj}$  and reduced by  $\lambda$ . The solution of the  $\delta a_j$  follows from Equation (E-16) after a matrix inversion:

$$\delta a_j = \sum_{k=1}^n (B_k a_{jk}) \quad (E-18)$$

The  $B_j$  are given by Equation (E-7), and the matrix ( $a$ ) is the inverse of the  $a'$  matrix, whose elements are defined by Equation (E-16).

A value of  $\lambda$  should be selected that is small enough to benefit from the analytical solution, but large enough so

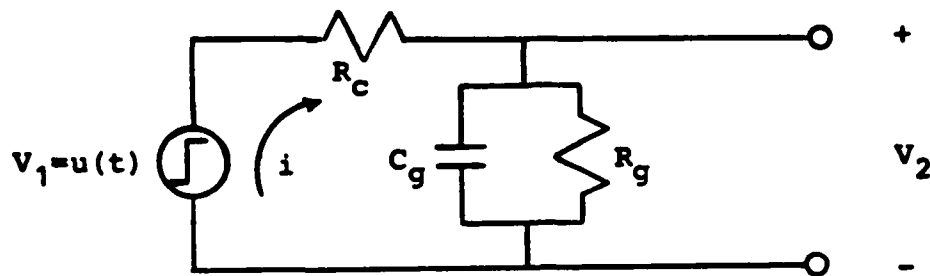
that  $x^2$  decreases. The Levenburg-Marquardt algorithm approaches the gradient search method with small steps for large  $\lambda$ , and values of  $\lambda$  should be found such that  $x^2(a+\delta a) < x^2(a)$ . Four steps summarize the Levenburg-Marquardt method (18:479):

1. Compute  $x^2$  using the trial solution values.
2. Initially, set  $\lambda=0.001$  and compute  $\delta a$  and  $x^2(a+\delta a)$ .
3. If  $x^2(a+\delta a) > x^2(a)$ , increase  $\lambda$  by a factor of 10 and repeat Step (3).
4. If  $x^2(a+\delta a) < x^2(a)$ , decrease  $\lambda$  by a factor of 10, consider  $a'=a+\delta a$  to be the new trial solution, and implement step (3) by substituting  $a'$  for  $a$ .

The increments  $(\delta a_j)$  are recomputed using Equation (E-18) until  $\lambda$  is optimized. The accumulation of the elements in the  $a_{jk}$  and  $B_j$  matrices is performed only once during each iteration of the loop. The solution will converge on a minimum value after several iterations of the loop as  $\lambda$  decreases.

## APPENDIX F

### Calculation of the Circuit Transfer Function



Kirchhoff's Voltage Laws:

$$V_1 = iR_c + i \left( \frac{R_g * 1/C_g s}{R_g + 1/C_g s} \right) \quad V_2 = i \left( \frac{R_g * 1/C_g s}{R_g + 1/C_g s} \right)$$

Transfer Function:

$$T(s) = V_2/V_1 = \frac{R_g (1/C_g s)}{R_c R_g + R_c / C_g s + R_g / C_g s} = \frac{1}{R_c C_g s + ((R_c + R_g) / R_g)}$$

Forced (Transient) Response:

$$\text{when } s=0, V_1 = u(t)$$

$$V_2^F = V_1 * \left( \frac{1}{R_c / R_g + 1} \right) = u(t) * \left( \frac{R_g}{R_c + R_g} \right)$$

Natural (Steady-State) Response:

$$V_2^N = u(t) * A * \exp \left( \frac{-(R_c + R_g)}{R_c R_g C_g} t \right)$$



Total (Entire) Response:

$$V_2 T = u(t) \left( \frac{R_g}{R_c + R_g} + A \exp \left( \frac{-(R_c + R_g)}{R_c R_g C_g} t \right) \right)$$

Use Initial Conditions:

$$V_2 T(0+) = u(0+) * \left( \frac{R_g}{R_c + R_g} + A \exp \left( \frac{-(R_c + R_g)(0+)}{R_c R_g C_g} \right) \right)$$

Solve for A:

$$\frac{R_g}{R_c + R_g} + A = 0$$

$$A = -\frac{R_g}{R_c + R_g}$$

Write Total Response:

$$V_2 T = u(t) \frac{R_g}{R_c + R_g} \left( 1 - \exp \left( \frac{-(R_c + R_g)}{R_c R_g C_g} t \right) \right)$$

## APPENDIX G

### Calibration and Baseline Measurements

#### Section A

#### 1000 ohm Resistor ( $R_c$ )

<u>F(Hz)</u>	<u><math>R_c</math> (ohm)</u>
5	1007
50	1006
100	1006
250	1006
500	1006
750	1006
1K↓	1006
2	1006
3	1006
4	1006
5	1006
7.5	1006
10	1006
25	1007
50	1006
75	1006
100	1006
250	1007
500	1007
750	1007
1M↓	1007
2	1008
3	1009
4	1010
5	1011
6	1013
7	1015
8	1018
9	1020
10	1023
11	1026
12	1030
13	1033

40 megohm Resistor ( $R_g$ )

<u>F (Hz)</u>	<u><math>R_g</math> (megohm)</u>
5	50
50	50
100	50
250	50
500	43.5
750	38.5
1K↓	38.5
2	38.5
3	38.5
4	38.5
5	38.5
7.5	38.5
10	38.5
25	38.5
50	38.5
75	38.5
100	38.5
250	37
500	34.5
750	32.3
1M↓	32.3
2	25
3	25
4	20
5	25
6	25
7	20
8	16.7
9	14.3
10	12.5
11	10
12	8.3
13	7.1

5000 microfarad Capacitor ( $C_g$ )

<u>F (Hz)</u>	<u><math>C_g</math> (microfarad)</u>
5	7320
50	7510
100	7460
250	7420
500	7400
750	7380
1K↓	7340
2	7270
3	7220
4	7200
5	7160
7.5	7110
10	7080
25	6960
50	6870
75	6810
100	6760
250	7350
500	6470
750	6390
1M↓	6460
2	6410
3	6510
4	6800
5	7260
6	7960
7	9050
8	10740
9	13600

Section B

Measurements of Circuit in Figure 5-2

<u>F (Hz)</u>	<u>R<sub>p</sub> (ohm)</u>
5	33.3M↓
50	20.0
100	11.1
200	5.26
300	2.86
400	1.85
500	1.28
1K↓	392K↓
2	112
3	53.1
4	31.2
5	20.7
7.5	10.0
10	6.20
50	1.25
100	1.08
500	1.01
1M↓	1.01
2	1.01
3	1.01
4	1.01
5	1.01
6	1.02
7	1.02
8	1.02
9	1.02
10	1.03
11	1.03
12	1.03
13	1.04

Section C

Measurement of Circuit in Figure 5-5  
(d=1.0 inch)

F (Hz)	R <sub>p</sub> (ohm)
5	33.3M↓
50	20.0
100	12.5
250	5.26
500	3.03
1K↓	1.18
2.5	350K↓
5	133
7.5	74.6
10	48.8
25	11.9
50	3.86
75	1.96
100	1.22
250	270 (ohm)↓
500	102
750	66.2
1M↓	52.6
2.5	40.3
5	52.4
7.5	76.9
10	113

(d=0.5 inch)

F (Hz)	R <sub>p</sub> (ohm)
5	33.3M↓
50	20.0
100	12.5
250	5.26
500	3.23
1K↓	1.22
2.5	350K↓
5	133
7.5	73.5
10	47.8
25	11.7
50	3.83
75	1.95
100	1.21
250	270 (ohm) ↓
500	102
750	65.8
1M↓	52.6
2.5	40.0
5	52.1
7.5	76.3
10	112

(d=0.1 inch)

F (Hz)	R <sub>p</sub> (ohm)
5	33.3M↓
50	16.7
100	11.1
250	4.55
500	2.27
1K↓	1.03
2.5	346K↓
5	145
7.5	84.7
10	57.8
25	16.2
50	5.99
75	3.26
100	2.11
250	500 (ohm) ↓
500	159
750	78.7
1M↓	46.9
2.5	14.8
5	48.3
7.5	118.6
10	222



## APPENDIX H

### Experimental and Calculated Frequency Response Data

The frequency response data of the three experimental chips are provided in this appendix. The model parameters are unscaled in this appendix. Table H-1 identifies the data in this appendix.

TABLE H-1

#### Identification of Frequency Response Data

<u>Electrode</u>	<u>Page</u> <u>Start</u>	<u>Page</u> <u>Stop</u>
188	H-2	H-4
144	H-5	H-7
1CC	H-8	H-10
111	H-11	H-13
1GG	H-14	H-16
199	H-17	H-19
177	H-20	H-22
14D	H-23	H-25
288	H-26	H-29
244	H-30	H-33
2CC	H-34	H-37
211	H-38	H-41
2GG	H-42	H-45
299	H-46	H-49
277	H-50	H-53
24D	H-54	H-57
2D4	H-58	H-61
388	H-62	H-65
344	H-66	H-69
3CC	H-70	H-73
311	H-74	H-77
3GG	H-78	H-81
399	H-82	H-85
377	H-86	H-89
34D	H-90	H-93
3D4	H-94	H-97

# VARIABLES USED IN THE CALCULATIONS

THE ESTIMATED METAL CLUSTER RESISTANCE (Rc) = 1.000000E+02

THE ESTIMATED GAP RESISTANCE (Rg) = 1.000000E+05

THE ESTIMATED GAP  
CAPACITANCE (Cg) = 6.000000E-07

THE LEAST SQUARE VALUE OF THE METAL CLUSTER  
RESISTANCE, Rc = 1.493154E+03

THE LEAST SQUARE VALUE OF THE GAP  
RESISTANCE, Rg = 8.374804E+04

THE LEAST SQUARE VALUE OF THE GAP  
CAPACITANCE, Cg = 6.690231E-07

THE RESIDUALS ARE CALCULATED BY THE FOLLOWING  
EQUATION: [MEASURED VALUE-CALCULATED VALUE]

SAMPLE	R(f)	R(cal)	R(resid)	Cg(est)
1	8.6400E+04	8.5241E+04	1.1588E+03	6.6902E-07
2	8.0000E+04	8.0930E+04	-9.2990E+02	6.6902E-07
3	3.5100E+04	3.7027E+04	-1.9273E+03	6.6902E-07
4	1.4400E+04	1.4523E+04	-1.2314E+02	6.6902E-07
5	1.0900E+04	7.8322E+03	3.0678E+03	6.6902E-07
6	9.3500E+03	5.1810E+03	4.1690E+03	6.6902E-07
7	6.9900E+03	3.1733E+03	3.8167E+03	6.6902E-07
8	5.3200E+03	2.4466E+03	2.8734E+03	6.6902E-07
9	4.2900E+03	2.1059E+03	2.1841E+03	6.6902E-07
10	3.5500E+03	1.9196E+03	1.6304E+03	6.6902E-07
11	3.0400E+03	1.8069E+03	1.2331E+03	6.6902E-07
12	2.7000E+03	1.7336E+03	9.6643E+02	6.6902E-07
13	2.4600E+03	1.6832E+03	7.7678E+02	6.6902E-07
14	2.2800E+03	1.6472E+03	6.3282E+02	6.6902E-07
15	2.0300E+03	1.6002E+03	4.2983E+02	6.6902E-07
16	1.8600E+03	1.5718E+03	2.8819E+02	6.6902E-07
17	1.7200E+03	1.5534E+03	1.6661E+02	6.6902E-07
18	1.6400E+03	1.5408E+03	9.9248E+01	6.6902E-07
19	1.5600E+03	1.5317E+03	2.8287E+01	6.6902E-07
20	1.3900E+03	1.5178E+03	-1.2784E+02	6.6902E-07
21	9.5200E+02	1.5103E+03	-5.5830E+02	6.6902E-07

22	8.4000E+02	1.5057E+03	-6.6575E+02	6.6902E-07
23	7.8100E+02	1.5028E+03	-7.2180E+02	6.6902E-07
24	6.8000E+02	1.4993E+03	-8.1933E+02	6.6902E-07
25	6.1000E+02	1.4974E+03	-8.8744E+02	6.6902E-07
26	5.6000E+02	1.4963E+03	-9.3630E+02	6.6902E-07
27	5.2400E+02	1.4956E+03	-9.7156E+02	6.6902E-07
28	4.9300E+02	1.4951E+03	-1.0021E+03	6.6902E-07
29	4.7200E+02	1.4947E+03	-1.0227E+03	6.6902E-07
30	4.2400E+02	1.4938E+03	-1.0698E+03	6.6902E-07
31	3.6500E+02	1.4935E+03	-1.1285E+03	6.6902E-07
32	2.4950E+02	1.4932E+03	-1.2437E+03	6.6902E-07
33	1.9900E+02	1.4932E+03	-1.2942E+03	6.6902E-07
34	1.8000E+02	1.4932E+03	-1.3132E+03	6.6902E-07
35	1.6500E+02	1.4932E+03	-1.3282E+03	6.6902E-07
36	1.3800E+02	1.4932E+03	-1.3552E+03	6.6902E-07
37	1.3000E+02	1.4932E+03	-1.3632E+03	6.6902E-07
38	1.2700E+02	1.4932E+03	-1.3662E+03	6.6902E-07
39	1.2700E+02	1.4932E+03	-1.3662E+03	6.6902E-07

SUM OF SQUARED RESIDUALS= 8.9924E+07

VARIANCE= 2.4304E+06

STANDARD DEVIATION= 1.5590E+03

ADDITIONAL PARAMETERS CALCULATED BY THE LEAST SQUARES SUBROUTINE.

THE RESIDUAL SUM OF SQUARES = 8.992372E+07

THE NUMBER OF SIGNIFICANT DIGITS IN THE CALCULATED PARAMETERS = 6.212452E+00

THE NUMBER OF FUNCTION EVALUATIONS REQUIRED = 1.020000E+02

THE NUMBER OF ITERATIONS REQUIRED = 3.000000E+01

AN INTEGER WHICH INDICATES THE CONVERGENCE CRITERION SATISFIED - INFER = 1

INFER=0 INDICATES THAT CONVERGENCE FAILED -- SEE THE (IER) PARAMETER

INFER=1 INDICATES THAT THE FOLLOWING CONVERGENCE CONDITION IS SATISFIED.

FOR TWO SUCCESSIVE ITERATIONS THE PARAMETER  
ESTIMATES AGREE, COMPONENT BY COMPONENT  
TO NSIG (SIGNIFICANT) DIGITS

- INFER-2 INDICATES THAT THE FOLLOWING CONVERGENCE CONDITION IS SATISFIED.  
FOR TWO SUCCESSIVE ITERATIONS THE RESIDUAL  
SUM OF THE SQUARE ESTIMATES HAVE RELATIVE  
DIFFERENCE LESS THAN OR EQUAL TO (EPS)
- INFER-4 INDICATES THAT THE FOLLOWING CONVERGENCE CONDITION IS SATISFIED.  
THE (EUCLIDEAN) NORM OF THE APPROXIMATE  
GRADIENT IS LESS THAN OR EQUAL TO (DELTA)
- INFER-X IF MORE THAN ONE OF THE ABOVE CONVERGENCE CRITERIA IS SATISFIED.  
(INFER) REPRESENTS THE CORRESPONDING SUM OF  
THE INTEGERS

THE ERROR PARAMETER: IER = 0

- IER-0 INDICATES SUCCESSFUL EXECUTION OF THE PROGRAM
- IER-38 INDICATES THAT THE JACOBIAN IS ZERO.  
THE SOLUTION IS A STATIONARY POINT (WARNING)
- IER-129 INDICATES THAT A SINGULARITY WAS  
DETECTED IN THE JACOBIAN
- IER-130 INDICATES THAT AT LEAST ONE OF THE  
SUBROUTINE CALL PARAMETERS WAS SPECIFIED  
INCORRECTLY -- VERIFY: M,N,IOPT,PARM(1),PARM(2)
- IER-131 INDICATES THAT THE MARQUARDT PARAMETER  
EXCEEDED THE DEFAULT VALUE OF (120.0)
- IER-132 INDICATES THAT AFTER A SUCCESSFUL  
RECOVERY FROM A SINGULAR JACOBIAN, THE SOLUTION  
HAS CYCLED BACK TO THE FIRST SINGULARITY
- IER-133 INDICATES THAT THE (MAXFN) PARAMETER  
WAS EXCEEDED

# VARIABLES USED IN THE CALCULATIONS

THE ESTIMATED METAL CLUSTER RESISTANCE (Rc) = 1.000000E+02

THE ESTIMATED GAP RESISTANCE (Rg) = 1.000000E+05

THE ESTIMATED GAP  
CAPACITANCE (Cg) = 6.000000E-07

THE LEAST SQUARE VALUE OF THE METAL CLUSTER  
RESISTANCE, Rc = 1.548297E+03

THE LEAST SQUARE VALUE OF THE GAP  
RESISTANCE, Rg = 8.898205E+04

THE LEAST SQUARE VALUE OF THE GAP  
CAPACITANCE, Cg = 6.550003E-07

THE RESIDUALS ARE CALCULATED BY THE FOLLOWING  
EQUATION: [MEASURED VALUE-CALCULATED VALUE]

SAMPLE	R(f)	R(cal)	R(resid)	Cg(est)
1	9.1100E+04	9.0530E+04	5.6965E-02	6.5500E-07
2	8.5500E+04	8.5705E+04	-2.0492E-02	6.5500E-07
3	3.5600E+04	3.8114E+04	-2.5142E-03	6.5500E-07
4	1.5000E+04	1.4762E+04	2.3760E-02	6.5500E-07
5	1.2600E+04	7.9493E+03	4.6507E+03	6.5500E-07
6	9.5200E+03	5.2659E+03	4.2541E+03	6.5500E-07
7	6.2500E+03	3.2398E+03	3.0102E+03	6.5500E-07
8	4.7600E+03	2.5078E+03	2.2522E+03	6.5500E-07
9	3.9100E+03	2.1647E+03	1.7453E+03	6.5500E-07
10	3.3300E+03	1.9773E+03	1.3527E+03	6.5500E-07
11	2.9500E+03	1.8639E+03	1.0861E+03	6.5500E-07
12	2.6900E+03	1.7901E+03	8.9988E-02	6.5500E-07
13	2.4900E+03	1.7395E+03	7.5053E+02	6.5500E-07
14	2.3400E+03	1.7032E+03	6.3679E+02	6.5500E-07
15	2.1000E+03	1.6559E+03	4.4406E+02	6.5500E-07
16	1.9200E+03	1.6274E+03	2.9260E+02	6.5500E-07
17	1.8000E+03	1.6089E+03	1.9112E+02	6.5500E-07
18	1.7000E+03	1.5962E+03	1.0383E+02	6.5500E-07
19	1.6200E+03	1.5871E+03	3.2923E+01	6.5500E-07
20	1.4700E+03	1.5731E+03	-1.0312E+02	6.5500E-07
21	1.3800E+03	1.5655E+03	-1.8554E+02	6.5500E-07

22	1.2600E+03	1.5610E+03	-3.0096E+02	6.5500E-07
23	1.2300E+03	1.5580E+03	-3.2800E+02	6.5500E-07
24	7.6000E+02	1.5545E+03	-7.9450E+02	6.5500E-07
25	6.8500E+02	1.5526E+03	-8.6761E+02	6.5500E-07
26	6.2500E+02	1.5515E+03	-9.2646E+02	6.5500E-07
27	5.8800E+02	1.5507E+03	-9.6272E+02	6.5500E-07
28	5.5900E+02	1.5502E+03	-9.9121E+02	6.5500E-07
29	5.3200E+02	1.5498E+03	-1.0178E+03	6.5500E-07
30	4.4600E+02	1.5490E+03	-1.1030E+03	6.5500E-07
31	4.0000E+02	1.5487E+03	-1.1487E+03	6.5500E-07
32	2.6900E+02	1.5484E+03	-1.2794E+03	6.5500E-07
33	2.1000E+02	1.5483E+03	-1.3383E+03	6.5500E-07
34	1.8500E+02	1.5483E+03	-1.3633E+03	6.5500E-07
35	1.6900E+02	1.5483E+03	-1.3793E+03	6.5500E-07
36	1.3300E+02	1.5483E+03	-1.4153E+03	6.5500E-07
37	1.2200E+02	1.5483E+03	-1.4263E+03	6.5500E-07
38	1.1900E+02	1.5483E+03	-1.4293E+03	6.5500E-07
39	1.1800E+02	1.5483E+03	-1.4303E+03	6.5500E-07

SUM OF SQUARED RESIDUALS= 9.2052E+07

VARIANCE= 2.4879E+06

STANDARD DEVIATION= 1.5773E+03

ADDITIONAL PARAMETERS CALCULATED BY THE LEAST SQUARES SUBROUTINE.

THE RESIDUAL SUM OF SQUARES = 9.205157E+07

THE NUMBER OF SIGNIFICANT DIGITS IN THE CALCULATED PARAMETERS = 6.960299E+00

THE NUMBER OF FUNCTION EVALUATIONS REQUIRED = 1.050000E+02

THE NUMBER OF ITERATIONS REQUIRED = 3.200000E+01

AN INTEGER WHICH INDICATES THE CONVERGENCE CRITERION SATISFIED - INFER = 1

INFER=0 INDICATES THAT CONVERGENCE FAILED -- SEE THE (IER) PARAMETER

INFER=1 INDICATES THAT THE FOLLOWING CONVERGENCE CONDITION IS SATISFIED.

FOR TWO SUCCESSIVE ITERATIONS THE PARAMETER  
ESTIMATES AGREE, COMPONENT BY COMPONENT  
TO NSIG (SIGNIFICANT) DIGITS

- INFER-2 INDICATES THAT THE FOLLOWING CONVERGENCE CONDITION IS SATISFIED.  
FOR TWO SUCCESSIVE ITERATIONS THE RESIDUAL  
SUM OF THE SQUARE ESTIMATES HAVE RELATIVE  
DIFFERENCE LESS THAN OR EQUAL TO (EPS)
- INFER-4 INDICATES THAT THE FOLLOWING CONVERGENCE CONDITION IS SATISFIED.  
THE (EUCLIDEAN) NORM OF THE APPROXIMATE  
GRADIENT IS LESS THAN OR EQUAL TO (DELTA)
- INFER-X IF MORE THAN ONE OF THE ABOVE CONVERGENCE CRITERIA IS SATISFIED.  
(INFER) REPRESENTS THE CORRESPONDING SUM OF  
THE INTEGERS

THE ERROR PARAMETER: IER = 0

- IER-0 INDICATES SUCCESSFUL EXECUTION OF THE PROGRAM
- IER-38 INDICATES THAT THE JACOBIAN IS ZERO.  
THE SOLUTION IS A STATIONARY POINT (WARNING)
- IER-129 INDICATES THAT A SINGULARITY WAS  
DETECTED IN THE JACOBIAN
- IER-130 INDICATES THAT AT LEAST ONE OF THE  
SUBROUTINE CALL PARAMETERS WAS SPECIFIED  
INCORRECTLY -- VERIFY: M,N,IOPT,PARM(1),PARM(2)
- IER-131 INDICATES THAT THE MARQUARDT PARAMETER  
EXCEEDED THE DEFAULT VALUE OF (120.0)
- IER-132 INDICATES THAT AFTER A SUCCESSFUL  
RECOVERY FROM A SINGULAR JACOBIAN, THE SOLUTION  
HAS CYCLED BACK TO THE FIRST SINGULARITY
- IER-133 INDICATES THAT THE (MAXFN) PARAMETER  
WAS EXCEEDED

# VARIABLES USED IN THE CALCULATIONS

THE ESTIMATED METAL CLUSTER RESISTANCE (Rc) = 1.000000E+02

THE ESTIMATED GAP RESISTANCE (Rg) = 1.000000E+05

THE ESTIMATED GAP  
CAPACITANCE (Cg) = 6.000000E-07

THE LEAST SQUARE VALUE OF THE METAL CLUSTER  
RESISTANCE, Rc = 1.272882E+03

THE LEAST SQUARE VALUE OF THE GAP  
RESISTANCE, Rg = 7.372166E+04

THE LEAST SQUARE VALUE OF THE GAP  
CAPACITANCE, Cg = 8.088382E-07

THE RESIDUALS ARE CALCULATED BY THE FOLLOWING  
EQUATION: [MEASURED VALUE-CALCULATED VALUE]

SAMPLE	R(f)	R(cal)	R(resid)	Cg(est)
1	7.6500E+04	7.4995E+04	1.5055E+03	8.0884E-07
2	6.9400E+04	7.0850E+04	-1.4503E+03	8.0884E-07
3	2.9400E+04	3.0891E+04	-1.4912E+03	8.0884E-07
4	1.2200E+04	1.1871E+04	3.2919E+02	8.0884E-07
5	9.3400E+03	6.3919E+03	2.9481E+03	8.0884E-07
6	7.3000E+03	4.2425E+03	3.0575E+03	8.0884E-07
7	5.0500E+03	2.6229E+03	2.4271E+03	8.0884E-07
8	3.8500E+03	2.0384E+03	1.8116E+03	8.0884E-07
9	3.2200E+03	1.7647E+03	1.4553E+03	8.0884E-07
10	2.7800E+03	1.6151E+03	1.1649E+03	8.0884E-07
11	2.5000E+03	1.5246E+03	9.7538E+02	8.0884E-07
12	2.3000E+03	1.4658E+03	8.3423E+02	8.0884E-07
13	2.1400E+03	1.4254E+03	7.1463E+02	8.0884E-07
14	2.0300E+03	1.3964E+03	6.3355E+02	8.0884E-07
15	1.8200E+03	1.3587E+03	4.6127E+02	8.0884E-07
16	1.6900E+03	1.3360E+03	3.5402E+02	8.0884E-07
17	1.5900E+03	1.3212E+03	2.6880E+02	8.0884E-07
18	1.5100E+03	1.3111E+03	1.9894E+02	8.0884E-07
19	1.4500E+03	1.3038E+03	1.4619E+02	8.0884E-07
20	1.3100E+03	1.2927E+03	1.7320E+01	8.0884E-07
21	9.0100E+02	1.2866E+03	-3.8563E+02	8.0884E-07



22	7.8100E+02	1.2830E+03	-5.0198E+02	8.0884E-07
23	7.3000E+02	1.2806E+03	-5.5062E+02	8.0884E-07
24	6.5400E+02	1.2778E+03	-6.2383E+02	8.0884E-07
25	6.0200E+02	1.2763E+03	-6.7432E+02	8.0884E-07
26	5.6200E+02	1.2754E+03	-7.1341E+02	8.0884E-07
27	5.3500E+02	1.2748E+03	-7.3982E+02	8.0884E-07
28	5.1000E+02	1.2744E+03	-7.6441E+02	8.0884E-07
29	4.9300E+02	1.2741E+03	-7.8112E+02	8.0884E-07
30	4.1700E+02	1.2734E+03	-8.5643E+02	8.0884E-07
31	3.7900E+02	1.2732E+03	-8.9419E+02	8.0884E-07
32	2.6900E+02	1.2729E+03	-1.0039E+03	8.0884E-07
33	2.1300E+02	1.2729E+03	-1.0599E+03	8.0884E-07
34	1.8700E+02	1.2729E+03	-1.0859E+03	8.0884E-07
35	1.7000E+02	1.2729E+03	-1.1029E+03	8.0884E-07
36	1.3000E+02	1.2729E+03	-1.1429E+03	8.0884E-07
37	1.1600E+02	1.2729E+03	-1.1569E+03	8.0884E-07
38	1.1200E+02	1.2729E+03	-1.1609E+03	8.0884E-07
39	1.1000E+02	1.2729E+03	-1.1629E+03	8.0884E-07

SUM OF SQUARED RESIDUALS= 5.5622E+07

VARIANCE= 1.5033E+06

STANDARD DEVIATION= 1.2261E+03

ADDITIONAL PARAMETERS CALCULATED BY THE LEAST SQUARES SUBROUTINE.

THE RESIDUAL SUM OF SQUARES = 5.562241E+07

THE NUMBER OF SIGNIFICANT DIGITS IN THE CALCULATED PARAMETERS = 6.070780E+00

THE NUMBER OF FUNCTION EVALUATIONS REQUIRED = 7.900000E+01

THE NUMBER OF ITERATIONS REQUIRED = 2.300000E+01

AN INTEGER WHICH INDICATES THE CONVERGENCE CRITERION SATISFIED.

INFER=0 INDICATES THAT CONVERGENCE FAILED -- SEE THE (IER) PARAMETER

INFER=1 INDICATES THAT THE FOLLOWING CONVERGENCE CONDITION IS SATISFIED.

FOR TWO SUCCESSIVE ITERATIONS THE PARAMETER  
ESTIMATES AGREE, COMPONENT BY COMPONENT  
TO NSIG (SIGNIFICANT) DIGITS

- INFER=2 INDICATES THAT THE FOLLOWING CONVERGENCE CONDITION IS SATISFIED.  
FOR TWO SUCCESSIVE ITERATIONS THE RESIDUAL  
SUM OF THE SQUARE ESTIMATES HAVE RELATIVE  
DIFFERENCE LESS THAN OR EQUAL TO (EPS)
- INFER=4 INDICATES THAT THE FOLLOWING CONVERGENCE CONDITION IS SATISFIED.  
THE (EUCLIDEAN) NORM OF THE APPROXIMATE  
GRADIENT IS LESS THAN OR EQUAL TO (DELTA)
- INFER=X IF MORE THAN ONE OF THE ABOVE CONVERGENCE CRITERIA IS SATISFIED.  
(INFER) REPRESENTS THE CORRESPONDING SUM OF  
THE INTEGERS

THE ERROR PARAMETER: IER = 0

- IER=0 INDICATES SUCCESSFUL EXECUTION OF THE PROGRAM
- IER=38 INDICATES THAT THE JACOBIAN IS ZERO.  
THE SOLUTION IS A STATIONARY POINT (WARNING)
- IER=129 INDICATES THAT A SINGULARITY WAS  
DETECTED IN THE JACOBIAN
- IER=130 INDICATES THAT AT LEAST ONE OF THE  
SUBROUTINE CALL PARAMETERS WAS SPECIFIED  
INCORRECTLY -- VERIFY: M,N,IOP,T,PARM(1),PARM(2)
- IER=131 INDICATES THAT THE MARQUARDT PARAMETER  
EXCEEDED THE DEFAULT VALUE OF (120.0)
- IER=132 INDICATES THAT AFTER A SUCCESSFUL  
RECOVERY FROM A SINGULAR JACOBIAN, THE SOLUTION  
HAS CYCLED BACK TO THE FIRST SINGULARITY
- IER=133 INDICATES THAT THE (MAXFN) PARAMETER  
WAS EXCEEDED

# VARIABLES USED IN THE CALCULATIONS

THE ESTIMATED METAL CLUSTER RESISTANCE (Rc) = 1.000000E+02

THE ESTIMATED GAP RESISTANCE (Rg) = 1.000000E+05

THE ESTIMATED GAP  
CAPACITANCE (Cg) = 6.000000E-07

THE LEAST SQUARE VALUE OF THE METAL CLUSTER  
RESISTANCE, Rc = 1.601662E+03

THE LEAST SQUARE VALUE OF THE GAP  
RESISTANCE, Rg = 1.002055E+05

THE LEAST SQUARE VALUE OF THE GAP  
CAPACITANCE, Cg = 6.252022E-07

THE RESIDUALS ARE CALCULATED BY THE FOLLOWING  
EQUATION: [MEASURED VALUE-CALCULATED VALUE]

SAMPLE	R(f)	R(cal)	R(resid)	Cg(est)
1	1.0200E+05	1.0181E+05	1.9288E+02	6.2520E-07
2	9.6200E+04	9.6051E+04	1.4881E+02	6.2520E-07
3	3.9100E+04	4.1310E+04	-2.2098E+03	6.2520E-07
4	1.5300E+04	1.5727E+04	-4.2666E+02	6.2520E-07
5	1.3300E+04	8.4128E+03	4.8872E+03	6.2520E-07
6	9.7100E+03	5.5504E+03	4.1556E+03	6.2520E-07
7	6.4900E+03	3.3959E+03	3.0941E+03	6.2520E-07
8	4.9000E+03	2.6189E+03	2.2811E+03	6.2520E-07
9	4.0000E+03	2.2551E+03	1.7449E+03	6.2520E-07
10	3.4700E+03	2.0563E+03	1.4137E+03	6.2520E-07
11	3.1000E+03	1.9361E+03	1.1639E+03	6.2520E-07
12	2.8200E+03	1.8579E+03	9.6208E+02	6.2520E-07
13	2.6200E+03	1.8042E+03	8.1575E+02	6.2520E-07
14	2.4900E+03	1.7658E+03	7.2418E+02	6.2520E-07
15	2.3700E+03	1.7157E+03	6.5428E+02	6.2520E-07
16	2.1100E+03	1.6855E+03	4.2452E+02	6.2520E-07
17	1.9400E+03	1.6659E+03	2.7415E+02	6.2520E-07
18	1.8200E+03	1.6524E+03	1.6761E+02	6.2520E-07
19	1.7200E+03	1.6428E+03	7.7248E+01	6.2520E-07
20	1.5200E+03	1.6280E+03	-1.0796E+02	6.2520E-07
21	1.4000E+03	1.6199E+03	-2.1993E+02	6.2520E-07

22	1.3100E+03	1.6151E+03	-3.0508E+02	6.2520E-07
23	1.2300E+03	1.6119E+03	-3.8194E+02	6.2520E-07
24	8.1300E+02	1.6082E+03	-7.9524E+02	6.2520E-07
25	7.0900E+02	1.6062E+03	-8.9723E+02	6.2520E-07
26	6.4900E+02	1.6050E+03	-9.5602E+02	6.2520E-07
27	6.0600E+02	1.6042E+03	-9.9823E+02	6.2520E-07
28	5.7500E+02	1.6037E+03	-1.0287E+03	6.2520E-07
29	5.4900E+02	1.6033E+03	-1.0543E+03	6.2520E-07
30	4.5500E+02	1.6024E+03	-1.1474E+03	6.2520E-07
31	4.0800E+02	1.6021E+03	-1.1941E+03	6.2520E-07
32	2.8200E+02	1.6017E+03	-1.3197E+03	6.2520E-07
33	2.2100E+02	1.6017E+03	-1.3807E+03	6.2520E-07
34	1.9400E+02	1.6017E+03	-1.4077E+03	6.2520E-07
35	1.7700E+02	1.6017E+03	-1.4247E+03	6.2520E-07
36	1.3200E+02	1.6017E+03	-1.4697E+03	6.2520E-07
37	1.1800E+02	1.6017E+03	-1.4837E+03	6.2520E-07
38	1.1400E+02	1.6017E+03	-1.4877E+03	6.2520E-07
39	1.1200E+02	1.6017E+03	-1.4897E+03	6.2520E-07

SUM OF SQUARED RESIDUALS= 9.5331E+07

VARIANCE= 2.5765E+06

STANDARD DEVIATION= 1.6051E+03

ADDITIONAL PARAMETERS CALCULATED BY THE LEAST SQUARES SUBROUTINE.

THE RESIDUAL SUM OF SQUARES = 9.533067E+07

THE NUMBER OF SIGNIFICANT DIGITS IN THE CALCULATED PARAMETERS = 6.850536E+00

THE NUMBER OF FUNCTION EVALUATIONS REQUIRED = 1.010000E+02

THE NUMBER OF ITERATIONS REQUIRED = 3.000000E+01

AN INTEGER WHICH INDICATES THE CONVERGENCE CRITERION SATISFIED.

INFER=0 INDICATES THAT CONVERGENCE FAILED -- SEE THE (IER) PARAMETER

INFER=1 INDICATES THAT THE FOLLOWING CONVERGENCE CONDITION IS SATISFIED.

FOR TWO SUCCESSIVE ITERATIONS THE PARAMETER  
ESTIMATES AGREE, COMPONENT BY COMPONENT  
TO NSIG (SIGNIFICANT) DIGITS

- INFER=2 INDICATES THAT THE FOLLOWING CONVERGENCE CONDITION IS SATISFIED.  
FOR TWO SUCCESSIVE ITERATIONS THE RESIDUAL  
SUM OF THE SQUARE ESTIMATES HAVE RELATIVE  
DIFFERENCE LESS THAN OR EQUAL TO (EPS)
- INFER=4 INDICATES THAT THE FOLLOWING CONVERGENCE CONDITION IS SATISFIED.  
THE (EUCLIDEAN) NORM OF THE APPROXIMATE  
GRADIENT IS LESS THAN OR EQUAL TO (DELTA)
- INFER=X IF MORE THAN ONE OF THE ABOVE CONVERGENCE CRITERIA IS SATISFIED.  
(INFER) REPRESENTS THE CORRESPONDING SUM OF  
THE INTEGERS

THE ERROR PARAMETER: IER = 0

- IER=0 INDICATES SUCCESSFUL EXECUTION OF THE PROGRAM
- IER=38 INDICATES THAT THE JACOBIAN IS ZERO.  
THE SOLUTION IS A STATIONARY POINT (WARNING)
- IER=129 INDICATES THAT A SINGULARITY WAS  
DETECTED IN THE JACOBIAN
- IER=130 INDICATES THAT AT LEAST ONE OF THE  
SUBROUTINE CALL PARAMETERS WAS SPECIFIED  
INCORRECTLY -- VERIFY: M,N,IOPT,PARM(1),PARM(2)
- IER=131 INDICATES THAT THE MARQUARDT PARAMETER  
EXCEEDED THE DEFAULT VALUE OF (120.0)
- IER=132 INDICATES THAT AFTER A SUCCESSFUL  
RECOVERY FROM A SINGULAR JACOBIAN, THE SOLUTION  
HAS CYCLED BACK TO THE FIRST SINGULARITY
- IER=133 INDICATES THAT THE (MAXFN) PARAMETER  
WAS EXCEEDED

# VARIABLES USED IN THE CALCULATIONS

THE ESTIMATED METAL CLUSTER RESISTANCE (Rc) = 1.000000E+02

THE ESTIMATED GAP RESISTANCE (Rg) = 1.000000E+05

THE ESTIMATED GAP  
CAPACITANCE (Cg) = 6.000000E-07

THE LEAST SQUARE VALUE OF THE METAL CLUSTER  
RESISTANCE, Rc = 1.573407E+03

THE LEAST SQUARE VALUE OF THE GAP  
RESISTANCE, Rg = 8.516865E+04

THE LEAST SQUARE VALUE OF THE GAP  
CAPACITANCE, Cg = 6.499758E-07

THE RESIDUALS ARE CALCULATED BY THE FOLLOWING  
EQUATION: [MEASURED VALUE-CALCULATED VALUE]

SAMPLE	R(f)	R(cal)	R(resid)	Cg(est)
1	8.7400E+04	8.6742E+04	6.5795E+02	6.4998E-07
2	8.2000E+04	8.2313E+04	-3.1261E+02	6.4998E-07
3	3.5200E+04	3.7486E+04	-2.2864E+03	6.4998E-07
4	1.4600E+04	1.4704E+04	-1.0432E+02	6.4998E-07
5	1.1700E+04	7.9561E+03	3.7439E+03	6.4998E-07
6	1.0100E+04	5.2854E+03	4.8146E+03	6.4998E-07
7	6.6700E+03	3.2641E+03	3.4059E+03	6.4998E-07
8	5.0000E+03	2.5328E+03	2.4672E+03	6.4998E-07
9	4.1200E+03	2.1899E+03	1.9301E+03	6.4998E-07
10	3.5300E+03	2.0025E+03	1.5275E+03	6.4998E-07
11	3.1300E+03	1.8891E+03	1.2409E+03	6.4998E-07
12	2.8200E+03	1.8153E+03	1.0047E+03	6.4998E-07
13	2.5900E+03	1.7646E+03	8.2536E+02	6.4998E-07
14	2.4200E+03	1.7284E+03	6.9163E+02	6.4998E-07
15	2.0800E+03	1.6811E+03	3.9892E+02	6.4998E-07
16	1.9400E+03	1.6525E+03	2.8746E+02	6.4998E-07
17	1.8100E+03	1.6340E+03	1.7599E+02	6.4998E-07
18	1.7000E+03	1.6213E+03	7.8705E+01	6.4998E-07
19	1.6200E+03	1.6122E+03	7.7996E+00	6.4998E-07
20	1.4500E+03	1.5982E+03	-1.4824E+02	6.4998E-07
21	1.3400E+03	1.5907E+03	-2.5065E+02	6.4998E-07

22	1.2700E+03	1.5861E+03	-3.1608E+02	6.4998E-07
23	1.2300E+03	1.5831E+03	-3.5311E+02	6.4998E-07
24	7.6900E+02	1.5796E+03	-8.1062E+02	6.4998E-07
25	6.5800E+02	1.5777E+03	-9.1972E+02	6.4998E-07
26	6.1000E+02	1.5766E+03	-9.6658E+02	6.4998E-07
27	5.7500E+02	1.5758E+03	-1.0008E+03	6.4998E-07
28	5.4500E+02	1.5753E+03	-1.0293E+03	6.4998E-07
29	5.2400E+02	1.5750E+03	-1.0510E+03	6.4998E-07
30	4.4400E+02	1.5741E+03	-1.1301E+03	6.4998E-07
31	4.0000E+02	1.5738E+03	-1.1738E+03	6.4998E-07
32	2.7400E+02	1.5735E+03	-1.2995E+03	6.4998E-07
33	2.1100E+02	1.5734E+03	-1.3624E+03	6.4998E-07
34	1.8000E+02	1.5734E+03	-1.3934E+03	6.4998E-07
35	1.6100E+02	1.5734E+03	-1.4124E+03	6.4998E-07
36	1.1000E+02	1.5734E+03	-1.4634E+03	6.4998E-07
37	8.7700E+01	1.5734E+03	-1.4857E+03	6.4998E-07
38	8.0600E+01	1.5734E+03	-1.4928E+03	6.4998E-07
39	7.7500E+01	1.5734E+03	-1.4959E+03	6.4998E-07

SUM OF SQUARED RESIDUALS= 9.5565E+07

VARIANCE= 2.5828E+06

STANDARD DEVIATION= 1.6071E+03

ADDITIONAL PARAMETERS CALCULATED BY THE LEAST SQUARES SUBROUTINE.

THE RESIDUAL SUM OF SQUARES = 9.556468E+07

THE NUMBER OF SIGNIFICANT DIGITS IN THE CALCULATED PARAMETERS = 6.770939E+00

THE NUMBER OF FUNCTION EVALUATIONS REQUIRED = 1.040000E+02

THE NUMBER OF ITERATIONS REQUIRED = 3.000000E+01

AN INTEGER WHICH INDICATES THE CONVERGENCE CRITERION SATISFIED - INFER = 1

INFER=0 INDICATES THAT CONVERGENCE FAILED -- SEE THE (IER) PARAMETER

INFER=1 INDICATES THAT THE FOLLOWING CONVERGENCE CONDITION IS SATISFIED.

FOR TWO SUCCESSIVE ITERATIONS THE PARAMETER  
ESTIMATES AGREE, COMPONENT BY COMPONENT  
TO NSIG (SIGNIFICANT) DIGITS

- INFER-2 INDICATES THAT THE FOLLOWING CONVERGENCE CONDITION IS SATISFIED.  
FOR TWO SUCCESSIVE ITERATIONS THE RESIDUAL  
SUM OF THE SQUARE ESTIMATES HAVE RELATIVE  
DIFFERENCE LESS THAN OR EQUAL TO (EPS)
- INFER-4 INDICATES THAT THE FOLLOWING CONVERGENCE CONDITION IS SATISFIED.  
THE (EUCLIDEAN) NORM OF THE APPROXIMATE  
GRADIENT IS LESS THAN OR EQUAL TO (DELTA)
- INFER-X IF MORE THAN ONE OF THE ABOVE CONVERGENCE CRITERIA IS SATISFIED.  
(INFER) REPRESENTS THE CORRESPONDING SUM OF  
THE INTEGERS

THE ERROR PARAMETER: IER = 0

- IER=0 INDICATES SUCCESSFUL EXECUTION OF THE PROGRAM
- IER=38 INDICATES THAT THE JACOBIAN IS ZERO.  
THE SOLUTION IS A STATIONARY POINT (WARNING)
- IER=129 INDICATES THAT A SINGULARITY WAS  
DETECTED IN THE JACOBIAN
- IER=130 INDICATES THAT AT LEAST ONE OF THE  
SUBROUTINE CALL PARAMETERS WAS SPECIFIED  
INCORRECTLY -- VERIFY: M,N,IOPT,PARM(1),PARM(2)
- IER=131 INDICATES THAT THE MARQUARDT PARAMETER  
EXCEEDED THE DEFAULT VALUE OF (120.0)
- IER=132 INDICATES THAT AFTER A SUCCESSFUL  
RECOVERY FROM A SINGULAR JACOBIAN, THE SOLUTION  
HAS CYCLED BACK TO THE FIRST SINGULARITY
- IER=133 INDICATES THAT THE (MAXFN) PARAMETER  
WAS EXCEEDED



# VARIABLES USED IN THE CALCULATIONS

THE ESTIMATED METAL CLUSTER RESISTANCE (Rc) = 1.000000E+02

THE ESTIMATED GAP RESISTANCE (Rg) = 1.000000E+05

THE ESTIMATED GAP  
CAPACITANCE (Cg) = 6.000000E-07

THE LEAST SQUARE VALUE OF THE METAL CLUSTER  
RESISTANCE, Rc = 1.571502E+03

THE LEAST SQUARE VALUE OF THE GAP  
RESISTANCE, Rg = 1.001552E+05

THE LEAST SQUARE VALUE OF THE GAP  
CAPACITANCE, Cg = 6.533406E-07

THE RESIDUALS ARE CALCULATED BY THE FOLLOWING  
EQUATION: [MEASURED VALUE-CALCULATED VALUE]

SAMPLE	R(f)	R(cal)	R(resid)	Cg(est)
1	1.0150E+05	1.0173E+05	-2.2669E+02	6.5334E-07
2	9.6200E+04	9.5589E+04	6.1113E+02	6.5334E-07
3	3.7300E+04	3.9623E+04	-2.3230E+03	6.5334E-07
4	1.4900E+04	1.4875E+04	2.4828E+01	6.5334E-07
5	1.1600E+04	7.9553E+03	3.6447E+03	6.5334E-07
6	1.0300E+04	5.2654E+03	5.0346E+03	6.5334E-07
7	6.8500E+03	3.2476E+03	3.6024E+03	6.5334E-07
8	5.1500E+03	2.5213E+03	2.6287E+03	6.5334E-07
9	4.2200E+03	2.1814E+03	2.0386E+03	6.5334E-07
10	3.6200E+03	1.9958E+03	1.6242E+03	6.5334E-07
11	3.1900E+03	1.8836E+03	1.3064E+03	6.5334E-07
12	2.8800E+03	1.8106E+03	1.0694E+03	6.5334E-07
13	2.6300E+03	1.7605E+03		

22	8.9300E+02	1.5840E+03	-6.9102E+02	6.5334E-07
23	8.2600E+02	1.5811E+03	-7.9509E+02	6.5334E-07
24	7.3000E+02	1.5776E+03	-8.4764E+02	6.5334E-07
25	6.6700E+02	1.5758E+03	-9.0876E+02	6.5334E-07
26	6.1700E+02	1.5746E+03	-9.9763E+02	6.5334E-07
27	5.8100E+02	1.5739E+03	-9.9290E+02	6.5334E-07
28	5.6200E+02	1.5734E+03	-1.0114E+03	6.5334E-07
29	5.4100E+02	1.5730E+03	-1.0320E+03	6.5334E-07
30	4.5700E+02	1.5722E+03	-1.1152E+03	6.5334E-07
31	4.1200E+02	1.5719E+03	-1.1599E+03	6.5334E-07
32	2.9100E+02	1.5716E+03	-1.2806E+03	6.5334E-07
33	2.3000E+02	1.5715E+03	-1.3415E+03	6.5334E-07
34	2.0000E+02	1.5715E+03	-1.3715E+03	6.5334E-07
35	1.8200E+02	1.5715E+03	-1.3895E+03	6.5334E-07
36	1.3300E+02	1.5715E+03	-1.4385E+03	6.5334E-07
37	1.1200E+02	1.5715E+03	-1.4595E+03	6.5334E-07
38	1.0500E+02	1.5715E+03	-1.4665E+03	6.5334E-07
39	1.0200E+02	1.5715E+03	-1.4695E+03	6.5334E-07

SUM OF SQUARED RESIDUALS= 1.0119E+08

VARIANCE= 2.7350E+06

STANDARD DEVIATION= 1.6538E+03

ADDITIONAL PARAMETERS CALCULATED BY THE LEAST SQUARES SUBROUTINE.

THE RESIDUAL SUM OF SQUARES = 1.011938E+08

THE NUMBER OF SIGNIFICANT DIGITS IN THE CALCULATED PARAMETERS = 7.241604E+00

THE NUMBER OF FUNCTION EVALUATIONS REQUIRED = 1.030000E+02

THE NUMBER OF ITERATIONS REQUIRED = 3.000000E+01

AN INTEGER WHICH INDICATES THE CONVERGENCE CRITERION SATISFIED - INFER = 1

INFER=0 INDICATES THAT CONVERGENCE FAILED -- SEE THE (IER) PARAMETER

INFER=1 INDICATES THAT THE FOLLOWING CONVERGENCE CONDITION IS SATISFIED.

FOR TWO SUCCESSIVE ITERATIONS THE PARAMETER  
ESTIMATES AGREE, COMPONENT BY COMPONENT  
TO NSIG (SIGNIFICANT) DIGITS

- INFER=2 INDICATES THAT THE FOLLOWING CONVERGENCE CONDITION IS SATISFIED.  
FOR TWO SUCCESSIVE ITERATIONS THE RESIDUAL  
SUM OF THE SQUARE ESTIMATES HAVE RELATIVE  
DIFFERENCE LESS THAN OR EQUAL TO (EPS)
- INFER=4 INDICATES THAT THE FOLLOWING CONVERGENCE CONDITION IS SATISFIED.  
THE (EUCLIDEAN) NORM OF THE APPROXIMATE  
GRADIENT IS LESS THAN OR EQUAL TO (DELTA)
- INFER=X IF MORE THAN ONE OF THE ABOVE CONVERGENCE CRITERIA IS SATISFIED.  
(INFER) REPRESENTS THE CORRESPONDING SUM OF  
THE INTEGERS

THE ERROR PARAMETER: IER = 0

- IER=0 INDICATES SUCCESSFUL EXECUTION OF THE PROGRAM
- IER=38 INDICATES THAT THE JACOBIAN IS ZERO.  
THE SOLUTION IS A STATIONARY POINT (WARNING)
- IER=129 INDICATES THAT A SINGULARITY WAS  
DETECTED IN THE JACOBIAN
- IER=130 INDICATES THAT AT LEAST ONE OF THE  
SUBROUTINE CALL PARAMETERS WAS SPECIFIED  
INCORRECTLY -- VERIFY: M,N,IOPT,PARM(1),PARM(2)
- IER=131 INDICATES THAT THE MARQUARDT PARAMETER  
EXCEEDED THE DEFAULT VALUE OF (120.0)
- IER=132 INDICATES THAT AFTER A SUCCESSFUL  
RECOVERY FROM A SINGULAR JACOBIAN, THE SOLUTION  
HAS CYCLED BACK TO THE FIRST SINGULARITY
- IER=133 INDICATES THAT THE (MAXFN) PARAMETER  
WAS EXCEEDED

# VARIABLES USED IN THE CALCULATIONS

THE ESTIMATED METAL CLUSTER RESISTANCE (Rc) = 1.000000E+02

THE ESTIMATED GAP RESISTANCE (Rg) = 1.000000E+05

THE ESTIMATED GAP  
CAPACITANCE (Cg) = 6.000000E-07

THE LEAST SQUARE VALUE OF THE METAL CLUSTER  
RESISTANCE, Rc = 1.609475E+03

THE LEAST SQUARE VALUE OF THE GAP  
RESISTANCE, Rg = 9.154079E+04

THE LEAST SQUARE VALUE OF THE GAP  
CAPACITANCE, Cg = 6.375048E-07

THE RESIDUALS ARE CALCULATED BY THE FOLLOWING  
EQUATION: [MEASURED VALUE-CALCULATED VALUE]

SAMPLE	R(f)	R(cal)	R(resid)	Cg(est)
1	9.3800E+04	9.3150E+04	6.4974E+02	6.3750E-07
2	8.7700E+04	8.8126E+04	-4.2575E+02	6.3750E-07
3	3.7300E+04	3.8944E+04	-1.6441E+03	6.3750E-07
4	1.3900E+04	1.5056E+04	-1.1563E+03	6.3750E-07
5	1.1900E+04	8.1169E+03	3.7831E+03	6.3750E-07
6	1.0200E+04	5.3874E+03	4.8126E+03	6.3750E-07
7	6.8000E+03	3.3280E+03	3.4720E+03	6.3750E-07
8	5.1500E+03	2.5841E+03	2.5659E+03	6.3750E-07
9	4.2700E+03	2.2357E+03	2.0343E+03	6.3750E-07
10	3.6800E+03	2.0452E+03	1.6348E+03	6.3750E-07
11	3.2600E+03	1.9300E+03	1.3300E+03	6.3750E-07
12	2.9400E+03	1.8551E+03	1.0849E+03	6.3750E-07
13	2.7000E+03	1.8037E+03	8.9634E+02	6.3750E-07
14	2.5000E+03	1.7668E+03	7.3317E+02	6.3750E-07
15	2.1700E+03	1.7188E+03	4.5120E+02	6.3750E-07
16	2.0200E+03	1.6898E+03	3.3018E+02	6.3750E-07
17	1.8600E+03	1.6710E+03	1.8900E+02	6.3750E-07
18	1.7400E+03	1.6581E+03	8.1902E+01	6.3750E-07
19	1.6500E+03	1.6489E+03	1.1364E+00	6.3750E-07
20	1.4600E+03	1.6347E+03	-1.7469E+02	6.3750E-07
21	1.3300E+03	1.6270E+03	-2.9699E+02	6.3750E-07

22	1.2500E+03	1.6223E+03	-3.7234E+02	6.3750E-07
23	1.1800E+03	1.6193E+03	-4.3933E+02	6.3750E-07
24	8.2600E+02	1.6158E+03	-7.8978E+02	6.3750E-07
25	7.1900E+02	1.6139E+03	-8.9485E+02	6.3750E-07
26	6.6200E+02	1.6127E+03	-9.5069E+02	6.3750E-07
27	6.2100E+02	1.6119E+03	-9.9094E+02	6.3750E-07
28	5.8800E+02	1.6114E+03	-1.0234E+03	6.3750E-07
29	5.6200E+02	1.6111E+03	-1.0491E+03	6.3750E-07
30	4.6500E+02	1.6102E+03	-1.1452E+03	6.3750E-07
31	4.1700E+02	1.6099E+03	-1.1929E+03	6.3750E-07
32	2.9400E+02	1.6095E+03	-1.3155E+03	6.3750E-07
33	2.3300E+02	1.6095E+03	-1.3765E+03	6.3750E-07
34	2.0300E+02	1.6095E+03	-1.4065E+03	6.3750E-07
35	1.8500E+02	1.6095E+03	-1.4245E+03	6.3750E-07
36	1.3700E+02	1.6095E+03	-1.4725E+03	6.3750E-07
37	1.1400E+02	1.6095E+03	-1.4955E+03	6.3750E-07
38	1.0500E+02	1.6095E+03	-1.5045E+03	6.3750E-07
39	1.0100E+02	1.6095E+03	-1.5085E+03	6.3750E-07

SUM OF SQUARED RESIDUALS= 9.7427E+07

VARIANCE= 2.6332E+06

STANDARD DEVIATION= 1.6227E+03

ADDITIONAL PARAMETERS CALCULATED BY THE LEAST SQUARES SUBROUTINE.

THE RESIDUAL SUM OF SQUARES = 9.742725E+07

THE NUMBER OF SIGNIFICANT DIGITS IN THE CALCULATED PARAMETERS = 7.200335E+00

THE NUMBER OF FUNCTION EVALUATIONS REQUIRED = 8.500000E+01

THE NUMBER OF ITERATIONS REQUIRED = 2.300000E+01

AN INTEGER WHICH INDICATES THE CONVERGENCE CRITERION SATISFIED - INFER = 1

INFER=0 INDICATES THAT CONVERGENCE FAILED -- SEE THE (IER) PARAMETER

INFER=1 INDICATES THAT THE FOLLOWING CONVERGENCE CONDITION IS SATISFIED.

FOR TWO SUCCESSIVE ITERATIONS THE PARAMETER  
ESTIMATES AGREE, COMPONENT BY COMPONENT  
TO NSIG (SIGNIFICANT) DIGITS

INFER-2 INDICATES THAT THE FOLLOWING CONVERGENCE CONDITION IS SATISFIED.  
FOR TWO SUCCESSIVE ITERATIONS THE RESIDUAL  
SUM OF THE SQUARE ESTIMATES HAVE RELATIVE  
DIFFERENCE LESS THAN OR EQUAL TO (EPS)

INFER-4 INDICATES THAT THE FOLLOWING CONVERGENCE CONDITION IS SATISFIED.  
THE (EUCLIDEAN) NORM OF THE APPROXIMATE  
GRADIENT IS LESS THAN OR EQUAL TO (DELTA)

INFER-X IF MORE THAN ONE OF THE ABOVE CONVERGENCE CRITERIA IS SATISFIED.  
(INFER) REPRESENTS THE CORRESPONDING SUM OF  
THE INTEGERS

THE ERROR PARAMETER: IER = 0

IER=0 INDICATES SUCCESSFUL EXECUTION OF THE PROGRAM

IER=38 INDICATES THAT THE JACOBIAN IS ZERO.  
THE SOLUTION IS A STATIONARY POINT (WARNING)

IER=129 INDICATES THAT A SINGULARITY WAS  
DETECTED IN THE JACOBIAN

IER=130 INDICATES THAT AT LEAST ONE OF THE  
SUBROUTINE CALL PARAMETERS WAS SPECIFIED  
INCORRECTLY -- VERIFY: M,N,IOP,PARM(1),PARM(2)

IER=131 INDICATES THAT THE MARQUARDT PARAMETER  
EXCEEDED THE DEFAULT VALUE OF (120.0)

IER=132 INDICATES THAT AFTER A SUCCESSFUL  
RECOVERY FROM A SINGULAR JACOBIAN, THE SOLUTION  
HAS CYCLED BACK TO THE FIRST SINGULARITY

IER=133 INDICATES THAT THE (MAXFN) PARAMETER  
WAS EXCEEDED

# VARIABLES USED IN THE CALCULATIONS

THE ESTIMATED METAL CLUSTER RESISTANCE (Rc) = 1.000000E+02

THE ESTIMATED GAP RESISTANCE (Rg) = 1.000000E+05

THE ESTIMATED GAP  
CAPACITANCE (Cg) = 6.000000E-07

THE LEAST SQUARE VALUE OF THE METAL CLUSTER  
RESISTANCE, Rc = 1.668688E+03

THE LEAST SQUARE VALUE OF THE GAP  
RESISTANCE, Rg = 9.734966E+04

THE LEAST SQUARE VALUE OF THE GAP  
CAPACITANCE, Cg = 6.614898E-07

THE RESIDUALS ARE CALCULATED BY THE FOLLOWING  
EQUATION: [MEASURED VALUE-CALCULATED VALUE]

SAMPLE	R(f)	R(cal)	R(resid)	Cg(est)
1	9.9400E+04	9.9018E+04	3.8166E+02	6.6149E-07
2	9.2600E+04	9.2737E+04	-1.3715E+02	6.6149E-07
3	3.5300E+04	3.7402E+04	-2.1024E+03	6.6149E-07
4	1.4000E+04	1.3996E+04	4.2179E+00	6.6149E-07
5	1.1400E+04	7.5620E+03	3.8380E+03	6.6149E-07
6	1.0200E+04	5.0738E+03	5.1262E+03	6.6149E-07
7	6.9000E+03	3.2121E+03	3.6879E+03	6.6149E-07
8	5.0800E+03	2.5429E+03	2.5371E+03	6.6149E-07
9	4.1500E+03	2.2300E+03	1.9200E+03	6.6149E-07
10	3.5500E+03	2.0592E+03	1.4908E+03	6.6149E-07
11	3.1500E+03	1.9559E+03	1.1941E+03	6.6149E-07
12	2.8700E+03	1.8887E+03	9.8127E+02	6.6149E-07
13	2.5640E+03	1.8426E+03	7.2137E+02	6.6149E-07
14	2.5000E+03	1.8096E+03	6.9037E+02	6.6149E-07
15	2.2700E+03	1.7666E+03	5.0339E+02	6.6149E-07
16	1.0700E+03	1.7406E+03	-6.7065E+02	6.6149E-07
17	1.9100E+03	1.7238E+03	1.8621E+02	6.6149E-07
18	1.8200E+03	1.7122E+03	1.0777E+02	6.6149E-07
19	1.7200E+03	1.7040E+03	1.6039E+01	6.6149E-07
20	1.5500E+03	1.6913E+03	-1.4127E+02	6.6149E-07
21	1.4200E+03	1.6844E+03	-2.6437E+02	6.6149E-07

22	1.3300E+03	1.6802E+03	-3.5021E+02	6.6149E-07
23	1.2600E+03	1.6775E+03	-4.1751E+02	6.6149E-07
24	1.2000E+03	1.6743E+03	-4.7433E+02	6.6149E-07
25	8.2000E+02	1.6726E+03	-8.5261E+02	6.6149E-07
26	7.5200E+02	1.6716E+03	-9.1957E+02	6.6149E-07
27	7.0900E+02	1.6709E+03	-9.6189E+02	6.6149E-07
28	6.7600E+02	1.6704E+03	-9.9443E+02	6.6149E-07
29	6.4500E+02	1.6701E+03	-1.0251E+03	6.6149E-07
30	5.4600E+02	1.6693E+03	-1.1233E+03	6.6149E-07
31	4.9500E+02	1.6690E+03	-1.1740E+03	6.6149E-07
32	3.5300E+02	1.6687E+03	-1.3157E+03	6.6149E-07
33	2.7800E+02	1.6687E+03	-1.3907E+03	6.6149E-07
34	2.4000E+02	1.6687E+03	-1.4287E+03	6.6149E-07
35	2.1700E+02	1.6687E+03	-1.4517E+03	6.6149E-07
36	1.5400E+02	1.6687E+03	-1.5147E+03	6.6149E-07
37	1.2200E+02	1.6687E+03	-1.5467E+03	6.6149E-07
38	1.0800E+02	1.6687E+03	-1.5607E+03	6.6149E-07
39	1.0000E+02	1.6687E+03	-1.5687E+03	6.6149E-07

SUM OF SQUARED RESIDUALS= 1.0086E+08

VARIANCE= 2.7260E+06

STANDARD DEVIATION= 1.6511E+03

ADDITIONAL PARAMETERS CALCULATED BY THE LEAST SQUARES SUBROUTINE.

THE RESIDUAL SUM OF SQUARES = 1.008610E+08

THE NUMBER OF SIGNIFICANT DIGITS IN THE CALCULATED PARAMETERS = 6.893553E+00

THE NUMBER OF FUNCTION EVALUATIONS REQUIRED = 9.200000E+01

THE NUMBER OF ITERATIONS REQUIRED = 2.600000E+01

AN INTEGER WHICH INDICATES THE CONVERGENCE CRITERION SATISFIED - INFER = 1

INFER=0 INDICATES THAT CONVERGENCE FAILED -- SEE THE (IER) PARAMETER

INFER=1 INDICATES THAT THE FOLLOWING CONVERGENCE CONDITION IS SATISFIED.



FOR TWO SUCCESSIVE ITERATIONS THE PARAMETER  
ESTIMATES AGREE, COMPONENT BY COMPONENT  
TO NSIG (SIGNIFICANT) DIGITS

- INFER-2 INDICATES THAT THE FOLLOWING CONVERGENCE CONDITION IS SATISFIED.  
FOR TWO SUCCESSIVE ITERATIONS THE RESIDUAL  
SUM OF THE SQUARE ESTIMATES HAVE RELATIVE  
DIFFERENCE LESS THAN OR EQUAL TO (EPS)
- INFER-4 INDICATES THAT THE FOLLOWING CONVERGENCE CONDITION IS SATISFIED.  
THE (EUCLIDEAN) NORM OF THE APPROXIMATE  
GRADIENT IS LESS THAN OR EQUAL TO (DELTA)
- INFER-X IF MORE THAN ONE OF THE ABOVE CONVERGENCE CRITERIA IS SATISFIED.  
(INFER) REPRESENTS THE CORRESPONDING SUM OF  
THE INTEGERS

THE ERROR PARAMETER: IER = 0

- IER=0 INDICATES SUCCESSFUL EXECUTION OF THE PROGRAM
- IER=38 INDICATES THAT THE JACOBIAN IS ZERO.  
THE SOLUTION IS A STATIONARY POINT (WARNING)
- IER=129 INDICATES THAT A SINGULARITY WAS  
DETECTED IN THE JACOBIAN
- IER=130 INDICATES THAT AT LEAST ONE OF THE  
SUBROUTINE CALL PARAMETERS WAS SPECIFIED  
INCORRECTLY -- VERIFY: M,N,IOPT,PARM(1),PARM(2)
- IER=131 INDICATES THAT THE MARQUARDT PARAMETER  
EXCEEDED THE DEFAULT VALUE OF (120.0)
- IER=132 INDICATES THAT AFTER A SUCCESSFUL  
RECOVERY FROM A SINGULAR JACOBIAN, THE SOLUTION  
HAS CYCLED BACK TO THE FIRST SINGULARITY
- IER=133 INDICATES THAT THE (MAXFN) PARAMETER  
WAS EXCEEDED

# VARIABLES USED IN THE CALCULATIONS

THE ESTIMATED METAL CLUSTER RESISTANCE ( $R_c$ ) =  $1.000000E+02$

THE ESTIMATED GAP RESISTANCE ( $R_g$ ) =  $1.000000E+05$

THE ESTIMATED GAP  
CAPACITANCE ( $C_g$ ) =  $6.000000E-07$

THE LEAST SQUARE VALUE OF THE METAL CLUSTER  
RESISTANCE,  $R_c$  =  $3.165796E+03$

THE LEAST SQUARE VALUE OF THE GAP  
RESISTANCE,  $R_g$  =  $9.547229E+04$

THE LEAST SQUARE VALUE OF THE GAP  
CAPACITANCE,  $C_g$  =  $4.753741E-07$

THE RESIDUALS ARE CALCULATED BY THE FOLLOWING  
EQUATION: [MEASURED VALUE-CALCULATED VALUE]

SAMPLE	R(f)	R(cal)	R(resid)	Cg(est)
1	9.5200E+04	9.8638E+04	-3.4381E+03	4.7537E-07
2	8.8500E+04	9.2790E+04	-4.2903E+03	4.7537E-07
3	8.7000E+04	9.0438E+04	-3.4383E+03	4.7537E-07
4	8.6200E+04	8.7813E+04	-1.6130E+03	4.7537E-07
5	8.4700E+04	8.4973E+04	-2.7346E+02	4.7537E-07
6	8.3300E+04	8.1977E+04	1.3228E+03	4.7537E-07
7	8.1300E+04	7.8878E+04	2.4220E+03	4.7537E-07
8	7.6900E+04	7.2559E+04	4.3415E+03	4.7537E-07
9	7.3000E+04	6.6328E+04	6.6719E+03	4.7537E-07
10	6.8000E+04	6.0399E+04	7.6012E+03	4.7537E-07
11	6.2900E+04	5.4895E+04	8.0047E+03	4.7537E-07
12	5.5600E+04	4.9875E+04	5.7247E+03	4.7537E-07
13	4.8500E+04	4.5351E+04	3.1494E+03	4.7537E-07
14	4.1800E+04	4.1304E+04	4.9566E+02	4.7537E-07
15	3.5100E+04	3.7704E+04	-2.6035E+03	4.7537E-07
16	2.9600E+04	3.4508E+04	-4.9076E+03	4.7537E-07
17	2.5500E+04	3.1674E+04	-6.1743E+03	4.7537E-07
18	2.2900E+04	2.9162E+04	-6.2621E+03	4.7537E-07
19	2.1500E+04	2.6933E+04	-5.4326E+03	4.7537E-07
20	1.9100E+04	2.4951E+04	-5.8510E+03	4.7537E-07
21	1.8000E+04	2.3186E+04	-5.1864E+03	4.7537E-07

22	1.7100E+04	2.1612E+04	-4.5116E+03	4.7537E-07
23	1.6400E+04	2.0203E+04	-3.8027E+03	4.7537E-07
24	1.5600E+04	1.8939E+04	-3.3391E+03	4.7537E-07
25	1.4900E+04	1.7803E+04	-2.9031E+03	4.7537E-07
26	1.4300E+04	1.6779E+04	-2.4790E+03	4.7537E-07
27	1.3900E+04	1.5854E+04	-1.9536E+03	4.7537E-07
28	1.3500E+04	1.5015E+04	-1.5152E+03	4.7537E-07
29	1.3000E+04	1.4254E+04	-1.2537E+03	4.7537E-07
30	1.2800E+04	1.3561E+04	-7.6057E+02	4.7537E-07
31	1.2700E+04	1.2928E+04	-2.2809E+02	4.7537E-07
32	1.2700E+04	1.2350E+04	3.5032E+02	4.7537E-07
33	1.2500E+04	1.1820E+04	6.8043E+02	4.7537E-07
34	1.2300E+04	1.1333E+04	9.6730E+02	4.7537E-07
35	1.2200E+04	1.0885E+04	1.3154E+03	4.7537E-07
36	1.2000E+04	1.0472E+04	1.5285E+03	4.7537E-07
37	1.1800E+04	1.0090E+04	1.7102E+03	4.7537E-07
38	1.1600E+04	9.7366E+03	1.8634E+03	4.7537E-07
39	1.1400E+04	9.4092E+03	1.9908E+03	4.7537E-07
40	1.1200E+04	9.1051E+03	2.0949E+03	4.7537E-07
41	1.0900E+04	8.8222E+03	2.0778E+03	4.7537E-07
42	1.0800E+04	8.5587E+03	2.2413E+03	4.7537E-07
43	1.0600E+04	8.3128E+03	2.2872E+03	4.7537E-07
44	1.0400E+04	8.0831E+03	2.3169E+03	4.7537E-07
45	1.0200E+04	7.8682E+03	2.3318E+03	4.7537E-07
46	1.0100E+04	7.6669E+03	2.4331E+03	4.7537E-07
47	1.0000E+04	7.4780E+03	2.5220E+03	4.7537E-07
48	9.9000E+03	3.1662E+03	6.7338E+03	4.7537E-07
49	9.8200E+03	3.1662E+03	6.6538E+03	4.7537E-07
50	9.7100E+03	3.1662E+03	6.5438E+03	4.7537E-07
51	9.6200E+03	3.1662E+03	6.4538E+03	4.7537E-07
52	9.5200E+03	6.6889E+03	2.8311E+03	4.7537E-07
53	6.3400E+03	4.7644E+03	1.5756E+03	4.7537E-07
54	4.8200E+03	4.0716E+03	7.4836E+02	4.7537E-07
55	4.1200E+03	3.7475E+03	3.7248E+02	4.7537E-07
56	3.5500E+03	3.5705E+03	-2.0527E+01	4.7537E-07
57	3.1700E+03	3.4635E+03	-2.9348E+02	4.7537E-07
58	2.7800E+03	3.3939E+03	-6.1388E+02	4.7537E-07
59	2.5400E+03	3.3461E+03	-8.0610E+02	4.7537E-07
60	2.3700E+03	3.3119E+03	-9.4190E+02	4.7537E-07
61	1.8900E+03	3.2308E+03	-1.3408E+03	4.7537E-07
62	1.6100E+03	3.2024E+03	-1.5924E+03	4.7537E-07
63	7.8700E+02	3.1716E+03	-2.3846E+03	4.7537E-07
64	5.2100E+02	3.1673E+03	-2.6463E+03	4.7537E-07
65	4.6500E+02	3.1664E+03	-2.7014E+03	4.7537E-07
66	4.0700E+02	3.1662E+03	-2.7592E+03	4.7537E-07
67	2.2800E+02	3.1658E+03	-2.9378E+03	4.7537E-07
68	1.8100E+02	3.1658E+03	-2.9848E+03	4.7537E-07
69	1.1200E+02	3.1658E+03	-3.0538E+03	4.7537E-07
70	1.0200E+02	3.1658E+03	-3.0638E+03	4.7537E-07

SUM OF SQUARED RESIDUALS= 8.6166E+08

VARIANCE= 1.2671E+07

STANDARD DEVIATION= 3.5597E+03

H-27

ADDITIONAL PARAMETERS CALCULATED BY THE LEAST SQUARES SUBROUTINE.

THE RESIDUAL SUM OF SQUARES = 8.616601E+08

THE NUMBER OF SIGNIFICANT DIGITS IN THE CALCULATED PARAMETERS = 6.150249E+00

THE NUMBER OF FUNCTION EVALUATIONS REQUIRED = 1.50000E+02

THE NUMBER OF ITERATIONS REQUIRED = 3.800000E+0

AN INTEGER WHICH INDICATES THE CONVERGENCE CRITERION SATISFIED - INFER = 1

INFER=0 INDICATES THAT CONVERGENCE FAILED -- SEE THE (IER) PARAMETER

INFER=1 INDICATES THAT THE FOLLOWING CONVERGENCE CONDITION IS SATISFIED.  
FOR TWO SUCCESSIVE ITERATIONS THE PARAMETER  
ESTIMATES AGREE, COMPONENT BY COMPONENT  
TO NSIG (SIGNIFICANT) DIGITS

INFER=2 INDICATES THAT THE FOLLOWING CONVERGENCE CONDITION IS SATISFIED.  
FOR TWO SUCCESSIVE ITERATIONS THE RESIDUAL  
SUM OF THE SQUARE ESTIMATES HAVE RELATIVE  
DIFFERENCE LESS THAN OR EQUAL TO (EPS)

INFER=4 INDICATES THAT THE FOLLOWING CONVERGENCE CONDITION IS SATISFIED.  
THE (EUCLIDEAN) NORM OF THE APPROXIMATE  
GRADIENT IS LESS THAN OR EQUAL TO (DELTA)

INFER=X IF MORE THAN ONE OF THE ABOVE CONVERGENCE CRITERIA IS SATISFIED.  
(INFER) REPRESENTS THE CORRESPONDING SUM OF  
THE INTEGERS

THE ERROR PARAMETER: IER = 0

IER=0    INDICATES SUCCESSFUL EXECUTION OF THE PROGRAM

IER=38    INDICATES THAT THE JACOBIAN IS ZERO.  
          THE SOLUTION IS A STATIONARY POINT (WARNING)

IER=129    INDICATES THAT A SINGULARITY WAS  
          DETECTED IN THE JACOBIAN

IER=130    INDICATES THAT AT LEAST ONE OF THE  
          SUBROUTINE CALL PARAMETERS WAS SPECIFIED  
          INCORRECTLY -- VERIFY: M,N,IOPT,PARM(1),PARM(2)

IER=131    INDICATES THAT THE MARQUARDT PARAMETER  
          EXCEEDED THE DEFAULT VALUE OF (120.0)

IER=132    INDICATES THAT AFTER A SUCCESSFUL  
          RECOVERY FROM A SINGULAR JACOBIAN, THE SOLUTION  
          HAS CYCLED BACK TO THE FIRST SINGULARITY

IER=133    INDICATES THAT THE (MAXFN) PARAMETER  
          WAS EXCEEDED

# VARIABLES USED IN THE CALCULATIONS

THE ESTIMATED METAL CLUSTER RESISTANCE ( $R_c$ ) = 1.000000E+02

THE ESTIMATED GAP RESISTANCE ( $R_g$ ) = 1.000000E+05

THE ESTIMATED GAP  
CAPACITANCE ( $C_g$ ) = 6.000000E-07

THE LEAST SQUARE VALUE OF THE METAL CLUSTER  
RESISTANCE,  $R_c$  = 2.508572E+03

THE LEAST SQUARE VALUE OF THE GAP  
RESISTANCE,  $R_g$  = 9.060034E+04

THE LEAST SQUARE VALUE OF THE GAP  
CAPACITANCE,  $C_g$  = 5.525615E-07

THE RESIDUALS ARE CALCULATED BY THE FOLLOWING  
EQUATION: [MEASURED VALUE-CALCULATED VALUE]

SAMPLE	R(f)	R(cal)	R(resid)	Cg(est)
1	8.8500E+04	9.3109E+04	-4.6089E+03	5.5256E-07
2	8.2600E+04	8.7448E+04	-4.8483E+03	5.5256E-07
3	8.1300E+04	8.5176E+04	-3.8757E+03	5.5256E-07
4	8.0600E+04	8.2642E+04	-2.0418E+03	5.5256E-07
5	7.9400E+04	7.9905E+04	-5.0463E+02	5.5256E-07
6	7.8100E+04	7.7020E+04	1.0799E+03	5.5256E-07
7	7.6900E+04	7.4040E+04	2.8595E+03	5.5256E-07
8	7.4100E+04	6.7978E+04	6.1224E+03	5.5256E-07
9	7.0900E+04	6.2017E+04	8.8831E+03	5.5256E-07
10	6.6700E+04	5.6360E+04	1.0340E+04	5.5256E-07
11	5.9200E+04	5.1122E+04	8.0782E+03	5.5256E-07
12	5.2100E+04	4.6355E+04	5.7446E+03	5.5256E-07
13	4.5300E+04	4.2068E+04	3.2316E+03	5.5256E-07
14	3.8800E+04	3.8242E+04	5.5813E+02	5.5256E-07
15	3.2400E+04	3.4842E+04	-2.4424E+03	5.5256E-07
16	2.6700E+04	3.1830E+04	-5.1297E+03	5.5256E-07
17	2.2300E+04	2.9162E+04	-6.8623E+03	5.5256E-07
18	1.9300E+04	2.6800E+04	-7.5001E+03	5.5256E-07
19	1.7700E+04	2.4706E+04	-7.0059E+03	5.5256E-07
20	1.6400E+04	2.2846E+04	-6.4463E+03	5.5256E-07
21	1.5500E+04	2.1192E+04	-5.6917E+03	5.5256E-07

22	1.4800E+04	1.9716E+04	-4.9161E+03	5.5256E-07
23	1.4300E+04	1.8397E+04	-4.0968E+03	5.5256E-07
24	1.3700E+04	1.7214E+04	-3.5144E+03	5.5256E-07
25	1.3200E+04	1.6152E+04	-2.9518E+03	5.5256E-07
26	1.2700E+04	1.5194E+04	-2.4944E+03	5.5256E-07
27	1.2100E+04	1.4330E+04	-2.2296E+03	5.5256E-07
28	1.1700E+04	1.3546E+04	-1.8464E+03	5.5256E-07
29	1.1400E+04	1.2835E+04	-1.4354E+03	5.5256E-07
30	1.1100E+04	1.2188E+04	-1.0884E+03	5.5256E-07
31	1.0900E+04	1.1598E+04	-6.9813E+02	5.5256E-07
32	1.0700E+04	1.1058E+04	-3.5850E+02	5.5256E-07
33	1.0600E+04	1.0564E+04	3.5962E+01	5.5256E-07
34	1.0500E+04	1.0110E+04	3.8998E+02	5.5256E-07
35	1.0300E+04	9.6923E+03	6.0772E+02	5.5256E-07
36	1.0300E+04	9.3072E+03	9.9283E+02	5.5256E-07
37	1.0200E+04	8.9515E+03	1.2485E+03	5.5256E-07
38	1.0100E+04	8.6223E+03	1.4777E+03	5.5256E-07
39	9.9000E+03	8.3172E+03	1.5828E+03	5.5256E-07
40	9.7100E+03	8.0339E+03	1.6761E+03	5.5256E-07
41	9.6200E+03	7.7704E+03	1.8496E+03	5.5256E-07
42	9.5200E+03	7.5250E+03	1.9950E+03	5.5256E-07
43	9.3500E+03	7.2961E+03	2.0539E+03	5.5256E-07
44	9.1700E+03	7.0822E+03	2.0878E+03	5.5256E-07
45	9.0100E+03	6.8821E+03	2.1279E+03	5.5256E-07
46	8.9300E+03	6.6946E+03	2.2354E+03	5.5256E-07
47	8.8500E+03	6.5188E+03	2.3312E+03	5.5256E-07
48	8.7700E+03	2.5090E+03	6.2610E+03	5.5256E-07
49	8.7000E+03	2.5090E+03	6.1910E+03	5.5256E-07
50	8.6200E+03	2.5089E+03	6.1111E+03	5.5256E-07
51	8.5500E+03	2.5089E+03	6.0411E+03	5.5256E-07
52	8.4800E+03	5.7844E+03	2.6956E+03	5.5256E-07
53	6.2100E+03	3.9943E+03	2.2157E+03	5.5256E-07
54	4.7400E+03	3.3504E+03	1.3896E+03	5.5256E-07
55	4.0500E+03	3.0491E+03	1.0009E+03	5.5256E-07
56	3.4000E+03	2.8846E+03	5.1536E+02	5.5256E-07
57	3.0900E+03	2.7852E+03	3.0483E+02	5.5256E-07
58	2.7200E+03	2.7205E+03	-4.9467E-01	5.5256E-07
59	2.4800E+03	2.6761E+03	-1.9610E+02	5.5256E-07
60	2.3200E+03	2.6443E+03	-3.2432E+02	5.5256E-07
61	1.8100E+03	2.5690E+03	-7.5895E+02	5.5256E-07
62	1.5600E+03	2.5425E+03	-9.8255E+02	5.5256E-07
63	7.1900E+02	2.5140E+03	-1.7950E+03	5.5256E-07
64	4.8300E+02	2.5099E+03	-2.0269E+03	5.5256E-07
65	4.2900E+02	2.5092E+03	-2.0802E+03	5.5256E-07
66	3.8900E+02	2.5089E+03	-2.1199E+03	5.5256E-07
67	2.1500E+02	2.5086E+03	-2.2936E+03	5.5256E-07
68	1.7000E+02	2.5086E+03	-2.3386E+03	5.5256E-07
69	1.0400E+02	2.5086E+03	-2.4046E+03	5.5256E-07
70	1.0100E+02	2.5086E+03	-2.4076E+03	5.5256E-07

SUM OF SQUARED RESIDUALS= 9.9349E+08

VARIANCE= 1.4610E+07

STANDARD DEVIATION= 3.8223E+03

H-31

ADDITIONAL PARAMETERS CALCULATED BY THE LEAST SQUARES SUBROUTINE.

THE RESIDUAL SUM OF SQUARES = 9.934858E+08

THE NUMBER OF SIGNIFICANT DIGITS IN THE CALCULATED PARAMETERS = 6.196203E+00

THE NUMBER OF FUNCTION EVALUATIONS REQUIRED = 1.330000E+02

THE NUMBER OF ITERATIONS REQUIRED = 4.500000E+01

AN INTEGER WHICH INDICATES THE CONVERGENCE CRITERION SATISFIED - INFER = 1

INFER=0 INDICATES THAT CONVERGENCE FAILED -- SEE THE (IER) PARAMETER

INFER=1 INDICATES THAT THE FOLLOWING CONVERGENCE CONDITION IS SATISFIED  
FOR TWO SUCCESSIVE ITERATIONS THE PARAMETER  
ESTIMATES AGREE, COMPONENT BY COMPONENT  
TO NSIG (SIGNIFICANT) DIGITS

INFER=2 INDICATES THAT THE FOLLOWING CONVERGENCE CONDITION IS SATISFIED  
FOR TWO SUCCESSIVE ITERATIONS THE RESIDUAL  
SUM OF THE SQUARE ESTIMATES HAVE RELATIVE  
DIFFERENCE LESS THAN OR EQUAL TO (EPS)

INFER=4 INDICATES THAT THE FOLLOWING CONVERGENCE CONDITION IS SATISFIED  
THE (EUCLIDEAN) NORM OF THE APPROXIMATE  
GRADIENT IS LESS THAN OR EQUAL TO (DELTA)

INFER=X IF MORE THAN ONE OF THE ABOVE CONVERGENCE CRITERIA IS SATISFIED  
(INFER) REPRESENTS THE CORRESPONDING SUM OF  
THE INTEGERS

THE ERROR PARAMETER: IER = 0



IER=0 INDICATES SUCCESSFUL EXECUTION OF THE PROGRAM

IER=38 INDICATES THAT THE JACOBIAN IS ZERO.  
THE SOLUTION IS A STATIONARY POINT (WARNING)

IER=129 INDICATES THAT A SINGULARITY WAS  
DETECTED IN THE JACOBIAN

IER=130 INDICATES THAT AT LEAST ONE OF THE  
SUBROUTINE CALL PARAMETERS WAS SPECIFIED  
INCORRECTLY -- VERIFY: M,N,IOPT,PARM(1),PARM(2)

IER=131 INDICATES THAT THE MARQUARDT PARAMETER  
EXCEEDED THE DEFAULT VALUE OF (120.0)

IER=132 INDICATES THAT AFTER A SUCCESSFUL  
RECOVERY FROM A SINGULAR JACOBIAN, THE SOLUTION  
HAS CYCLED BACK TO THE FIRST SINGULARITY

IER=133 INDICATES THAT THE (MAXFN) PARAMETER  
WAS EXCEEDED

# VARIABLES USED IN THE CALCULATIONS

THE ESTIMATED METAL CLUSTER RESISTANCE (Rc) = 1.000000E+02

THE ESTIMATED GAP RESISTANCE (Rg) = 1.000000E+05

THE ESTIMATED GAP  
CAPACITANCE (Cg) = 6.000000E-07

THE LEAST SQUARE VALUE OF THE METAL CLUSTER  
RESISTANCE, Rc = 2.961782E+03

THE LEAST SQUARE VALUE OF THE GAP  
RESISTANCE, Rg = 1.050164E+05

THE LEAST SQUARE VALUE OF THE GAP  
CAPACITANCE, Cg = 4.848386E-07

THE RESIDUALS ARE CALCULATED BY THE FOLLOWING  
EQUATION: [MEASURED VALUE-CALCULATED VALUE]

SAMPLE	R(f)	R(cal)	R(resid)	Cg(est)
1	1.0100E+05	1.0798E+05	-6.9781E+03	4.8484E-07
2	9.6200E+04	1.0109E+05	-4.8912E+03	4.8484E-07
3	9.5200E+04	9.8339E+04	-3.1391E+03	4.8484E-07
4	9.3500E+04	9.5279E+04	-1.7793E+03	4.8484E-07
5	9.1700E+04	9.1984E+04	-2.8392E+02	4.8484E-07
6	9.0900E+04	8.8523E+04	2.3775E+03	4.8484E-07
7	8.9300E+04	8.4959E+04	4.3408E+03	4.8484E-07
8	8.5500E+04	7.7747E+04	7.7534E+03	4.8484E-07
9	8.0000E+04	7.0704E+04	9.2956E+03	4.8484E-07
10	7.2500E+04	6.4065E+04	8.4347E+03	4.8484E-07
11	6.6200E+04	5.7957E+04	8.2431E+03	4.8484E-07
12	5.7800E+04	5.2430E+04	5.3701E+03	4.8484E-07
13	5.0300E+04	4.7484E+04	2.8157E+03	4.8484E-07
14	4.3100E+04	4.3090E+04	9.5595E+00	4.8484E-07
15	3.5800E+04	3.9203E+04	-3.4028E+03	4.8484E-07
16	3.0000E+04	3.5770E+04	-5.7701E+03	4.8484E-07
17	2.5800E+04	3.2741E+04	-6.9406E+03	4.8484E-07
18	2.3200E+04	3.0065E+04	-6.8652E+03	4.8484E-07
19	2.1700E+04	2.7699E+04	-5.9994E+03	4.8484E-07
20	1.9800E+04	2.5603E+04	-5.8033E+03	4.8484E-07
21	1.8600E+04	2.3742E+04	-5.1418E+03	4.8484E-07

22	1.6900E+04	2.2085E+04	-5.1847E+03	4.8484E-07
23	1.5800E+04	2.0606E+04	-4.8056E+03	4.8484E-07
24	1.5100E+04	1.9282E+04	-4.1816E+03	4.8484E-07
25	1.4500E+04	1.8093E+04	-3.5934E+03	4.8484E-07
26	1.4100E+04	1.7024E+04	-2.9240E+03	4.8484E-07
27	1.3700E+04	1.6059E+04	-2.3590E+03	4.8484E-07
28	1.3200E+04	1.5186E+04	-1.9860E+03	4.8484E-07
29	1.3000E+04	1.4394E+04	-1.3940E+03	4.8484E-07
30	1.2980E+01	1.3674E+04	-1.3661E+04	4.8484E-07
31	1.2800E+04	1.3017E+04	-2.1728E+02	4.8484E-07
32	1.2700E+04	1.2417E+04	2.8256E+02	4.8484E-07
33	1.2600E+04	1.1868E+04	7.3186E+02	4.8484E-07
34	1.2500E+04	1.1364E+04	1.1360E+03	4.8484E-07
35	1.2400E+04	1.0900E+04	1.4996E+03	4.8484E-07
36	1.2300E+04	1.0473E+04	1.8268E+03	4.8484E-07
37	1.2200E+04	1.0079E+04	2.1212E+03	4.8484E-07
38	1.2200E+04	9.7140E+03	2.4860E+03	4.8484E-07
39	1.2100E+04	9.3759E+03	2.7241E+03	4.8484E-07
40	1.1900E+04	9.0621E+03	2.8379E+03	4.8484E-07
41	1.1600E+04	8.7704E+03	2.8296E+03	4.8484E-07
42	1.1300E+04	8.4987E+03	2.8013E+03	4.8484E-07
43	1.1200E+04	8.2453E+03	2.9547E+03	4.8484E-07
44	1.1000E+04	8.0087E+03	2.9913E+03	4.8484E-07
45	1.0700E+04	7.7873E+03	2.9127E+03	4.8484E-07
46	1.0600E+04	7.5800E+03	3.0200E+03	4.8484E-07
47	1.0400E+04	7.3856E+03	3.0144E+03	4.8484E-07
48	1.0300E+04	2.9622E+03	7.3378E+03	4.8484E-07
49	1.0100E+04	2.9622E+03	7.1378E+03	4.8484E-07
50	1.0000E+04	2.9622E+03	7.0378E+03	4.8484E-07
51	9.9000E+03	2.9622E+03	6.9378E+03	4.8484E-07
52	9.8000E+03	6.5740E+03	3.2260E+03	4.8484E-07
53	6.9400E+03	4.5985E+03	2.3415E+03	4.8484E-07
54	5.2400E+03	3.8887E+03	1.3513E+03	4.8484E-07
55	4.3700E+03	3.5569E+03	8.1307E+02	4.8484E-07
56	3.7300E+03	3.3758E+03	3.5421E+02	4.8484E-07
57	3.3100E+03	3.2663E+03	4.3727E+01	4.8484E-07
58	3.0100E+03	3.1951E+03	-1.8507E+02	4.8484E-07
59	2.7200E+03	3.1462E+03	-4.2619E+02	4.8484E-07
60	2.5400E+03	3.1112E+03	-5.7120E+02	4.8484E-07
61	1.9800E+03	3.0282E+03	-1.0482E+03	4.8484E-07
62	1.7000E+03	2.9992E+03	-1.2992E+03	4.8484E-07
63	9.0900E+02	2.9678E+03	-2.0588E+03	4.8484E-07
64	6.1300E+02	2.9633E+03	-2.3503E+03	4.8484E-07
65	5.0700E+02	2.9624E+03	-2.4554E+03	4.8484E-07
66	4.5700E+02	2.9622E+03	-2.5052E+03	4.8484E-07
67	2.4400E+02	2.9618E+03	-2.7178E+03	4.8484E-07
68	1.9300E+02	2.9618E+03	-2.7688E+03	4.8484E-07
69	1.1400E+02	2.9618E+03	-2.8478E+03	4.8484E-07
70	1.0600E+02	2.9618E+03	-2.8558E+03	4.8484E-07

SUM OF SQUARED RESIDUALS= 1.3275E+09

VARIANCE= 1.9522E+07

STANDARD DEVIATION= 4.4183E+03

ADDITIONAL PARAMETERS CALCULATED BY THE LEAST SQUARES SUBROUTINE.

THE RESIDUAL SUM OF SQUARES = 1.327465E+09

THE NUMBER OF SIGNIFICANT DIGITS IN THE CALCULATED PARAMETERS = 6.274597E+00

THE NUMBER OF FUNCTION EVALUATIONS REQUIRED = 1.110000E+02

THE NUMBER OF ITERATIONS REQUIRED = 3.800000E+01

AN INTEGER WHICH INDICATES THE CONVERGENCE CRITERION SATISFIED - INFER = 1

INFER=0 INDICATES THAT CONVERGENCE FAILED -- SEE THE (IER) PARAMETER

INFER=1 INDICATES THAT THE FOLLOWING CONVERGENCE CONDITION IS SATISFIED  
FOR TWO SUCCESSIVE ITERATIONS THE PARAMETER  
ESTIMATES AGREE, COMPONENT BY COMPONENT  
TO NSIG (SIGNIFICANT) DIGITS

INFER=2 INDICATES THAT THE FOLLOWING CONVERGENCE CONDITION IS SATISFIED  
FOR TWO SUCCESSIVE ITERATIONS THE RESIDUAL  
SUM OF THE SQUARE ESTIMATES HAVE RELATIVE  
DIFFERENCE LESS THAN OR EQUAL TO (EPS)

INFER=4 INDICATES THAT THE FOLLOWING CONVERGENCE CONDITION IS SATISFIED  
THE (EUCLIDEAN) NORM OF THE APPROXIMATE  
GRADIENT IS LESS THAN OR EQUAL TO (DELTA)

INFER=X IF MORE THAN ONE OF THE ABOVE CONVERGENCE CRITERIA IS SATISFIED  
(INFER) REPRESENTS THE CORRESPONDING SUM OF  
THE INTEGERS

THE ERROR PARAMETER: IER = 0

IER=0    INDICATES SUCCESSFUL EXECUTION OF THE PROGRAM

IER=38    INDICATES THAT THE JACOBIAN IS ZERO.  
          THE SOLUTION IS A STATIONARY POINT (WARNING)

IER=129    INDICATES THAT A SINGULARITY WAS  
          DETECTED IN THE JACOBIAN

IER=130    INDICATES THAT AT LEAST ONE OF THE  
          SUBROUTINE CALL PARAMETERS WAS SPECIFIED  
          INCORRECTLY -- VERIFY: M,N,IOPT,PARM(1),PARM(2)

IER=131    INDICATES THAT THE MARQUARDT PARAMETER  
          EXCEEDED THE DEFAULT VALUE OF (120.0)

IER=132    INDICATES THAT AFTER A SUCCESSFUL  
          RECOVERY FROM A SINGULAR JACOBIAN, THE SOLUTION  
          HAS CYCLED BACK TO THE FIRST SINGULARITY

IER=133    INDICATES THAT THE (MAXFN) PARAMETER  
          WAS EXCEEDED

# VARIABLES USED IN THE CALCULATIONS

THE ESTIMATED METAL CLUSTER RESISTANCE (Rc) = 1.000000E+02

THE ESTIMATED GAP RESISTANCE (Rg) = 1.000000E+05

THE ESTIMATED GAP  
CAPACITANCE (Cg) = 6.000000E-07

THE LEAST SQUARE VALUE OF THE METAL CLUSTER  
RESISTANCE, Rc = 3.477256E+03

THE LEAST SQUARE VALUE OF THE GAP  
RESISTANCE, Rg = 8.796331E+04

THE LEAST SQUARE VALUE OF THE GAP  
CAPACITANCE, Cg = 4.860128E-07

THE RESIDUALS ARE CALCULATED BY THE FOLLOWING  
EQUATION: [MEASURED VALUE-CALCULATED VALUE]

SAMPLE	R(f)	R(cal)	R(resid)	Cg(est)
1	8.7000E+04	9.1441E+04	-4.4406E+03	4.8601E-07
2	8.1300E+04	8.5794E+04	-4.4940E+03	4.8601E-07
3	8.0000E+04	8.3533E+04	-3.5329E+03	4.8601E-07
4	7.9400E+04	8.1016E+04	-1.6157E+03	4.8601E-07
5	7.8100E+04	7.8301E+04	-2.0115E+02	4.8601E-07
6	7.6900E+04	7.5446E+04	1.4544E+03	4.8601E-07
7	7.5200E+04	7.2502E+04	2.6985E+03	4.8601E-07
8	7.2500E+04	6.6528E+04	5.9716E+03	4.8601E-07
9	6.9000E+04	6.0678E+04	8.3216E+03	4.8601E-07
10	6.4500E+04	5.5147E+04	9.3531E+03	4.8601E-07
11	5.7800E+04	5.0043E+04	7.7566E+03	4.8601E-07
12	5.0800E+04	4.5414E+04	5.3861E+03	4.8601E-07
13	4.3500E+04	4.1262E+04	2.2380E+03	4.8601E-07
14	3.6600E+04	3.7566E+04	-9.6572E+02	4.8601E-07
15	3.0400E+04	3.4289E+04	-3.8894E+03	4.8601E-07
16	2.5400E+04	3.1392E+04	-5.9919E+03	4.8601E-07
17	2.2100E+04	2.8831E+04	-6.7310E+03	4.8601E-07
18	1.9500E+04	2.6567E+04	-7.0667E+03	4.8601E-07
19	1.8100E+04	2.4562E+04	-6.4622E+03	4.8601E-07
20	1.6800E+04	2.2784E+04	-5.9844E+03	4.8601E-07
21	1.5900E+04	2.1204E+04	-5.3044E+03	4.8601E-07

22	1.5200E+04	1.9797E+04	-4.5966E+03	4.8601E-07
23	1.4700E+04	1.8539E+04	-3.8392E+03	4.8601E-07
24	1.4000E+04	1.7413E+04	-3.4131E+03	4.8601E-07
25	1.3600E+04	1.6402E+04	-2.8018E+03	4.8601E-07
26	1.3200E+04	1.5491E+04	-2.2912E+03	4.8601E-07
27	1.2900E+04	1.4669E+04	-1.7691E+03	4.8601E-07
28	1.2600E+04	1.3925E+04	-1.3251E+03	4.8601E-07
29	1.2300E+04	1.3250E+04	-9.4988E+02	4.8601E-07
30	1.2100E+04	1.2636E+04	-5.3569E+02	4.8601E-07
31	1.1900E+04	1.2076E+04	-1.7563E+02	4.8601E-07
32	1.1900E+04	1.1564E+04	3.3622E+02	4.8601E-07
33	1.1800E+04	1.1095E+04	7.0506E+02	4.8601E-07
34	1.1700E+04	1.0665E+04	1.0354E+03	4.8601E-07
35	1.1500E+04	1.0269E+04	1.2313E+03	4.8601E-07
36	1.1300E+04	9.9038E+03	1.3962E+03	4.8601E-07
37	1.1200E+04	9.5669E+03	1.6331E+03	4.8601E-07
38	1.1200E+04	9.2552E+03	1.9448E+03	4.8601E-07
39	1.1100E+04	8.9663E+03	2.1337E+03	4.8601E-07
40	1.1000E+04	8.6982E+03	2.3018E+03	4.8601E-07
41	1.0900E+04	8.4488E+03	2.4512E+03	4.8601E-07
42	1.0800E+04	8.2165E+03	2.5835E+03	4.8601E-07
43	1.0800E+04	7.9999E+03	2.8001E+03	4.8601E-07
44	1.0700E+04	7.7976E+03	2.9024E+03	4.8601E-07
45	1.0600E+04	7.6083E+03	2.9917E+03	4.8601E-07
46	1.0500E+04	7.4310E+03	3.0690E+03	4.8601E-07
47	1.0500E+04	7.2647E+03	3.2353E+03	4.8601E-07
48	1.0400E+04	3.4776E+03	6.9224E+03	4.8601E-07
49	1.0400E+04	3.4776E+03	6.9224E+03	4.8601E-07
50	1.0300E+04	3.4776E+03	6.8224E+03	4.8601E-07
51	1.0200E+04	3.4776E+03	6.7224E+03	4.8601E-07
52	1.0200E+04	6.5704E+03	3.6296E+03	4.8601E-07
53	6.9900E+03	4.8794E+03	2.1106E+03	4.8601E-07
54	5.2900E+03	4.2715E+03	1.0185E+03	4.8601E-07
55	4.2400E+03	3.9872E+03	2.5278E+02	4.8601E-07
56	3.6800E+03	3.8320E+03	-1.5203E+02	4.8601E-07
57	3.2400E+03	3.7382E+03	-4.9818E+02	4.8601E-07
58	2.9300E+03	3.6772E+03	-7.4717E+02	4.8601E-07
59	2.7000E+03	3.6353E+03	-9.3529E+02	4.8601E-07
60	2.4900E+03	3.6053E+03	-1.1153E+03	4.8601E-07
61	1.9100E+03	3.5342E+03	-1.6242E+03	4.8601E-07
62	1.7100E+03	3.5093E+03	-1.7993E+03	4.8601E-07
63	7.4100E+02	3.4824E+03	-2.7414E+03	4.8601E-07
64	5.7100E+02	3.4785E+03	-2.9075E+03	4.8601E-07
65	4.6300E+02	3.4778E+03	-3.0148E+03	4.8601E-07
66	4.1200E+02	3.4776E+03	-3.0656E+03	4.8601E-07
67	2.2300E+02	3.4773E+03	-3.2543E+03	4.8601E-07
68	1.6300E+02	3.4773E+03	-3.3143E+03	4.8601E-07
69	8.9300E+01	3.4773E+03	-3.3880E+03	4.8601E-07
70	8.0000E+01	3.4773E+03	-3.3973E+03	4.8601E-07

SUM OF SQUARED RESIDUALS= 1.0441E+09

VARIANCE= 1.5354E+07

STANDARD DEVIATION= 3.9184E+03

ADDITIONAL PARAMETERS CALCULATED BY THE LEAST SQUARES SUBROUTINE.

THE RESIDUAL SUM OF SQUARES = 1.044067E+09

THE NUMBER OF SIGNIFICANT DIGITS IN THE CALCULATED PARAMETERS = 6.197449E+00

THE NUMBER OF FUNCTION EVALUATIONS REQUIRED = 1.360000E+02

THE NUMBER OF ITERATIONS REQUIRED = 4.700000E+01

AN INTEGER WHICH INDICATES THE CONVERGENCE CRITERION SATISFIED - INFER = 1

INFER=0 INDICATES THAT CONVERGENCE FAILED -- SEE THE (IER) PARAMETER

INFER=1 INDICATES THAT THE FOLLOWING CONVERGENCE CONDITION IS SATISFIED  
FOR TWO SUCCESSIVE ITERATIONS THE PARAMETER  
ESTIMATES AGREE, COMPONENT BY COMPONENT  
TO NSIG (SIGNIFICANT) DIGITS

INFER=2 INDICATES THAT THE FOLLOWING CONVERGENCE CONDITION IS SATISFIED  
FOR TWO SUCCESSIVE ITERATIONS THE RESIDUAL  
SUM OF THE SQUARE ESTIMATES HAVE RELATIVE  
DIFFERENCE LESS THAN OR EQUAL TO (EPS)

INFER=4 INDICATES THAT THE FOLLOWING CONVERGENCE CONDITION IS SATISFIED  
THE (EUCLIDEAN) NORM OF THE APPROXIMATE  
GRADIENT IS LESS THAN OR EQUAL TO (DELTA)

INFER=X IF MORE THAN ONE OF THE ABOVE CONVERGENCE CRITERIA IS SATISFIED  
(INFER) REPRESENTS THE CORRESPONDING SUM OF  
THE INTEGERS

THE ERROR PARAMETER: IER = 0



IER=0    INDICATES SUCCESSFUL EXECUTION OF THE PROGRAM

IER=38    INDICATES THAT THE JACOBIAN IS ZERO.  
          THE SOLUTION IS A STATIONARY POINT (WARNING)

IER=129    INDICATES THAT A SINGULARITY WAS  
          DETECTED IN THE JACOBIAN

IER=130    INDICATES THAT AT LEAST ONE OF THE  
          SUBROUTINE CALL PARAMETERS WAS SPECIFIED  
          INCORRECTLY -- VERIFY: M,N,IOPT,PARM(1),PARM(2)

IER=131    INDICATES THAT THE MARQUARDT PARAMETER  
          EXCEEDED THE DEFAULT VALUE OF (120.0)

IER=132    INDICATES THAT AFTER A SUCCESSFUL  
          RECOVERY FROM A SINGULAR JACOBIAN, THE SOLUTION  
          HAS CYCLED BACK TO THE FIRST SINGULARITY

IER=133    INDICATES THAT THE (MAXFN) PARAMETER  
          WAS EXCEEDED

# VARIABLES USED IN THE CALCULATIONS

THE ESTIMATED METAL CLUSTER RESISTANCE (Rc) = 1.000000E+02

THE ESTIMATED GAP RESISTANCE (Rg) = 1.000000E+05

THE ESTIMATED GAP  
CAPACITANCE (Cg) = 6.000000E-07

THE LEAST SQUARE VALUE OF THE METAL CLUSTER  
RESISTANCE, Rc = 3.167636E+03

THE LEAST SQUARE VALUE OF THE GAP  
RESISTANCE, Rg = 1.032931E+05

THE LEAST SQUARE VALUE OF THE GAP  
CAPACITANCE, Cg = 4.617742E-07

THE RESIDUALS ARE CALCULATED BY THE FOLLOWING  
EQUATION: [MEASURED VALUE-CALCULATED VALUE]

SAMPLE	R(f)	R(cal)	R(resid)	Cg(est)
1	9.8500E+04	1.0646E+05	-7.9607E+03	4.6177E-07
2	9.4300E+04	9.9992E+04	-5.6918E+03	4.6177E-07
3	9.3500E+04	9.7395E+04	-3.8953E+03	4.6177E-07
4	9.2600E+04	9.4501E+04	-1.9007E+03	4.6177E-07
5	9.1700E+04	9.1374E+04	3.2579E+02	4.6177E-07
6	9.0100E+04	8.8080E+04	2.0200E+03	4.6177E-07
7	8.9300E+04	8.4678E+04	4.6223E+03	4.6177E-07
8	8.6200E+04	7.7757E+04	8.4434E+03	4.6177E-07
9	8.2000E+04	7.0954E+04	1.1046E+04	4.6177E-07
10	7.5800E+04	6.4500E+04	1.1300E+04	4.6177E-07
11	6.8500E+04	5.8527E+04	9.9731E+03	4.6177E-07
12	5.9900E+04	5.3092E+04	6.8076E+03	4.6177E-07
13	5.0800E+04	4.8206E+04	2.5943E+03	4.6177E-07
14	4.1200E+04	4.3845E+04	-2.6450E+03	4.6177E-07
15	3.3700E+04	3.9972E+04	-6.2717E+03	4.6177E-07
16	2.8700E+04	3.6540E+04	-7.8398E+03	4.6177E-07
17	2.4600E+04	3.3502E+04	-8.9016E+03	4.6177E-07
18	2.2400E+04	3.0811E+04	-8.4114E+03	4.6177E-07
19	2.1100E+04	2.8427E+04	-7.3268E+03	4.6177E-07
20	2.0000E+04	2.6309E+04	-6.3095E+03	4.6177E-07
21	1.8800E+04	2.4426E+04	-5.6257E+03	4.6177E-07

22	1.7700E+04	2.2746E+04	-5.0459E+03	4.6177E-07
23	1.6800E+04	2.1244E+04	-4.4443E+03	4.6177E-07
24	1.6100E+04	1.9898E+04	-3.7984E+03	4.6177E-07
25	1.5700E+04	1.8689E+04	-2.9890E+03	4.6177E-07
26	1.5300E+04	1.7599E+04	-2.2995E+03	4.6177E-07
27	1.4900E+04	1.6615E+04	-1.7153E+03	4.6177E-07
28	1.4300E+04	1.5724E+04	-1.4241E+03	4.6177E-07
29	1.3900E+04	1.4915E+04	-1.0151E+03	4.6177E-07
30	1.3500E+04	1.4179E+04	-6.7880E+02	4.6177E-07
31	1.3200E+04	1.3507E+04	-3.0720E+02	4.6177E-07
32	1.2900E+04	1.2893E+04	6.7934E+00	4.6177E-07
33	1.2700E+04	1.2331E+04	3.6937E+02	4.6177E-07
34	1.2600E+04	1.1814E+04	7.8592E+02	4.6177E-07
35	1.2400E+04	1.1339E+04	1.0612E+03	4.6177E-07
36	1.2200E+04	1.0901E+04	1.2993E+03	4.6177E-07
37	1.2100E+04	1.0496E+04	1.6040E+03	4.6177E-07
38	1.1900E+04	1.0122E+04	1.7784E+03	4.6177E-07
39	1.1700E+04	9.7745E+03	1.9255E+03	4.6177E-07
40	1.1600E+04	9.4522E+03	2.1478E+03	4.6177E-07
41	1.1400E+04	9.1525E+03	2.2475E+03	4.6177E-07
42	1.1300E+04	8.8733E+03	2.4267E+03	4.6177E-07
43	1.1200E+04	8.6129E+03	2.5871E+03	4.6177E-07
44	1.1100E+04	8.3696E+03	2.7304E+03	4.6177E-07
45	1.1100E+04	8.1419E+03	2.9581E+03	4.6177E-07
46	1.1000E+04	7.9287E+03	3.0713E+03	4.6177E-07
47	1.0900E+04	7.7287E+03	3.1713E+03	4.6177E-07
48	1.0800E+04	3.1681E+03	7.6319E+03	4.6177E-07
49	1.0600E+04	3.1681E+03	7.4319E+03	4.6177E-07
50	1.0600E+04	3.1681E+03	7.4319E+03	4.6177E-07
51	1.0500E+04	3.1680E+03	7.3320E+03	4.6177E-07
52	1.0300E+04	6.8934E+03	3.4066E+03	4.6177E-07
53	6.9400E+03	4.8574E+03	2.0826E+03	4.6177E-07
54	5.2400E+03	4.1250E+03	1.1150E+03	4.6177E-07
55	4.2600E+03	3.7824E+03	4.7762E+02	4.6177E-07
56	3.6000E+03	3.5953E+03	4.6832E+00	4.6177E-07
57	3.2500E+03	3.4822E+03	-2.3220E+02	4.6177E-07
58	2.9100E+03	3.4086E+03	-4.9864E+02	4.6177E-07
59	2.6600E+03	3.3582E+03	-6.9815E+02	4.6177E-07
60	2.4900E+03	3.3220E+03	-8.3201E+02	4.6177E-07
61	1.9000E+03	3.2363E+03	-1.3363E+03	4.6177E-07
62	1.6300E+03	3.2063E+03	-1.5763E+03	4.6177E-07
63	7.5200E+02	3.1738E+03	-2.4218E+03	4.6177E-07
64	5.4900E+02	3.1692E+03	-2.6202E+03	4.6177E-07
65	4.6300E+02	3.1683E+03	-2.7053E+03	4.6177E-07
66	4.1200E+02	3.1680E+03	-2.7560E+03	4.6177E-07
67	2.3300E+02	3.1677E+03	-2.9347E+03	4.6177E-07
68	1.8100E+02	3.1676E+03	-2.9866E+03	4.6177E-07
69	1.1300E+02	3.1676E+03	-3.0546E+03	4.6177E-07
70	1.0100E+02	3.1676E+03	-3.0666E+03	4.6177E-07

SUM OF SQUARED RESIDUALS= 1.4575E+09

VARIANCE= 2.1433E+07

STANDARD DEVIATION= 4.6296E+03

ADDITIONAL PARAMETERS CALCULATED BY THE LEAST SQUARES SUBROUTINE.

THE RESIDUAL SUM OF SQUARES = 1.457473E+09

THE NUMBER OF SIGNIFICANT DIGITS IN THE CALCULATED PARAMETERS = 6.070937E+00

THE NUMBER OF FUNCTION EVALUATIONS REQUIRED = 1.090000E+02

THE NUMBER OF ITERATIONS REQUIRED = 3.600000E+01

AN INTEGER WHICH INDICATES THE CONVERGENCE CRITERION SATISFIED - INFER = 1

INFER=0 INDICATES THAT CONVERGENCE FAILED -- SEE THE (IER) PARAMETER

INFER=1 INDICATES THAT THE FOLLOWING CONVERGENCE CONDITION IS SATISFIED  
FOR TWO SUCCESSIVE ITERATIONS THE PARAMETER  
ESTIMATES AGREE, COMPONENT BY COMPONENT  
TO NSIG (SIGNIFICANT) DIGITS

INFER=2 INDICATES THAT THE FOLLOWING CONVERGENCE CONDITION IS SATISFIED  
FOR TWO SUCCESSIVE ITERATIONS THE RESIDUAL  
SUM OF THE SQUARE ESTIMATES HAVE RELATIVE  
DIFFERENCE LESS THAN OR EQUAL TO (EPS)

INFER=4 INDICATES THAT THE FOLLOWING CONVERGENCE CONDITION IS SATISFIED  
THE (EUCLIDEAN) NORM OF THE APPROXIMATE  
GRADIENT IS LESS THAN OR EQUAL TO (DELTA)

INFER=X IF MORE THAN ONE OF THE ABOVE CONVERGENCE CRITERIA IS SATISFIED  
(INFER) REPRESENTS THE CORRESPONDING SUM OF  
THE INTEGERS

THE ERROR PARAMETER: IER = 0

IER=0 INDICATES SUCCESSFUL EXECUTION OF THE PROGRAM

IER=38 INDICATES THAT THE JACOBIAN IS ZERO.  
THE SOLUTION IS A STATIONARY POINT (WARNING)

IER=129 INDICATES THAT A SINGULARITY WAS  
DETECTED IN THE JACOBIAN

IER=130 INDICATES THAT AT LEAST ONE OF THE  
SUBROUTINE CALL PARAMETERS WAS SPECIFIED  
INCORRECTLY -- VERIFY: M,N,IOPT,PARM(1),PARM(2)

IER=131 INDICATES THAT THE MARQUARDT PARAMETER  
EXCEEDED THE DEFAULT VALUE OF (120.0)

IER=132 INDICATES THAT AFTER A SUCCESSFUL  
RECOVERY FROM A SINGULAR JACOBIAN, THE SOLUTION  
HAS CYCLED BACK TO THE FIRST SINGULARITY

IER=133 INDICATES THAT THE (MAXFN) PARAMETER  
WAS EXCEEDED

# VARIABLES USED IN THE CALCULATIONS

THE ESTIMATED METAL CLUSTER RESISTANCE ( $R_c$ ) = 1.000000E+02

THE ESTIMATED GAP RESISTANCE ( $R_g$ ) = 1.000000E+05

THE ESTIMATED GAP  
CAPACITANCE ( $C_g$ ) = 6.000000E-07

THE LEAST SQUARE VALUE OF THE METAL CLUSTER  
RESISTANCE,  $R_c$  = 3.340187E+03

THE LEAST SQUARE VALUE OF THE GAP  
RESISTANCE,  $R_g$  = 1.012427E+05

THE LEAST SQUARE VALUE OF THE GAP  
CAPACITANCE,  $C_g$  = 4.702941E-07

THE RESIDUALS ARE CALCULATED BY THE FOLLOWING  
EQUATION: [MEASURED VALUE-CALCULATED VALUE]

SAMPLE	R(f)	R(cal)	R(resid)	Cg(est)
1	9.9200E+04	1.0458E+05	-5.3829E+03	4.7029E-07
2	9.2600E+04	9.7830E+04	-5.2304E+03	4.7029E-07
3	9.1700E+04	9.5137E+04	-3.4365E+03	4.7029E-07
4	9.0100E+04	9.2144E+04	-2.0444E+03	4.7029E-07
5	8.8500E+04	8.8926E+04	-4.2561E+02	4.7029E-07
6	8.7700E+04	8.5549E+04	2.1514E+03	4.7029E-07
7	8.6200E+04	8.2076E+04	4.1237E+03	4.7029E-07
8	8.2600E+04	7.5061E+04	7.5390E+03	4.7029E-07
9	7.8100E+04	6.8228E+04	9.8716E+03	4.7029E-07
10	7.1900E+04	6.1802E+04	1.0098E+04	4.7029E-07
11	6.3700E+04	5.5902E+04	7.7976E+03	4.7029E-07
12	5.5600E+04	5.0575E+04	5.0251E+03	4.7029E-07
13	4.6700E+04	4.5817E+04	8.8347E+02	4.7029E-07
14	3.8800E+04	4.1596E+04	-2.7957E+03	4.7029E-07
15	3.2700E+04	3.7866E+04	-5.1665E+03	4.7029E-07
16	2.7800E+04	3.4578E+04	-6.7778E+03	4.7029E-07
17	2.4700E+04	3.1679E+04	-6.9785E+03	4.7029E-07
18	2.2200E+04	2.9121E+04	-6.9208E+03	4.7029E-07
19	2.0800E+04	2.6861E+04	-6.0609E+03	4.7029E-07
20	1.8700E+04	2.4860E+04	-6.1601E+03	4.7029E-07
21	1.7800E+04	2.3085E+04	-5.2846E+03	4.7029E-07

22	1.7000E+04	2.1505E+04	-4.5049E+03	4.7029E-07
23	1.6300E+04	2.0096E+04	-3.7956E+03	4.7029E-07
24	1.5600E+04	1.8835E+04	-3.2349E+03	4.7029E-07
25	1.4900E+04	1.7704E+04	-2.8038E+03	4.7029E-07
26	1.4400E+04	1.6686E+04	-2.2863E+03	4.7029E-07
27	1.3900E+04	1.5768E+04	-1.8684E+03	4.7029E-07
28	1.3600E+04	1.4938E+04	-1.3382E+03	4.7029E-07
29	1.3200E+04	1.4185E+04	-9.8528E+02	4.7029E-07
30	1.3000E+04	1.3501E+04	-5.0081E+02	4.7029E-07
31	1.2700E+04	1.2877E+04	-1.7703E+02	4.7029E-07
32	1.2600E+04	1.2307E+04	2.9279E+02	4.7029E-07
33	1.2400E+04	1.1786E+04	6.1450E+02	4.7029E-07
34	1.2300E+04	1.1307E+04	9.9319E+02	4.7029E-07
35	1.2200E+04	1.0867E+04	1.3334E+03	4.7029E-07
36	1.2000E+04	1.0461E+04	1.5389E+03	4.7029E-07
37	1.1800E+04	1.0087E+04	1.7133E+03	4.7029E-07
38	1.1600E+04	9.7405E+03	1.8595E+03	4.7029E-07
39	1.1400E+04	9.4197E+03	1.9803E+03	4.7029E-07
40	1.1200E+04	9.1220E+03	2.0780E+03	4.7029E-07
41	1.1100E+04	8.8452E+03	2.2548E+03	4.7029E-07
42	1.1000E+04	8.5875E+03	2.4125E+03	4.7029E-07
43	1.0900E+04	8.3471E+03	2.5529E+03	4.7029E-07
44	1.0900E+04	8.1227E+03	2.7773E+03	4.7029E-07
45	1.0800E+04	7.9127E+03	2.8873E+03	4.7029E-07
46	1.0800E+04	7.7161E+03	3.0839E+03	4.7029E-07
47	1.0700E+04	7.5318E+03	3.1682E+03	4.7029E-07
48	1.0600E+04	3.3406E+03	7.2594E+03	4.7029E-07
49	1.0500E+04	3.3406E+03	7.1594E+03	4.7029E-07
50	1.0400E+04	3.3406E+03	7.0594E+03	4.7029E-07
51	1.0300E+04	3.3406E+03	6.9594E+03	4.7029E-07
52	1.0200E+04	6.7623E+03	3.4377E+03	4.7029E-07
53	6.8000E+03	4.8902E+03	1.9098E+03	4.7029E-07
54	4.9500E+03	4.2180E+03	7.3203E+02	4.7029E-07
55	4.1000E+03	3.9037E+03	1.9627E+02	4.7029E-07
56	3.5000E+03	3.7322E+03	-2.3220E+02	4.7029E-07
57	3.1100E+03	3.6285E+03	-5.1849E+02	4.7029E-07
58	2.8500E+03	3.5611E+03	-7.1107E+02	4.7029E-07
59	2.6200E+03	3.5148E+03	-8.9479E+02	4.7029E-07
60	2.4800E+03	3.4817E+03	-1.0017E+03	4.7029E-07
61	1.9900E+03	3.4031E+03	-1.4131E+03	4.7029E-07
62	1.7100E+03	3.3756E+03	-1.6656E+03	4.7029E-07
63	1.2000E+03	3.3459E+03	-2.1459E+03	4.7029E-07
64	6.3700E+02	3.3416E+03	-2.7046E+03	4.7029E-07
65	5.3800E+02	3.3408E+03	-2.8028E+03	4.7029E-07
66	5.0000E+02	3.3405E+03	-2.8405E+03	4.7029E-07
67	2.7500E+02	3.3402E+03	-3.0652E+03	4.7029E-07
68	2.1500E+02	3.3402E+03	-3.1252E+03	4.7029E-07
69	1.2000E+02	3.3402E+03	-3.2202E+03	4.7029E-07
70	9.7000E+01	3.3402E+03	-3.2432E+03	4.7029E-07

SUM OF SQUARED RESIDUALS= 1.1485E+09

VARIANCE= 1.6889E+07

STANDARD DEVIATION= 4.1097E+03

H-47

ADDITIONAL PARAMETERS CALCULATED BY THE LEAST SQUARES SUBROUTINE.

THE RESIDUAL SUM OF SQUARES = 1.148475E+09

THE NUMBER OF SIGNIFICANT DIGITS IN THE CALCULATED PARAMETERS = 6.081776E+00

THE NUMBER OF FUNCTION EVALUATIONS REQUIRED = 1.680000E+02

THE NUMBER OF ITERATIONS REQUIRED = 6.100000E+01

AN INTEGER WHICH INDICATES THE CONVERGENCE CRITERION SATISFIED - INFER = 1

INFER=0 INDICATES THAT CONVERGENCE FAILED -- SEE THE (IER) PARAMETER

INFER=1 INDICATES THAT THE FOLLOWING CONVERGENCE CONDITION IS SATISFIED  
FOR TWO SUCCESSIVE ITERATIONS THE PARAMETER  
ESTIMATES AGREE, COMPONENT BY COMPONENT  
TO NSIG (SIGNIFICANT) DIGITS

INFER=2 INDICATES THAT THE FOLLOWING CONVERGENCE CONDITION IS SATISFIED  
FOR TWO SUCCESSIVE ITERATIONS THE RESIDUAL  
SUM OF THE SQUARE ESTIMATES HAVE RELATIVE  
DIFFERENCE LESS THAN OR EQUAL TO (EPS)

INFER=4 INDICATES THAT THE FOLLOWING CONVERGENCE CONDITION IS SATISFIED  
THE (EUCLIDEAN) NORM OF THE APPROXIMATE  
GRADIENT IS LESS THAN OR EQUAL TO (DELTA)

INFER=X IF MORE THAN ONE OF THE ABOVE CONVERGENCE CRITERIA IS SATISFIED  
(INFER) REPRESENTS THE CORRESPONDING SUM OF  
THE INTEGERS

THE ERROR PARAMETER: IEP = 0



IER=0 INDICATES SUCCESSFUL EXECUTION OF THE PROGRAM

IER=38 INDICATES THAT THE JACOBIAN IS ZERO.  
THE SOLUTION IS A STATIONARY POINT (WARNING)

IER=129 INDICATES THAT A SINGULARITY WAS  
DETECTED IN THE JACOBIAN

IER=130 INDICATES THAT AT LEAST ONE OF THE  
SUBROUTINE CALL PARAMETERS WAS SPECIFIED  
INCORRECTLY -- VERIFY: M,N,IOPT,PARM(1),PARM(2)

IER=131 INDICATES THAT THE MARQUARDT PARAMETER  
EXCEEDED THE DEFAULT VALUE OF (120.0)

IER=132 INDICATES THAT AFTER A SUCCESSFUL  
RECOVERY FROM A SINGULAR JACOBIAN, THE SOLUTION  
HAS CYCLED BACK TO THE FIRST SINGULARITY

IER=133 INDICATES THAT THE (MAXFN) PARAMETER  
WAS EXCEEDED

# VARIABLES USED IN THE CALCULATIONS

THE ESTIMATED METAL CLUSTER RESISTANCE (Rc) = 1.000000E+02

THE ESTIMATED GAP RESISTANCE (Rg) = 1.000000E+05

THE ESTIMATED GAP  
CAPACITANCE (Cg) = 6.000000E-07

THE LEAST SQUARE VALUE OF THE METAL CLUSTER  
RESISTANCE, Rc = 3.502186E+03

THE LEAST SQUARE VALUE OF THE GAP  
RESISTANCE, Rg = 9.292173E+04

THE LEAST SQUARE VALUE OF THE GAP  
CAPACITANCE, Cg = 4.573935E-07

THE RESIDUALS ARE CALCULATED BY THE FOLLOWING  
EQUATION: [MEASURED VALUE-CALCULATED VALUE]

SAMPLE	R(f)	R(cal)	R(resid)	Cg(est)
1	9.1800E+04	9.6424E+04	-4.6239E+03	4.5739E-07
2	8.6200E+04	9.0773E+04	-4.5728E+03	4.5739E-07
3	8.5500E+04	8.8498E+04	-2.9983E+03	4.5739E-07
4	8.4000E+04	8.5959E+04	-1.9587E+03	4.5739E-07
5	8.3300E+04	8.3211E+04	8.9426E+01	4.5739E-07
6	8.2000E+04	8.0309E+04	1.6906E+03	4.5739E-07
7	8.0600E+04	7.7307E+04	3.2928E+03	4.5739E-07
8	7.7500E+04	7.1181E+04	6.3192E+03	4.5739E-07
9	7.3500E+04	6.5135E+04	8.3653E+03	4.5739E-07
10	6.7600E+04	5.9375E+04	8.2247E+03	4.5739E-07
11	6.0600E+04	5.4025E+04	6.5753E+03	4.5739E-07
12	5.3500E+04	4.9140E+04	4.3600E+03	4.5739E-07
13	4.6100E+04	4.4734E+04	1.3660E+03	4.5739E-07
14	3.8900E+04	4.0791E+04	-1.8911E+03	4.5739E-07
15	3.2200E+04	3.7280E+04	-5.0802E+03	4.5739E-07
16	2.7000E+04	3.4162E+04	-7.1624E+03	4.5739E-07
17	2.4300E+04	3.1397E+04	-7.0969E+03	4.5739E-07
18	2.2600E+04	2.8944E+04	-6.3439E+03	4.5739E-07
19	2.1300E+04	2.6766E+04	-5.4661E+03	4.5739E-07
20	2.0200E+04	2.4830E+04	-4.6298E+03	4.5739E-07
21	1.9100E+04	2.3105E+04	-4.0051E+03	4.5739E-07

22	1.8200E+04	2.1565E+04	-3.3653E+03	4.5739E-07
23	1.7400E+04	2.0188E+04	-2.7875E+03	4.5739E-07
24	1.6800E+04	1.8952E+04	-2.1516E+03	4.5739E-07
25	1.6100E+04	1.7840E+04	-1.7402E+03	4.5739E-07
26	1.5500E+04	1.6838E+04	-1.3381E+03	4.5739E-07
27	1.5000E+04	1.5932E+04	-9.3247E+02	4.5739E-07
28	1.4700E+04	1.5112E+04	-4.1185E+02	4.5739E-07
29	1.4400E+04	1.4366E+04	3.3517E+01	4.5739E-07
30	1.4100E+04	1.3688E+04	4.1214E+02	4.5739E-07
31	1.3800E+04	1.3069E+04	7.3141E+02	4.5739E-07
32	1.3400E+04	1.2502E+04	8.9780E+02	4.5739E-07
33	1.3100E+04	1.1983E+04	1.1169E+03	4.5739E-07
34	1.2800E+04	1.1506E+04	1.2938E+03	4.5739E-07
35	1.2600E+04	1.1067E+04	1.5326E+03	4.5739E-07
36	1.2300E+04	1.0663E+04	1.6373E+03	4.5739E-07
37	1.2000E+04	1.0289E+04	1.7112E+03	4.5739E-07
38	1.1800E+04	9.9428E+03	1.8572E+03	4.5739E-07
39	1.1700E+04	9.6220E+03	2.0780E+03	4.5739E-07
40	1.1500E+04	9.3240E+03	2.1760E+03	4.5739E-07
41	1.1200E+04	9.0469E+03	2.1531E+03	4.5739E-07
42	1.1000E+04	8.7887E+03	2.2113E+03	4.5739E-07
43	1.0800E+04	8.5478E+03	2.2522E+03	4.5739E-07
44	1.0600E+04	8.3227E+03	2.2773E+03	4.5739E-07
45	1.0500E+04	8.1121E+03	2.3879E+03	4.5739E-07
46	1.0300E+04	7.9148E+03	2.3852E+03	4.5739E-07
47	1.0200E+04	7.7297E+03	2.4703E+03	4.5739E-07
48	1.0000E+04	3.5026E+03	6.4974E+03	4.5739E-07
49	9.9000E+03	3.5026E+03	6.3974E+03	4.5739E-07
50	9.7100E+03	3.5026E+03	6.2074E+03	4.5739E-07
51	9.6200E+03	3.5026E+03	6.1174E+03	4.5739E-07
52	9.4300E+03	6.9563E+03	2.4737E+03	4.5739E-07
53	6.5400E+03	5.0697E+03	1.4703E+03	4.5739E-07
54	4.9500E+03	4.3905E+03	5.5952E+02	4.5739E-07
55	4.1700E+03	4.0727E+03	9.7342E+01	4.5739E-07
56	3.5300E+03	3.8991E+03	-3.6909E+02	4.5739E-07
57	3.1400E+03	3.7941E+03	-6.5412E+02	4.5739E-07
58	2.8400E+03	3.7259E+03	-8.8586E+02	4.5739E-07
59	2.5700E+03	3.6790E+03	-1.1090E+03	4.5739E-07
60	2.3600E+03	3.6455E+03	-1.2855E+03	4.5739E-07
61	1.7800E+03	3.5659E+03	-1.7859E+03	4.5739E-07
62	1.5700E+03	3.5380E+03	-1.9680E+03	4.5739E-07
63	8.4000E+02	3.5079E+03	-2.6679E+03	4.5739E-07
64	5.3200E+02	3.5036E+03	-2.9716E+03	4.5739E-07
65	4.8300E+02	3.5028E+03	-3.0198E+03	4.5739E-07
66	4.2600E+02	3.5025E+03	-3.0765E+03	4.5739E-07
67	2.3600E+02	3.5022E+03	-3.2662E+03	4.5739E-07
68	1.8600E+02	3.5022E+03	-3.3162E+03	4.5739E-07
69	1.1400E+02	3.5022E+03	-3.3882E+03	4.5739E-07
70	1.0300E+02	3.5022E+03	-3.3992E+03	4.5739E-07

SUM OF SQUARED RESIDUALS= 8.9912E+08

VARIANCE= 1.3222E+07

STANDARD DEVIATION= 3.6363E+03

H-51

ADDITIONAL PARAMETERS CALCULATED BY THE LEAST SQUARES SUBROUTINE.

THE RESIDUAL SUM OF SQUARES = 8.991247E+08

THE NUMBER OF SIGNIFICANT DIGITS IN THE CALCULATED PARAMETERS = 6.113810E+00

THE NUMBER OF FUNCTION EVALUATIONS REQUIRED = 1.320000E+02

THE NUMBER OF ITERATIONS REQUIRED = 4.800000E+01

AN INTEGER WHICH INDICATES THE CONVERGENCE CRITERION SATISFIED - INFER = 1

INFER=0 INDICATES THAT CONVERGENCE FAILED -- SEE THE (IER) PARAMETER

INFER=1 INDICATES THAT THE FOLLOWING CONVERGENCE CONDITION IS SATISFIED  
FOR TWO SUCCESSIVE ITERATIONS THE PARAMETER  
ESTIMATES AGREE, COMPONENT BY COMPONENT  
TO NSIG (SIGNIFICANT) DIGITS

INFER=2 INDICATES THAT THE FOLLOWING CONVERGENCE CONDITION IS SATISFIED  
FOR TWO SUCCESSIVE ITERATIONS THE RESIDUAL  
SUM OF THE SQUARE ESTIMATES HAVE RELATIVE  
DIFFERENCE LESS THAN OR EQUAL TO (EPS)

INFER=4 INDICATES THAT THE FOLLOWING CONVERGENCE CONDITION IS SATISFIED  
THE (EUCLIDEAN) NORM OF THE APPROXIMATE  
GRADIENT IS LESS THAN OR EQUAL TO (DELTA)

INFER=X IF MORE THAN ONE OF THE ABOVE CONVERGENCE CRITERIA IS SATISFIED  
(INFER) REPRESENTS THE CORRESPONDING SUM OF  
THE INTEGERS

THE ERROR PARAMETER: IER = 0

IER=0    INDICATES SUCCESSFUL EXECUTION OF THE PROGRAM

IER=38    INDICATES THAT THE JACOBIAN IS ZERO.  
          THE SOLUTION IS A STATIONARY POINT (WARNING)

IER=129    INDICATES THAT A SINGULARITY WAS  
          DETECTED IN THE JACOBIAN

IER=130    INDICATES THAT AT LEAST ONE OF THE  
          SUBROUTINE CALL PARAMETERS WAS SPECIFIED  
          INCORRECTLY -- VERIFY:  M,N,IOPT,PARM(1),PARM(2)

IER=131    INDICATES THAT THE MARQUARDT PARAMETER  
          EXCEEDED THE DEFAULT VALUE OF (120.0)

IER=132    INDICATES THAT AFTER A SUCCESSFUL  
          RECOVERY FROM A SINGULAR JACOBIAN, THE SOLUTION  
          HAS CYCLED BACK TO THE FIRST SINGULARITY

IER=133    INDICATES THAT THE (MAXFN) PARAMETER  
          WAS EXCEEDED

# VARIABLES USED IN THE CALCULATIONS

THE ESTIMATED METAL CLUSTER RESISTANCE ( $R_c$ ) = 1.000000E+02

THE ESTIMATED GAP RESISTANCE ( $R_g$ ) = 1.000000E+05

THE ESTIMATED GAP  
CAPACITANCE ( $C_g$ ) = 6.000000E-07

THE LEAST SQUARE VALUE OF THE METAL CLUSTER  
RESISTANCE,  $R_c$  = 2.702907E+03

THE LEAST SQUARE VALUE OF THE GAP  
RESISTANCE,  $R_g$  = 8.902660E+04

THE LEAST SQUARE VALUE OF THE GAP  
CAPACITANCE,  $C_g$  = 5.463141E-07

THE RESIDUALS ARE CALCULATED BY THE FOLLOWING  
EQUATION: [MEASURED VALUE-CALCULATED VALUE]

SAMPLE	R(f)	R(cal)	R(resid)	Cg(est)
1	8.6300E+04	9.1730E+04	-5.4295E+03	5.4631E-07
2	8.0600E+04	8.5999E+04	-5.3993E+03	5.4631E-07
3	8.0000E+04	8.3705E+04	-3.7052E+03	5.4631E-07
4	7.9400E+04	8.1152E+04	-1.7519E+03	5.4631E-07
5	7.8700E+04	7.8399E+04	3.0134E+02	5.4631E-07
6	7.7500E+04	7.5503E+04	1.9969E+03	5.4631E-07
7	7.6300E+04	7.2518E+04	3.7818E+03	5.4631E-07
8	7.3500E+04	6.6464E+04	7.0359E+03	5.4631E-07
9	6.9900E+04	6.0537E+04	9.3628E+03	5.4631E-07
10	6.4900E+04	5.4935E+04	9.9650E+03	5.4631E-07
11	5.7500E+04	4.9768E+04	7.7320E+03	5.4631E-07
12	5.0300E+04	4.5083E+04	5.2175E+03	5.4631E-07
13	4.2700E+04	4.0882E+04	1.8184E+03	5.4631E-07
14	3.5700E+04	3.7143E+04	-1.4426E+03	5.4631E-07
15	2.8800E+04	3.3829E+04	-5.0292E+03	5.4631E-07
16	2.3700E+04	3.0899E+04	-7.1995E+03	5.4631E-07
17	2.0000E+04	2.8311E+04	-8.3106E+03	5.4631E-07
18	1.8500E+04	2.6022E+04	-7.5219E+03	5.4631E-07
19	1.7300E+04	2.3996E+04	-6.6960E+03	5.4631E-07
20	1.6200E+04	2.2200E+04	-5.9996E+03	5.4631E-07
21	1.5400E+04	2.0603E+04	-5.2031E+03	5.4631E-07

22	1.4800E+04	1.9181E+04	-4.3809E+03	5.4631E-07
23	1.4300E+04	1.7911E+04	-3.6106E+03	5.4631E-07
24	1.3900E+04	1.6773E+04	-2.8730E+03	5.4631E-07
25	1.3500E+04	1.5752E+04	-2.2516E+03	5.4631E-07
26	1.3200E+04	1.4832E+04	-1.6319E+03	5.4631E-07
27	1.2900E+04	1.4002E+04	-1.1017E+03	5.4631E-07
28	1.2600E+04	1.3250E+04	-6.5023E+02	5.4631E-07
29	1.2300E+04	1.2568E+04	-2.6839E+02	5.4631E-07
30	1.2000E+04	1.1948E+04	5.1834E+01	5.4631E-07
31	1.1800E+04	1.1383E+04	4.1735E+02	5.4631E-07
32	1.1500E+04	1.0866E+04	6.3419E+02	5.4631E-07
33	1.1300E+04	1.0392E+04	9.0758E+02	5.4631E-07
34	1.1100E+04	9.9579E+03	1.1421E+03	5.4631E-07
35	1.0900E+04	9.5582E+03	1.3418E+03	5.4631E-07
36	1.0600E+04	9.1898E+03	1.4102E+03	5.4631E-07
37	1.0400E+04	8.8497E+03	1.5503E+03	5.4631E-07
38	1.0200E+04	8.5350E+03	1.6650E+03	5.4631E-07
39	1.0100E+04	8.2434E+03	1.8566E+03	5.4631E-07
40	9.9000E+03	7.9726E+03	1.9274E+03	5.4631E-07
41	9.8000E+03	7.7209E+03	2.0791E+03	5.4631E-07
42	9.7100E+03	7.4864E+03	2.2236E+03	5.4631E-07
43	9.5200E+03	7.2678E+03	2.2522E+03	5.4631E-07
44	9.4300E+03	7.0635E+03	2.3665E+03	5.4631E-07
45	9.2600E+03	6.8724E+03	2.3876E+03	5.4631E-07
46	9.0900E+03	6.6934E+03	2.3966E+03	5.4631E-07
47	8.9300E+03	6.5256E+03	2.4044E+03	5.4631E-07
48	8.7700E+03	2.7033E+03	6.0667E+03	5.4631E-07
49	8.5500E+03	2.7033E+03	5.8467E+03	5.4631E-07
50	8.4000E+03	2.7033E+03	5.6967E+03	5.4631E-07
51	8.2000E+03	2.7032E+03	5.4968E+03	5.4631E-07
52	8.0100E+03	5.8247E+03	2.1853E+03	5.4631E-07
53	5.7800E+03	4.1180E+03	1.6620E+03	5.4631E-07
54	4.1500E+03	3.5044E+03	6.4555E+02	5.4631E-07
55	3.4500E+03	3.2176E+03	2.3244E+02	5.4631E-07
56	2.9100E+03	3.0609E+03	-1.5094E+02	5.4631E-07
57	2.5900E+03	2.9662E+03	-3.7623E+02	5.4631E-07
58	2.3500E+03	2.9047E+03	-5.5465E+02	5.4631E-07
59	2.2100E+03	2.8624E+03	-6.5239E+02	5.4631E-07
60	2.0900E+03	2.8321E+03	-7.4213E+02	5.4631E-07
61	1.6900E+03	2.7604E+03	-1.0704E+03	5.4631E-07
62	1.5300E+03	2.7352E+03	-1.2052E+03	5.4631E-07
63	7.9400E+02	2.7081E+03	-1.9141E+03	5.4631E-07
64	5.0800E+02	2.7042E+03	-2.1962E+03	5.4631E-07
65	4.3700E+02	2.7035E+03	-2.2665E+03	5.4631E-07
66	3.9800E+02	2.7032E+03	-2.3052E+03	5.4631E-07
67	2.3000E+02	2.7029E+03	-2.4729E+03	5.4631E-07
68	1.8100E+02	2.7029E+03	-2.5219E+03	5.4631E-07
69	1.2200E+02	2.7029E+03	-2.5809E+03	5.4631E-07
70	1.1100E+02	2.7029E+03	-2.5919E+03	5.4631E-07

SUM OF SQUARED RESIDUALS= 1.0298E+09

VARIANCE= 1.5144E+07

STANDARD DEVIATION= 3.8915E+03

ADDITIONAL PARAMETERS CALCULATED BY THE LEAST SQUARES SUBROUTINE.

THE RESIDUAL SUM OF SQUARES = 1.029770E+09

THE NUMBER OF SIGNIFICANT DIGITS IN THE CALCULATED PARAMETERS = 6.641345E+00

THE NUMBER OF FUNCTION EVALUATIONS REQUIRED = 1.400000E+02

THE NUMBER OF ITERATIONS REQUIRED = 4.300000E+01

AN INTEGER WHICH INDICATES THE CONVERGENCE CRITERION SATISFIED - INFER = 1

INFER=0 INDICATES THAT CONVERGENCE FAILED -- SEE THE (IER) PARAMETER

INFER=1 INDICATES THAT THE FOLLOWING CONVERGENCE CONDITION IS SATISFIED  
FOR TWO SUCCESSIVE ITERATIONS THE PARAMETER  
ESTIMATES AGREE, COMPONENT BY COMPONENT  
TO NSIG (SIGNIFICANT) DIGITS

INFER=2 INDICATES THAT THE FOLLOWING CONVERGENCE CONDITION IS SATISFIED  
FOR TWO SUCCESSIVE ITERATIONS THE RESIDUAL  
SUM OF THE SQUARE ESTIMATES HAVE RELATIVE  
DIFFERENCE LESS THAN OR EQUAL TO (EPS)

INFER=4 INDICATES THAT THE FOLLOWING CONVERGENCE CONDITION IS SATISFIED  
THE (EUCLIDEAN) NORM OF THE APPROXIMATE  
GRADIENT IS LESS THAN OR EQUAL TO (DELTA)

INFER=X IF MORE THAN ONE OF THE ABOVE CONVERGENCE CRITERIA IS SATISFIED  
(INFER) REPRESENTS THE CORRESPONDING SUM OF  
THE INTEGERS

THE ERROR PARAMETER: IER = 0



IER=0 INDICATES SUCCESSFUL EXECUTION OF THE PROGRAM

IER=38 INDICATES THAT THE JACOBIAN IS ZERO.  
THE SOLUTION IS A STATIONARY POINT (WARNING)

IER=129 INDICATES THAT A SINGULARITY WAS  
DETECTED IN THE JACOBIAN

IER=130 INDICATES THAT AT LEAST ONE OF THE  
SUBROUTINE CALL PARAMETERS WAS SPECIFIED  
INCORRECTLY -- VERIFY: M,N,IOPT,PARM(1),PARM(2)

IER= 11 INDICATES THAT THE MARQUARDT PARAMETER  
EXCEEDED THE DEFAULT VALUE OF (120.0)

IER=132 INDICATES THAT AFTER A SUCCESSFUL  
RECOVERY FROM A SINGULAR JACOBIAN, THE SOLUTION  
HAS CYCLED BACK TO THE FIRST SINGULARITY

IER=133 INDICATES THAT THE (MAXFN) PARAMETER  
WAS EXCEEDED

# VARIABLES USED IN THE CALCULATIONS

THE ESTIMATED METAL CLUSTER RESISTANCE ( $R_c$ ) =  $1.000000E+02$

THE ESTIMATED GAP RESISTANCE ( $R_g$ ) =  $1.000000E+05$

THE ESTIMATED GAP  
CAPACITANCE ( $C_g$ ) =  $6.000000E-07$

THE LEAST SQUARE VALUE OF THE METAL CLUSTER  
RESISTANCE,  $R_c$  =  $4.008639E+03$

THE LEAST SQUARE VALUE OF THE GAP  
RESISTANCE,  $R_g$  =  $9.786128E+04$

THE LEAST SQUARE VALUE OF THE GAP  
CAPACITANCE,  $C_g$  =  $3.825098E-07$

THE RESIDUALS ARE CALCULATED BY THE FOLLOWING  
EQUATION: [MEASURED VALUE-CALCULATED VALUE]

SAMPLE	$R(f)$	$R(cal)$	$R(resid)$	$C_g(est)$
1	9.5800E+04	1.0187E+05	-6.0699E+03	3.8251E-07
2	9.1700E+04	9.6819E+04	-5.1192E+03	3.8251E-07
3	9.1700E+04	9.4758E+04	-3.0584E+03	3.8251E-07
4	9.0900E+04	9.2438E+04	-1.5378E+03	3.8251E-07
5	9.0000E+04	8.9903E+04	9.6514E+01	3.8251E-07
6	8.9300E+04	8.7201E+04	2.0987E+03	3.8251E-07
7	8.7700E+04	8.4376E+04	3.3243E+03	3.8251E-07
8	8.4700E+04	7.8515E+04	6.1848E+03	3.8251E-07
9	8.0600E+04	7.2604E+04	7.9963E+03	3.8251E-07
10	7.5200E+04	6.6851E+04	8.3494E+03	3.8251E-07
11	6.8500E+04	6.1396E+04	7.1042E+03	3.8251E-07
12	6.1300E+04	5.6321E+04	4.9792E+03	3.8251E-07
13	5.3800E+04	5.1663E+04	2.1371E+03	3.8251E-07
14	4.6700E+04	4.7429E+04	-7.2854E+02	3.8251E-07
15	3.9800E+04	4.3604E+04	-3.8043E+03	3.8251E-07
16	3.4000E+04	4.0165E+04	-6.1651E+03	3.8251E-07
17	2.9700E+04	3.7080E+04	-7.3798E+03	3.8251E-07
18	2.7000E+04	3.4315E+04	-7.3153E+03	3.8251E-07
19	2.5500E+04	3.1839E+04	-6.3388E+03	3.8251E-07
20	2.4200E+04	2.9619E+04	-5.4192E+03	3.8251E-07
21	2.2900E+04	2.7628E+04	-4.7278E+03	3.8251E-07

22	2.1900E+04	2.5839E+04	-3.9387E+03	3.8251E-07
23	2.1100E+04	2.4228E+04	-3.1285E+03	3.8251E-07
24	2.0400E+04	2.2777E+04	-2.3766E+03	3.8251E-07
25	1.9800E+04	2.1465E+04	-1.6649E+03	3.8251E-07
26	1.9200E+04	2.0277E+04	-1.0773E+03	3.8251E-07
27	1.8600E+04	1.9200E+04	-5.9980E+02	3.8251E-07
28	1.8100E+04	1.8220E+04	-1.2015E+02	3.8251E-07
29	1.7500E+04	1.7328E+04	1.7244E+02	3.8251E-07
30	1.7000E+04	1.6513E+04	4.8742E+02	3.8251E-07
31	1.6600E+04	1.5767E+04	8.3306E+02	3.8251E-07
32	1.6100E+04	1.5083E+04	1.0167E+03	3.8251E-07
33	1.5700E+04	1.4455E+04	1.2446E+03	3.8251E-07
34	1.5300E+04	1.3878E+04	1.4225E+03	3.8251E-07
35	1.5000E+04	1.3345E+04	1.6553E+03	3.8251E-07
36	1.4700E+04	1.2852E+04	1.8475E+03	3.8251E-07
37	1.4400E+04	1.2397E+04	2.0030E+03	3.8251E-07
38	1.4200E+04	1.1975E+04	2.2251E+03	3.8251E-07
39	1.3900E+04	1.1583E+04	2.3170E+03	3.8251E-07
40	1.3700E+04	1.1219E+04	2.4815E+03	3.8251E-07
41	1.3400E+04	1.0879E+04	2.5208E+03	3.8251E-07
42	1.3100E+04	1.0563E+04	2.5373E+03	3.8251E-07
43	1.2900E+04	1.0267E+04	2.6330E+03	3.8251E-07
44	1.2700E+04	9.9906E+03	2.7094E+03	3.8251E-07
45	1.2300E+04	9.7317E+03	2.5683E+03	3.8251E-07
46	1.2100E+04	9.4889E+03	2.6111E+03	3.8251E-07
47	1.1800E+04	9.2609E+03	2.5391E+03	3.8251E-07
48	1.1600E+04	4.0092E+03	7.5908E+03	3.8251E-07
49	1.1300E+04	4.0091E+03	7.2909E+03	3.8251E-07
50	1.1000E+04	4.0091E+03	6.9909E+03	3.8251E-07
51	1.0800E+04	4.0091E+03	6.7909E+03	3.8251E-07
52	1.0600E+04	8.3068E+03	2.2932E+03	3.8251E-07
53	7.1900E+03	5.9667E+03	1.2233E+03	3.8251E-07
54	5.4300E+03	5.1198E+03	3.1021E+02	3.8251E-07
55	4.4400E+03	4.7227E+03	-2.8270E+02	3.8251E-07
56	3.8000E+03	4.5056E+03	-7.0562E+02	3.8251E-07
57	3.3800E+03	4.3743E+03	-9.9426E+02	3.8251E-07
58	3.0200E+03	4.2888E+03	-1.2688E+03	3.8251E-07
59	2.7500E+03	4.2301E+03	-1.4801E+03	3.8251E-07
60	2.5500E+03	4.1881E+03	-1.6381E+03	3.8251E-07
61	1.9700E+03	4.0885E+03	-2.1185E+03	3.8251E-07
62	1.6900E+03	4.0536E+03	-2.3636E+03	3.8251E-07
63	8.0000E+02	4.0158E+03	-3.2158E+03	3.8251E-07
64	5.6500E+02	4.0104E+03	-3.4454E+03	3.8251E-07
65	4.8500E+02	4.0094E+03	-3.5244E+03	3.8251E-07
66	4.2200E+02	4.0091E+03	-3.5871E+03	3.8251E-07
67	2.4200E+02	4.0087E+03	-3.7667E+03	3.8251E-07
68	1.8500E+02	4.0086E+03	-3.8236E+03	3.8251E-07
69	1.1400E+02	4.0086E+03	-3.8946E+03	3.8251E-07
70	1.0200E+02	4.0086E+03	-3.9066E+03	3.8251E-07

SUM OF SQUARED RESIDUALS= 1.0467E+09

VARIANCE= 1.5393E+07

STANDARD DEVIATION= 3.9234E+03

ADDITIONAL PARAMETERS CALCULATED BY THE LEAST SQUARES SUBROUTINE.

THE RESIDUAL SUM OF SQUARES = 1.046728E+09

THE NUMBER OF SIGNIFICANT DIGITS IN THE CALCULATED PARAMETERS = 6.633811E+00

THE NUMBER OF FUNCTION EVALUATIONS REQUIRED = 1.740000E+02

THE NUMBER OF ITERATIONS REQUIRED = 6.900000E+01

AN INTEGER WHICH INDICATES THE CONVERGENCE CRITERION SATISFIED - INFER = 1

INFER=0 INDICATES THAT CONVERGENCE FAILED -- SEE THE (IER) PARAMETER

INFER=1 INDICATES THAT THE FOLLOWING CONVERGENCE CONDITION IS SATISFIED  
FOR TWO SUCCESSIVE ITERATIONS THE PARAMETER  
ESTIMATES AGREE, COMPONENT BY COMPONENT  
TO NSIG (SIGNIFICANT) DIGITS

INFER=2 INDICATES THAT THE FOLLOWING CONVERGENCE CONDITION IS SATISFIED  
FOR TWO SUCCESSIVE ITERATIONS THE RESIDUAL  
SUM OF THE SQUARE ESTIMATES HAVE RELATIVE  
DIFFERENCE LESS THAN OR EQUAL TO (EPS)

INFER=4 INDICATES THAT THE FOLLOWING CONVERGENCE CONDITION IS SATISFIED  
THE (EUCLIDEAN) NORM OF THE APPROXIMATE  
GRADIENT IS LESS THAN OR EQUAL TO (DELTA)

INFER=X IF MORE THAN ONE OF THE ABOVE CONVERGENCE CRITERIA IS SATISFIED  
(INFER) REPRESENTS THE CORRESPONDING SUM OF  
THE INTEGERS

THE ERROR PARAMETER: IER = 0

IER=0    INDICATES SUCCESSFUL EXECUTION OF THE PROGRAM

IER=38    INDICATES THAT THE JACOBIAN IS ZERO.  
          THE SOLUTION IS A STATIONARY POINT (WARNING)

IER=129    INDICATES THAT A SINGULARITY WAS  
          DETECTED IN THE JACOBIAN

IER=130    INDICATES THAT AT LEAST ONE OF THE  
          SUBROUTINE CALL PARAMETERS WAS SPECIFIED  
          INCORRECTLY -- VERIFY:  M,N,IOPT,PARM(1),PARM(2)

IER=131    INDICATES THAT THE MARQUARDT PARAMETER  
          EXCEEDED THE DEFAULT VALUE OF (120.0)

IER=132    INDICATES THAT AFTER A SUCCESSFUL  
          RECOVERY FROM A SINGULAR JACOBIAN, THE SOLUTION  
          HAS CYCLED BACK TO THE FIRST SINGULARITY

IER=133    INDICATES THAT THE (MAXFN) PARAMETER  
          WAS EXCEEDED

# VARIABLES USED IN THE CALCULATIONS

THE ESTIMATED METAL CLUSTER RESISTANCE (Rc) = 1.000000E+02

THE ESTIMATED GAP RESISTANCE (Rg) = 1.000000E+05

THE ESTIMATED GAP  
CAPACITANCE (Cg) = 6.000000E-07

THE LEAST SQUARE VALUE OF THE METAL CLUSTER  
RESISTANCE, Rc = 3.311159E+03

THE LEAST SQUARE VALUE OF THE GAP  
RESISTANCE, Rg = 9.134471E+04

THE LEAST SQUARE VALUE OF THE GAP  
CAPACITANCE, Cg = 4.891687E-07

THE RESIDUALS ARE CALCULATED BY THE FOLLOWING  
EQUATION: [MEASURED VALUE-CALCULATED VALUE]

SAMPLE	R(f)	R(cal)	R(resid)	Cg(est)
1	8.9400E+04	9.4656E+04	-5.2559E+03	4.8917E-07
2	8.4000E+04	8.8765E+04	-4.7654E+03	4.8917E-07
3	8.3300E+04	8.6408E+04	-3.1076E+03	4.8917E-07
4	8.2000E+04	8.3784E+04	-1.7836E+03	4.8917E-07
5	8.0600E+04	8.0955E+04	-3.5459E+02	4.8917E-07
6	7.9400E+04	7.7980E+04	1.4204E+03	4.8917E-07
7	7.8100E+04	7.4913E+04	3.1867E+03	4.8917E-07
8	7.5200E+04	6.8695E+04	6.5046E+03	4.8917E-07
9	7.1400E+04	6.2610E+04	8.7903E+03	4.8917E-07
10	6.6200E+04	5.6859E+04	9.3411E+03	4.8917E-07
11	5.9500E+04	5.1556E+04	7.9438E+03	4.8917E-07
12	5.2600E+04	4.6749E+04	5.8514E+03	4.8917E-07
13	4.5200E+04	4.2439E+04	2.7608E+03	4.8917E-07
14	3.8000E+04	3.8604E+04	-6.0423E+02	4.8917E-07
15	3.1600E+04	3.5206E+04	-3.6064E+03	4.8917E-07
16	2.6300E+04	3.2202E+04	-5.9023E+03	4.8917E-07
17	2.2800E+04	2.9548E+04	-6.7481E+03	4.8917E-07
18	2.0100E+04	2.7202E+04	-7.1020E+03	4.8917E-07
19	1.8600E+04	2.5125E+04	-6.5254E+03	4.8917E-07
20	1.7300E+04	2.3284E+04	-5.9842E+03	4.8917E-07
21	1.6200E+04	2.1648E+04	-5.4481E+03	4.8917E-07

22	1.5200E+04	2.0191E+04	-4.9906E+03	4.8917E-07
23	1.4400E+04	1.8889E+04	-4.4889E+03	4.8917E-07
24	1.3700E+04	1.7723E+04	-4.0233E+03	4.8917E-07
25	1.3200E+04	1.6677E+04	-3.4767E+03	4.8917E-07
26	1.2800E+04	1.5734E+04	-2.9344E+03	4.8917E-07
27	1.2500E+04	1.4884E+04	-2.3838E+03	4.8917E-07
28	1.2200E+04	1.4114E+04	-1.9140E+03	4.8917E-07
29	1.2000E+04	1.3416E+04	-1.4155E+03	4.8917E-07
30	1.1900E+04	1.2780E+04	-8.8013E+02	4.8917E-07
31	1.1700E+04	1.2201E+04	-5.0081E+02	4.8917E-07
32	1.1600E+04	1.1671E+04	-7.1386E+01	4.8917E-07
33	1.1500E+04	1.1186E+04	3.1353E+02	4.8917E-07
34	1.1400E+04	1.0741E+04	6.5864E+02	4.8917E-07
35	1.1400E+04	1.0332E+04	1.0680E+03	4.8917E-07
36	1.1300E+04	9.9546E+03	1.3454E+03	4.8917E-07
37	1.1200E+04	9.6062E+03	1.5938E+03	4.8917E-07
38	1.1200E+04	9.2839E+03	1.9161E+03	4.8917E-07
39	1.1100E+04	8.9852E+03	2.1148E+03	4.8917E-07
40	1.1000E+04	8.7079E+03	2.2921E+03	4.8917E-07
41	1.0900E+04	8.4501E+03	2.4499E+03	4.8917E-07
42	1.0900E+04	8.2099E+03	2.6901E+03	4.8917E-07
43	1.0800E+04	7.9860E+03	2.8140E+03	4.8917E-07
44	1.0700E+04	7.7768E+03	2.9232E+03	4.8917E-07
45	1.0700E+04	7.5811E+03	3.1189E+03	4.8917E-07
46	1.0600E+04	7.3978E+03	3.2022E+03	4.8917E-07
47	1.0500E+04	7.2259E+03	3.2741E+03	4.8917E-07
48	1.0500E+04	3.3116E+03	7.1884E+03	4.8917E-07
49	1.0400E+04	3.3115E+03	7.0885E+03	4.8917E-07
50	1.0400E+04	3.3115E+03	7.0885E+03	4.8917E-07
51	1.0300E+04	3.3115E+03	6.9885E+03	4.8917E-07
52	1.0200E+04	6.5081E+03	3.6919E+03	4.8917E-07
53	7.0400E+03	4.7602E+03	2.2798E+03	4.8917E-07
54	5.4100E+03	4.1319E+03	1.2781E+03	4.8917E-07
55	4.3100E+03	3.8382E+03	4.7184E+02	4.8917E-07
56	3.6200E+03	3.6778E+03	-5.7780E+01	4.8917E-07
57	3.1800E+03	3.5808E+03	-4.0080E+02	4.8917E-07
58	2.9200E+03	3.5177E+03	-5.9775E+02	4.8917E-07
59	2.7200E+03	3.4745E+03	-7.5447E+02	4.8917E-07
60	2.5600E+03	3.4435E+03	-8.8348E+02	4.8917E-07
61	1.9300E+03	3.3700E+03	-1.4400E+03	4.8917E-07
62	1.7400E+03	3.3443E+03	-1.6043E+03	4.8917E-07
63	7.8100E+02	3.3165E+03	-2.5355E+03	4.8917E-07
64	5.8500E+02	3.3125E+03	-2.7275E+03	4.8917E-07
65	4.6900E+02	3.3117E+03	-2.8427E+03	4.8917E-07
66	4.1800E+02	3.3115E+03	-2.8935E+03	4.8917E-07
67	2.2600E+02	3.3112E+03	-3.0852E+03	4.8917E-07
68	1.6800E+02	3.3112E+03	-3.1432E+03	4.8917E-07
69	1.0900E+02	3.3112E+03	-3.2022E+03	4.8917E-07
70	9.8000E+01	3.3112E+03	-3.2132E+03	4.8917E-07

SUM OF SQUARED RESIDUALS= 1.1122E+09

VARIANCE= 1.6356E+07

STANDARD DEVIATION= 4.0442E+03

ADDITIONAL PARAMETERS CALCULATED BY THE LEAST SQUARES SUBROUTINE.

THE RESIDUAL SUM OF SQUARES = 1.112179E+09

THE NUMBER OF SIGNIFICANT DIGITS IN THE CALCULATED PARAMETERS = 6.215111E+00

THE NUMBER OF FUNCTION EVALUATIONS REQUIRED = 1.440000E+02

THE NUMBER OF ITERATIONS REQUIRED = 5.600000E+01

AN INTEGER WHICH INDICATES THE CONVERGENCE CRITERION SATISFIED - INFER = 1

INFER=0 INDICATES THAT CONVERGENCE FAILED -- SEE THE (IER) PARAMETER

INFER=1 INDICATES THAT THE FOLLOWING CONVERGENCE CONDITION IS SATISFIED  
FOR TWO SUCCESSIVE ITERATIONS THE PARAMETER  
ESTIMATES AGREE, COMPONENT BY COMPONENT  
TO NSIG (SIGNIFICANT) DIGITS

INFER=2 INDICATES THAT THE FOLLOWING CONVERGENCE CONDITION IS SATISFIED  
FOR TWO SUCCESSIVE ITERATIONS THE RESIDUAL  
SUM OF THE SQUARE ESTIMATES HAVE RELATIVE  
DIFFERENCE LESS THAN OR EQUAL TO (EPS)

INFER=4 INDICATES THAT THE FOLLOWING CONVERGENCE CONDITION IS SATISFIED  
THE (EUCLIDEAN) NORM OF THE APPROXIMATE  
GRADIENT IS LESS THAN OR EQUAL TO (DELTA)

INFER=X IF MORE THAN ONE OF THE ABOVE CONVERGENCE CRITERIA IS SATISFIED  
(INFER) REPRESENTS THE CORRESPONDING SUM OF  
THE INTEGERS

THE ERROR PARAMETER: IER = 0



IER=0    INDICATES SUCCESSFUL EXECUTION OF THE PROGRAM

IER=38    INDICATES THAT THE JACOBIAN IS ZERO.  
          THE SOLUTION IS A STATIONARY POINT (WARNING)

IER=129    INDICATES THAT A SINGULARITY WAS  
          DETECTED IN THE JACOBIAN

IER=130    INDICATES THAT AT LEAST ONE OF THE  
          SUBROUTINE CALL PARAMETERS WAS SPECIFIED  
          INCORRECTLY -- VERIFY: M,N,IOPT,PARM(1),PARM(2)

IER=131    INDICATES THAT THE MARQUARDT PARAMETER  
          EXCEEDED THE DEFAULT VALUE OF (120.0)

IER=132    INDICATES THAT AFTER A SUCCESSFUL  
          RECOVERY FROM A SINGULAR JACOBIAN, THE SOLUTION  
          HAS CYCLED BACK TO THE FIRST SINGULARITY

IER=133    INDICATES THAT THE (MAXFN) PARAMETER  
          WAS EXCEEDED

# VARIABLES USED IN THE CALCULATIONS

THE ESTIMATED METAL CLUSTER RESISTANCE ( $R_c$ ) =  $1.000000E+02$

THE ESTIMATED GAP RESISTANCE ( $R_g$ ) =  $1.000000E+05$

THE ESTIMATED GAP  
CAPACITANCE ( $C_g$ ) =  $6.000000E-07$

THE LEAST SQUARE VALUE OF THE METAL CLUSTER  
RESISTANCE,  $R_c$  =  $3.771069E+03$

THE LEAST SQUARE VALUE OF THE GAP  
RESISTANCE,  $R_g$  =  $9.530865E+04$

THE LEAST SQUARE VALUE OF THE GAP  
CAPACITANCE,  $C_g$  =  $4.246093E-07$

THE RESIDUALS ARE CALCULATED BY THE FOLLOWING  
EQUATION: [MEASURED VALUE-CALCULATED VALUE]

SAMPLE	R(f)	R(cal)	R(resid)	Cg(est)
1	9.4500E+04	9.9080E+04	-4.5797E+03	4.2461E-07
2	9.0100E+04	9.3556E+04	-3.4561E+03	4.2461E-07
3	8.8500E+04	9.1323E+04	-2.8234E+03	4.2461E-07
4	8.7000E+04	8.8824E+04	-1.8240E+03	4.2461E-07
5	8.5500E+04	8.6112E+04	-6.1161E+02	4.2461E-07
6	8.4700E+04	8.3239E+04	1.4605E+03	4.2461E-07
7	8.2600E+04	8.0258E+04	2.3424E+03	4.2461E-07
8	7.9400E+04	7.4143E+04	5.2572E+03	4.2461E-07
9	7.5200E+04	6.8068E+04	7.1322E+03	4.2461E-07
10	6.9900E+04	6.2244E+04	7.6565E+03	4.2461E-07
11	6.3700E+04	5.6800E+04	6.9005E+03	4.2461E-07
12	5.7500E+04	5.1802E+04	5.6984E+03	4.2461E-07
13	4.9800E+04	4.7270E+04	2.5298E+03	4.2461E-07
14	4.2600E+04	4.3196E+04	-5.9647E+02	4.2461E-07
15	3.6000E+04	3.9554E+04	-3.5540E+03	4.2461E-07
16	3.0500E+04	3.6307E+04	-5.8074E+03	4.2461E-07
17	2.6700E+04	3.3418E+04	-6.7183E+03	4.2461E-07
18	2.4500E+04	3.0848E+04	-6.3482E+03	4.2461E-07
19	2.2900E+04	2.8561E+04	-5.6605E+03	4.2461E-07
20	2.1500E+04	2.6522E+04	-5.0219E+03	4.2461E-07
21	2.0200E+04	2.4702E+04	-4.5022E+03	4.2461E-07

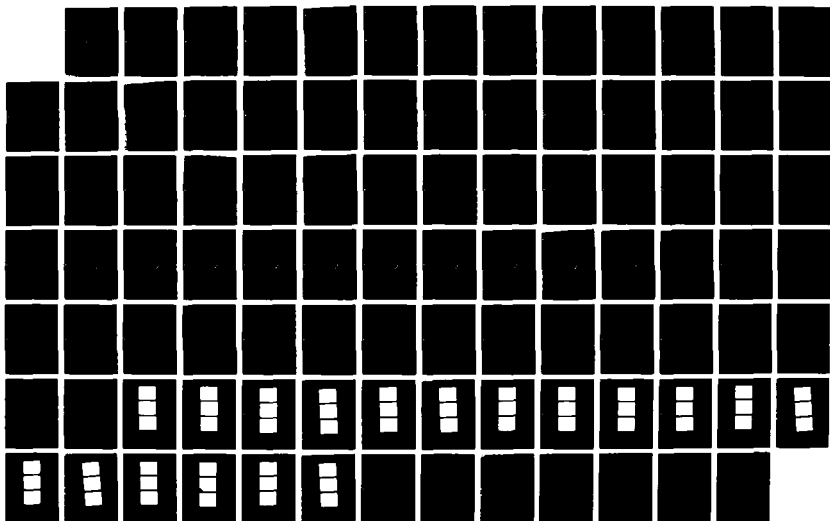
AD-A103 204

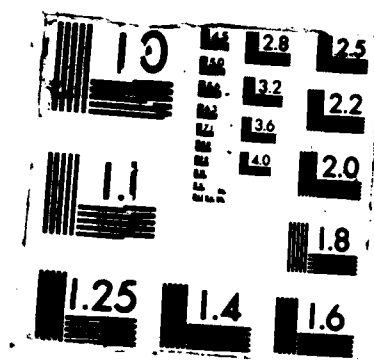
AN ELECTRICAL CIRCUIT MODEL OF THE INTERFACE BETWEEN AN  
ELECTRODE AND THE... (U) AIR FORCE INST OF TECH  
WRIGHT-PATTERSON AFB OH SCHOOL OF ENGI... J M SEDLAK  
31 JUL 87 AFIT/GE/EE/86D-48 F/G 9/1

4/4

UNCLASSIFIED

NL





22	1.9100E+04	2.3075E+04	-3.9747E+03	4.2461E-07
23	1.8200E+04	2.1616E+04	-3.4161E+03	4.2461E-07
24	1.7500E+04	2.0306E+04	-2.8057E+03	4.2461E-07
25	1.6800E+04	1.9126E+04	-2.3258E+03	4.2461E-07
26	1.6300E+04	1.8061E+04	-1.7607E+03	4.2461E-07
27	1.5800E+04	1.7097E+04	-1.2970E+03	4.2461E-07
28	1.5400E+04	1.6223E+04	-8.2303E+02	4.2461E-07
29	1.5100E+04	1.5428E+04	-3.2847E+02	4.2461E-07
30	1.4700E+04	1.4704E+04	-4.4866E+00	4.2461E-07
31	1.4400E+04	1.4043E+04	3.5667E+02	4.2461E-07
32	1.4100E+04	1.3438E+04	6.6177E+02	4.2461E-07
33	1.3800E+04	1.2883E+04	9.1674E+02	4.2461E-07
34	1.3600E+04	1.2373E+04	1.2268E+03	4.2461E-07
35	1.3400E+04	1.1904E+04	1.4964E+03	4.2461E-07
36	1.3200E+04	1.1470E+04	1.7297E+03	4.2461E-07
37	1.2900E+04	1.1070E+04	1.8301E+03	4.2461E-07
38	1.2600E+04	1.0699E+04	1.9009E+03	4.2461E-07
39	1.2400E+04	1.0355E+04	2.0448E+03	4.2461E-07
40	1.2200E+04	1.0036E+04	2.1643E+03	4.2461E-07
41	1.2000E+04	9.7384E+03	2.2616E+03	4.2461E-07
42	1.1900E+04	9.4614E+03	2.4386E+03	4.2461E-07
43	1.1700E+04	9.2028E+03	2.4972E+03	4.2461E-07
44	1.1600E+04	8.9611E+03	2.6389E+03	4.2461E-07
45	1.1400E+04	8.7350E+03	2.6650E+03	4.2461E-07
46	1.1300E+04	8.5230E+03	2.7770E+03	4.2461E-07
47	1.1100E+04	8.3241E+03	2.7759E+03	4.2461E-07
48	1.1000E+04	3.7715E+03	7.2285E+03	4.2461E-07
49	1.0900E+04	3.7715E+03	7.1285E+03	4.2461E-07
50	1.0800E+04	3.7715E+03	7.0285E+03	4.2461E-07
51	1.0700E+04	3.7715E+03	6.9285E+03	4.2461E-07
52	1.0500E+04	7.4928E+03	3.0072E+03	4.2461E-07
53	6.8500E+03	5.4619E+03	1.3881E+03	4.2461E-07
54	5.2600E+03	4.7296E+03	5.3042E+02	4.2461E-07
55	4.2200E+03	4.3867E+03	-1.6675E+02	4.2461E-07
56	3.6200E+03	4.1995E+03	-5.7947E+02	4.2461E-07
57	3.2600E+03	4.0862E+03	-8.2619E+02	4.2461E-07
58	2.9900E+03	4.0125E+03	-1.0225E+03	4.2461E-07
59	2.7900E+03	3.9619E+03	-1.1719E+03	4.2461E-07
60	2.6100E+03	3.9257E+03	-1.3157E+03	4.2461E-07
61	2.0100E+03	3.8399E+03	-1.8299E+03	4.2461E-07
62	1.7100E+03	3.8098E+03	-2.0998E+03	4.2461E-07
63	8.0600E+02	3.7773E+03	-2.9713E+03	4.2461E-07
64	5.4900E+02	3.7726E+03	-3.2236E+03	4.2461E-07
65	4.5000E+02	3.7718E+03	-3.3218E+03	4.2461E-07
66	4.0300E+02	3.7715E+03	-3.3685E+03	4.2461E-07
67	2.1900E+02	3.7711E+03	-3.5521E+03	4.2461E-07
68	1.7500E+02	3.7711E+03	-3.5961E+03	4.2461E-07
69	1.1700E+02	3.7711E+03	-3.6541E+03	4.2461E-07
70	1.1100E+02	3.7711E+03	-3.6601E+03	4.2461E-07

SUM OF SQUARED RESIDUALS= 9.2115E+08

VARIANCE= 1.3546E+07

STANDARD DEVIATION= 3.6805E+03

ADDITIONAL PARAMETERS CALCULATED BY THE LEAST SQUARES SUBROUTINE.

THE RESIDUAL SUM OF SQUARES = 9.211453E+08

THE NUMBER OF SIGNIFICANT DIGITS IN THE CALCULATED PARAMETERS = 6.521906E+00

THE NUMBER OF FUNCTION EVALUATIONS REQUIRED = 1.410000E+02

THE NUMBER OF ITERATIONS REQUIRED = 5.300000E+01

AN INTEGER WHICH INDICATES THE CONVERGENCE CRITERION SATISFIED - INFER = 1

INFER=0 INDICATES THAT CONVERGENCE FAILED -- SEE THE (IER) PARAMETER

INFER=1 INDICATES THAT THE FOLLOWING CONVERGENCE CONDITION IS SATISFIED  
FOR TWO SUCCESSIVE ITERATIONS THE PARAMETER  
ESTIMATES AGREE, COMPONENT BY COMPONENT  
TO NSIG (SIGNIFICANT) DIGITS

INFER=2 INDICATES THAT THE FOLLOWING CONVERGENCE CONDITION IS SATISFIED  
FOR TWO SUCCESSIVE ITERATIONS THE RESIDUAL  
SUM OF THE SQUARE ESTIMATES HAVE RELATIVE  
DIFFERENCE LESS THAN OR EQUAL TO (EPS)

INFER=4 INDICATES THAT THE FOLLOWING CONVERGENCE CONDITION IS SATISFIED  
THE (EUCLIDEAN) NORM OF THE APPROXIMATE  
GRADIENT IS LESS THAN OR EQUAL TO (DELTA)

INFER=X IF MORE THAN ONE OF THE ABOVE CONVERGENCE CRITERIA IS SATISFIED  
(INFER) REPRESENTS THE CORRESPONDING SUM OF  
THE INTEGERS

THE ERROR PARAMETER: IER = 0

IER=0 INDICATES SUCCESSFUL EXECUTION OF THE PROGRAM

IER=38 INDICATES THAT THE JACOBIAN IS ZERO.  
THE SOLUTION IS A STATIONARY POINT (WARNING)

IER=129 INDICATES THAT A SINGULARITY WAS  
DETECTED IN THE JACOBIAN

IER=130 INDICATES THAT AT LEAST ONE OF THE  
SUBROUTINE CALL PARAMETERS WAS SPECIFIED  
INCORRECTLY -- VERIFY: M,N,IOPT,PARM(1),PARM(2)

IER=131 INDICATES THAT THE MARQUARDT PARAMETER  
EXCEEDED THE DEFAULT VALUE OF (120.0)

IER=132 INDICATES THAT AFTER A SUCCESSFUL  
RECOVERY FROM A SINGULAR JACOBIAN, THE SOLUTION  
HAS CYCLED BACK TO THE FIRST SINGULARITY

IER=133 INDICATES THAT THE (MAXFN) PARAMETER  
WAS EXCEEDED

# VARIABLES USED IN THE CALCULATIONS

THE ESTIMATED METAL CLUSTER RESISTANCE ( $R_c$ ) = 1.000000E+02

THE ESTIMATED GAP RESISTANCE ( $R_g$ ) = 1.000000E+05

THE ESTIMATED GAP  
CAPACITANCE ( $C_g$ ) = 6.000000E-07

THE LEAST SQUARE VALUE OF THE METAL CLUSTER  
RESISTANCE,  $R_c$  = 3.723755E+03

THE LEAST SQUARE VALUE OF THE GAP  
RESISTANCE,  $R_g$  = 9.104829E+04

THE LEAST SQUARE VALUE OF THE GAP  
CAPACITANCE,  $C_g$  = 4.436065E-07

THE RESIDUALS ARE CALCULATED BY THE FOLLOWING  
EQUATION: [MEASURED VALUE-CALCULATED VALUE]

SAMPLE	R(f)	R(cal)	R(resid)	Cg(est)
1	9.1400E+04	9.4772E+04	-3.3721E+03	4.4361E-07
2	8.5500E+04	8.9355E+04	-3.8549E+03	4.4361E-07
3	8.4000E+04	8.7170E+04	-3.1703E+03	4.4361E-07
4	8.2600E+04	8.4728E+04	-2.1281E+03	4.4361E-07
5	8.1300E+04	8.2082E+04	-7.8197E+02	4.4361E-07
6	8.0000E+04	7.9285E+04	7.1546E+02	4.4361E-07
7	7.8700E+04	7.6385E+04	2.3147E+03	4.4361E-07
8	7.5800E+04	7.0456E+04	5.3442E+03	4.4361E-07
9	7.2500E+04	6.4586E+04	7.9139E+03	4.4361E-07
10	6.8000E+04	5.8978E+04	9.0217E+03	4.4361E-07
11	6.1300E+04	5.3754E+04	7.5461E+03	4.4361E-07
12	5.3800E+04	4.8972E+04	4.8278E+03	4.4361E-07
13	4.6500E+04	4.4649E+04	1.8510E+03	4.4361E-07
14	3.9500E+04	4.0772E+04	-1.2722E+03	4.4361E-07
15	3.3000E+04	3.7314E+04	-4.3136E+03	4.4361E-07
16	2.7900E+04	3.4237E+04	-6.3371E+03	4.4361E-07
17	2.4600E+04	3.1504E+04	-6.9043E+03	4.4361E-07
18	2.2500E+04	2.9077E+04	-6.5770E+03	4.4361E-07
19	2.1000E+04	2.6920E+04	-5.9195E+03	4.4361E-07
20	1.9800E+04	2.4999E+04	-5.1993E+03	4.4361E-07
21	1.8600E+04	2.3287E+04	-4.4873E+03	4.4361E-07



22	1.8000E+04	2.1758E+04	-3.7576E+03	4.4361E-07
23	1.7200E+04	2.0388E+04	-3.1879E+03	4.4361E-07
24	1.6500E+04	1.9158E+04	-2.6583E+03	4.4361E-07
25	1.5900E+04	1.8052E+04	-2.1520E+03	4.4361E-07
26	1.5400E+04	1.7054E+04	-1.6540E+03	4.4361E-07
27	1.4900E+04	1.6152E+04	-1.2516E+03	4.4361E-07
28	1.4600E+04	1.5334E+04	-7.3355E+02	4.4361E-07
29	1.4200E+04	1.4590E+04	-3.9022E+02	4.4361E-07
30	1.3900E+04	1.3913E+04	-1.3221E+01	4.4361E-07
31	1.3700E+04	1.3295E+04	4.0479E+02	4.4361E-07
32	1.3500E+04	1.2730E+04	7.7018E+02	4.4361E-07
33	1.3300E+04	1.2211E+04	1.0886E+03	4.4361E-07
34	1.3100E+04	1.1735E+04	1.3648E+03	4.4361E-07
35	1.3000E+04	1.1297E+04	1.7032E+03	4.4361E-07
36	1.2800E+04	1.0892E+04	1.9076E+03	4.4361E-07
37	1.2700E+04	1.0519E+04	2.1812E+03	4.4361E-07
38	1.2600E+04	1.0173E+04	2.4271E+03	4.4361E-07
39	1.2400E+04	9.8521E+03	2.5479E+03	4.4361E-07
40	1.2300E+04	9.5542E+03	2.7458E+03	4.4361E-07
41	1.2100E+04	9.2771E+03	2.8229E+03	4.4361E-07
42	1.1900E+04	9.0188E+03	2.8812E+03	4.4361E-07
43	1.1700E+04	8.7778E+03	2.9222E+03	4.4361E-07
44	1.1500E+04	8.5526E+03	2.9474E+03	4.4361E-07
45	1.1300E+04	8.3419E+03	2.9581E+03	4.4361E-07
46	1.1100E+04	8.1445E+03	2.9555E+03	4.4361E-07
47	1.0800E+04	7.9592E+03	2.8408E+03	4.4361E-07
48	1.0600E+04	3.7242E+03	6.8758E+03	4.4361E-07
49	1.0400E+04	3.7242E+03	6.6758E+03	4.4361E-07
50	1.0100E+04	3.7241E+03	6.3759E+03	4.4361E-07
51	9.9000E+03	3.7241E+03	6.1759E+03	4.4361E-07
52	9.6200E+03	7.1851E+03	2.4349E+03	4.4361E-07
53	6.5800E+03	5.2953E+03	1.2847E+03	4.4361E-07
54	4.9500E+03	4.6145E+03	3.3552E+02	4.4361E-07
55	4.0500E+03	4.2958E+03	-2.4583E+02	4.4361E-07
56	3.5000E+03	4.1218E+03	-6.2180E+02	4.4361E-07
57	3.0600E+03	4.0165E+03	-9.5653E+02	4.4361E-07
58	2.7500E+03	3.9481E+03	-1.1981E+03	4.4361E-07
59	2.5100E+03	3.9011E+03	-1.3911E+03	4.4361E-07
60	2.3400E+03	3.8675E+03	-1.5275E+03	4.4361E-07
61	1.8500E+03	3.7877E+03	-1.9377E+03	4.4361E-07
62	1.5700E+03	3.7597E+03	-2.1897E+03	4.4361E-07
63	8.0600E+02	3.7295E+03	-2.9235E+03	4.4361E-07
64	5.3800E+02	3.7252E+03	-3.1872E+03	4.4361E-07
65	4.5900E+02	3.7244E+03	-3.2654E+03	4.4361E-07
66	3.9700E+02	3.7241E+03	-3.3271E+03	4.4361E-07
67	2.2600E+02	3.7238E+03	-3.4978E+03	4.4361E-07
68	1.7600E+02	3.7238E+03	-3.5478E+03	4.4361E-07
69	1.1500E+02	3.7238E+03	-3.6088E+03	4.4361E-07
70	1.0300E+02	3.7238E+03	-3.6208E+03	4.4361E-07

SUM OF SQUARED RESIDUALS= 9.5745E+08

VARIANCE= 1.4080E+07

STANDARD DEVIATION= 3.7524E+03

ADDITIONAL PARAMETERS CALCULATED BY THE LEAST SQUARES SUBROUTINE.

THE RESIDUAL SUM OF SQUARES = 9.574542E+08

THE NUMBER OF SIGNIFICANT DIGITS IN THE CALCULATED PARAMETERS = 6.418320E+00

THE NUMBER OF FUNCTION EVALUATIONS REQUIRED = 1.280000E+02

THE NUMBER OF ITERATIONS REQUIRED = 4.800000E+01

AN INTEGER WHICH INDICATES THE CONVERGENCE CRITERION SATISFIED - INFER = 1

INFER=0 INDICATES THAT CONVERGENCE FAILED -- SEE THE (IER) PARAMETER

INFER=1 INDICATES THAT THE FOLLOWING CONVERGENCE CONDITION IS SATISFIED  
FOR TWO SUCCESSIVE ITERATIONS THE PARAMETER  
ESTIMATES AGREE, COMPONENT BY COMPONENT  
TO NSIG (SIGNIFICANT) DIGITS

INFER=2 INDICATES THAT THE FOLLOWING CONVERGENCE CONDITION IS SATISFIED  
FOR TWO SUCCESSIVE ITERATIONS THE RESIDUAL  
SUM OF THE SQUARE ESTIMATES HAVE RELATIVE  
DIFFERENCE LESS THAN OR EQUAL TO (EPS)

INFER=4 INDICATES THAT THE FOLLOWING CONVERGENCE CONDITION IS SATISFIED  
THE (EUCLIDEAN) NORM OF THE APPROXIMATE  
GRADIENT IS LESS THAN OR EQUAL TO (DELTA)

INFER=X IF MORE THAN ONE OF THE ABOVE CONVERGENCE CRITERIA IS SATISFIED  
(INFER) REPRESENTS THE CORRESPONDING SUM OF  
THE INTEGERS

THE ERROR PARAMETER: IER = 0

IER=0    INDICATES SUCCESSFUL EXECUTION OF THE PROGRAM

IER=38    INDICATES THAT THE JACOBIAN IS ZERO.  
          THE SOLUTION IS A STATIONARY POINT (WARNING)

IER=129    INDICATES THAT A SINGULARITY WAS  
          DETECTED IN THE JACOBIAN

IER=130    INDICATES THAT AT LEAST ONE OF THE  
          SUBROUTINE CALL PARAMETERS WAS SPECIFIED  
          INCORRECTLY -- VERIFY:  M,N,IOPT,PARM(1),PARM(2)

IER=131    INDICATES THAT THE MARQUARDT PARAMETER  
          EXCEEDED THE DEFAULT VALUE OF (120.0)

IER=132    INDICATES THAT AFTER A SUCCESSFUL  
          RECOVERY FROM A SINGULAR JACOBIAN, THE SOLUTION  
          HAS CYCLED BACK TO THE FIRST SINGULARITY

IER=133    INDICATES THAT THE (MAXFN) PARAMETER  
          WAS EXCEEDED

# VARIABLES USED IN THE CALCULATIONS

THE ESTIMATED METAL CLUSTER RESISTANCE (Rc) = 1.000000E+02

THE ESTIMATED GAP RESISTANCE (Rg) = 1.000000E+05

THE ESTIMATED GAP  
CAPACITANCE (Cg) = 6.000000E-07

THE LEAST SQUARE VALUE OF THE METAL CLUSTER  
RESISTANCE, Rc = 2.936657E+03

THE LEAST SQUARE VALUE OF THE GAP  
RESISTANCE, Rg = 1.045968E+05

THE LEAST SQUARE VALUE OF THE GAP  
CAPACITANCE, Cg = 4.690154E-07

THE RESIDUALS ARE CALCULATED BY THE FOLLOWING  
EQUATION: [MEASURED VALUE-CALCULATED VALUE]

SAMPLE	R(f)	R(cal)	R(resid)	Cg(est)
1	1.0300E+05	1.0753E+05	-4.5334E+03	4.6902E-07
2	9.6200E+04	1.0116E+05	-4.9619E+03	4.6902E-07
3	9.5200E+04	9.8598E+04	-3.3979E+03	4.6902E-07
4	9.3500E+04	9.5735E+04	-2.2352E+03	4.6902E-07
5	9.1700E+04	9.2638E+04	-9.3781E+02	4.6902E-07
6	9.0100E+04	8.9368E+04	7.3169E+02	4.6902E-07
7	8.8500E+04	8.5985E+04	2.5148E+03	4.6902E-07
8	8.5500E+04	7.9083E+04	6.4171E+03	4.6902E-07
9	8.1300E+04	7.2272E+04	9.0275E+03	4.6902E-07
10	7.5800E+04	6.5787E+04	1.0013E+04	4.6902E-07
11	6.8500E+04	5.9762E+04	8.7379E+03	4.6902E-07
12	6.1000E+04	5.4263E+04	6.7367E+03	4.6902E-07
13	5.2900E+04	4.9304E+04	3.5957E+03	4.6902E-07
14	4.5500E+04	4.4867E+04	6.3278E+02	4.6902E-07
15	3.8300E+04	4.0917E+04	-2.6168E+03	4.6902E-07
16	3.1700E+04	3.7409E+04	-5.7091E+03	4.6902E-07
17	2.6700E+04	3.4298E+04	-7.5982E+03	4.6902E-07
18	2.3500E+04	3.1539E+04	-8.0390E+03	4.6902E-07
19	2.1600E+04	2.9090E+04	-7.4896E+03	4.6902E-07
20	2.0100E+04	2.6912E+04	-6.8120E+03	4.6902E-07
21	1.8900E+04	2.4972E+04	-6.0724E+03	4.6902E-07

22	1.7900E+04	2.3241E+04	-5.3410E+03	4.6902E-07
23	1.7100E+04	2.1692E+04	-4.5918E+03	4.6902E-07
24	1.6500E+04	2.0302E+04	-3.8021E+03	4.6902E-07
25	1.6000E+04	1.9053E+04	-3.0525E+03	4.6902E-07
26	1.5600E+04	1.7926E+04	-2.3260E+03	4.6902E-07
27	1.5200E+04	1.6908E+04	-1.7078E+03	4.6902E-07
28	1.4800E+04	1.5985E+04	-1.1852E+03	4.6902E-07
29	1.4400E+04	1.5147E+04	-7.4731E+02	4.6902E-07
30	1.4100E+04	1.4384E+04	-2.8445E+02	4.6902E-07
31	1.3700E+04	1.3688E+04	1.1684E+01	4.6902E-07
32	1.3400E+04	1.3052E+04	3.4835E+02	4.6902E-07
33	1.3100E+04	1.2468E+04	6.3190E+02	4.6902E-07
34	1.2800E+04	1.1932E+04	8.6788E+02	4.6902E-07
35	1.2400E+04	1.1439E+04	9.6115E+02	4.6902E-07
36	1.2200E+04	1.0984E+04	1.2160E+03	4.6902E-07
37	1.1900E+04	1.0564E+04	1.3362E+03	4.6902E-07
38	1.1700E+04	1.0175E+04	1.5252E+03	4.6902E-07
39	1.1500E+04	9.8142E+03	1.6858E+03	4.6902E-07
40	1.1300E+04	9.4794E+03	1.8206E+03	4.6902E-07
41	1.1100E+04	9.1679E+03	1.9321E+03	4.6902E-07
42	1.0900E+04	8.8777E+03	2.0223E+03	4.6902E-07
43	1.0700E+04	8.6069E+03	2.0931E+03	4.6902E-07
44	1.0600E+04	8.3540E+03	2.2460E+03	4.6902E-07
45	1.0500E+04	8.1173E+03	2.3827E+03	4.6902E-07
46	1.0400E+04	7.8955E+03	2.5045E+03	4.6902E-07
47	1.0200E+04	7.6874E+03	2.5126E+03	4.6902E-07
48	1.0100E+04	2.9371E+03	7.1629E+03	4.6902E-07
49	1.0000E+04	2.9371E+03	7.0629E+03	4.6902E-07
50	9.9000E+03	2.9371E+03	6.9629E+03	4.6902E-07
51	9.8000E+03	2.9371E+03	6.8629E+03	4.6902E-07
52	9.7000E+03	6.8183E+03	2.8817E+03	4.6902E-07
53	6.7600E+03	4.6981E+03	2.0619E+03	4.6902E-07
54	4.8500E+03	3.9348E+03	9.1515E+02	4.6902E-07
55	3.9700E+03	3.5777E+03	3.9230E+02	4.6902E-07
56	3.4100E+03	3.3827E+03	2.7338E+01	4.6902E-07
57	3.0200E+03	3.2647E+03	-2.4471E+02	4.6902E-07
58	2.7400E+03	3.1880E+03	-4.4800E+02	4.6902E-07
59	2.5300E+03	3.1354E+03	-6.0535E+02	4.6902E-07
60	2.3400E+03	3.0977E+03	-7.5766E+02	4.6902E-07
61	1.8500E+03	3.0083E+03	-1.1583E+03	4.6902E-07
62	1.5400E+03	2.9770E+03	-1.4370E+03	4.6902E-07
63	7.5200E+02	2.9431E+03	-2.1911E+03	4.6902E-07
64	5.5200E+02	2.9383E+03	-2.3863E+03	4.6902E-07
65	4.5500E+02	2.9374E+03	-2.4824E+03	4.6902E-07
66	4.0800E+02	2.9371E+03	-2.5291E+03	4.6902E-07
67	2.1400E+02	2.9367E+03	-2.7227E+03	4.6902E-07
68	1.6900E+02	2.9367E+03	-2.7677E+03	4.6902E-07
69	1.1100E+02	2.9367E+03	-2.8257E+03	4.6902E-07
70	9.8000E+01	2.9367E+03	-2.8387E+03	4.6902E-07

SUM OF SQUARED RESIDUALS= 1.1309E+09

VARIANCE= 1.6632E+07

STANDARD DEVIATION= 4.0782E+03

H-75

ADDITIONAL PARAMETERS CALCULATED BY THE LEAST SQUARES SUBROUTINE.

THE RESIDUAL SUM OF SQUARES = 1.130943E+09

THE NUMBER OF SIGNIFICANT DIGITS IN THE CALCULATED PARAMETERS = 6.314055E+00

THE NUMBER OF FUNCTION EVALUATIONS REQUIRED = 1.140000E+02

THE NUMBER OF ITERATIONS REQUIRED = 4.000000E+01

AN INTEGER WHICH INDICATES THE CONVERGENCE CRITERION SATISFIED - INFER = 1

INFER=0 INDICATES THAT CONVERGENCE FAILED -- SEE THE (IER) PARAMETER

INFER=1 INDICATES THAT THE FOLLOWING CONVERGENCE CONDITION IS SATISFIED  
FOR TWO SUCCESSIVE ITERATIONS THE PARAMETER  
ESTIMATES AGREE, COMPONENT BY COMPONENT  
TO NSIG (SIGNIFICANT) DIGITS

INFER=2 INDICATES THAT THE FOLLOWING CONVERGENCE CONDITION IS SATISFIED  
FOR TWO SUCCESSIVE ITERATIONS THE RESIDUAL  
SUM OF THE SQUARE ESTIMATES HAVE RELATIVE  
DIFFERENCE LESS THAN OR EQUAL TO (EPS)

INFER=4 INDICATES THAT THE FOLLOWING CONVERGENCE CONDITION IS SATISFIED  
THE (EUCLIDEAN) NORM OF THE APPROXIMATE  
GRADIENT IS LESS THAN OR EQUAL TO (DELTA)

INFER=X IF MORE THAN ONE OF THE ABOVE CONVERGENCE CRITERIA IS SATISFIED  
(INFER) REPRESENTS THE CORRESPONDING SUM OF  
THE INTEGERS

THE ERROR PARAMETER: IER = 0

IER=0    INDICATES SUCCESSFUL EXECUTION OF THE PROGRAM

IER=38    INDICATES THAT THE JACOBIAN IS ZERO.  
          THE SOLUTION IS A STATIONARY POINT (WARNING)

IER=129    INDICATES THAT A SINGULARITY WAS  
          DETECTED IN THE JACOBIAN

IER=130    INDICATES THAT AT LEAST ONE OF THE  
          SUBROUTINE CALL PARAMETERS WAS SPECIFIED  
          INCORRECTLY -- VERIFY: M,N,IOPT,PARM(1),PARM(2)

IER=131    INDICATES THAT THE MARQUARDT PARAMETER  
          EXCEEDED THE DEFAULT VALUE OF (120.0)

IER=132    INDICATES THAT AFTER A SUCCESSFUL  
          RECOVERY FROM A SINGULAR JACOBIAN, THE SOLUTION  
          HAS CYCLED BACK TO THE FIRST SINGULARITY

IER=133    INDICATES THAT THE (MAXFN) PARAMETER  
          WAS EXCEEDED

# VARIABLES USED IN THE CALCULATIONS

THE ESTIMATED METAL CLUSTER RESISTANCE (Rc) = 1.000000E+02

THE ESTIMATED GAP RESISTANCE (Rg) = 1.000000E+05

THE ESTIMATED GAP  
CAPACITANCE (Cg) = 6.000000E-07

THE LEAST SQUARE VALUE OF THE METAL CLUSTER  
RESISTANCE, Rc = 4.270775E+03

THE LEAST SQUARE VALUE OF THE GAP  
RESISTANCE, Rg = 8.386926E+04

THE LEAST SQUARE VALUE OF THE GAP  
CAPACITANCE, Cg = 4.212615E-07

THE RESIDUALS ARE CALCULATED BY THE FOLLOWING  
EQUATION: [MEASURED VALUE-CALCULATED VALUE]

SAMPLE	R(f)	R(cal)	R(resid)	Cg(est)
1	8.6400E+04	8.8140E+04	-1.7400E+03	4.2126E-07
2	8.0000E+04	8.3415E+04	-3.4154E+03	4.2126E-07
3	7.8700E+04	8.1501E+04	-2.8012E+03	4.2126E-07
4	7.8100E+04	7.9355E+04	-1.2549E+03	4.2126E-07
5	7.6900E+04	7.7022E+04	-1.2212E+02	4.2126E-07
6	7.5800E+04	7.4548E+04	1.2525E+03	4.2126E-07
7	7.4100E+04	7.1974E+04	2.1262E+03	4.2126E-07
8	7.0900E+04	6.6681E+04	4.2194E+03	4.2126E-07
9	6.7100E+04	6.1402E+04	5.6981E+03	4.2126E-07
10	6.2500E+04	5.6322E+04	6.1780E+03	4.2126E-07
11	5.6500E+04	5.1557E+04	4.9431E+03	4.2126E-07
12	4.9500E+04	4.7168E+04	2.3322E+03	4.2126E-07
13	4.2600E+04	4.3176E+04	-5.7646E+02	4.2126E-07
14	3.6000E+04	3.9578E+04	-3.5784E+03	4.2126E-07
15	3.1300E+04	3.6353E+04	-5.0533E+03	4.2126E-07
16	2.7900E+04	3.3473E+04	-5.5726E+03	4.2126E-07
17	2.5900E+04	3.0904E+04	-5.0040E+03	4.2126E-07
18	2.4400E+04	2.8615E+04	-4.2151E+03	4.2126E-07
19	2.3100E+04	2.6575E+04	-3.4745E+03	4.2126E-07
20	2.1800E+04	2.4754E+04	-2.9536E+03	4.2126E-07
21	2.0700E+04	2.3126E+04	-2.4262E+03	4.2126E-07



22	1.9600E+04	2.1669E+04	-2.0692E+03	4.2126E-07
23	1.8800E+04	2.0362E+04	-1.5620E+03	4.2126E-07
24	1.8100E+04	1.9187E+04	-1.0866E+03	4.2126E-07
25	1.7500E+04	1.8127E+04	-6.2743E+02	4.2126E-07
26	1.7000E+04	1.7171E+04	-1.7067E+02	4.2126E-07
27	1.6400E+04	1.6304E+04	9.5573E+01	4.2126E-07
28	1.5900E+04	1.5518E+04	3.8169E+02	4.2126E-07
29	1.5600E+04	1.4803E+04	7.9672E+02	4.2126E-07
30	1.5200E+04	1.4151E+04	1.0486E+03	4.2126E-07
31	1.4700E+04	1.3556E+04	1.1441E+03	4.2126E-07
32	1.4400E+04	1.3011E+04	1.3894E+03	4.2126E-07
33	1.4100E+04	1.2510E+04	1.5896E+03	4.2126E-07
34	1.3800E+04	1.2050E+04	1.7495E+03	4.2126E-07
35	1.3500E+04	1.1627E+04	1.8732E+03	4.2126E-07
36	1.3200E+04	1.1236E+04	1.9641E+03	4.2126E-07
37	1.2900E+04	1.0874E+04	2.0255E+03	4.2126E-07
38	1.2700E+04	1.0540E+04	2.1603E+03	4.2126E-07
39	1.2400E+04	1.0229E+04	2.1708E+03	4.2126E-07
40	1.2200E+04	9.9407E+03	2.2593E+03	4.2126E-07
41	1.2000E+04	9.6721E+03	2.3279E+03	4.2126E-07
42	1.1800E+04	9.4218E+03	2.3782E+03	4.2126E-07
43	1.1600E+04	9.1881E+03	2.4119E+03	4.2126E-07
44	1.1400E+04	8.9697E+03	2.4303E+03	4.2126E-07
45	1.1200E+04	8.7653E+03	2.4347E+03	4.2126E-07
46	1.1100E+04	8.5737E+03	2.5263E+03	4.2126E-07
47	1.0900E+04	8.3939E+03	2.5061E+03	4.2126E-07
48	1.0800E+04	4.2712E+03	6.5288E+03	4.2126E-07
49	1.0600E+04	4.2712E+03	6.3288E+03	4.2126E-07
50	1.0400E+04	4.2712E+03	6.1288E+03	4.2126E-07
51	1.0300E+04	4.2711E+03	6.0289E+03	4.2126E-07
52	1.0100E+04	7.6420E+03	2.4580E+03	4.2126E-07
53	6.4900E+03	5.8033E+03	6.8670E+02	4.2126E-07
54	5.1000E+03	5.1398E+03	-3.9770E+01	4.2126E-07
55	4.2600E+03	4.8290E+03	-5.6901E+02	4.2126E-07
56	3.6100E+03	4.6592E+03	-1.0492E+03	4.2126E-07
57	3.1600E+03	4.5565E+03	-1.3965E+03	4.2126E-07
58	2.8300E+03	4.4897E+03	-1.6597E+03	4.2126E-07
59	2.6000E+03	4.4439E+03	-1.8439E+03	4.2126E-07
60	2.4100E+03	4.4110E+03	-2.0010E+03	4.2126E-07
61	1.8200E+03	4.3332E+03	-2.5132E+03	4.2126E-07
62	1.6300E+03	4.3059E+03	-2.6759E+03	4.2126E-07
63	8.7700E+02	4.2764E+03	-3.3994E+03	4.2126E-07
64	6.1300E+02	4.2722E+03	-3.6592E+03	4.2126E-07
65	5.1300E+02	4.2714E+03	-3.7584E+03	4.2126E-07
66	4.3500E+02	4.2711E+03	-3.8361E+03	4.2126E-07
67	2.2900E+02	4.2708E+03	-4.0418E+03	4.2126E-07
68	1.7500E+02	4.2708E+03	-4.0958E+03	4.2126E-07
69	1.1100E+02	4.2708E+03	-4.1598E+03	4.2126E-07
70	1.0000E+02	4.2708E+03	-4.1708E+03	4.2126E-07

SUM OF SQUARED RESIDUALS= 6.8584E+08

VARIANCE= 1.0086E+07

STANDARD DEVIATION= 3.1758E+03

ADDITIONAL PARAMETERS CALCULATED BY THE LEAST SQUARES SUBROUTINE.

THE RESIDUAL SUM OF SQUARES = 6.858428E+08

THE NUMBER OF SIGNIFICANT DIGITS IN THE CALCULATED PARAMETERS = 6.116623E+00

THE NUMBER OF FUNCTION EVALUATIONS REQUIRED = 1.180000E+02

THE NUMBER OF ITERATIONS REQUIRED = 4.200000E+01

AN INTEGER WHICH INDICATES THE CONVERGENCE CRITERION SATISFIED - INFER = 1

INFER=0 INDICATES THAT CONVERGENCE FAILED -- SEE THE (IER) PARAMETER

INFER=1 INDICATES THAT THE FOLLOWING CONVERGENCE CONDITION IS SATISFIED  
FOR TWO SUCCESSIVE ITERATIONS THE PARAMETER  
ESTIMATES AGREE, COMPONENT BY COMPONENT  
TO NSIG (SIGNIFICANT) DIGITS

INFER=2 INDICATES THAT THE FOLLOWING CONVERGENCE CONDITION IS SATISFIED  
FOR TWO SUCCESSIVE ITERATIONS THE RESIDUAL  
SUM OF THE SQUARE ESTIMATES HAVE RELATIVE  
DIFFERENCE LESS THAN OR EQUAL TO (EPS)

INFER=4 INDICATES THAT THE FOLLOWING CONVERGENCE CONDITION IS SATISFIED  
THE (EUCLIDEAN) NORM OF THE APPROXIMATE  
GRADIENT IS LESS THAN OR EQUAL TO (DELTA)

INFER=X IF MORE THAN ONE OF THE ABOVE CONVERGENCE CRITERIA IS SATISFIED  
(INFER) REPRESENTS THE CORRESPONDING SUM OF  
THE INTEGERS

THE ERROR PARAMETER: IER = 0

IER-0 INDICATES SUCCESSFUL EXECUTION OF THE PROGRAM

IER-38 INDICATES THAT THE JACOBIAN IS ZERO.  
THE SOLUTION IS A STATIONARY POINT (WARNING)

IER-129 INDICATES THAT A SINGULARITY WAS  
DETECTED IN THE JACOBIAN

IER-130 INDICATES THAT AT LEAST ONE OF THE  
SUBROUTINE CALL PARAMETERS WAS SPECIFIED  
INCORRECTLY -- VERIFY: M,N,IOPT,PARM(1),PARM(2)

IER-131 INDICATES THAT THE MARQUARDT PARAMETER  
EXCEEDED THE DEFAULT VALUE OF (120.0)

IER-132 INDICATES THAT AFTER A SUCCESSFUL  
RECOVERY FROM A SINGULAR JACOBIAN, THE SOLUTION  
HAS CYCLED BACK TO THE FIRST SINGULARITY

IER-133 INDICATES THAT THE (MAXFN) PARAMETER  
WAS EXCEEDED

VARIABLES USED IN THE CALCULATIONS

THE ESTIMATED METAL CLUSTER RESISTANCE (Rc) = 1.000000E+02

THE ESTIMATED GAP RESISTANCE (Rg) = 1.000000E+05

THE ESTIMATED GAP  
CAPACITANCE (Cg) = 6.000000E-07

THE LEAST SQUARE VALUE OF THE METAL CLUSTER  
RESISTANCE, Rc = 2.759014E+03

THE LEAST SQUARE VALUE OF THE GAP  
RESISTANCE, Rg = 9.577902E+04

THE LEAST SQUARE VALUE OF THE GAP  
CAPACITANCE, Cg = 5.326584E-07

THE RESIDUALS ARE CALCULATED BY THE FOLLOWING  
EQUATION: [MEASURED VALUE-CALCULATED VALUE]

SAMPLE	R(f)	R(cal)	R(resid)	Cg(est)
1	9.2200E+04	9.8538E+04	-6.3380E+03	5.3266E-07
2	8.7000E+04	9.2111E+04	-5.1113E+03	5.3266E-07
3	8.6200E+04	8.9549E+04	-3.3489E+03	5.3266E-07
4	8.4700E+04	8.6704E+04	-2.0039E+03	5.3266E-07
5	8.3300E+04	8.3644E+04	-3.4448E+02	5.3266E-07
6	8.2000E+04	8.0436E+04	1.5639E+03	5.3266E-07
7	8.0600E+04	7.7139E+04	3.4614E+03	5.3266E-07
8	7.7500E+04	7.0481E+04	7.0189E+03	5.3266E-07
9	7.3500E+04	6.4003E+04	9.4974E+03	5.3266E-07
10	6.8500E+04	5.7915E+04	1.0585E+04	5.3266E-07
11	6.2100E+04	5.2330E+04	9.7702E+03	5.3266E-07
12	5.4900E+04	4.7290E+04	7.6096E+03	5.3266E-07
13	4.7400E+04	4.2792E+04	4.6079E+03	5.3266E-07
14	3.9800E+04	3.8804E+04	9.9567E+02	5.3266E-07
15	3.2500E+04	3.5283E+04	-2.7828E+03	5.3266E-07
16	2.6200E+04	3.2179E+04	-5.9787E+03	5.3266E-07
17	2.1100E+04	2.9443E+04	-8.3432E+03	5.3266E-07
18	1.7600E+04	2.7031E+04	-9.4308E+03	5.3266E-07
19	1.5800E+04	2.4900E+04	-9.1000E+03	5.3266E-07
20	1.4600E+04	2.3014E+04	-8.4140E+03	5.3266E-07
21	1.3800E+04	2.1341E+04	-7.5408E+03	5.3266E-07

22	1.3200E+04	1.9852E+04	-6.6524E+03	5.3266E-07
23	1.2800E+04	1.8525E+04	-5.7248E+03	5.3266E-07
24	1.2500E+04	1.7337E+04	-4.8373E+03	5.3266E-07
25	1.2300E+04	1.6272E+04	-3.9721E+03	5.3266E-07
26	1.2000E+04	1.5314E+04	-3.3140E+03	5.3266E-07
27	1.1800E+04	1.4450E+04	-2.6499E+03	5.3266E-07
28	1.1600E+04	1.3668E+04	-2.0683E+03	5.3266E-07
29	1.1400E+04	1.2960E+04	-1.8897E+03	5.3266E-07
30	1.1300E+04	1.2315E+04	-1.0155E+03	5.3266E-07
31	1.1200E+04	1.1728E+04	-5.2842E+02	5.3266E-07
32	1.1100E+04	1.1192E+04	-9.2198E+01	5.3266E-07
33	1.1000E+04	1.0701E+04	2.9871E+02	5.3266E-07
34	1.0900E+04	1.0251E+04	6.4913E+02	5.3266E-07
35	1.0800E+04	9.8367E+03	9.6326E+02	5.3266E-07
36	1.0700E+04	9.4552E+03	1.2448E+03	5.3266E-07
37	1.0600E+04	9.1030E+03	1.4970E+03	5.3266E-07
38	1.0500E+04	8.7773E+03	1.7227E+03	5.3266E-07
39	1.0500E+04	8.4755E+03	2.0245E+03	5.3266E-07
40	1.0400E+04	8.1955E+03	2.2045E+03	5.3266E-07
41	1.0300E+04	7.9351E+03	2.3649E+03	5.3266E-07
42	1.0200E+04	7.6927E+03	2.5073E+03	5.3266E-07
43	1.0200E+04	7.4667E+03	2.7333E+03	5.3266E-07
44	1.0100E+04	7.2556E+03	2.8444E+03	5.3266E-07
45	1.0100E+04	7.0581E+03	3.0419E+03	5.3266E-07
46	1.0000E+04	6.8732E+03	3.1268E+03	5.3266E-07
47	9.9000E+03	6.6999E+03	3.2001E+03	5.3266E-07
48	9.8000E+03	2.7594E+03	7.0406E+03	5.3266E-07
49	9.8000E+03	2.7594E+03	7.0406E+03	5.3266E-07
50	9.7100E+03	2.7594E+03	6.9506E+03	5.3266E-07
51	9.6200E+03	2.7594E+03	6.8606E+03	5.3266E-07
52	9.5200E+03	5.9763E+03	3.5437E+03	5.3266E-07
53	6.6700E+03	4.2161E+03	2.4539E+03	5.3266E-07
54	5.1800E+03	3.5841E+03	1.5959E+03	5.3266E-07
55	4.3300E+03	3.2887E+03	1.0413E+03	5.3266E-07
56	3.7500E+03	3.1275E+03	6.2251E+02	5.3266E-07
57	3.3100E+03	3.0300E+03	2.7999E+02	5.3266E-07
58	2.9400E+03	2.9666E+03	-2.6629E+01	5.3266E-07
59	2.6700E+03	2.9231E+03	-2.5313E+02	5.3266E-07
60	2.4200E+03	2.8920E+03	-4.7199E+02	5.3266E-07
61	1.8700E+03	2.8182E+03	-9.4816E+02	5.3266E-07
62	1.6200E+03	2.7923E+03	-1.1723E+03	5.3266E-07
63	8.6200E+02	2.7643E+03	-1.9023E+03	5.3266E-07
64	5.9500E+02	2.7603E+03	-2.1653E+03	5.3266E-07
65	5.2100E+02	2.7596E+03	-2.2386E+03	5.3266E-07
66	4.6500E+02	2.7593E+03	-2.2943E+03	5.3266E-07
67	2.6700E+02	2.7590E+03	-2.4920E+03	5.3266E-07
68	2.1000E+02	2.7590E+03	-2.5490E+03	5.3266E-07
69	1.1800E+02	2.7590E+03	-2.6410E+03	5.3266E-07
70	1.0200E+02	2.7590E+03	-2.6570E+03	5.3266E-07

SUM OF SQUARED RESIDUALS= 1.4169E+09

VARIANCE= 2.0836E+07

STANDARD DEVIATION= 4.5647E+03

ADDITIONAL PARAMETERS CALCULATED BY THE LEAST SQUARES SUBROUTINE.

THE RESIDUAL SUM OF SQUARES = 1.416870E+09

THE NUMBER OF SIGNIFICANT DIGITS IN THE CALCULATED PARAMETERS = 6.177295E+00

THE NUMBER OF FUNCTION EVALUATIONS REQUIRED = 1.200000E+02

THE NUMBER OF ITERATIONS REQUIRED = 4.000000E+01

AN INTEGER WHICH INDICATES THE CONVERGENCE CRITERION SATISFIED - INFER = 1

INFER=0 INDICATES THAT CONVERGENCE FAILED -- SEE THE (IER) PARAMETER

INFER=1 INDICATES THAT THE FOLLOWING CONVERGENCE CONDITION IS SATISFIED  
FOR TWO SUCCESSIVE ITERATIONS THE PARAMETER  
ESTIMATES AGREE, COMPONENT BY COMPONENT  
TO NSIG (SIGNIFICANT) DIGITS

INFER=2 INDICATES THAT THE FOLLOWING CONVERGENCE CONDITION IS SATISFIED  
FOR TWO SUCCESSIVE ITERATIONS THE RESIDUAL  
SUM OF THE SQUARE ESTIMATES HAVE RELATIVE  
DIFFERENCE LESS THAN OR EQUAL TO (EPS)

INFER=4 INDICATES THAT THE FOLLOWING CONVERGENCE CONDITION IS SATISFIED  
THE (EUCLIDEAN) NORM OF THE APPROXIMATE  
GRADIENT IS LESS THAN OR EQUAL TO (DELTA)

INFER=X IF MORE THAN ONE OF THE ABOVE CONVERGENCE CRITERIA IS SATISFIED  
(INFER) REPRESENTS THE CORRESPONDING SUM OF  
THE INTEGERS

THE ERROR PARAMETER: IER = 0

IER=0 INDICATES SUCCESSFUL EXECUTION OF THE PROGRAM

IER=38 INDICATES THAT THE JACOBIAN IS ZERO.  
THE SOLUTION IS A STATIONARY POINT (WARNING)

IER=129 INDICATES THAT A SINGULARITY WAS  
DETECTED IN THE JACOBIAN

IER=130 INDICATES THAT AT LEAST ONE OF THE  
SUBROUTINE CALL PARAMETERS WAS SPECIFIED  
INCORRECTLY -- VERIFY: M,N,IOPT,PARM(1),PARM(2)

IER=131 INDICATES THAT THE MARQUARDT PARAMETER  
EXCEEDED THE DEFAULT VALUE OF (120.0)

IER=132 INDICATES THAT AFTER A SUCCESSFUL  
RECOVERY FROM A SINGULAR JACOBIAN, THE SOLUTION  
HAS CYCLED BACK TO THE FIRST SINGULARITY

IER=133 INDICATES THAT THE (MAXFN) PARAMETER  
WAS EXCEEDED

# VARIABLES USED IN THE CALCULATIONS

THE ESTIMATED METAL CLUSTER RESISTANCE (Rc) = 1.000000E+02

THE ESTIMATED GAP RESISTANCE (Rg) = 1.000000E+05

THE ESTIMATED GAP  
CAPACITANCE (Cg) = 6.000000E-07

THE LEAST SQUARE VALUE OF THE METAL CLUSTER  
RESISTANCE, Rc = 3.411801E+03

THE LEAST SQUARE VALUE OF THE GAP  
RESISTANCE, Rg = 9.098428E+04

THE LEAST SQUARE VALUE OF THE GAP  
CAPACITANCE, Cg = 5.140541E-07

THE RESIDUALS ARE CALCULATED BY THE FOLLOWING  
EQUATION: [MEASURED VALUE-CALCULATED VALUE]

SAMPLE	R(f)	R(cal)	R(resid)	Cg(est)
1	8.8200E+04	9.4396E+04	-6.1961E+03	5.1405E-07
2	8.4000E+04	8.7810E+04	-3.8102E+03	5.1405E-07
3	8.2600E+04	8.5205E+04	-2.6051E+03	5.1405E-07
4	8.1300E+04	8.2326E+04	-1.0265E+03	5.1405E-07
5	8.0000E+04	7.9247E+04	7.5312E+02	5.1405E-07
6	7.8100E+04	7.6035E+04	2.0651E+03	5.1405E-07
7	7.6300E+04	7.2753E+04	3.5475E+03	5.1405E-07
8	7.3000E+04	6.6182E+04	6.8175E+03	5.1405E-07
9	6.8500E+04	5.9861E+04	8.6387E+03	5.1405E-07
10	6.2500E+04	5.3985E+04	8.5150E+03	5.1405E-07
11	5.5200E+04	4.8648E+04	6.5519E+03	5.1405E-07
12	4.7600E+04	4.3876E+04	3.7243E+03	5.1405E-07
13	4.0200E+04	3.9650E+04	5.4994E+02	5.1405E-07
14	3.3600E+04	3.5931E+04	-2.3307E+03	5.1405E-07
15	2.8100E+04	3.2667E+04	-4.5670E+03	5.1405E-07
16	2.3600E+04	2.9806E+04	-6.2061E+03	5.1405E-07
17	2.0200E+04	2.7297E+04	-7.0972E+03	5.1405E-07
18	1.7700E+04	2.5094E+04	-7.3941E+03	5.1405E-07
19	1.6400E+04	2.3156E+04	-6.7555E+03	5.1405E-07
20	1.5500E+04	2.1445E+04	-5.9455E+03	5.1405E-07
21	1.4800E+04	1.9933E+04	-5.1328E+03	5.1405E-07



22	1.4200E+04	1.8591E+04	-4.3907E+03	5.1405E-07
23	1.3800E+04	1.7396E+04	-3.5964E+03	5.1405E-07
24	1.3400E+04	1.6330E+04	-2.9304E+03	5.1405E-07
25	1.3000E+04	1.5376E+04	-2.3760E+03	5.1405E-07
26	1.2700E+04	1.4519E+04	-1.8189E+03	5.1405E-07
27	1.2400E+04	1.3747E+04	-1.3470E+03	5.1405E-07
28	1.2200E+04	1.3050E+04	-8.4988E+02	5.1405E-07
29	1.1900E+04	1.2419E+04	-5.1854E+02	5.1405E-07
30	1.1700E+04	1.1845E+04	-1.4526E+02	5.1405E-07
31	1.1500E+04	1.1323E+04	1.7663E+02	5.1405E-07
32	1.1300E+04	1.0847E+04	4.5289E+02	5.1405E-07
33	1.1200E+04	1.0411E+04	7.8855E+02	5.1405E-07
34	1.1100E+04	1.0012E+04	1.0879E+03	5.1405E-07
35	1.1000E+04	9.6451E+03	1.3549E+03	5.1405E-07
36	1.0900E+04	9.3072E+03	1.5928E+03	5.1405E-07
37	1.0800E+04	8.9955E+03	1.8045E+03	5.1405E-07
38	1.0800E+04	8.7074E+03	2.0926E+03	5.1405E-07
39	1.0700E+04	8.4407E+03	2.2593E+03	5.1405E-07
40	1.0600E+04	8.1932E+03	2.4068E+03	5.1405E-07
41	1.0500E+04	7.9632E+03	2.5368E+03	5.1405E-07
42	1.0500E+04	7.7492E+03	2.7508E+03	5.1405E-07
43	1.0400E+04	7.5497E+03	2.8503E+03	5.1405E-07
44	1.0300E+04	7.3635E+03	2.9365E+03	5.1405E-07
45	1.0300E+04	7.1894E+03	3.1106E+03	5.1405E-07
46	1.0200E+04	7.0264E+03	3.1736E+03	5.1405E-07
47	1.0100E+04	6.8735E+03	3.2265E+03	5.1405E-07
48	1.0100E+04	3.4121E+03	6.6879E+03	5.1405E-07
49	1.0000E+04	3.4121E+03	6.5879E+03	5.1405E-07
50	1.0000E+04	3.4121E+03	6.5879E+03	5.1405E-07
51	9.9000E+03	3.4121E+03	6.4879E+03	5.1405E-07
52	9.8000E+03	6.2362E+03	3.5638E+03	5.1405E-07
53	6.5400E+03	4.6891E+03	1.8509E+03	5.1405E-07
54	5.0000E+03	4.1347E+03	8.6526E+02	5.1405E-07
55	4.1000E+03	3.8758E+03	2.2419E+02	5.1405E-07
56	3.5100E+03	3.7345E+03	-2.2453E+02	5.1405E-07
57	3.1200E+03	3.6491E+03	-5.2913E+02	5.1405E-07
58	2.7900E+03	3.5936E+03	-8.0362E+02	5.1405E-07
59	2.5500E+03	3.5555E+03	-1.0055E+03	5.1405E-07
60	2.3400E+03	3.5282E+03	-1.1882E+03	5.1405E-07
61	1.9000E+03	3.4636E+03	-1.5636E+03	5.1405E-07
62	1.6100E+03	3.4409E+03	-1.8309E+03	5.1405E-07
63	7.7500E+02	3.4165E+03	-2.6415E+03	5.1405E-07
64	5.7100E+02	3.4130E+03	-2.8420E+03	5.1405E-07
65	4.7600E+02	3.4123E+03	-2.9363E+03	5.1405E-07
66	4.1500E+02	3.4121E+03	-2.9971E+03	5.1405E-07
67	2.3100E+02	3.4118E+03	-3.1808E+03	5.1405E-07
68	1.8300E+02	3.4118E+03	-3.2288E+03	5.1405E-07
69	1.1300E+02	3.4118E+03	-3.2988E+03	5.1405E-07
70	1.0200E+02	3.4118E+03	-3.3098E+03	5.1405E-07

SUM OF SQUARED RESIDUALS= 1.0193E+09

VARIANCE= 1.4989E+07

STANDARD DEVIATION= 3.8716E+03

H-87

ADDITIONAL PARAMETERS CALCULATED BY THE LEAST SQUARES SUBROUTINE.

THE RESIDUAL SUM OF SQUARES = 1.019270E+09

THE NUMBER OF SIGNIFICANT DIGITS IN THE CALCULATED PARAMETERS = 6.716306E+00

THE NUMBER OF FUNCTION EVALUATIONS REQUIRED = 1.420000E+02

THE NUMBER OF ITERATIONS REQUIRED = 4.700000E+01

AN INTEGER WHICH INDICATES THE CONVERGENCE CRITERION SATISFIED - INFER = 1

INFER=0 INDICATES THAT CONVERGENCE FAILED -- SEE THE (IER) PARAMETER

INFER=1 INDICATES THAT THE FOLLOWING CONVERGENCE CONDITION IS SATISFIED  
FOR TWO SUCCESSIVE ITERATIONS THE PARAMETER  
ESTIMATES AGREE, COMPONENT BY COMPONENT  
TO NSIG (SIGNIFICANT) DIGITS

INFER=2 INDICATES THAT THE FOLLOWING CONVERGENCE CONDITION IS SATISFIED  
FOR TWO SUCCESSIVE ITERATIONS THE RESIDUAL  
SUM OF THE SQUARE ESTIMATES HAVE RELATIVE  
DIFFERENCE LESS THAN OR EQUAL TO (EPS)

INFER=4 INDICATES THAT THE FOLLOWING CONVERGENCE CONDITION IS SATISFIED  
THE (EUCLIDEAN) NORM OF THE APPROXIMATE  
GRADIENT IS LESS THAN OR EQUAL TO (DELTA)

INFER=X IF MORE THAN ONE OF THE ABOVE CONVERGENCE CRITERIA IS SATISFIED  
(INFER) REPRESENTS THE CORRESPONDING SUM OF  
THE INTEGERS

THE ERROR PARAMETER: IER = 0

IER=0    INDICATES SUCCESSFUL EXECUTION OF THE PROGRAM

IER=38    INDICATES THAT THE JACOBIAN IS ZERO.  
          THE SOLUTION IS A STATIONARY POINT (WARNING)

IER=129    INDICATES THAT A SINGULARITY WAS  
          DETECTED IN THE JACOBIAN

IER=130    INDICATES THAT AT LEAST ONE OF THE  
          SUBROUTINE CALL PARAMETERS WAS SPECIFIED  
          INCORRECTLY -- VERIFY: M,N,IOPT,PARM(1),PARM(2)

IER=131    INDICATES THAT THE MARQUARDT PARAMETER  
          EXCEEDED THE DEFAULT VALUE OF (120.0)

IER=132    INDICATES THAT AFTER A SUCCESSFUL  
          RECOVERY FROM A SINGULAR JACOBIAN, THE SOLUTION  
          HAS CYCLED BACK TO THE FIRST SINGULARITY

IER=133    INDICATES THAT THE (MAXFN) PARAMETER  
          WAS EXCEEDED

# VARIABLES USED IN THE CALCULATIONS

THE ESTIMATED METAL CLUSTER RESISTANCE ( $R_c$ ) =  $1.000000E+02$

THE ESTIMATED GAP RESISTANCE ( $R_g$ ) =  $1.000000E+05$

THE ESTIMATED GAP  
CAPACITANCE ( $C_g$ ) =  $6.000000E-07$

THE LEAST SQUARE VALUE OF THE METAL CLUSTER  
RESISTANCE,  $R_c$  =  $2.782984E+03$

THE LEAST SQUARE VALUE OF THE GAP  
RESISTANCE,  $R_g$  =  $9.878537E+04$

THE LEAST SQUARE VALUE OF THE GAP  
CAPACITANCE,  $C_g$  =  $4.518085E-07$

THE RESIDUALS ARE CALCULATED BY THE FOLLOWING  
EQUATION: [MEASURED VALUE-CALCULATED VALUE]

SAMPLE	R(f)	R(cal)	R(resid)	Cg(est)
1	9.7000E+04	1.0157E+05	-4.5684E+03	4.5181E-07
2	9.1700E+04	9.6519E+04	-4.8188E+03	4.5181E-07
3	9.0900E+04	9.4457E+04	-3.5570E+03	4.5181E-07
4	9.0000E+04	9.2134E+04	-2.1342E+03	4.5181E-07
5	8.9300E+04	8.9596E+04	-2.9621E+02	4.5181E-07
6	8.7700E+04	8.6889E+04	8.1132E+02	4.5181E-07
7	8.6200E+04	8.4056E+04	2.1443E+03	4.5181E-07
8	8.3300E+04	7.8175E+04	5.1251E+03	4.5181E-07
9	8.0000E+04	7.2236E+04	7.7643E+03	4.5181E-07
10	7.5200E+04	6.6449E+04	8.7514E+03	4.5181E-07
11	6.9000E+04	6.0955E+04	8.0448E+03	4.5181E-07
12	6.1700E+04	5.5839E+04	5.8613E+03	4.5181E-07
13	5.4300E+04	5.1138E+04	3.1621E+03	4.5181E-07
14	4.6700E+04	4.6861E+04	-1.6072E+02	4.5181E-07
15	4.0200E+04	4.2995E+04	-2.7945E+03	4.5181E-07
16	3.5100E+04	3.9515E+04	-4.4149E+03	4.5181E-07
17	3.1200E+04	3.6391E+04	-5.1913E+03	4.5181E-07
18	2.8100E+04	3.3591E+04	-5.4907E+03	4.5181E-07
19	2.5800E+04	3.1081E+04	-5.2806E+03	4.5181E-07
20	2.4100E+04	2.8830E+04	-4.7298E+03	4.5181E-07
21	2.2700E+04	2.6809E+04	-4.1094E+03	4.5181E-07

22	2.1500E+04	2.4994E+04	-3.4936E+03	4.5181E-07
23	2.0400E+04	2.3359E+04	-2.9587E+03	4.5181E-07
24	1.9400E+04	2.1884E+04	-2.4842E+03	4.5181E-07
25	1.8400E+04	2.0552E+04	-2.1516E+03	4.5181E-07
26	1.7600E+04	1.9345E+04	-1.7448E+03	4.5181E-07
27	1.6900E+04	1.8250E+04	-1.3496E+03	4.5181E-07
28	1.6100E+04	1.7254E+04	-1.1537E+03	4.5181E-07
29	1.5400E+04	1.6346E+04	-9.4610E+02	4.5181E-07
30	1.4800E+04	1.5517E+04	-7.1726E+02	4.5181E-07
31	1.4300E+04	1.4759E+04	-4.5881E+02	4.5181E-07
32	1.3800E+04	1.4063E+04	-2.6338E+02	4.5181E-07
33	1.3400E+04	1.3424E+04	-2.4480E+01	4.5181E-07
34	1.3000E+04	1.2836E+04	1.6359E+02	4.5181E-07
35	1.2600E+04	1.2294E+04	3.0588E+02	4.5181E-07
36	1.2200E+04	1.1793E+04	4.0686E+02	4.5181E-07
37	1.1900E+04	1.1330E+04	5.7046E+02	4.5181E-07
38	1.1600E+04	1.0900E+04	7.0020E+02	4.5181E-07
39	1.1300E+04	1.0501E+04	7.9920E+02	4.5181E-07
40	1.1000E+04	1.0130E+04	8.7025E+02	4.5181E-07
41	1.0800E+04	9.7842E+03	1.0158E+03	4.5181E-07
42	1.0600E+04	9.4619E+03	1.1381E+03	4.5181E-07
43	1.0400E+04	9.1608E+03	1.2392E+03	4.5181E-07
44	1.0300E+04	8.8793E+03	1.4207E+03	4.5181E-07
45	1.0200E+04	8.6155E+03	1.5845E+03	4.5181E-07
46	1.0100E+04	8.3683E+03	1.7317E+03	4.5181E-07
47	1.0000E+04	8.1361E+03	1.8639E+03	4.5181E-07
48	1.0000E+04	2.7835E+03	7.2165E+03	4.5181E-07
49	9.9000E+03	2.7835E+03	7.1165E+03	4.5181E-07
50	9.8000E+03	2.7835E+03	7.0165E+03	4.5181E-07
51	9.8000E+03	2.7835E+03	7.0165E+03	4.5181E-07
52	9.7100E+03	7.1641E+03	2.5459E+03	4.5181E-07
53	6.2500E+03	4.7793E+03	1.4707E+03	4.5181E-07
54	4.6700E+03	3.9160E+03	7.5405E+02	4.5181E-07
55	3.9700E+03	3.5111E+03	4.5891E+02	4.5181E-07
56	3.3700E+03	3.2898E+03	8.0246E+01	4.5181E-07
57	2.9500E+03	3.1558E+03	-2.0581E+02	4.5181E-07
58	2.6600E+03	3.0687E+03	-4.0868E+02	4.5181E-07
59	2.4400E+03	3.0089E+03	-5.6886E+02	4.5181E-07
60	2.2800E+03	2.9660E+03	-6.8602E+02	4.5181E-07
61	1.7800E+03	2.8644E+03	-1.0844E+03	4.5181E-07
62	1.5500E+03	2.8288E+03	-1.2788E+03	4.5181E-07
63	7.0900E+02	2.7903E+03	-2.0813E+03	4.5181E-07
64	4.9000E+02	2.7848E+03	-2.2948E+03	4.5181E-07
65	4.3900E+02	2.7838E+03	-2.3448E+03	4.5181E-07
66	4.0200E+02	2.7834E+03	-2.3814E+03	4.5181E-07
67	2.2600E+02	2.7830E+03	-2.5570E+03	4.5181E-07
68	1.7100E+02	2.7830E+03	-2.6120E+03	4.5181E-07
69	1.1100E+02	2.7830E+03	-2.6720E+03	4.5181E-07
70	1.0100E+02	2.7830E+03	-2.6820E+03	4.5181E-07

SUM OF SQUARED RESIDUALS= 8.1032E+08

VARIANCE= 1.1916E+07

STANDARD DEVIATION= 3.4520E+03

H-91

ADDITIONAL PARAMETERS CALCULATED BY THE LEAST SQUARES SUBROUTINE.

THE RESIDUAL SUM OF SQUARES = 8.103179E+08

THE NUMBER OF SIGNIFICANT DIGITS IN THE CALCULATED PARAMETERS = 6.614308E+00

THE NUMBER OF FUNCTION EVALUATIONS REQUIRED = 2.050000E+02

THE NUMBER OF ITERATIONS REQUIRED = 7.800000E+01

ADDITIONAL PARAMETERS CALCULATED BY THE LEAST SQUARES SUBROUTINE.

INFER=0 INDICATES THAT CONVERGENCE FAILED -- SEE THE (IER) PARAMETER

INFER=1 INDICATES THAT THE FOLLOWING CONVERGENCE CONDITION IS SATISFIED  
FOR TWO SUCCESSIVE ITERATIONS THE PARAMETER  
ESTIMATES AGREE, COMPONENT BY COMPONENT  
TO NSIG (SIGNIFICANT) DIGITS

INFER=2 INDICATES THAT THE FOLLOWING CONVERGENCE CONDITION IS SATISFIED  
FOR TWO SUCCESSIVE ITERATIONS THE RESIDUAL  
SUM OF THE SQUARE ESTIMATES HAVE RELATIVE  
DIFFERENCE LESS THAN OR EQUAL TO (EPS)

INFER=4 INDICATES THAT THE FOLLOWING CONVERGENCE CONDITION IS SATISFIED  
THE (EUCLIDEAN) NORM OF THE APPROXIMATE  
GRADIENT IS LESS THAN OR EQUAL TO (DELTA)

INFER=X IF MORE THAN ONE OF THE ABOVE CONVERGENCE CRITERIA IS SATISFIED  
(INFER) REPRESENTS THE CORRESPONDING SUM OF  
THE INTEGERS

THE ERROR PARAMETER: IER = 0

IER=0    INDICATES SUCCESSFUL EXECUTION OF THE PROGRAM

IER=38    INDICATES THAT THE JACOBIAN IS ZERO.  
          THE SOLUTION IS A STATIONARY POINT (WARNING)

IER=129    INDICATES THAT A SINGULARITY WAS  
          DETECTED IN THE JACOBIAN

IER=130    INDICATES THAT AT LEAST ONE OF THE  
          SUBROUTINE CALL PARAMETERS WAS SPECIFIED  
          INCORRECTLY -- VERIFY: M,N,IOPT,PARM(1),PARM(2)

IER=131    INDICATES THAT THE MARQUARDT PARAMETER  
          EXCEEDED THE DEFAULT VALUE OF (120.0)

IER=132    INDICATES THAT AFTER A SUCCESSFUL  
          RECOVERY FROM A SINGULAR JACOBIAN, THE SOLUTION  
          HAS CYCLED BACK TO THE FIRST SINGULARITY

IER=133    INDICATES THAT THE (MAXFN) PARAMETER  
          WAS EXCEEDED

# VARIABLES USED IN THE CALCULATIONS

THE ESTIMATED METAL CLUSTER RESISTANCE (Rc) = 1.000000E+02

THE ESTIMATED GAP RESISTANCE (Rg) = 1.000000E+05

THE ESTIMATED GAP  
CAPACITANCE (Cg) = 6.000000E-07

THE LEAST SQUARE VALUE OF THE METAL CLUSTER  
RESISTANCE, Rc = 3.644387E+03

THE LEAST SQUARE VALUE OF THE GAP  
RESISTANCE, Rg = 8.713729E+04

THE LEAST SQUARE VALUE OF THE GAP  
CAPACITANCE, Cg = 4.334767E-07

THE RESIDUALS ARE CALCULATED BY THE FOLLOWING  
EQUATION: [MEASURED VALUE-CALCULATED VALUE]

SAMPLE	R(f)	R(cal)	R(resid)	Cg(est)
1	8.6300E+04	9.0782E+04	-4.4817E+03	4.3348E-07
2	8.2000E+04	8.6120E+04	-4.1195E+03	4.3348E-07
3	8.1300E+04	8.4223E+04	-2.9226E+03	4.3348E-07
4	8.0600E+04	8.2090E+04	-1.4902E+03	4.3348E-07
5	8.0000E+04	7.9766E+04	2.3405E+02	4.3348E-07
6	7.8700E+04	7.7293E+04	1.4072E+03	4.3348E-07
7	7.7500E+04	7.4712E+04	2.7877E+03	4.3348E-07
8	7.4600E+04	6.9378E+04	5.2215E+03	4.3348E-07
9	7.0900E+04	6.4023E+04	6.8770E+03	4.3348E-07
10	6.6200E+04	5.8835E+04	7.3652E+03	4.3348E-07
11	6.0200E+04	5.3937E+04	6.2630E+03	4.3348E-07
12	5.2900E+04	4.9399E+04	3.5011E+03	4.3348E-07
13	4.5900E+04	4.5250E+04	6.5046E+02	4.3348E-07
14	3.9400E+04	4.1490E+04	-2.0905E+03	4.3348E-07
15	3.4000E+04	3.8106E+04	-4.1061E+03	4.3348E-07
16	3.0100E+04	3.5071E+04	-4.9710E+03	4.3348E-07
17	2.7400E+04	3.2355E+04	-4.9550E+03	4.3348E-07
18	2.5500E+04	2.9927E+04	-4.4270E+03	4.3348E-07
19	2.3900E+04	2.7756E+04	-3.8563E+03	4.3348E-07
20	2.2500E+04	2.5814E+04	-3.3143E+03	4.3348E-07
21	2.1200E+04	2.4075E+04	-2.8748E+03	4.3348E-07



22	2.0000E+04	2.2514E+04	-2.5142E+03	4.3348E-07
23	1.8900E+04	2.1112E+04	-2.2116E+03	4.3348E-07
24	1.7900E+04	1.9848E+04	-1.9483E+03	4.3348E-07
25	1.7000E+04	1.8708E+04	-1.7082E+03	4.3348E-07
26	1.6300E+04	1.7677E+04	-1.3770E+03	4.3348E-07
27	1.5600E+04	1.6742E+04	-1.1422E+03	4.3348E-07
28	1.5100E+04	1.5893E+04	-7.9293E+02	4.3348E-07
29	1.4600E+04	1.5120E+04	-5.1970E+02	4.3348E-07
30	1.4100E+04	1.4414E+04	-3.1417E+02	4.3348E-07
31	1.4700E+04	1.3769E+04	9.3095E+02	4.3348E-07
32	1.3200E+04	1.3178E+04	2.2065E+01	4.3348E-07
33	1.2900E+04	1.2635E+04	2.6477E+02	4.3348E-07
34	1.2500E+04	1.2136E+04	3.6402E+02	4.3348E-07
35	1.2300E+04	1.1676E+04	6.2414E+02	4.3348E-07
36	1.2000E+04	1.1251E+04	7.4900E+02	4.3348E-07
37	1.1900E+04	1.0858E+04	1.0420E+03	4.3348E-07
38	1.1700E+04	1.0494E+04	1.2061E+03	4.3348E-07
39	1.1600E+04	1.0156E+04	1.4441E+03	4.3348E-07
40	1.1500E+04	9.8418E+03	1.6582E+03	4.3348E-07
41	1.1400E+04	9.5493E+03	1.8507E+03	4.3348E-07
42	1.1300E+04	9.2766E+03	2.0234E+03	4.3348E-07
43	1.1100E+04	9.0220E+03	2.0780E+03	4.3348E-07
44	1.1000E+04	8.7839E+03	2.2161E+03	4.3348E-07
45	1.0900E+04	8.5609E+03	2.3391E+03	4.3348E-07
46	1.0800E+04	8.3519E+03	2.4481E+03	4.3348E-07
47	1.0700E+04	8.1557E+03	2.5443E+03	4.3348E-07
48	1.0700E+04	3.6448E+03	7.0552E+03	4.3348E-07
49	1.0500E+04	3.6448E+03	6.8552E+03	4.3348E-07
50	1.0400E+04	3.6448E+03	6.7552E+03	4.3348E-07
51	1.0300E+04	3.6448E+03	6.6552E+03	4.3348E-07
52	1.0200E+04	7.3349E+03	2.8651E+03	4.3348E-07
53	6.8000E+03	5.3241E+03	1.4759E+03	4.3348E-07
54	5.2900E+03	4.5973E+03	6.9272E+02	4.3348E-07
55	4.3900E+03	4.2566E+03	1.3335E+02	4.3348E-07
56	3.8000E+03	4.0705E+03	-2.7048E+02	4.3348E-07
57	3.3100E+03	3.9578E+03	-6.4784E+02	4.3348E-07
58	2.9700E+03	3.8846E+03	-9.1458E+02	4.3348E-07
59	2.7000E+03	3.8343E+03	-1.1343E+03	4.3348E-07
60	2.4800E+03	3.7983E+03	-1.3183E+03	4.3348E-07
61	1.8900E+03	3.7128E+03	-1.8228E+03	4.3348E-07
62	1.6100E+03	3.6829E+03	-2.0729E+03	4.3348E-07
63	7.9400E+02	3.6506E+03	-2.8566E+03	4.3348E-07
64	5.4300E+02	3.6459E+03	-3.1029E+03	4.3348E-07
65	4.8500E+02	3.6451E+03	-3.1601E+03	4.3348E-07
66	4.3300E+02	3.6448E+03	-3.2118E+03	4.3348E-07
67	2.3000E+02	3.6444E+03	-3.4144E+03	4.3348E-07
68	1.7800E+02	3.6444E+03	-3.4664E+03	4.3348E-07
69	1.1500E+02	3.6444E+03	-3.5294E+03	4.3348E-07
70	1.0400E+02	3.6444E+03	-3.5404E+03	4.3348E-07

SUM OF SQUARED RESIDUALS= 7.2506E+08

VARIANCE= 1.0663E+07

STANDARD DEVIATION= 3.2654E+03

ADDITIONAL PARAMETERS CALCULATED BY THE LEAST SQUARES SUBROUTINE.

THE RESIDUAL SUM OF SQUARES = 7.250584E+08

THE NUMBER OF SIGNIFICANT DIGITS IN THE CALCULATED PARAMETERS = 6.370527E+00

THE NUMBER OF FUNCTION EVALUATIONS REQUIRED = 1.240000E+02

THE NUMBER OF ITERATIONS REQUIRED = 4.600000E+01

AN INTEGER WHICH INDICATES THE CONVERGENCE CRITERION SATISFIED - INFER = 1

INFER=0 INDICATES THAT CONVERGENCE FAILED -- SEE THE (IER) PARAMETER

INFER=1 INDICATES THAT THE FOLLOWING CONVERGENCE CONDITION IS SATISFIED  
FOR TWO SUCCESSIVE ITERATIONS THE PARAMETER  
ESTIMATES AGREE, COMPONENT BY COMPONENT  
TO NSIG (SIGNIFICANT) DIGITS

INFER=2 INDICATES THAT THE FOLLOWING CONVERGENCE CONDITION IS SATISFIED  
FOR TWO SUCCESSIVE ITERATIONS THE RESIDUAL  
SUM OF THE SQUARE ESTIMATES HAVE RELATIVE  
DIFFERENCE LESS THAN OR EQUAL TO (EPS)

INFER=4 INDICATES THAT THE FOLLOWING CONVERGENCE CONDITION IS SATISFIED  
THE (EUCLIDEAN) NORM OF THE APPROXIMATE  
GRADIENT IS LESS THAN OR EQUAL TO (DELTA)

INFER=X IF MORE THAN ONE OF THE ABOVE CONVERGENCE CRITERIA IS SATISFIED  
(INFER) REPRESENTS THE CORRESPONDING SUM OF  
THE INTEGERS

THE ERROR PARAMETER: IER = 0

IER-0 INDICATES SUCCESSFUL EXECUTION OF THE PROGRAM

IER-38 INDICATES THAT THE JACOBIAN IS ZERO.  
THE SOLUTION IS A STATIONARY POINT (WARNING)

IER-129 INDICATES THAT A SINGULARITY WAS  
DETECTED IN THE JACOBIAN

IER-130 INDICATES THAT AT LEAST ONE OF THE  
SUBROUTINE CALL PARAMETERS WAS SPECIFIED  
INCORRECTLY -- VERIFY: M,N,IOPT,PARM(1),PARM(2)

IER-131 INDICATES THAT THE MARQUARDT PARAMETER  
EXCEEDED THE DEFAULT VALUE OF (120.0)

IER-132 INDICATES THAT AFTER A SUCCESSFUL  
RECOVERY FROM A SINGULAR JACOBIAN, THE SOLUTION  
HAS CYCLED BACK TO THE FIRST SINGULARITY

IER-133 INDICATES THAT THE (MAXFN) PARAMETER  
WAS EXCEEDED

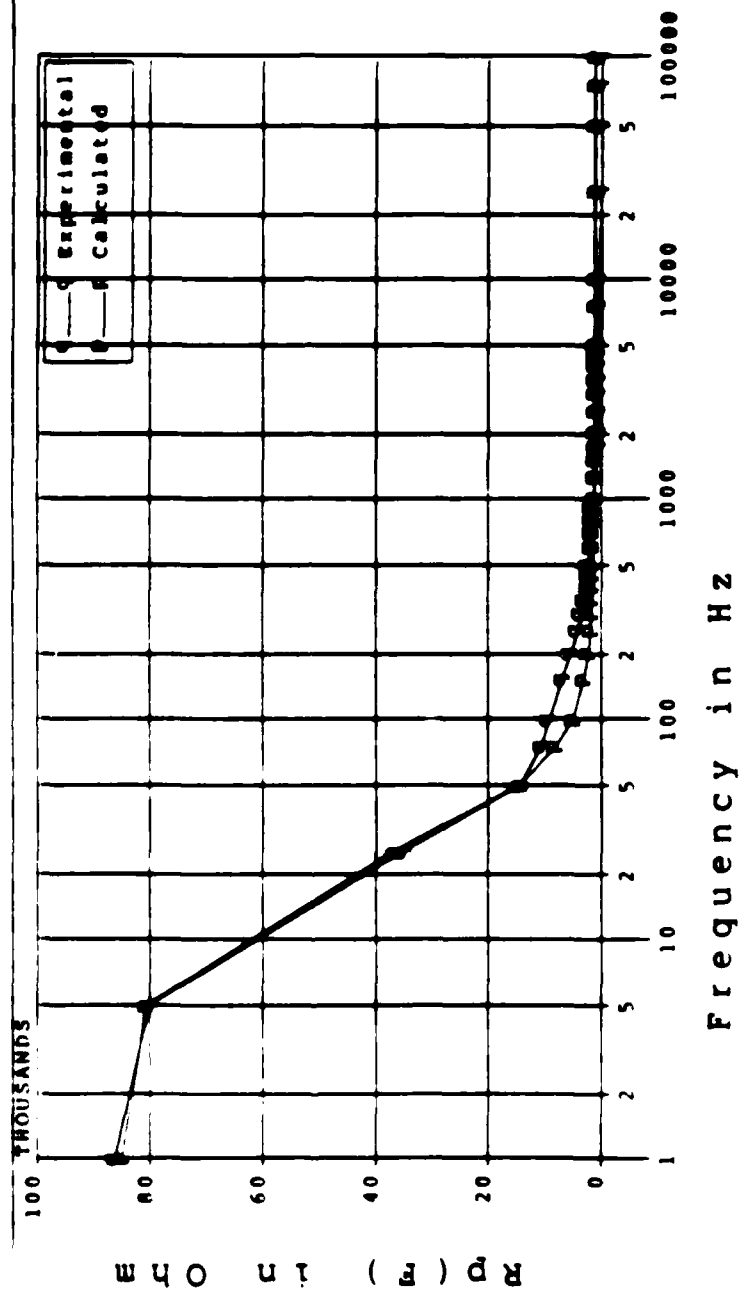
## APPENDIX I

### Frequency Response Graphs of the Brain Chip Electrodes

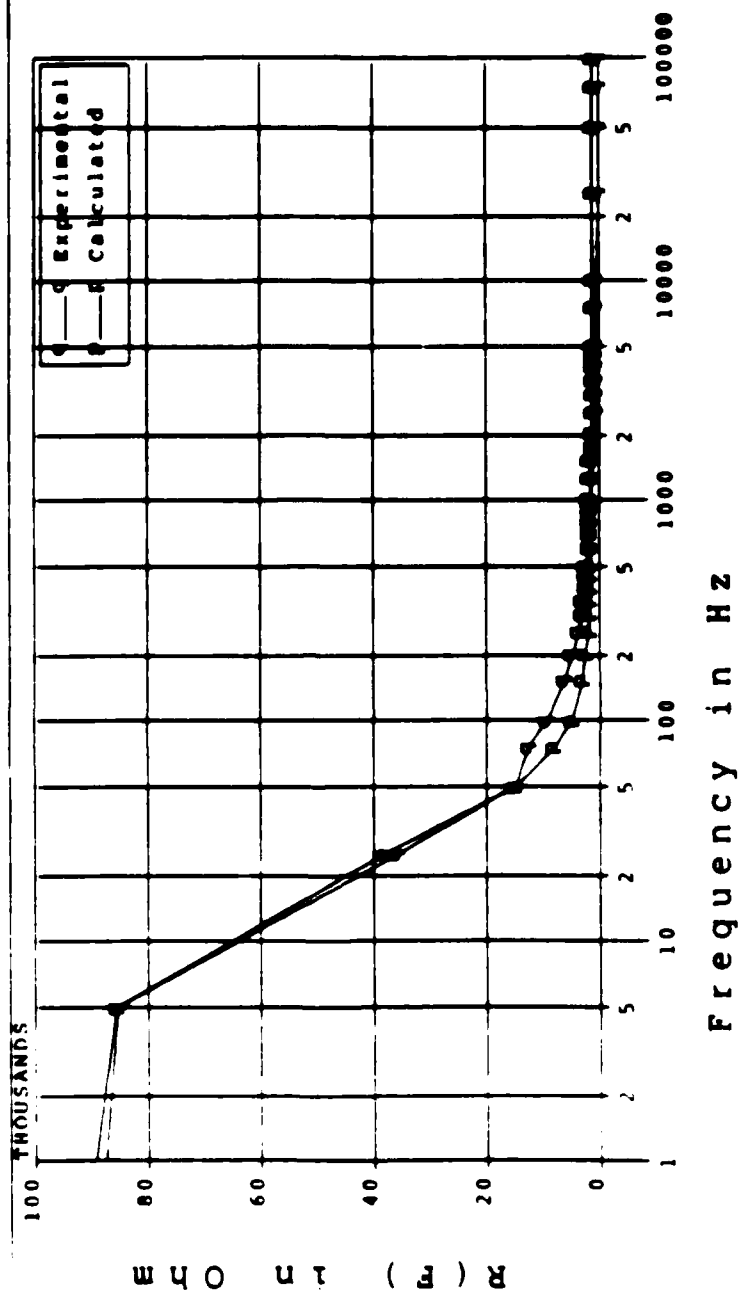
Each of the graphs in this appendix provides the frequency response of an electrode. The symbol "q" denotes experimental data, and the symbol "p" denotes calculated data. Semilogarithmic scales are used in the graphs.

# PLOT $R_p(f)$ VS $f$

Date Set 100

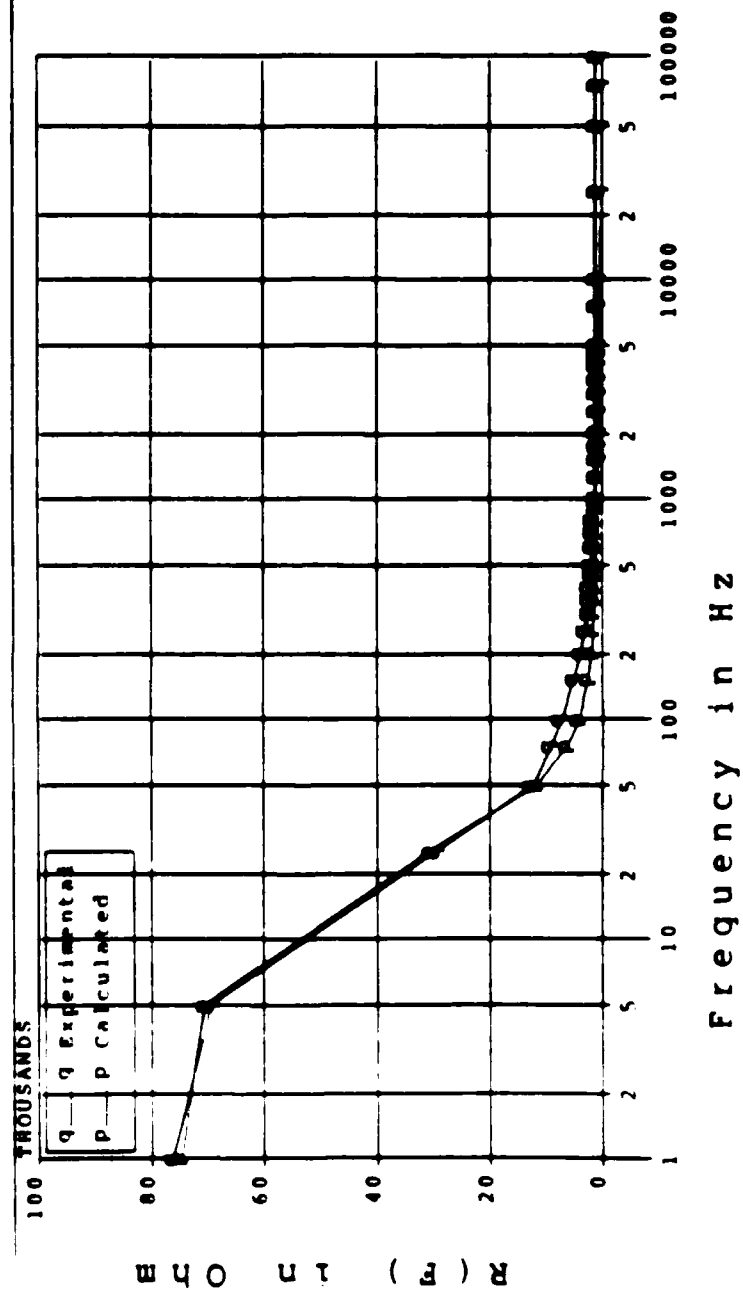


# PLOT $R_p(F)$ VS $F$ Data Set 144

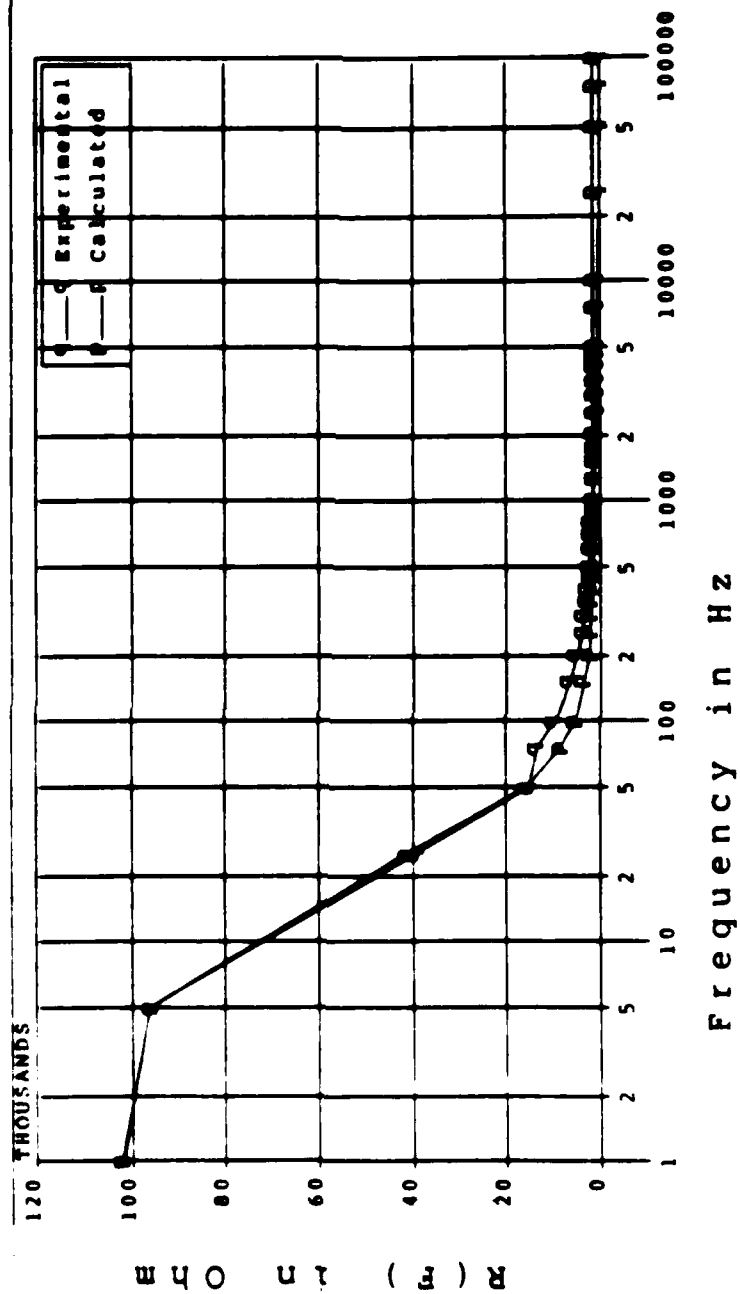


# PLOT $R_p(F)$ VS $F$

Data Set 112



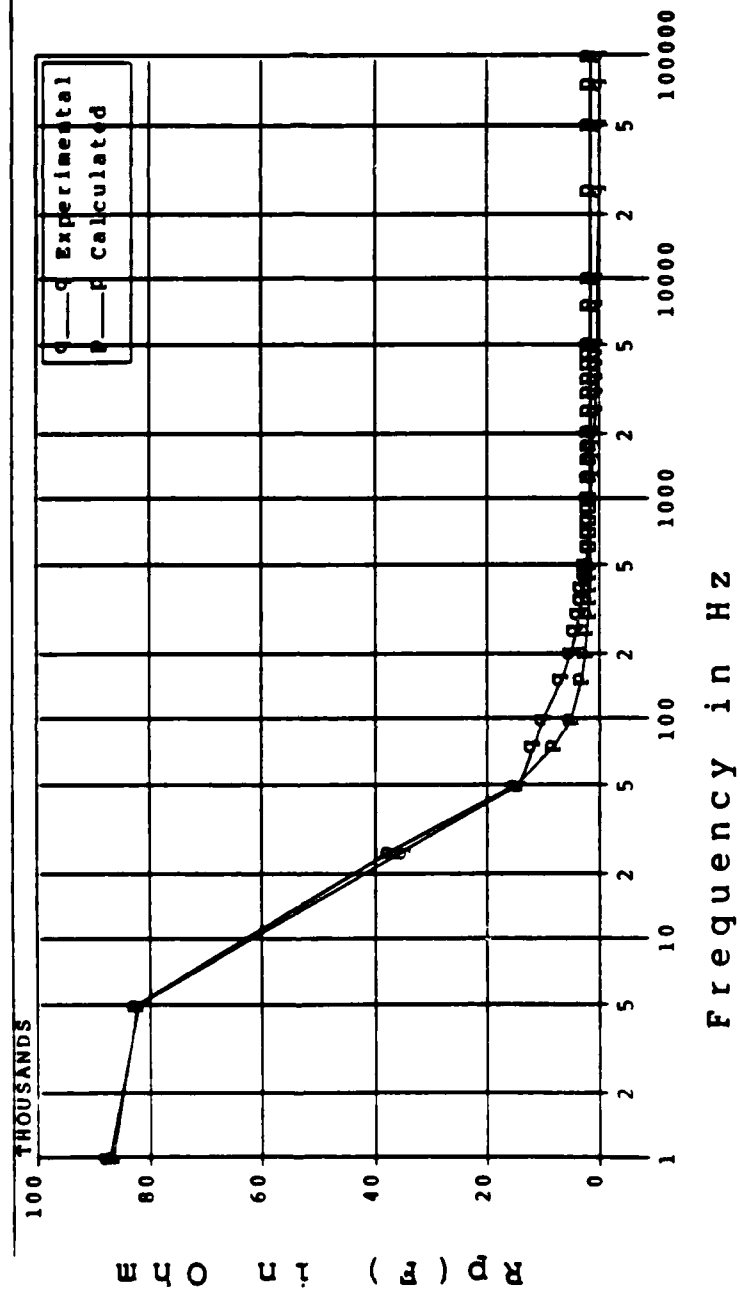
PLOT  $R_p(F)$  VS  $F$   
Data Set 111



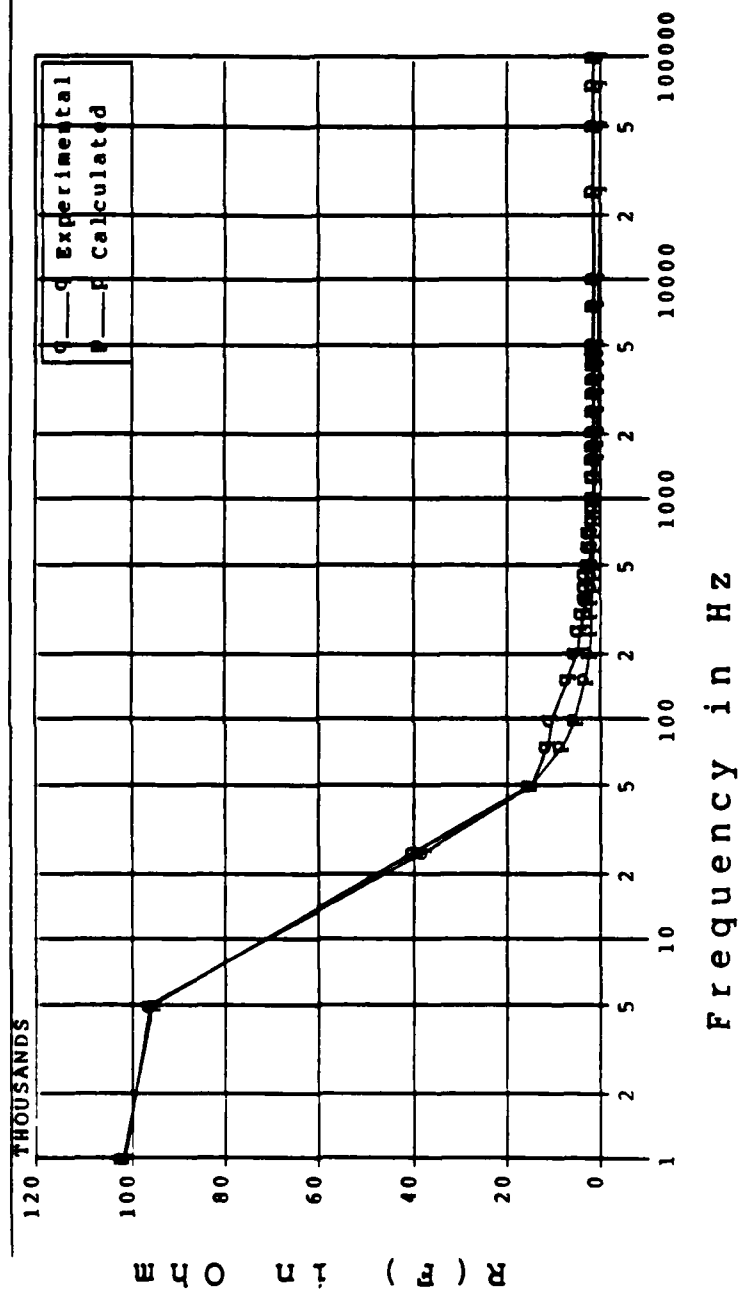


# PLOT $R_p(F)$ VS $F$

Data Set 116

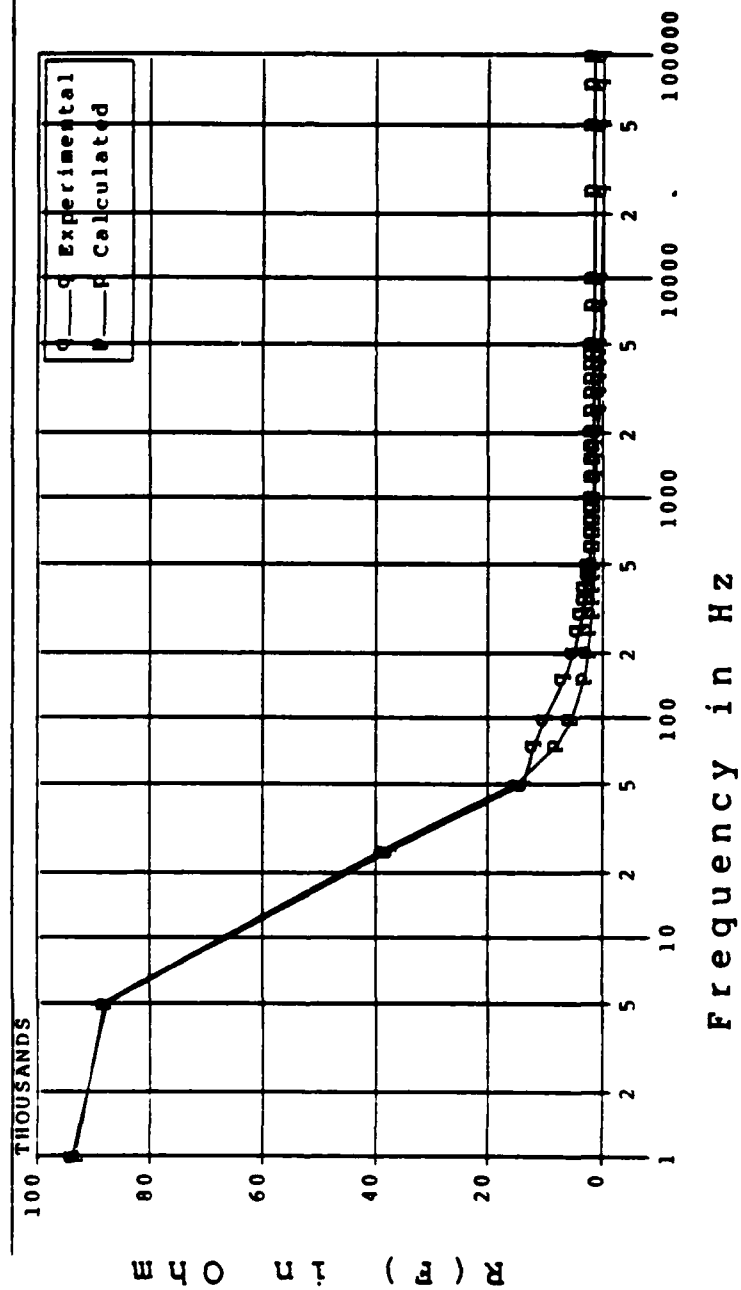


PLOT  $R_p(f)$  VS  $f$   
Data Set 199

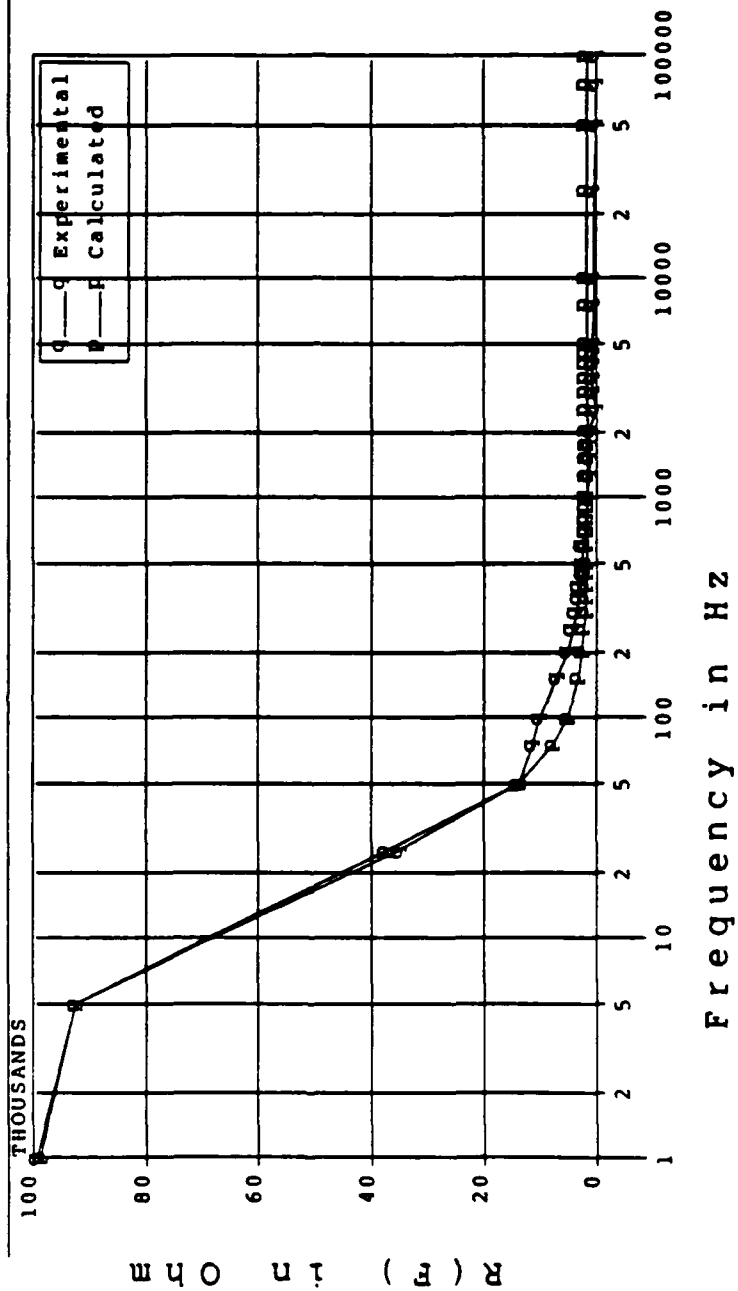


# PLOT $R_p(F)$ VS $F$

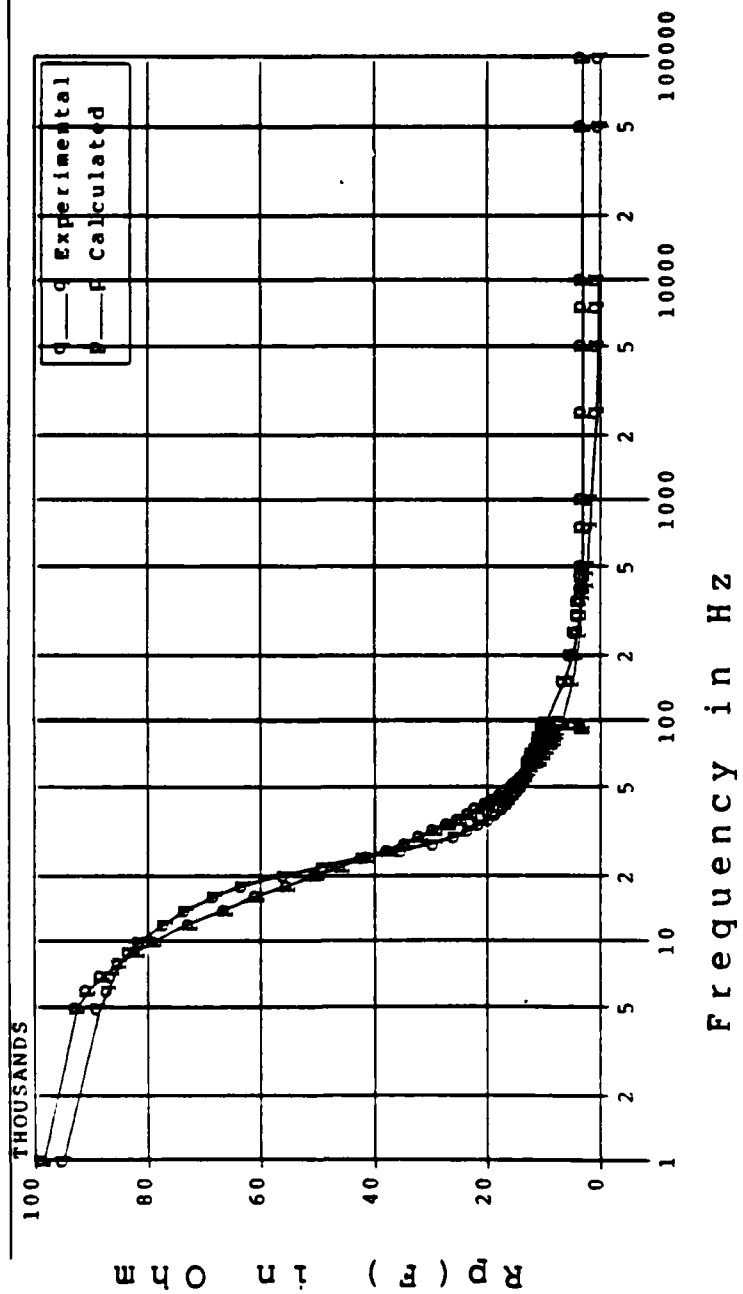
Data Set 177



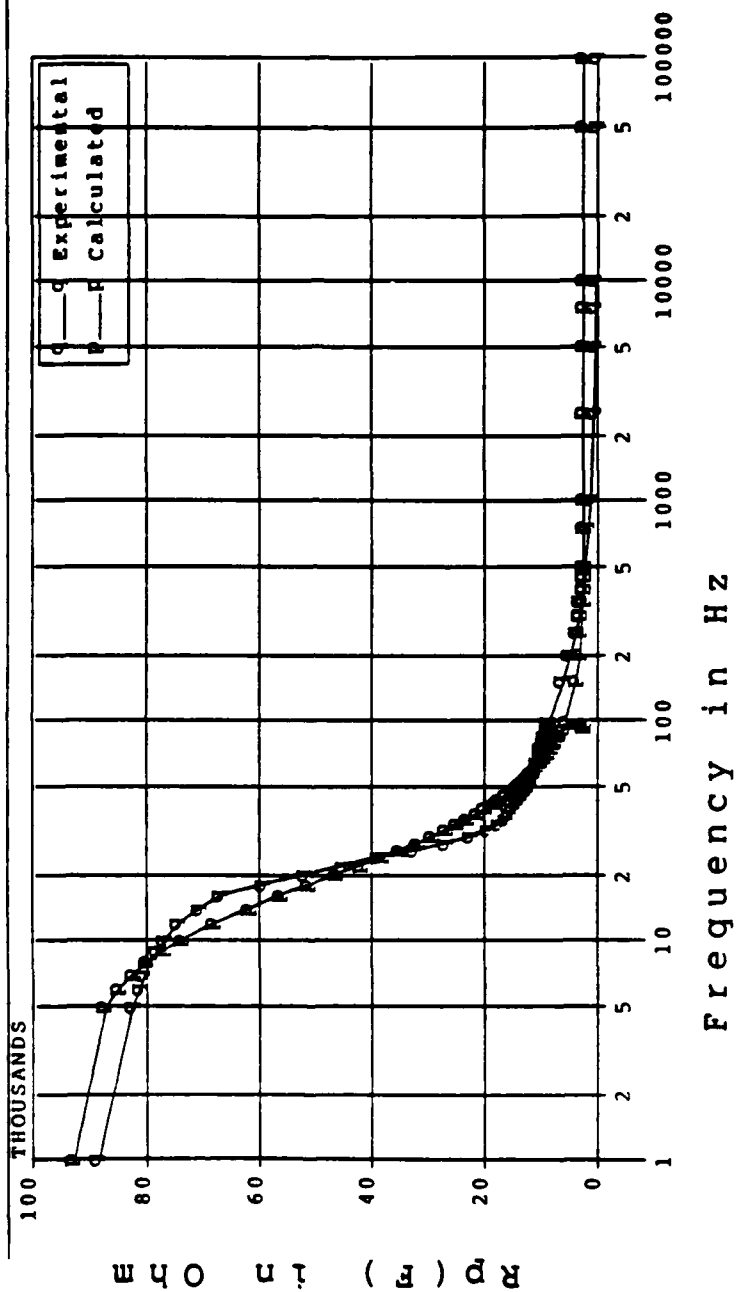
# PLOT $R_p(F)$ VS $F$ Data Set 131



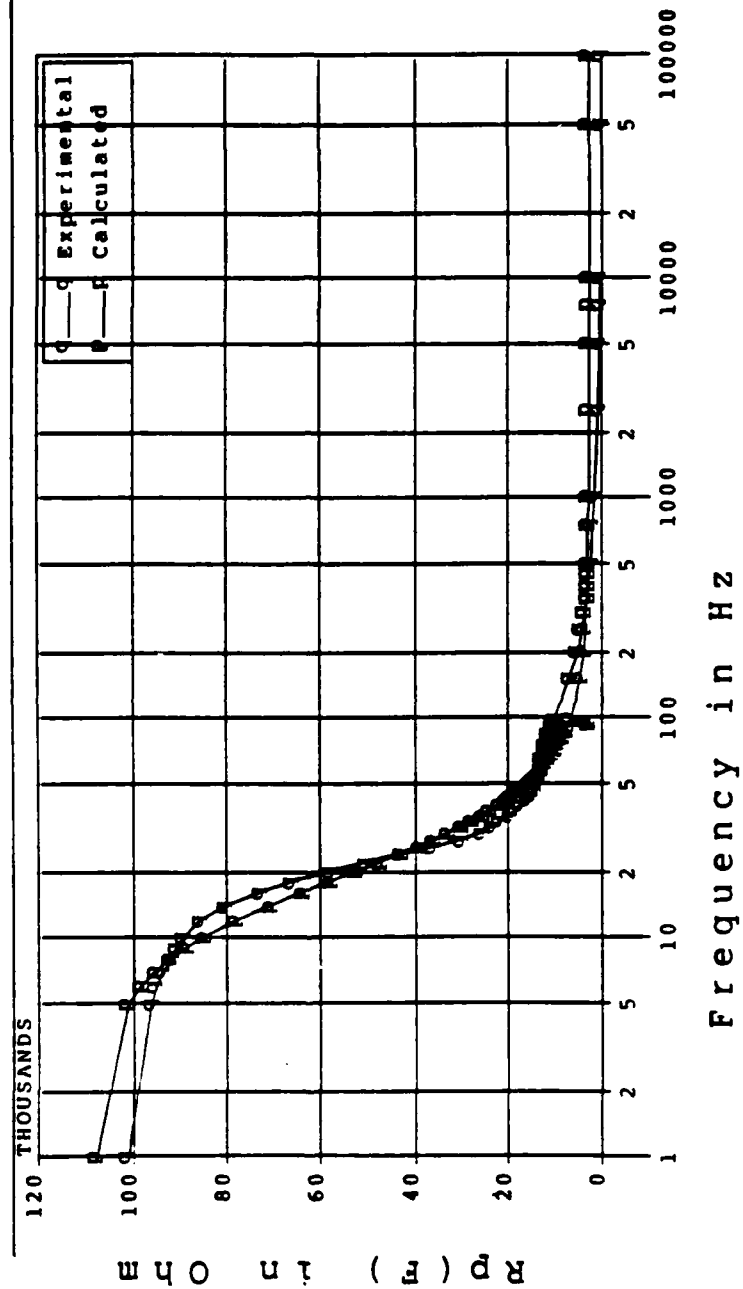
# PLOT $R_p(F)$ VS $F$ Data Set 288



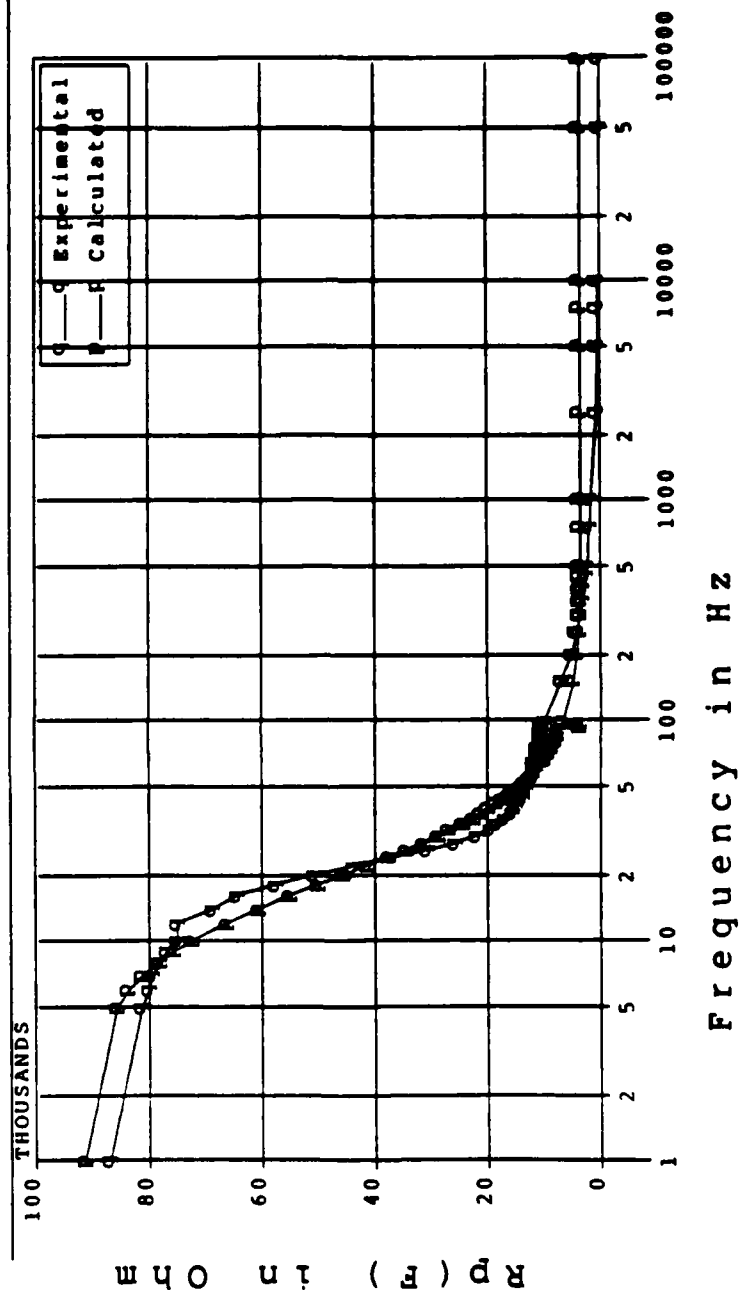
PLOT  $R_p(F)$  VS  $F$   
Data Set 244



# PLOT $R_p(F)$ VS $F$ Data Set 212



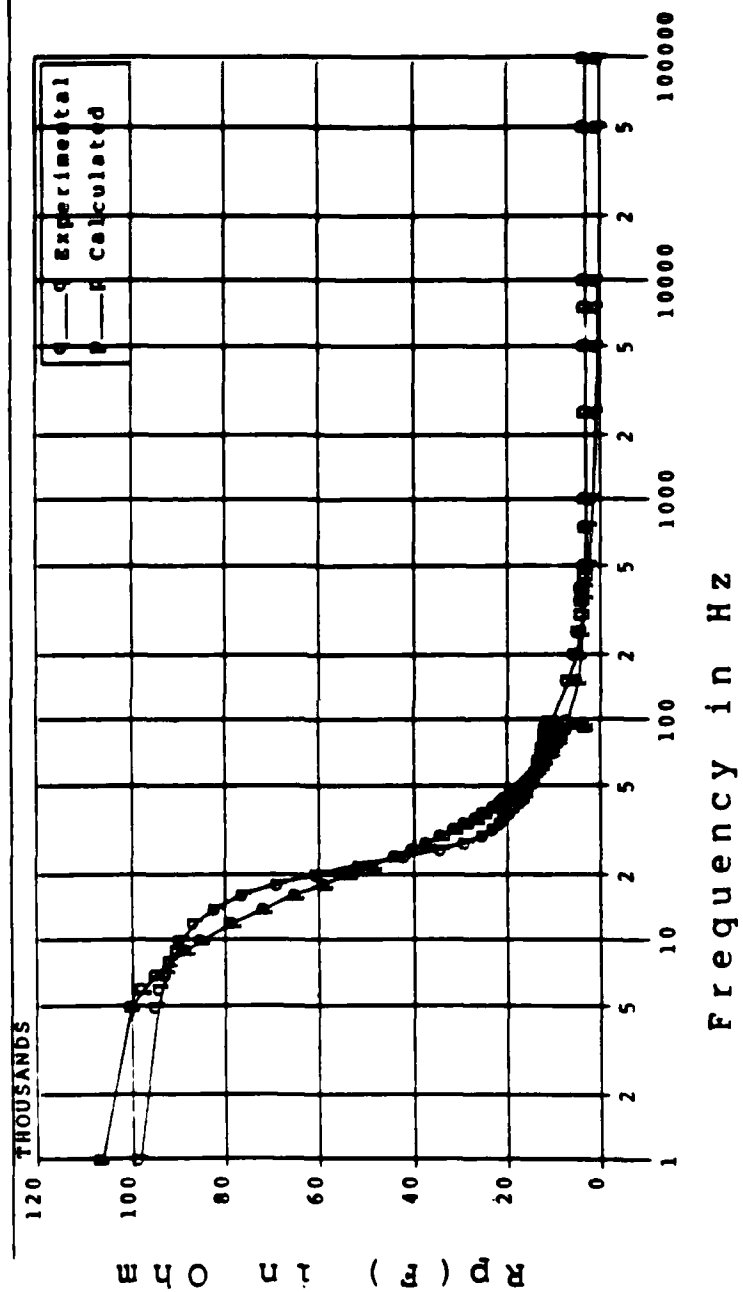
PLOT  $R_p(F)$  VS  $F$   
Data Set 211





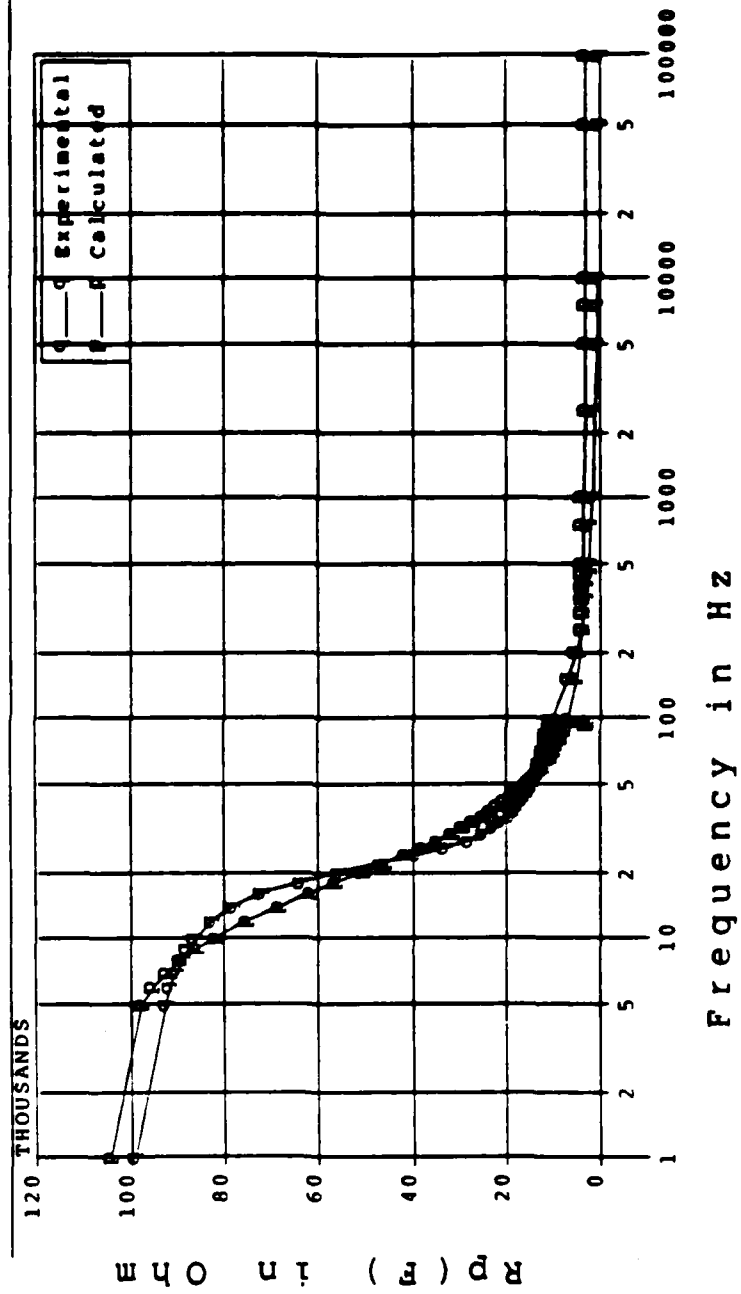
# PLOT $R_p(F)$ VS F

Data Set 216



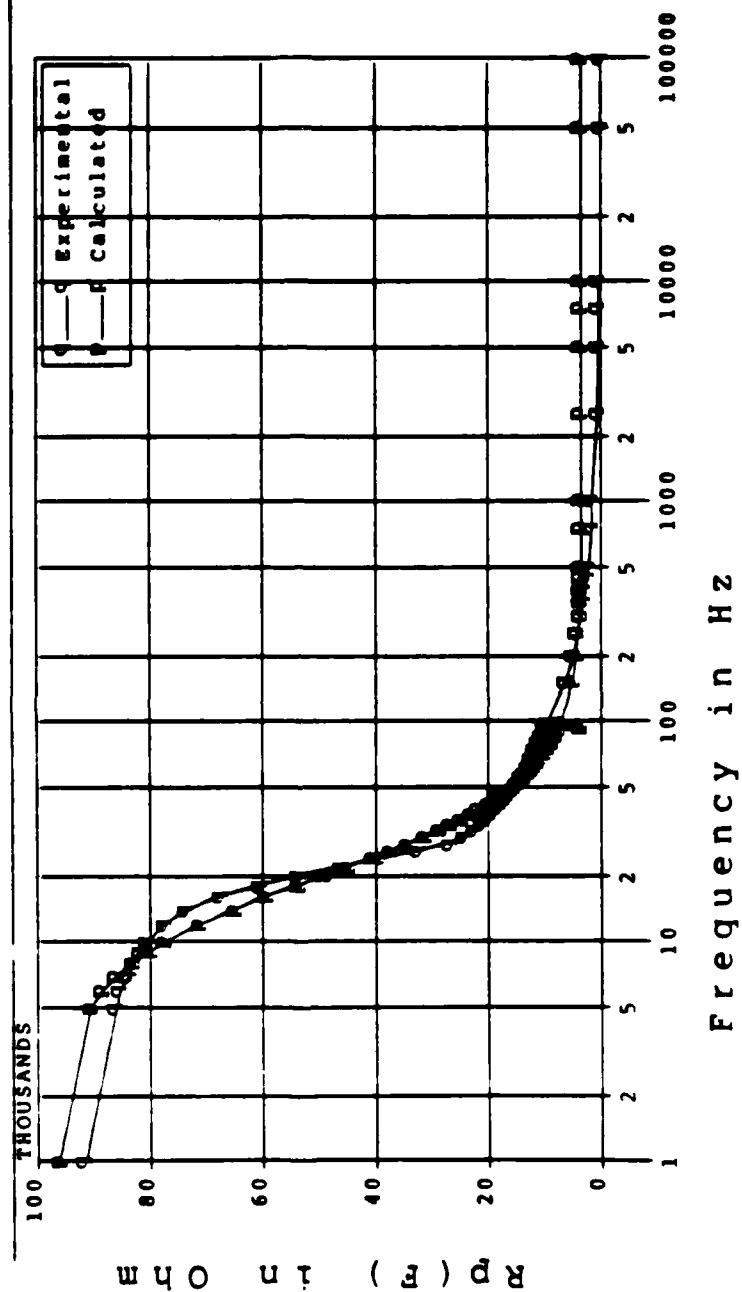
# PLOT $R_p(F)$ VS $F$

Data Set 299



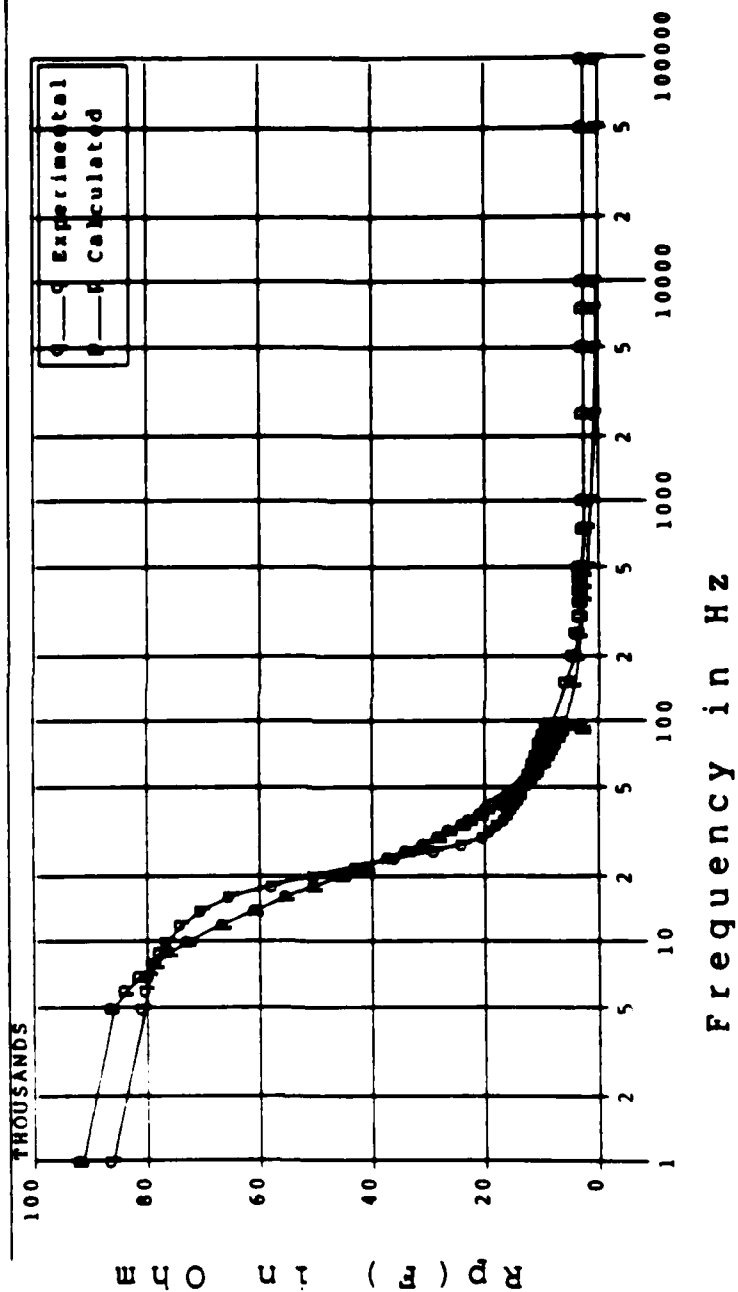
# PLOT $R_p(F)$ VS $F$

Data Set 277



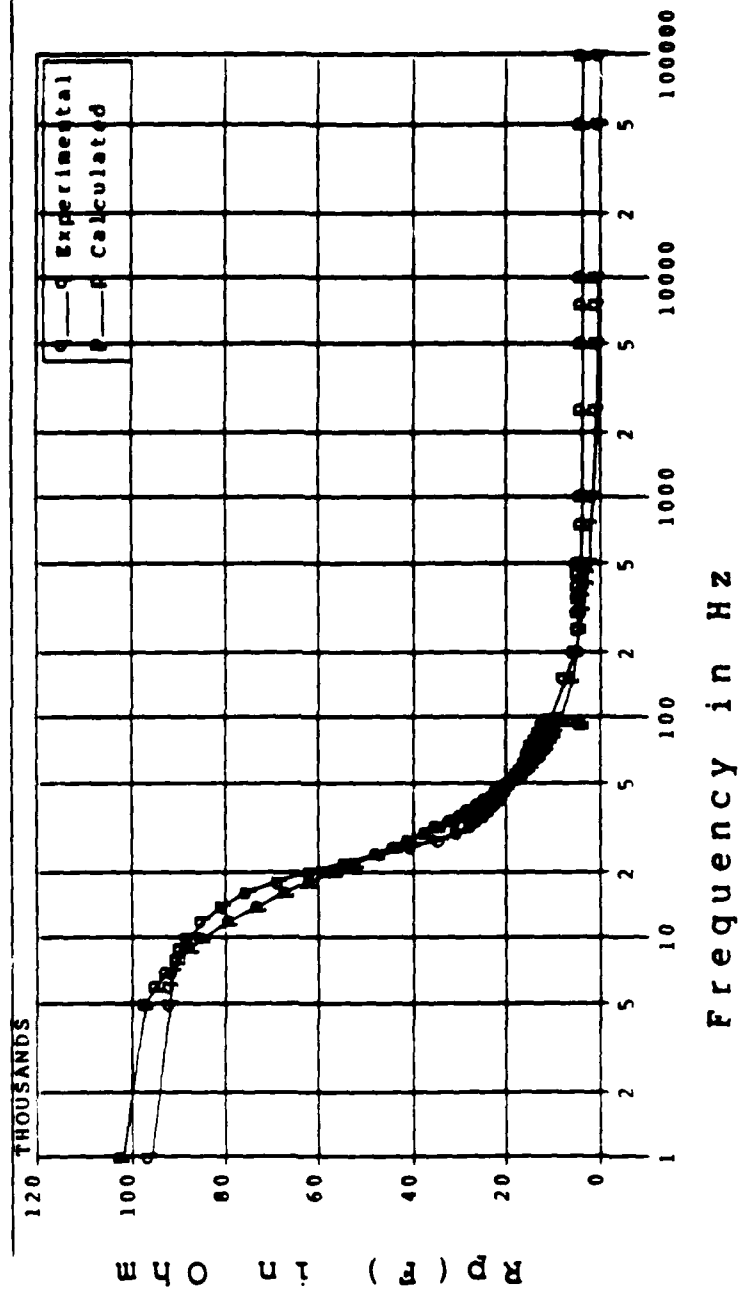
# PLOT $R_p(F)$ VS $F$

Data Set 243



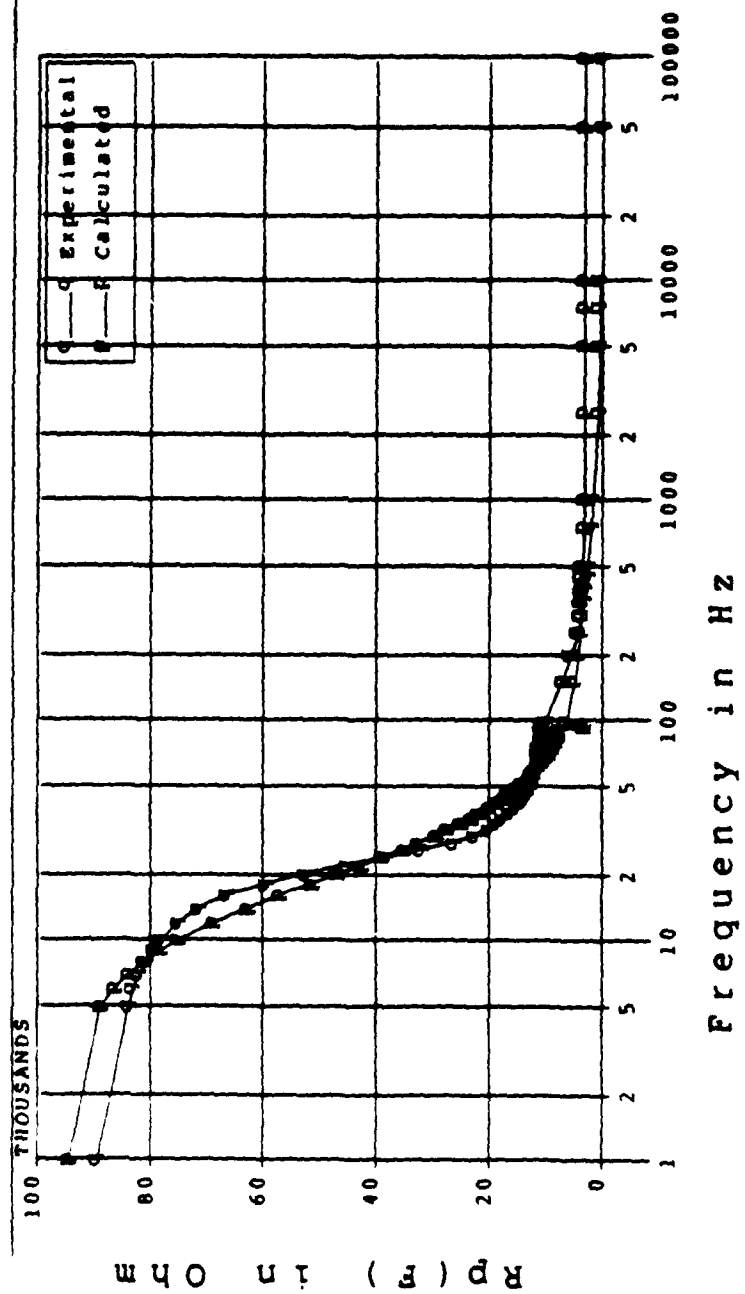
# PLOT $R_p(F)$ VS $F$

Date Set 214



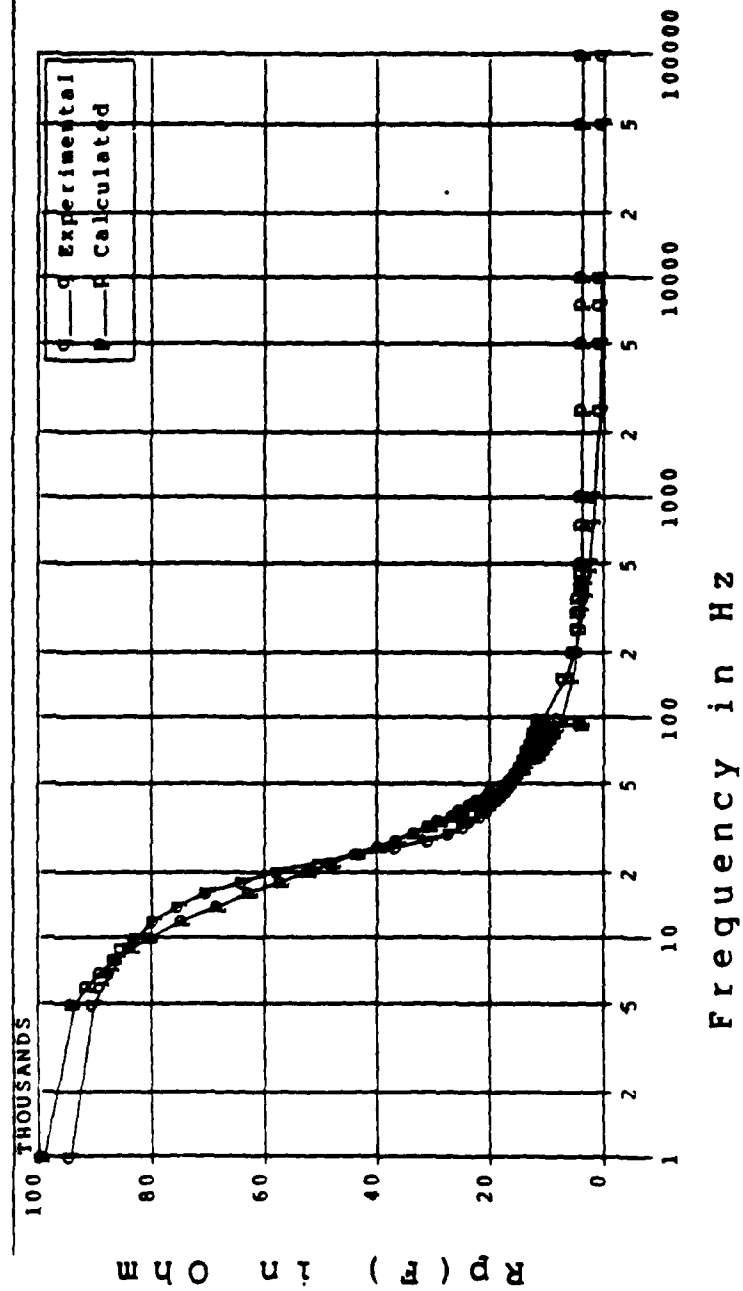
# PLOT $R_p(F)$ VS $F$

Data Set 388

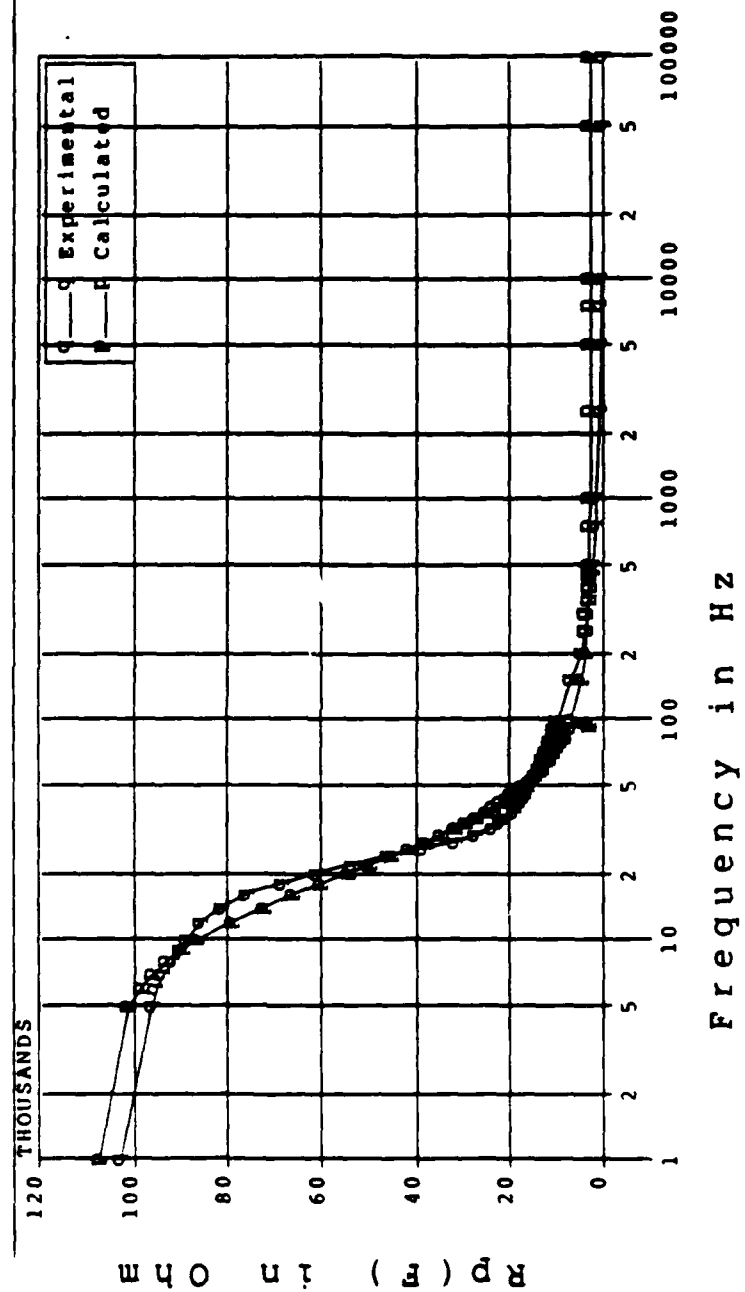


# PLOT $R_p(F)$ VS F

Data Set 344

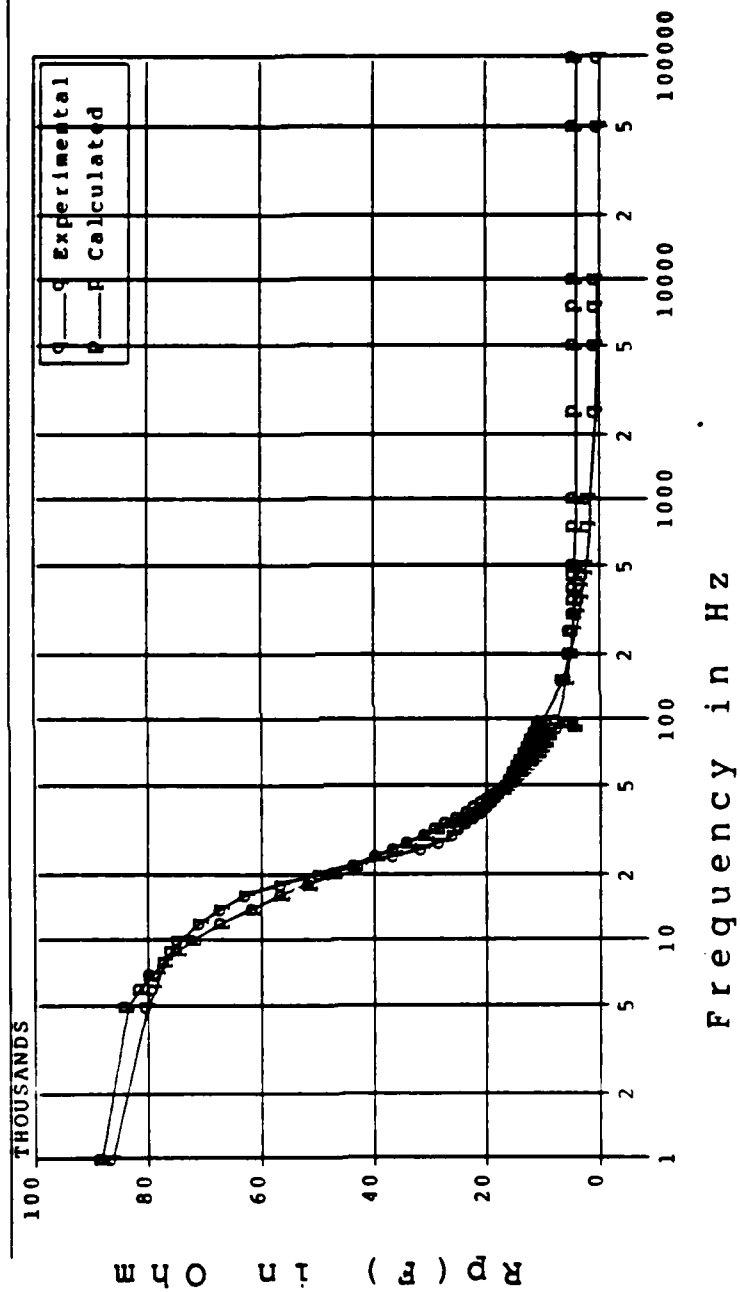


# PLOT $R_p(F)$ VS $F$ Data Set 311

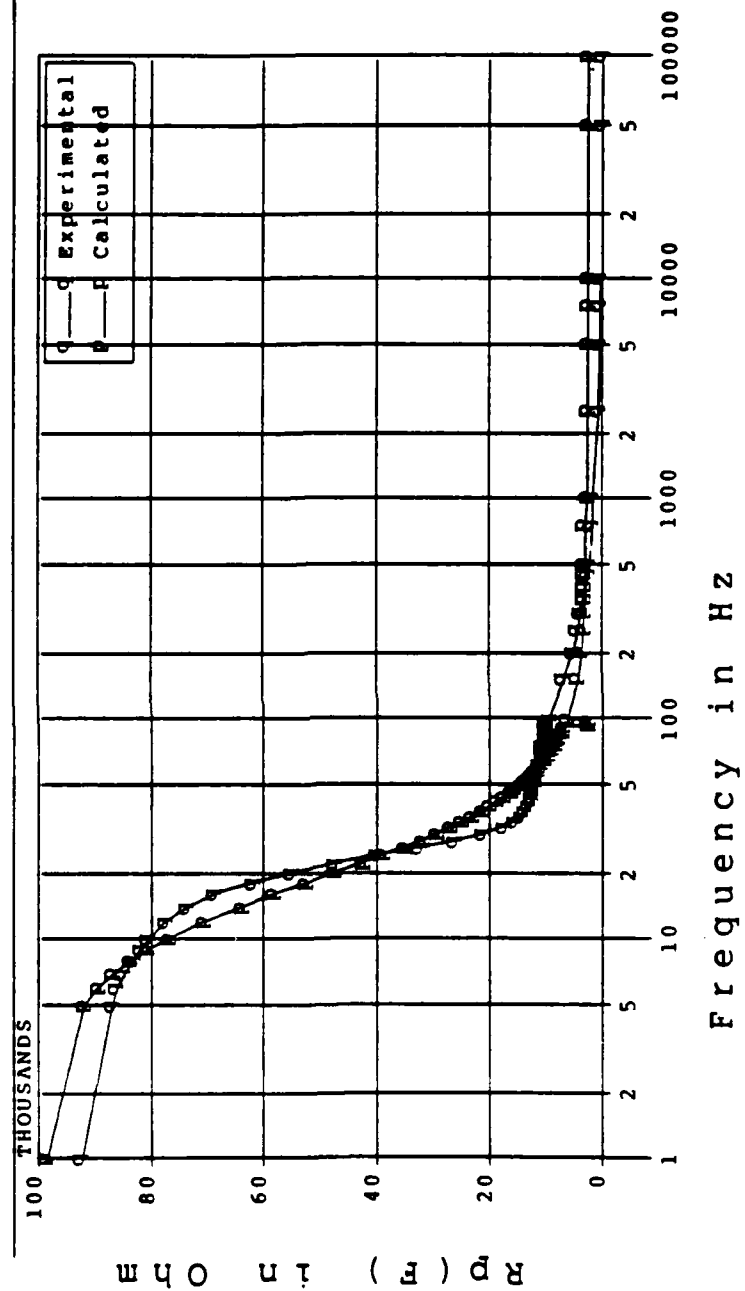




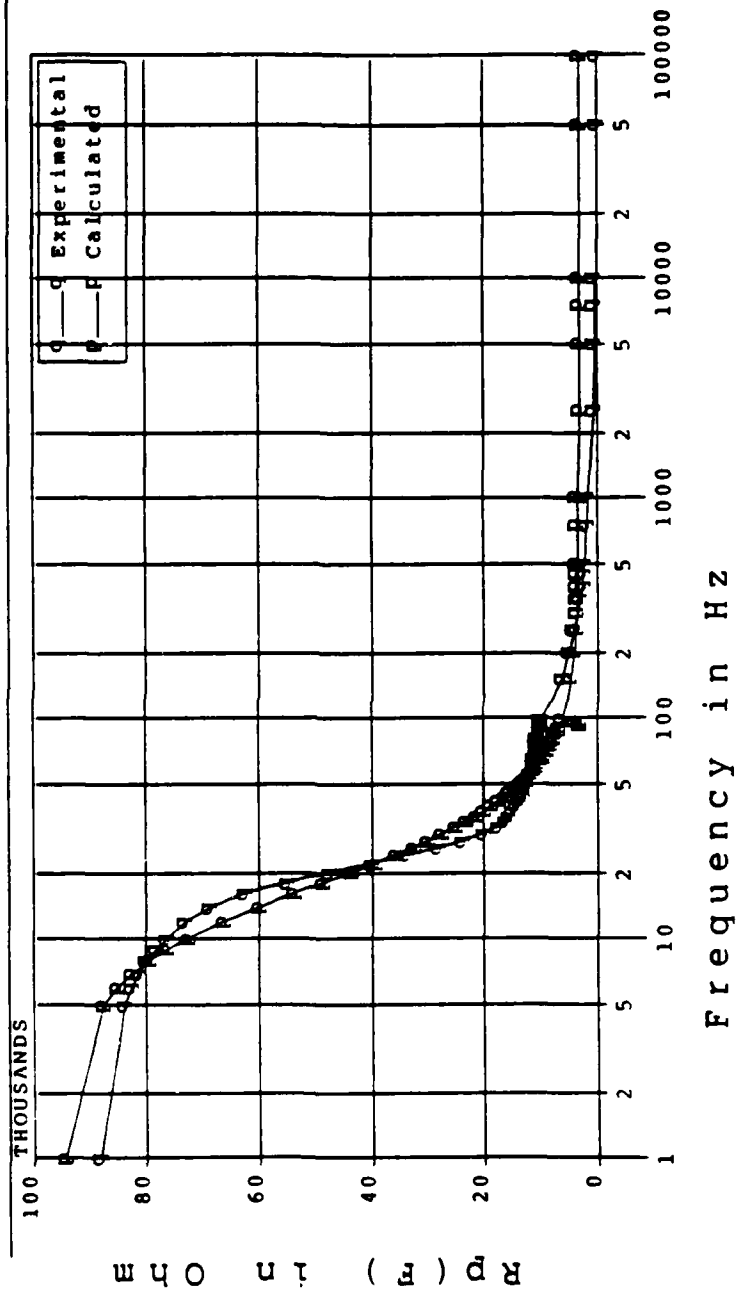
PLOT  $R_p(F)$  VS  $F$   
Data Set 316



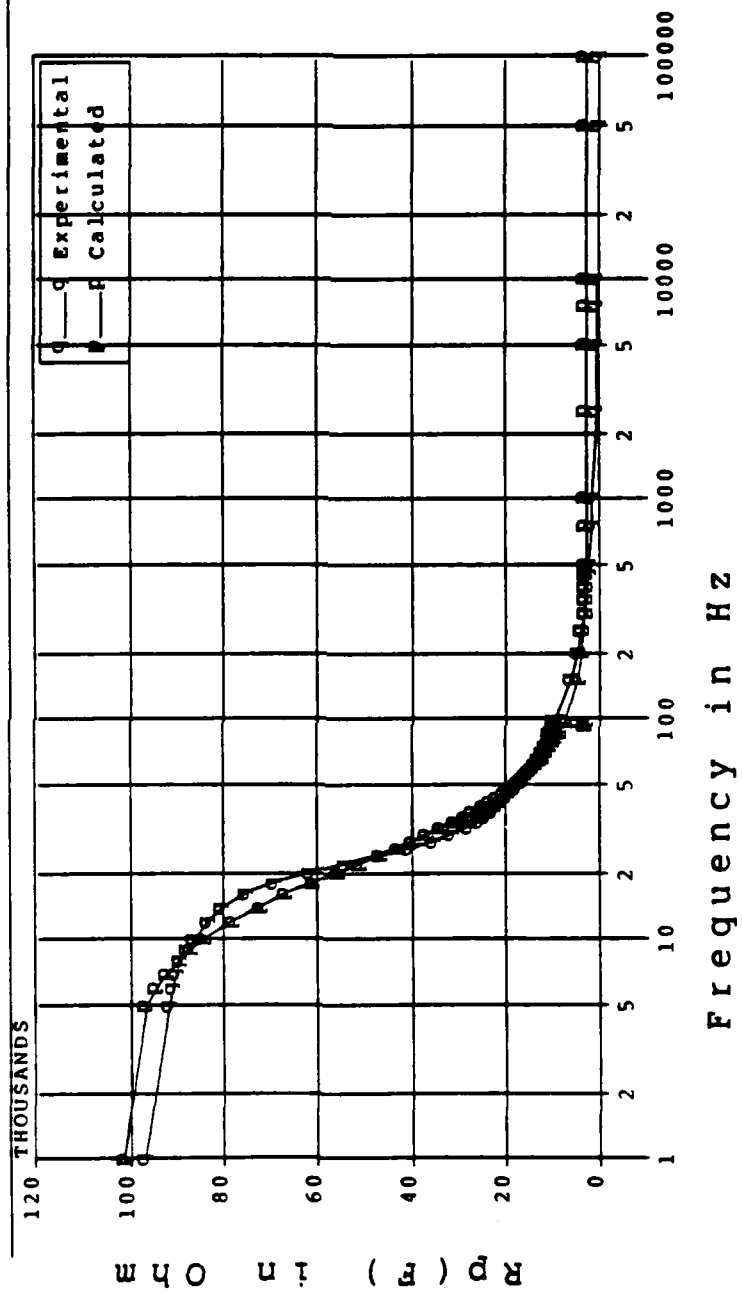
# PLOT $R_p(F)$ VS $F$ Data Set 399



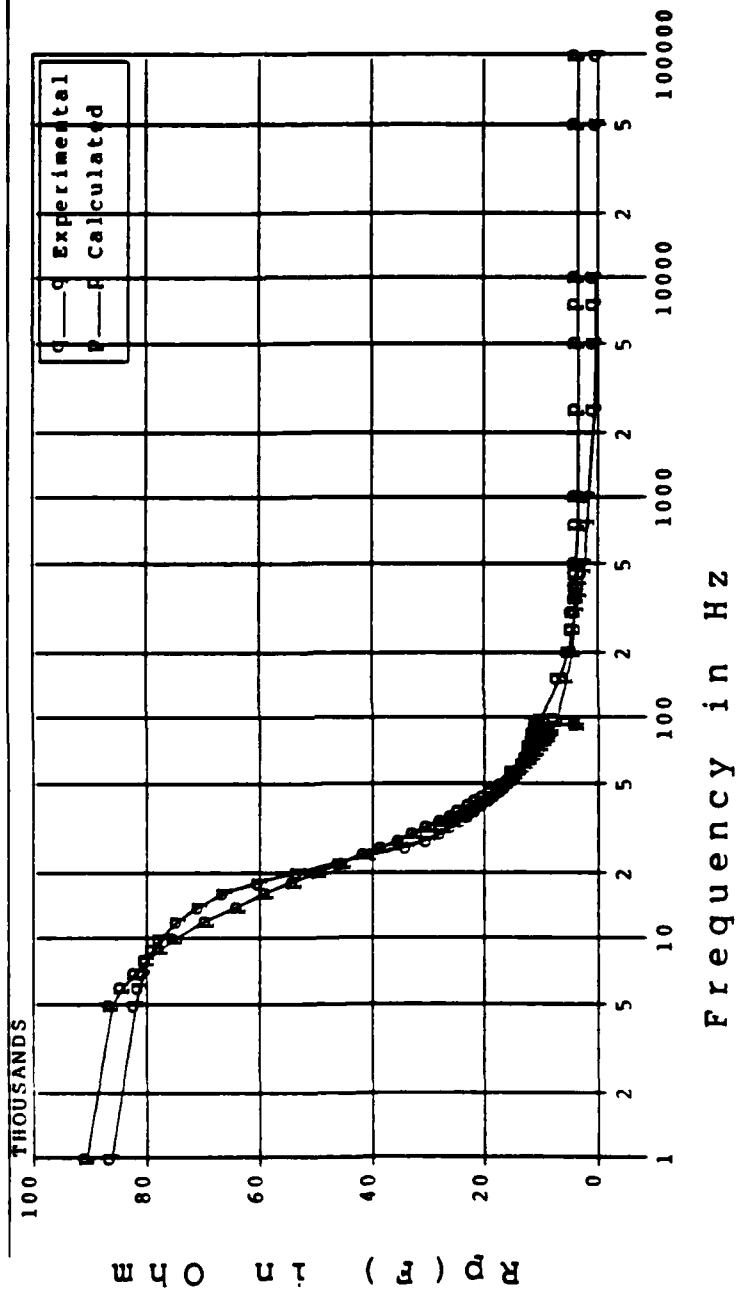
# PLOT $R_p(F)$ VS F Data Set 377



# PLOT $R_p(F)$ VS $F$ Data Set 343



PLOT  $R_p(F)$  VS  $F$   
Data Set 314



## APPENDIX J

### Frequency Response Calculations for Scaled Inputs

The frequency responses of three separate electrodes were calculated for inputs scaled between zero and one. Data for electrode 188 (see Figure 5-1 for nomenclature identification) are provided on pages J-2 through J-4; data for electrode 288 are provided on pages J-5 through J-8; data for electrode 388 are provided on pages J-9 through J-12.

# VARIABLES USED IN THE CALCULATIONS

THE ESTIMATED METAL CLUSTER RESISTANCE ( $R_c$ ) =  $1.000000E+02$

THE ESTIMATED GAP RESISTANCE ( $R_g$ ) =  $1.000000E+05$

THE ESTIMATED GAP  
CAPACITANCE ( $C_g$ ) =  $6.000000E-07$

## SCALED VALUES OF INPUTS ARE

$5.000000E-01$   
 $1.000000E+00$   
 $6.000000E-01$

THE LEAST SQUARE VALUE OF THE METAL CLUSTER  
RESISTANCE,  $R_c$  =  $1.493154E+03$

THE LEAST SQUARE VALUE OF THE GAP  
RESISTANCE,  $R_g$  =  $8.374804E+04$

THE LEAST SQUARE VALUE OF THE GAP  
CAPACITANCE,  $C_g$  =  $6.690232E-07$

THE RESIDUALS ARE CALCULATED BY THE FOLLOWING  
EQUATION: [MEASURED VALUE-CALCULATED VALUE]

SAMPLE	R(f)	R(cal)	R(resid)	Cg(est)
1	8.6400E+04	8.5241E+04	1.1588E+03	6.6902E-07
2	8.0000E+04	8.0930E+04	-9.2990E+02	6.6902E-07
3	3.5100E+04	3.7027E+04	-1.9273E+03	6.6902E-07
4	1.4400E+04	1.4523E+04	-1.2314E+02	6.6902E-07
5	1.0900E+04	7.8322E+03	3.0678E+03	6.6902E-07
6	9.3500E+03	5.1810E+03	4.1690E+03	6.6902E-07
7	6.9900E+03	3.1733E+03	3.8167E+03	6.6902E-07
8	5.3200E+03	2.4466E+03	2.8734E+03	6.6902E-07
9	4.2900E+03	2.1059E+03	2.1841E+03	6.6902E-07
10	3.5500E+03	1.9196E+03	1.6304E+03	6.6902E-07
11	3.0400E+03	1.8069E+03	1.2331E+03	6.6902E-07
12	2.7000E+03	1.7336E+03	9.6643E+02	6.6902E-07
13	2.4600E+03	1.6832E+03	7.7678E+02	6.6902E-07
14	2.2800E+03	1.6472E+03	6.3282E+02	6.6902E-07
15	2.0300E+03	1.6002E+03	4.2983E+02	6.6902E-07
16	1.8600E+03	1.5718E+03	2.8819E+02	6.6902E-07

17	1.7200E+03	1.5534E+03	1.6661E+02	6.6902E-07
18	1.6400E+03	1.5408E+03	9.9248E+01	6.6902E-07
19	1.5600E+03	1.5317E+03	2.8287E+01	6.6902E-07
20	1.3900E+03	1.5178E+03	-1.2784E+02	6.6902E-07
21	9.5200E+02	1.5103E+03	-5.5830E+02	6.6902E-07
22	8.4000E+02	1.5057E+03	-6.6575E+02	6.6902E-07
23	7.8100E+02	1.5028E+03	-7.2180E+02	6.6902E-07
24	6.8000E+02	1.4993E+03	-8.1933E+02	6.6902E-07
25	6.1000E+02	1.4974E+03	-8.8744E+02	6.6902E-07
26	5.6000E+02	1.4963E+03	-9.3630E+02	6.6902E-07
27	5.2400E+02	1.4956E+03	-9.7156E+02	6.6902E-07
28	4.9300E+02	1.4951E+03	-1.0021E+03	6.6902E-07
29	4.7200E+02	1.4947E+03	-1.0227E+03	6.6902E-07
30	4.2400E+02	1.4938E+03	-1.0698E+03	6.6902E-07
31	3.6500E+02	1.4935E+03	-1.1285E+03	6.6902E-07
32	2.4950E+02	1.4932E+03	-1.2437E+03	6.6902E-07
33	1.9900E+02	1.4932E+03	-1.2942E+03	6.6902E-07
34	1.8000E+02	1.4932E+03	-1.3132E+03	6.6902E-07
35	1.6500E+02	1.4932E+03	-1.3282E+03	6.6902E-07
36	1.3800E+02	1.4932E+03	-1.3552E+03	6.6902E-07
37	1.3000E+02	1.4932E+03	-1.3632E+03	6.6902E-07
38	1.2700E+02	1.4932E+03	-1.3662E+03	6.6902E-07
39	1.2700E+02	1.4932E+03	-1.3662E+03	6.6902E-07

SUM OF SQUARED RESIDUALS= 9.9924E+07

VARIANCE = 2.4304E+07

STANDARD DEVIATION = 1.5590E+03

ADDITIONAL PARAMETERS CALCULATED BY THE LEAST SQUARES ROUTINE

THE RESIDUAL SUM OF SQUARES = 8.992372E+07

THE NUMBER OF SIGNIFICANT DIGITS IN THE CALCULATED PARAMETERS = 6.001317E+00

THE NUMBER OF FUNCTION EVALUATIONS REQUIRED = 6.200000E+01

THE NUMBER OF ITERATIONS REQUIRED = 1.500000E+01

AN INTEGER WHICH INDICATES THE CONVERGENCE CRITERION SATISFIED: INFER = 1



INFER=0 INDICATES THAT CONVERGENCE FAILED -- SEE THE (IER) PARAMETER

INFER=1 INDICATES THAT THE FOLLOWING CONVERGENCE CONDITION IS SATISFIED IF FOR TWO SUCCESSIVE ITERATIONS THE PARAMETER ESTIMATES AGREE, COMPONENT BY COMPONENT TO NSIG (SIGNIFICANT) DIGITS

INFER=2 INDICATES THAT THE FOLLOWING CONVERGENCE CONDITION IS SATISFIED IF FOR TWO SUCCESSIVE ITERATIONS THE RESIDUAL SUM OF THE SQUARE ESTIMATES HAVE RELATIVE DIFFERENCE LESS THAN OR EQUAL TO (EPS)

INFER=4 INDICATES THAT THE FOLLOWING CONVERGENCE CONDITION IS SATISFIED IF THE (EUCLIDEAN) NORM OF THE APPROXIMATE GRADIENT IS LESS THAN OR EQUAL TO (DELTA)

INFER=X IF MORE THAN ONE OF THE ABOVE CONVERGENCE CRITERIA IS SATISFIED (INFER) REPRESENTS THE CORRESPONDING SUM OF THE INTEGERS

THE ERROR PARAMETER: IER = 0

IER=0 INDICATES SUCCESSFUL EXECUTION OF THE PROGRAM

IER=38 INDICATES THAT THE JACOBIAN IS ZERO.  
THE SOLUTION IS A STATIONARY POINT (WARNING)

IER=129 INDICATES THAT A SINGULARITY WAS  
DETECTED IN THE JACOBIAN

IER=130 INDICATES THAT AT LEAST ONE OF THE  
SUBROUTINE CALL PARAMETERS WAS SPECIFIED  
INCORRECTLY -- VERIFY: M,N,IOPT,PARM(1),PARM(2)

IER=131 INDICATES THAT THE MARQUARDT PARAMETER  
EXCEEDED THE DEFAULT VALUE OF (120.0)

IER=132 INDICATES THAT AFTER A SUCCESSFUL  
RECOVERY FROM A SINGULAR JACOBIAN, THE SOLUTION  
HAS CYCLED BACK TO THE FIRST SINGULARITY

IER=133 INDICATES THAT THE (MAXFN) PARAMETER WAS EXCEEDED

# VARIABLES USED IN THE CALCULATIONS

THE ESTIMATED METAL CLUSTER RESISTANCE ( $R_c$ ) =  $1.000000E+02$

THE ESTIMATED GAP RESISTANCE ( $R_g$ ) =  $1.000000E+05$

THE ESTIMATED GAP  
CAPACITANCE ( $C_g$ ) =  $6.000000E-07$

## SCALED VALUES OF INPUTS ARE

$5.000000E-01$   
 $1.000000E+00$   
 $6.000000E-01$

THE LEAST SQUARE VALUE OF THE METAL CLUSTER  
RESISTANCE,  $R_c$  =  $3.165797E+03$

THE LEAST SQUARE VALUE OF THE GAP  
RESISTANCE,  $R_g$  =  $9.547230E+04$

THE LEAST SQUARE VALUE OF THE GAP  
CAPACITANCE,  $C_g$  =  $4.753740E-07$

THE RESIDUALS ARE CALCULATED BY THE FOLLOWING  
EQUATION: [MEASURED VALUE-CALCULATED VALUE]

SAMPLE	R(f)	R(cal)	R(resid)	Cg(est)
1	9.5200E+04	9.8638E+04	-3.4381E+03	4.7537E-07
2	8.8500E+04	9.2790E+04	-4.2903E+03	4.7537E-07
3	8.7000E+04	9.0438E+04	-3.4383E+03	4.7537E-07
4	8.6200E+04	8.7813E+04	-1.6130E+03	4.7537E-07
5	8.4700E+04	8.4973E+04	-2.7347E+02	4.7537E-07
6	8.3300E+04	8.1977E+04	1.3228E+03	4.7537E-07
7	8.1300E+04	7.8878E+04	2.4220E+03	4.7537E-07
8	7.6900E+04	7.2559E+04	4.3415E+03	4.7537E-07
9	7.3000E+04	6.6328E+04	6.6719E+03	4.7537E-07
10	6.8000E+04	6.0399E+04	7.6012E+03	4.7537E-07
11	6.2900E+04	5.4895E+04	8.0047E+03	4.7537E-07
12	5.5600E+04	4.9875E+04	5.7247E+03	4.7537E-07
13	4.8500E+04	4.5351E+04	3.1494E+03	4.7537E-07
14	4.1800E+04	4.1304E+04	4.9566E+02	4.7537E-07
15	3.5100E+04	3.7703E+04	-2.6035E+03	4.7537E-07
16	2.9600E+04	3.4508E+04	-4.9076E+03	4.7537E-07

17	2.5500E+04	3.1674E+04	-6.1743E+03	4.7537E-07
18	2.2900E+04	2.9162E+04	-6.2621E+03	4.7537E-07
19	2.1500E+04	2.6933E+04	-5.4326E+03	4.7537E-07
20	1.9100E+04	2.4951E+04	-5.8510E+03	4.7537E-07
21	1.8000E+04	2.3186E+04	-5.1864E+03	4.7537E-07
22	1.7100E+04	2.1612E+04	-4.5116E+03	4.7537E-07
23	1.6400E+04	2.0203E+04	-3.8027E+03	4.7537E-07
24	1.5600E+04	1.8939E+04	-3.3391E+03	4.7537E-07
25	1.4900E+04	1.7803E+04	-2.9031E+03	4.7537E-07
26	1.4300E+04	1.6779E+04	-2.4790E+03	4.7537E-07
27	1.3900E+04	1.5854E+04	-1.9536E+03	4.7537E-07
28	1.3500E+04	1.5015E+04	-1.5152E+03	4.7537E-07
29	1.3000E+04	1.4254E+04	-1.2537E+03	4.7537E-07
30	1.2800E+04	1.3561E+04	-7.6057E+02	4.7537E-07
31	1.2700E+04	1.2928E+04	-2.2809E+02	4.7537E-07
32	1.2700E+04	1.2350E+04	3.5032E+02	4.7537E-07
33	1.2500E+04	1.1820E+04	6.8043E+02	4.7537E-07
34	1.2300E+04	1.1333E+04	9.6730E+02	4.7537E-07
35	1.2200E+04	1.0885E+04	1.3154E+03	4.7537E-07
36	1.2000E+04	1.0472E+04	1.5285E+03	4.7537E-07
37	1.1800E+04	1.0090E+04	1.7102E+03	4.7537E-07
38	1.1600E+04	9.7366E+03	1.8634E+03	4.7537E-07
39	1.1400E+04	9.4092E+03	1.9908E+03	4.7537E-07
40	1.1200E+04	9.1051E+03	2.0949E+03	4.7537E-07
41	1.0900E+04	8.8222E+03	2.0778E+03	4.7537E-07
42	1.0800E+04	8.5587E+03	2.2413E+03	4.7537E-07
43	1.0600E+04	8.3128E+03	2.2872E+03	4.7537E-07
44	1.0400E+04	8.0831E+03	2.3169E+03	4.7537E-07
45	1.0200E+04	7.8682E+03	2.3318E+03	4.7537E-07
46	1.0100E+04	7.6669E+03	2.4331E+03	4.7537E-07
47	1.0000E+04	7.4780E+03	2.5220E+03	4.7537E-07
48	9.9000E+03	3.1662E+03	6.7338E+03	4.7537E-07
49	9.8200E+03	3.1662E+03	6.6538E+03	4.7537E-07
50	9.7100E+03	3.1662E+03	6.5438E+03	4.7537E-07
51	9.6200E+03	3.1662E+03	6.4538E+03	4.7537E-07
52	9.5200E+03	6.6889E+03	2.8311E+03	4.7537E-07
53	6.3400E+03	4.7644E+03	1.5756E+03	4.7537E-07
54	4.8200E+03	4.0716E+03	7.4836E+02	4.7537E-07
55	4.1200E+03	3.7475E+03	3.7248E+02	4.7537E-07
56	3.5500E+03	3.5705E+03	-2.0528E+01	4.7537E-07
57	3.1700E+03	3.4635E+03	-2.9349E+02	4.7537E-07
58	2.7800E+03	3.3939E+03	-6.1388E+02	4.7537E-07
59	2.5400E+03	3.3461E+03	-8.0610E+02	4.7537E-07
60	2.3700E+03	3.3119E+03	-9.4190E+02	4.7537E-07
61	1.8900E+03	3.2308E+03	-1.3408E+03	4.7537E-07
62	1.6100E+03	3.2024E+03	-1.5924E+03	4.7537E-07
63	7.8700E+02	3.1716E+03	-2.3846E+03	4.7537E-07
64	5.2100E+02	3.1673E+03	-2.6463E+03	4.7537E-07
65	4.6500E+02	3.1664E+03	-2.7014E+03	4.7537E-07
66	4.0700E+02	3.1662E+03	-2.7592E+03	4.7537E-07
67	2.2800E+02	3.1658E+03	-2.9378E+03	4.7537E-07
68	1.8100E+02	3.1658E+03	-2.9848E+03	4.7537E-07
69	1.1200E+02	3.1658E+03	-3.0538E+03	4.7537E-07
70	1.0200E+02	3.1658E+03	-3.0638E+03	4.7537E-07

SUM OF SQUARED RESIDUALS= 8.6166E+08

VARIANCE = 1.2671E+07

STANDARD DEVIATION = 3.5597E+03

ADDITIONAL PARAMETERS CALCULATED BY THE LEAST SQUARES ROUTINE

THE RESIDUAL SUM OF SQUARES = 8.616601E+08

THE NUMBER OF SIGNIFICANT DIGITS IN THE CALCULATED PARAMETERS = 6.073827E+00

THE NUMBER OF FUNCTION EVALUATIONS REQUIRED = 6.900000E+01

THE NUMBER OF ITERATIONS REQUIRED = 2.600000E+01

AN INTEGER WHICH INDICATES THE CONVERGENCE CRITERION SATISFIED: INFER = 1

INFER=0 INDICATES THAT CONVERGENCE FAILED -- SEE THE (IER) PARAMETER

INFER=1 INDICATES THAT THE FOLLOWING CONVERGENCE CONDITION IS SATISFIED IF  
FOR TWO SUCCESSIVE ITERATIONS THE PARAMETER  
ESTIMATES AGREE, COMPONENT BY COMPONENT  
TO NSIG (SIGNIFICANT) DIGITS

INFER=2 INDICATES THAT THE FOLLOWING CONVERGENCE CONDITION IS SATISFIED IF  
FOR TWO SUCCESSIVE ITERATIONS THE RESIDUAL  
SUM OF THE SQUARE ESTIMATES HAVE RELATIVE  
DIFFERENCE LESS THAN OR EQUAL TO (EPS)

INFER=4 INDICATES THAT THE FOLLOWING CONVERGENCE CONDITION IS SATISFIED IF  
THE (EUCLIDEAN) NORM OF THE APPROXIMATE  
GRADIENT IS LESS THAN OR EQUAL TO (DELTA)

INFER=X IF MORE THAN ONE OF THE ABOVE CONVERGENCE CRITERIA IS SATISFIED  
(INFER) REPRESENTS THE CORRESPONDING SUM OF  
THE INTEGERS

THE ERROR PARAMETER: IER = 0

- IER=0 INDICATES SUCCESSFUL EXECUTION OF THE PROGRAM
- IER=38 INDICATES THAT THE JACOBIAN IS ZERO.  
THE SOLUTION IS A STATIONARY POINT (WARNING)
- IER=129 INDICATES THAT A SINGULARITY WAS  
DETECTED IN THE JACOBIAN
- IER=130 INDICATES THAT AT LEAST ONE OF THE  
SUBROUTINE CALL PARAMETERS WAS SPECIFIED  
INCORRECTLY -- VERIFY: M,N,IOPT,PARM(1),PARM(2)
- IER=131 INDICATES THAT THE MARQUARDT PARAMETER  
EXCEEDED THE DEFAULT VALUE OF (120.0)
- IER=132 INDICATES THAT AFTER A SUCCESSFUL  
RECOVERY FROM A SINGULAR JACOBIAN, THE SOLUTION  
HAS CYCLED BACK TO THE FIRST SINGULARITY
- IER=133 INDICATES THAT THE (MAXFN) PARAMETER  
WAS EXCEEDED

# VARIABLES USED IN THE CALCULATIONS

THE ESTIMATED METAL CLUSTER RESISTANCE (Rc) = 1.000000E+02

THE ESTIMATED GAP RESISTANCE (Rg) = 1.000000E+05

THE ESTIMATED GAP  
CAPACITANCE (Cg) = 6.000000E-07

## SCALED VALUES OF INPUTS ARE

5.000000E-01  
1.000000E+00  
6.000000E-01

THE LEAST SQUARE VALUE OF THE METAL CLUSTER  
RESISTANCE, Rc = 3.311153E+03

THE LEAST SQUARE VALUE OF THE GAP  
RESISTANCE, Rg = 9.134469E+04

THE LEAST SQUARE VALUE OF THE GAP  
CAPACITANCE, Cg = 4.891686E-07

THE RESIDUALS ARE CALCULATED BY THE FOLLOWING  
EQUATION: [MEASURED VALUE-CALCULATED VALUE]

SAMPLE	R(f)	R(cal)	R(resid)	Cg(est)
1	8.9400E+04	9.4656E+04	-5.2558E+03	4.8917E-07
2	8.4000E+04	8.8765E+04	-4.7654E+03	4.8917E-07
3	8.3300E+04	8.6408E+04	-3.1076E+03	4.8917E-07
4	8.2000E+04	8.3784E+04	-1.7836E+03	4.8917E-07
5	8.0600E+04	8.0955E+04	-3.5460E+02	4.8917E-07
6	7.9400E+04	7.7980E+04	1.4204E+03	4.8917E-07
7	7.8100E+04	7.4913E+04	3.1866E+03	4.8917E-07
8	7.5200E+04	6.8695E+04	6.5045E+03	4.8917E-07
9	7.1400E+04	6.2610E+04	8.7903E+03	4.8917E-07
10	6.6200E+04	5.6859E+04	9.3411E+03	4.8917E-07
11	5.9500E+04	5.1556E+04	7.9438E+03	4.8917E-07
12	5.2600E+04	4.6749E+04	5.8513E+03	4.8917E-07
13	4.5200E+04	4.2439E+04	2.7608E+03	4.8917E-07
14	3.8000E+04	3.8604E+04	-6.0427E+02	4.8917E-07
15	3.1600E+04	3.5206E+04	-3.6064E+03	4.8917E-07
16	2.6300E+04	3.2202E+04	-5.9023E+03	4.8917E-07

17	2.2800E+04	2.9548E+04	-6.7482E+03	4.8917E-07
18	2.0100E+04	2.7202E+04	-7.1020E+03	4.8917E-07
19	1.8600E+04	2.5125E+04	-6.5255E+03	4.8917E-07
20	1.7300E+04	2.3284E+04	-5.9842E+03	4.8917E-07
21	1.6200E+04	2.1648E+04	-5.4481E+03	4.8917E-07
22	1.5200E+04	2.0191E+04	-4.9906E+03	4.8917E-07
23	1.4400E+04	1.8889E+04	-4.4889E+03	4.8917E-07
24	1.3700E+04	1.7723E+04	-4.0233E+03	4.8917E-07
25	1.3200E+04	1.6677E+04	-3.4767E+03	4.8917E-07
26	1.2800E+04	1.5734E+04	-2.9345E+03	4.8917E-07
27	1.2500E+04	1.4884E+04	-2.3839E+03	4.8917E-07
28	1.2200E+04	1.4114E+04	-1.9140E+03	4.8917E-07
29	1.2000E+04	1.3416E+04	-1.4155E+03	4.8917E-07
30	1.1900E+04	1.2780E+04	-8.8014E+02	4.8917E-07
31	1.1700E+04	1.2201E+04	-5.0083E+02	4.8917E-07
32	1.1600E+04	1.1671E+04	-7.1396E+01	4.8917E-07
33	1.1500E+04	1.1186E+04	3.1352E+02	4.8917E-07
34	1.1400E+04	1.0741E+04	6.5863E+02	4.8917E-07
35	1.1400E+04	1.0332E+04	1.0680E+03	4.8917E-07
36	1.1300E+04	9.9546E+03	1.3454E+03	4.8917E-07
37	1.1200E+04	9.6062E+03	1.5938E+03	4.8917E-07
38	1.1200E+04	9.2839E+03	1.9161E+03	4.8917E-07
39	1.1100E+04	8.9852E+03	2.1148E+03	4.8917E-07
40	1.1000E+04	8.7079E+03	2.2921E+03	4.8917E-07
41	1.0900E+04	8.4501E+03	2.4499E+03	4.8917E-07
42	1.0900E+04	8.2099E+03	2.6901E+03	4.8917E-07
43	1.0800E+04	7.9860E+03	2.8140E+03	4.8917E-07
44	1.0700E+04	7.7768E+03	2.9232E+03	4.8917E-07
45	1.0700E+04	7.5811E+03	3.1189E+03	4.8917E-07
46	1.0600E+04	7.3978E+03	3.2022E+03	4.8917E-07
47	1.0500E+04	7.2259E+03	3.2741E+03	4.8917E-07
48	1.0500E+04	3.3115E+03	7.1885E+03	4.8917E-07
49	1.0400E+04	3.3115E+03	7.0885E+03	4.8917E-07
50	1.0400E+04	3.3115E+03	7.0885E+03	4.8917E-07
51	1.0300E+04	3.3115E+03	6.9885E+03	4.8917E-07
52	1.0200E+04	6.5081E+03	3.6919E+03	4.8917E-07
53	7.0400E+03	4.7602E+03	2.2798E+03	4.8917E-07
54	5.4100E+03	4.1319E+03	1.2781E+03	4.8917E-07
55	4.3100E+03	3.8382E+03	4.7184E+02	4.8917E-07
56	3.6200E+03	3.6778E+03	-5.7775E+01	4.8917E-07
57	3.1800E+03	3.5808E+03	-4.0079E+02	4.8917E-07
58	2.9200E+03	3.5177E+03	-5.9774E+02	4.8917E-07
59	2.7200E+03	3.4745E+03	-7.5446E+02	4.8917E-07
60	2.5600E+03	3.4435E+03	-8.8348E+02	4.8917E-07
61	1.9300E+03	3.3700E+03	-1.4400E+03	4.8917E-07
62	1.7400E+03	3.3443E+03	-1.6043E+03	4.8917E-07
63	7.8100E+02	3.3165E+03	-2.5355E+03	4.8917E-07
64	5.8500E+02	3.3125E+03	-2.7275E+03	4.8917E-07
65	4.6900E+02	3.3117E+03	-2.8427E+03	4.8917E-07
66	4.1800E+02	3.3115E+03	-2.8935E+03	4.8917E-07
67	2.2600E+02	3.3112E+03	-3.0852E+03	4.8917E-07
68	1.6800E+02	3.3112E+03	-3.1432E+03	4.8917E-07
69	1.0900E+02	3.3112E+03	-3.2022E+03	4.8917E-07
70	9.8000E+01	3.3112E+03	-3.2132E+03	4.8917E-07

SUM OF SQUARED RESIDUALS= 1.1122E+09

VARIANCE = 1.6356E+07

STANDARD DEVIATION = 4.0442E+03

ADDITIONAL PARAMETERS CALCULATED BY THE LEAST SQUARES ROUTINE

THE RESIDUAL SUM OF SQUARES = 1.112179E+09

THE NUMBER OF SIGNIFICANT DIGITS IN THE CALCULATED PARAMETERS = 6.692512E+00

THE NUMBER OF FUNCTION EVALUATIONS REQUIRED = 9.500000E+01

THE NUMBER OF ITERATIONS REQUIRED = 2.800000E+01

AN INTEGER WHICH INDICATES THE CONVERGENCE CRITERION SATISFIED: INFER = 1

INFER=0 INDICATES THAT CONVERGENCE FAILED -- SEE THE (IER) PARAMETER

INFER=1 INDICATES THAT THE FOLLOWING CONVERGENCE CONDITION IS SATISFIED IF  
FOR TWO SUCCESSIVE ITERATIONS THE PARAMETER  
ESTIMATES AGREE, COMPONENT BY COMPONENT  
TO NSIG (SIGNIFICANT) DIGITS

INFER=2 INDICATES THAT THE FOLLOWING CONVERGENCE CONDITION IS SATISFIED IF  
FOR TWO SUCCESSIVE ITERATIONS THE RESIDUAL  
SUM OF THE SQUARE ESTIMATES HAVE RELATIVE  
DIFFERENCE LESS THAN OR EQUAL TO (EPS)

INFER=4 INDICATES THAT THE FOLLOWING CONVERGENCE CONDITION IS SATISFIED IF  
THE (EUCLIDEAN) NORM OF THE APPROXIMATE  
GRADIENT IS LESS THAN OR EQUAL TO (DELTA)

INFER=X IF MORE THAN ONE OF THE ABOVE CONVERGENCE CRITERIA IS SATISFIED  
(INFER) REPRESENTS THE CORRESPONDING SUM OF  
THE INTEGERS



THE ERROR PARAMETER: IER = 0

- IER=0 INDICATES SUCCESSFUL EXECUTION OF THE PROGRAM
- IER=38 INDICATES THAT THE JACOBIAN IS ZERO.  
THE SOLUTION IS A STATIONARY POINT (WARNING)
- IER=129 INDICATES THAT A SINGULARITY WAS  
DETECTED IN THE JACOBIAN
- IER=130 INDICATES THAT AT LEAST ONE OF THE  
SUBROUTINE CALL PARAMETERS WAS SPECIFIED  
INCORRECTLY -- VERIFY: M,N,IOPT,PARM(1),PARM(2)
- IER=131 INDICATES THAT THE MARQUARDT PARAMETER  
EXCEEDED THE DEFAULT VALUE OF (120.0)
- IER=132 INDICATES THAT AFTER A SUCCESSFUL  
RECOVERY FROM A SINGULAR JACOBIAN, THE SOLUTION  
HAS CYCLED BACK TO THE FIRST SINGULARITY
- IER=133 INDICATES THAT THE (MAXFN) PARAMETER  
WAS EXCEEDED

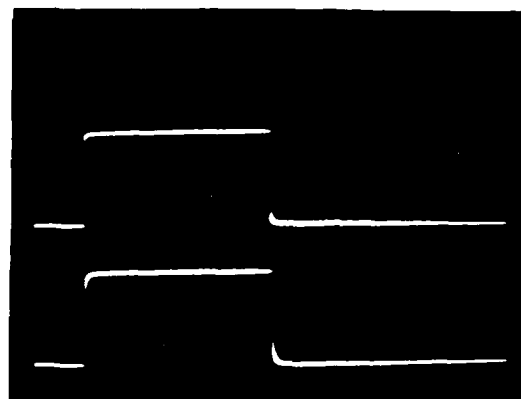
## APPENDIX K

### The Distortion of Simulated Brain Signals

Signal traces of the distorted waveforms of simulated brain signals are presented in this appendix. Three oscilloscope pictures were obtained for each electrode, and the pictures of an electrode appear on each page. The uppermost picture on each page in this appendix was obtained by using a 100 ohm series-connected load resistance. The middle and bottom pictures on each page of the appendix were obtained with series-connected load resistances of 1000 ohms and 10,000 ohms, respectively. In each oscilloscope picture, the uppermost trace is the control signal, and the bottom trace is the signal received by an electrode. The electrodes are identified with the coding scheme presented in Figure 5-1.

control  
signal →

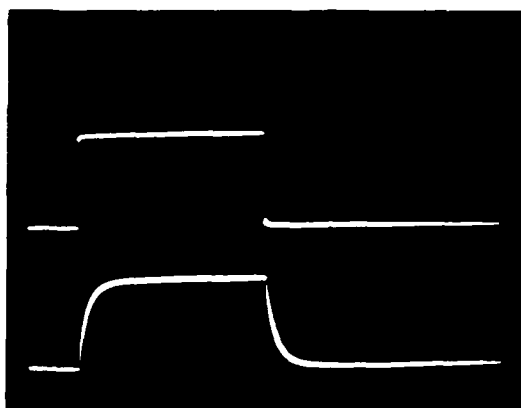
received  
signal →



100 Ohm  
Series-Connected  
Load Resistance

control  
signal →

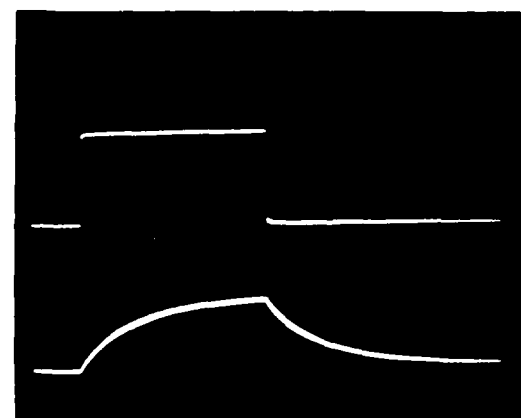
received  
signal →



1000 Ohm  
Series-Connected  
Load Resistance

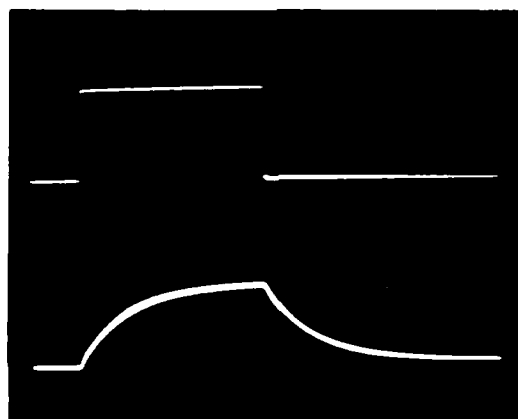
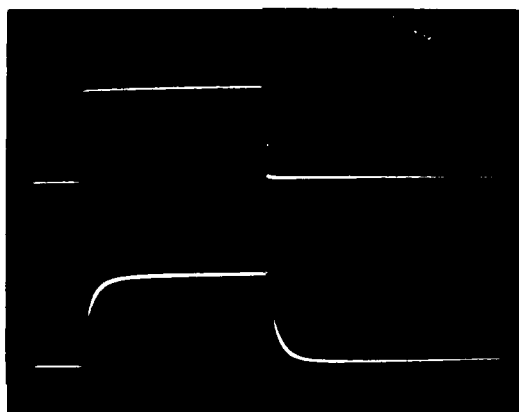
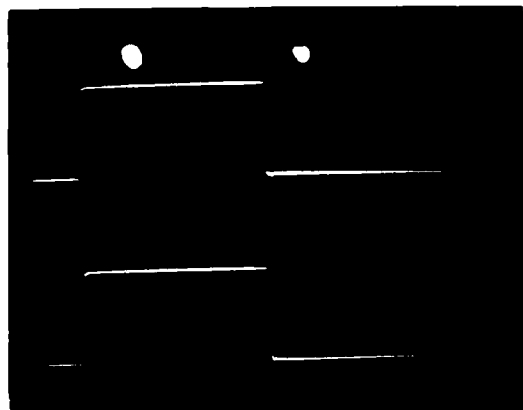
control  
signal →

received  
signal →



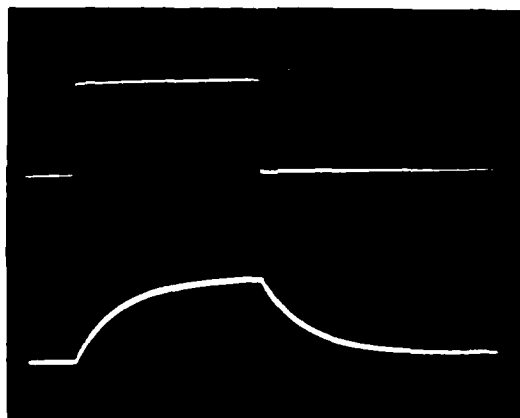
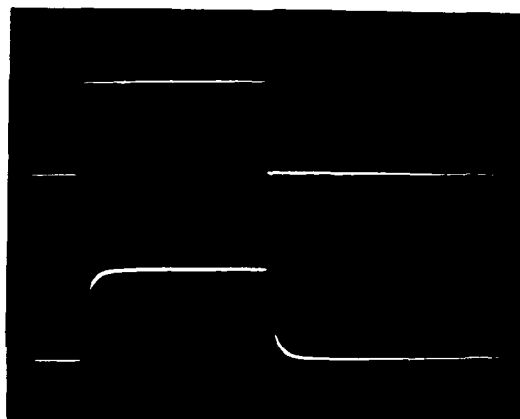
10,000 Ohm  
Series-Connected  
Load Resistance

Electrode 288



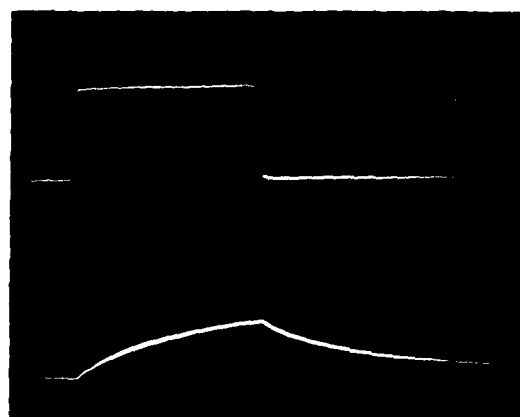
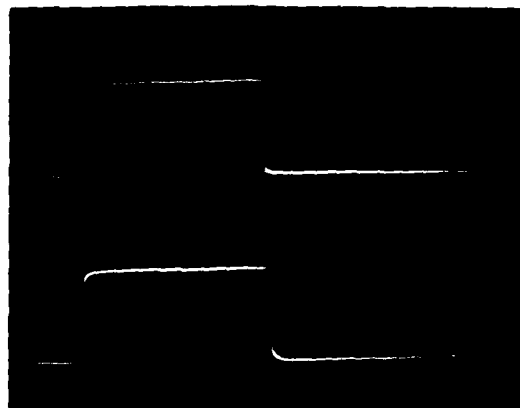
Electrode 244

K-3



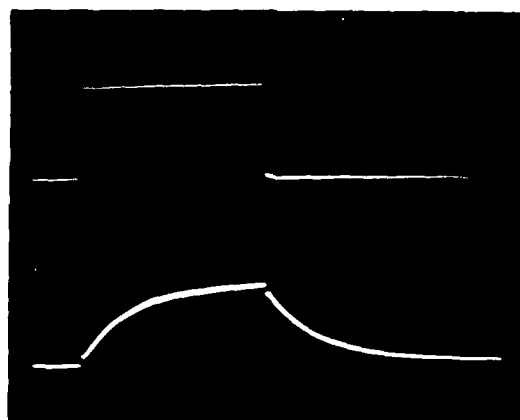
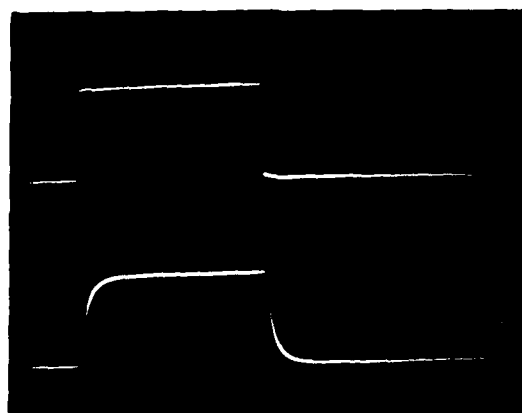
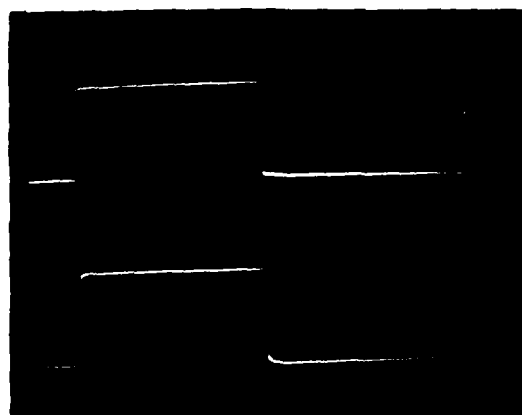
Electrode 2CC

K-4



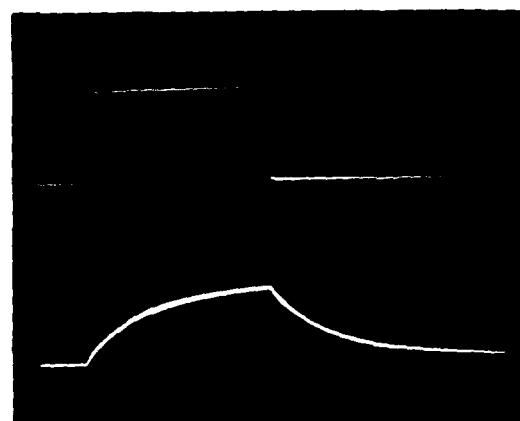
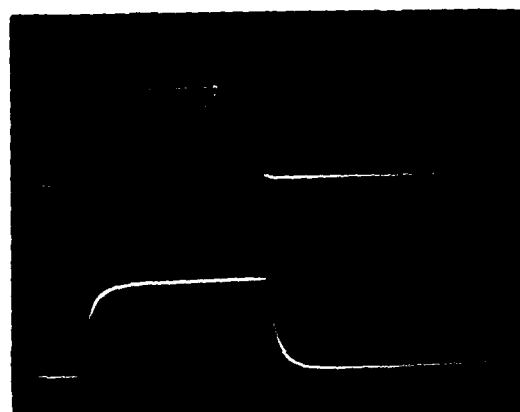
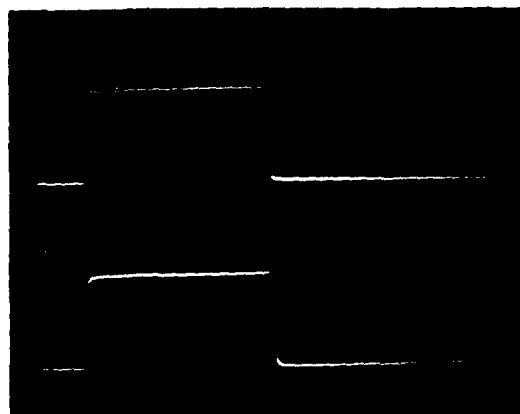
Electrode 211

K-5



Electrode 2GG

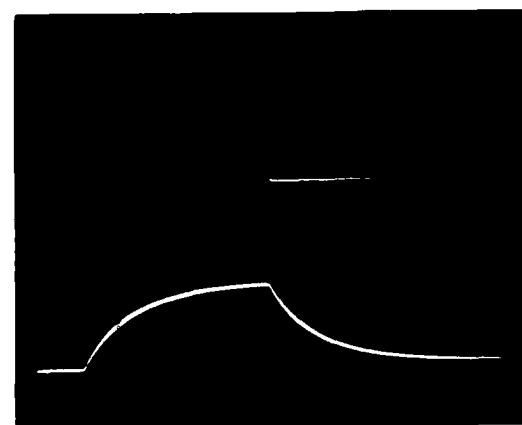
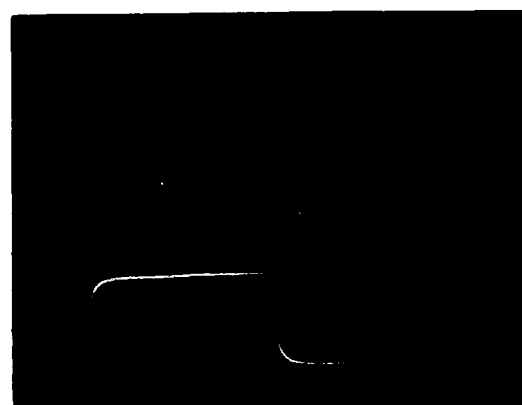
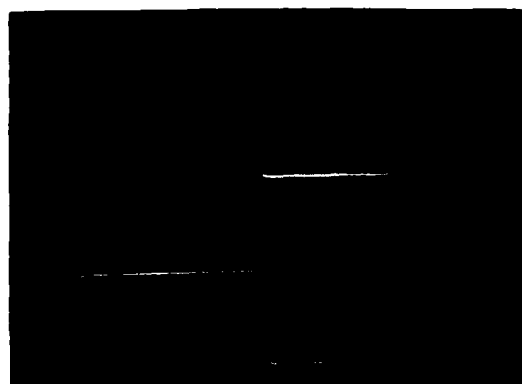
K-6



Electrode 299

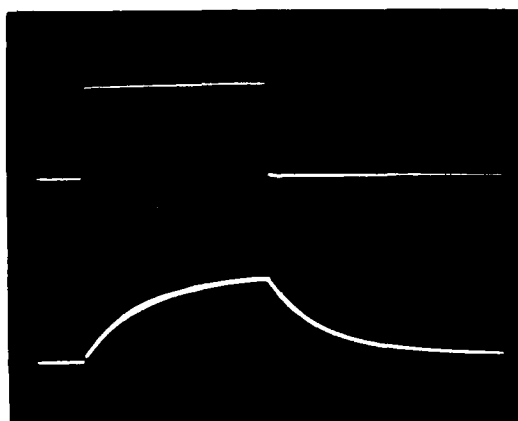
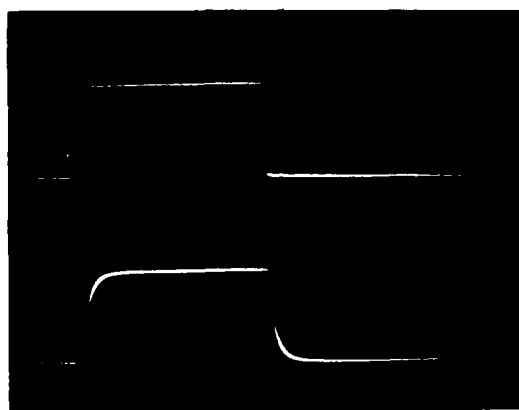
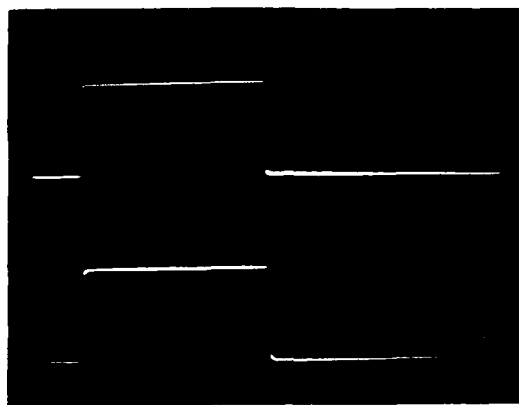
K-7





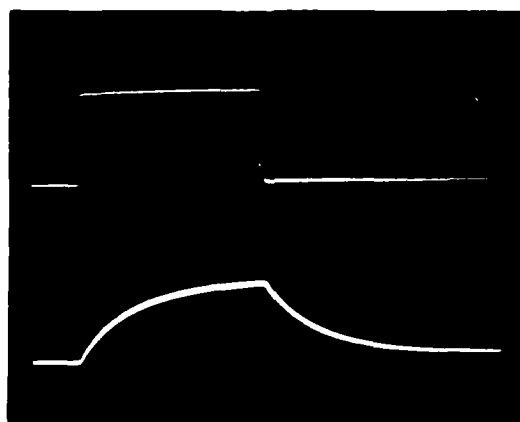
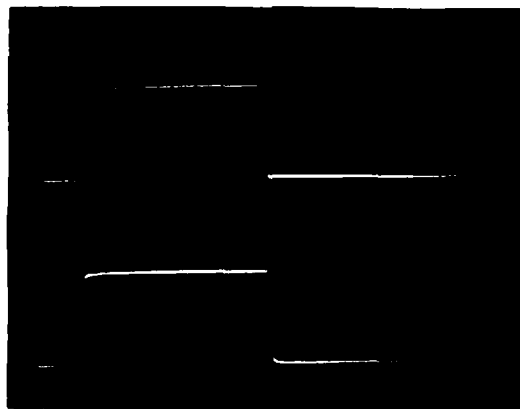
Electrode 277

K-8



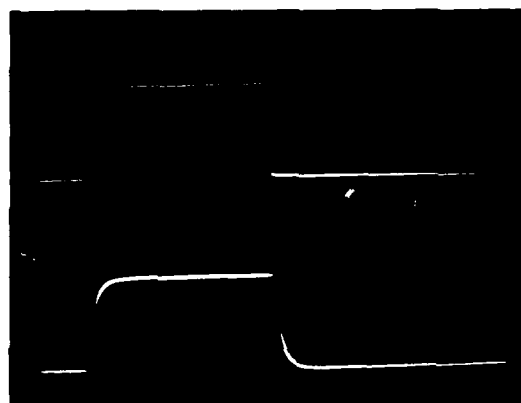
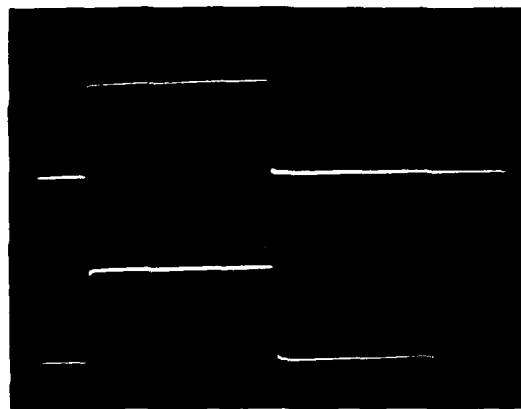
Electrode 24D

K-9



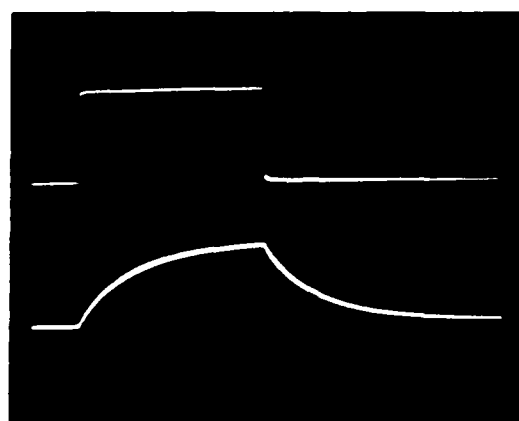
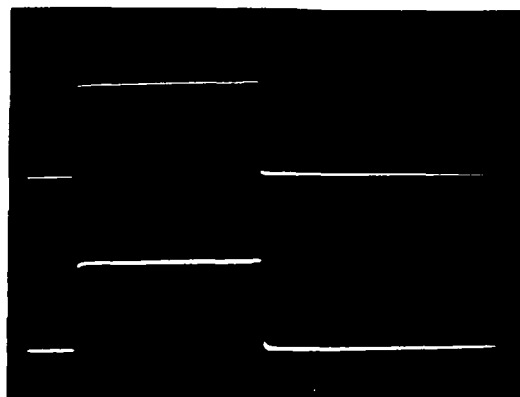
Electrode 2D4

K-10



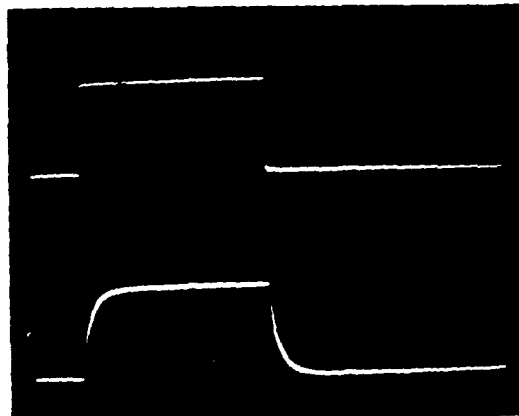
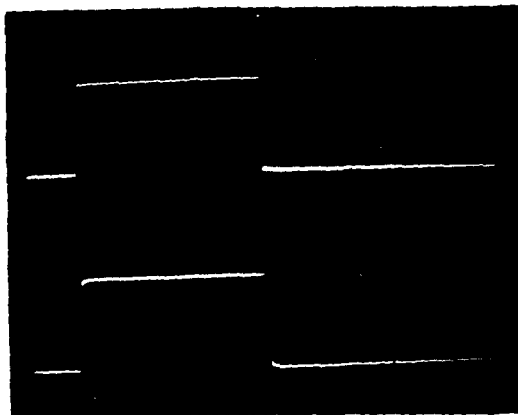
Electrode 388

K-11



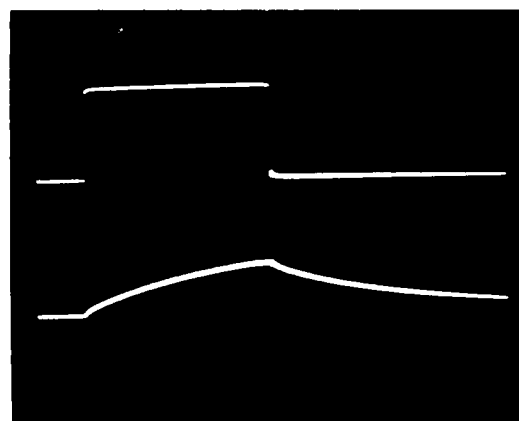
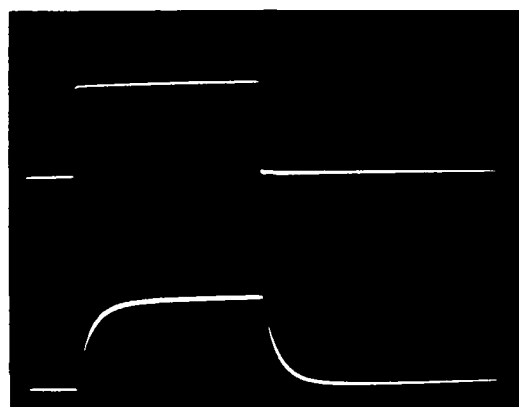
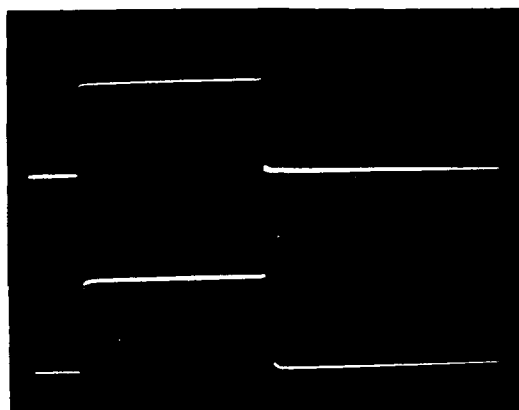
Electrode 344

K-12

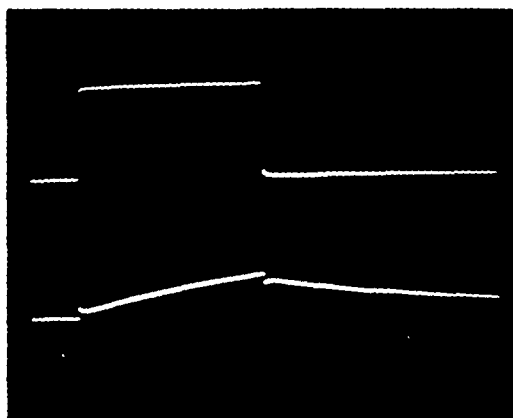
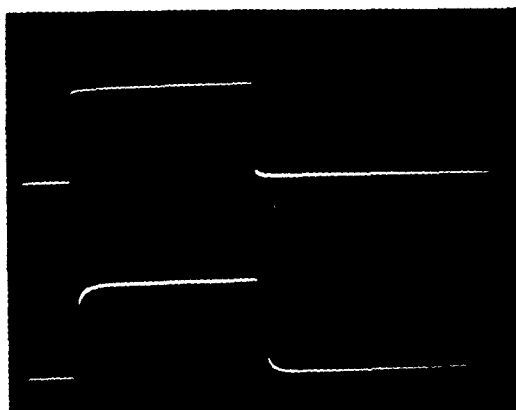


Electrode 3CC

K-13



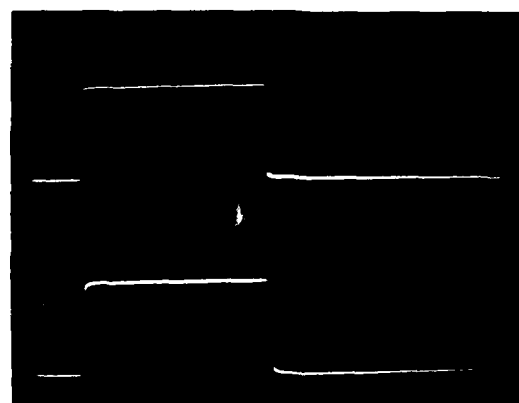
Electrode 311



Electrode 3GG

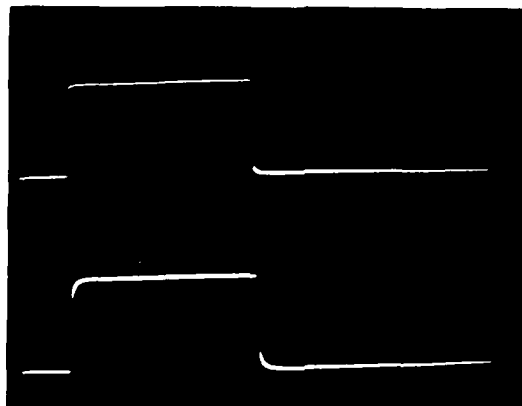
K-15





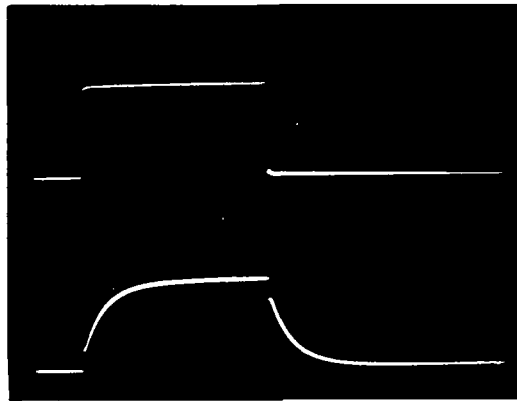
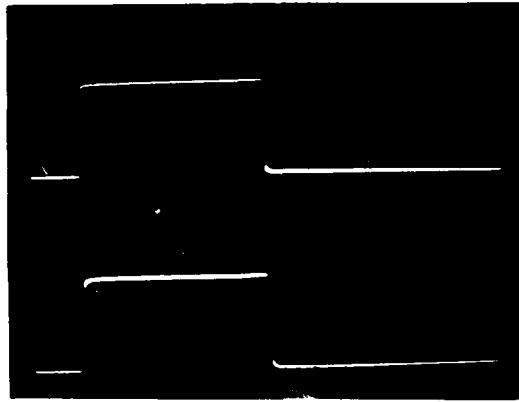
Electrode 399

K-16



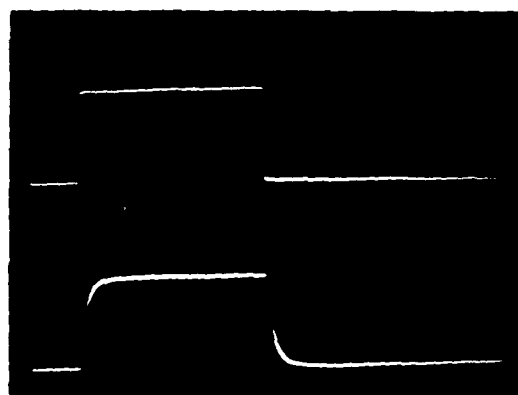
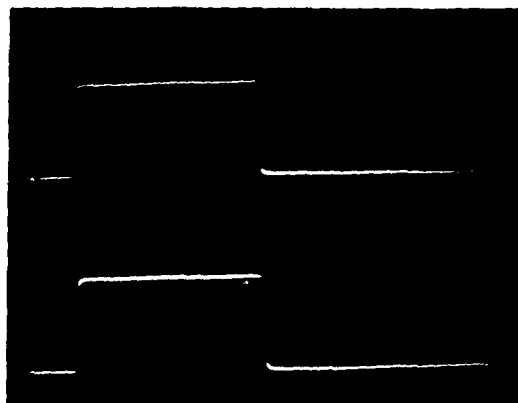
Electrode 377

K-17



Electrode 34D

K-18



Electrode 3D4

## Bibliography

1. Hensley, Capt Russell W. and 1Lt David C. Denton. The First Cortical Implant of a Semiconductor Multielectrode Array: Electrode Development and Data Collection. MS Thesis, GE/EE/82D-29. School of Engineering, Air Force Institute of Technology (AU), Wright-Patterson AFB OH, December 1982.
2. Zeman, 2Lt Gregory S. A Communications Link for an Implantable Electrode Array. MS Thesis, GE/ENG/84D-70. School of Engineering, Air Force Institute of Technology (AU), Wright-Patterson AFB OH, December 1984.
3. Turner, Capt Ricardo R. Encapsulation and Packaging of a Semiconductor Multielectrode Array for Cortical Implantation. MS Thesis, GSC/ENG/84D-30. School of Engineering, Air Force Institute of Technology (AU), Wright-Patterson AFB OH, December 1984.
4. Brindley, G.S. Physiology of the Retina and Visual Pathway. Baltimore: The Williams and Wilkins Company, 1970.
5. Kabrisky, Matthew. A Proposed Model for Visual Information Processing in the Human Brain. Urbana: University of Illinois Press, 1966.
6. Tatman, 2Lt Joseph A. A Two-Dimensional Multielectrode Microprobe for the Visual Cortex. MS Thesis, GE/EE/79-37. School of Engineering, Air Force Institute of Technology (AU), Wright-Patterson AFB, OH, December 1979 (AD-A080378).
7. Fitzgerald, Capt Gary H. The Development of a Two-Dimensional Multielectrode Array for Visual Perception Research in the Mammalian Brain. MS Thesis, GE/BE/80D-21. School of Engineering, Air Force Institute of Technology (AU), Wright-Patterson AFB OH, December 1980.
8. German, Capt George W. A Cortically Implantable Multielectrode Array for Investigating the Mammalian Visual System. MS Thesis, GE/EE/81D-24. School of Engineering, Air Force Institute of Technology (AU), Wright-Patterson AFB OH, December 1981 (AD-A115484).
9. Ballantine, Capt Robert B. The Development and Fabrication of an Implantable, Multiplexed, Semiconductor Multielectrode Array. MS Thesis, GE/EE/83D-9. School of Engineering, Air Force Institute of Technology (AU),

Wright-Patterson AFB, OH, December 1983.

10. Carstensen, Edwin L. "Ceramic Electrodes for ELF Bioeffects Studies," IEEE Transactions on Biomedical Engineering, BME-31 (8): 557-560 (August 1984).
11. Gandhi, Om P. Microwave Engineering and Applications. New York: Pergamon Press, 1985.
12. Robinson, D. A. "The Electrical Properties of Metal Microelectrodes," Proceedings of the IEEE, 56: 1065-1071 (June 1968).
13. Geddes, L. A. "Interface Design for Bioelectrode Systems," IEEE Spectrum, 9: 41-48 (October 1972).
14. Restak, Richard M. The Brain: The Last Frontier. Garden City: Doubleday and Company, 1979.
15. Wise, K. D. "A Multichannel Microprobe for Intracortical Single-Unit Recording," IEEE 1984 Symposium on Biosensors, 6: 87-89 (August 1984).
16. Sedlak, Jeffrey M. "Status Report--The AFIT Brain Chip." Unpublished report for AFIT COMM 698, Seminar in Technical Communication. School of Engineering, Air Force Institute of Technology (AU), Wright-Patterson AFB OH, 24 April 1986.
17. Zimmerman, A. H. Transient Passivation Kinetics of Reactive Metal Electrodes. Report SD-TR-82-78. Washington: Government Printing Office, 27 September 1982.
18. Kolesar, Edward Steven, Jr. Electronic Detection of Low Concentrations of Organophosphorus Compounds with a Solid State Device Utilizing Supported Copper + Cuprous Oxide Island Films. PhD dissertation. School of Engineering, Air Force Institute of Technology (AU), Wright-patterson AFB OH, May 1985 (AD-A158181).
19. Wise, K. D. "An Integrated Circuit Approach to Extracellular Microelectronics," IEEE Transactions on Biomedical Engineering, BME-17: 238-247 (July 1970).
20. Gesteland, R. C. "Comments on Microelectrodes," Proceeding of the IRE, 1856-1862 (November 1959).
21. Wise, K. D. and J. B. Angell. "A Low-Capacitance Multielectrode Probe for use in Extracellular

Neurophysiology," IEEE Transactions on Biomedical Engineering, BME-22: 212-219 (May 1975).

22. Geddes, L. A. and L. E. Baker. Principles of Applied Biomedical Instrumentation. New York: Wiley, 1968.
23. Cooke, Harry F. "Microwave Transistors: Theory and Design," Proceedings of the IEEE, 59 (8): 1163-1181 (August 1971).
24. Delahay, P. Double Layer and Electrode Kinetics. New York: Wiley, 1965.
25. Wise, K. D. and others. "An Integrated Circuit Approach to Extracellular Microelectrodes," IEEE Transactions on Bio-Medical Engineering, BME-17: 238-246 (July 1970).
26. Kip, Arthur F. Fundamentals of Electricity and Magnetism. New York: McGraw-Hill Book Company, 1969.
27. Onaral, B. and others. "The Effect of Metal Electrodes on Stimulation Thresholds," IEEE 1983 Frontiers of Engineering and Computing in Health Care, 94-99 (1983).
28. Carlson and Gisser. Electrical Engineering Concepts and Applications. Reading: Addison-Wesley Publishing Company, 1981.
29. Van Valkenburg, M.E. Network Analysis. Englewood Cliffs: Prentice Hall, Incorporated, 1974.
30. Sopko, 2Lt Michael E. Fabrication of a Biologically-Implantable, Multiplexed, Multielectrode Array of JFETs for Cortical Implantation. MS Thesis, GE/EE/84D-63. School of Engineering, Air Force Institute of Technology (AU), Wright-Patterson AFB OH, December 1984.
31. Eshraghian, Kamran and Neil Weste. Principles of CMOS VLSI Design. Reading: Addison-Wesley Publishing Company, 1985.
32. CMOS Databook. Pittsburg: National Semiconductor, 1985.
33. Daniel, Cuthbert and Fred S. Wood. Fitting Equations to Data. New York: John Wiley and Sons, 1980.
34. Christian, Sherril D. and others. "Least Squares Analysis: A Primer," American Laboratory, 41-49 (June 1986).

Vita

Jeffrey Michael Sedlak was born on 2 September 1958 in Meadville, Pennsylvania. He graduated from Meadville Senior High School in 1976. He entered Grove City College, Grove City, Pennsylvania in September 1976. He joined the ROTC program and accepted a scholarship to study electrical engineering. Jeffrey obtained a BS in electrical engineering in May 1980 and was commissioned into the USAF. His first assignment was at the Foreign Technology Division (FTD) at Wright-Patterson AFB, Ohio where he specialized in telecommunications. In June 1984, he was transferred to Headquarters Air Force Logistics Command at Wright-Patterson AFB, Ohio. While at HQ AFLC, Jeffrey supported mission requirements for the maintenance of embedded computer systems. He entered the Air Force Institute of Technology in June 1985.

Permanent Address:

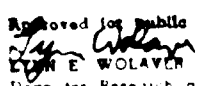
R.D.#5, Box 154  
Meadville, Pennsylvania 16335



UNCLASSIFIED

SECURITY CLASSIFICATION OF THIS PAGE

## REPORT DOCUMENTATION PAGE

1a REPORT SECURITY CLASSIFICATION <b>UNCLASSIFIED</b>			1b RESTRICTIVE MARKINGS		
2a SECURITY CLASSIFICATION AUTHORITY			3 DISTRIBUTION/AVAILABILITY OF REPORT		
2b DECLASSIFICATION/DOWNGRADING SCHEDULE			Approved for public release; Distribution unlimited		
4. PERFORMING ORGANIZATION REPORT NUMBER(S)  AFIT/GE/EE/86D-48			5. MONITORING ORGANIZATION REPORT NUMBER(S)		
6a NAME OF PERFORMING ORGANIZATION  School of Engineering	6b OFFICE SYMBOL (if applicable)  AFIT/ENG	7a NAME OF MONITORING ORGANIZATION			
6c ADDRESS (City, State, and ZIP Code)  Air Force Institute of Technology Wright-Patterson AFB, Ohio 45433		7b ADDRESS (City, State, and ZIP Code)			
8a NAME OF FUNDING/SPONSORING ORGANIZATION Air Force Institute of Technology	8b OFFICE SYMBOL (if applicable)  AFIT/ENG	9 PROCUREMENT INSTRUMENT IDENTIFICATION NUMBER			
8c ADDRESS (City, State, and ZIP Code)  Air Force Institute of Technology Wright-Patterson AFB, Ohio 45433		10 SOURCE OF FUNDING NUMBERS			
		PROGRAM ELEMENT NO	PROJECT NO	TASK NO	WORK UNIT ACCESSION NO
11 TITLE (Include Security Classification)  See Block 19					
12 PERSONAL AUTHOR(S) Jeffrey M. Sedlak, B.S., Capt, USAF					
13a TYPE OF REPORT Thesis	13b TIME COVERED FROM TO	14 DATE OF REPORT (Year, Month, Day) 1987, July 31		15 PAGE COUNT 381	
16 SUPPLEMENTARY NOTES					
17 COSATI CODES			18 SUBJECT TERMS (Continue on reverse if necessary and identify by block number)		
FIELD 09	GROUP 01	SUB-GROUP	Multielectrode Array, Polyimide, Cortex, Brain Chip, Electrolyte, Electrical Equivalent Circuit, Metal Electrode, Cerebrospinal Fluid, Passivation,		
19 ABSTRACT (Continue on reverse if necessary and identify by block number)					
Title: AN ELECTRICAL CIRCUIT MODEL OF THE INTERFACE BETWEEN AN ELECTRODE AND THE ELECTROLYTIC MEDIUM OF THE CORTEX					
Thesis Chairman: Edward S. Kolesar, Maj, USAF					
<div style="text-align: right;">             Approved for public release; LAW AFB 190-17                LYNN E. WOLAYER              Dean for Research and Professional Development              Air Force Institute of Technology (AFIT)              Wright-Patterson AFB OH 45433           </div>					
20 DISTRIBUTION STATEMENT OF ABSTRACT <input checked="" type="checkbox"/> UNCLASSIFIED/UNLIMITED <input type="checkbox"/> SAME AS RPT <input type="checkbox"/> DTIC USERS			21 ABSTRACT SECURITY CLASSIFICATION <b>UNCLASSIFIED</b>		
22a NAME OF RESPONSIBLE INDIVIDUAL Edward S. Kolesar, Maj, USAF			22b TELEPHONE (Include Area Code) (513) 255-3576		22c OFFICE SYMBOL AFIT/ENG

DD FORM 1473, 84 MAR

83 APR edition may be used until exhausted  
All other editions are obsolete

SECURITY CLASSIFICATION OF THIS PAGE

UNCLASSIFIED

18. (cont.)

Interface Kinetics, Nonlinear Least Squares, Biopotential, Levenburg-Marquardt Algorithm, Visual Evoked Response, Maximum Scan Rate, Photolithography, Signal Distortion, Helmholtz Double Layer, Amplifier Input Impedance, Frequency Response, Polarization

19. (cont.)

An equivalent electrical circuit model of an electrode in contact with a saline electrolyte was proposed and evaluated to characterize the performance of the implantable AFIT brain chip. The proposed model consists of three frequency-independent lumped elements; a resistance connected in series with the parallel combination of a resistance and capacitance. This model accounts for the electrical characteristics of the Helmholtz double layer that forms at the interface between an electrode and the saline electrolyte. Values of the resistance and capacitance parameters were calculated using a nonlinear least squares technique and compared with the empirical data obtained from brain chips immersed in a saline bath. The impact of the Helmholtz double layer capacitance upon the maximum scan rate of the 256-electrode array was also examined. A square wave input pulse was used to simulate the visual evoked response of a mammal, and the maximum scan rate of the array was determined by varying the resistance of a series-connected load that could represent the input impedance of an amplifier.

END

9-87

Dtic